

Alternative splicing in sodium channels:
Biophysical and functional effects in
Na_v1.1, Na_v1.2 & Na_v1.7.

Andrianos Liavas

A thesis submitted to University College London for the
degree of Doctor of Philosophy

Department of Clinical and Experimental Epilepsy

Institute of Neurology

Queen Square

London

WC1N 3BG

Declaration

I, Andrianos Liavas, confirm that the work presented in this thesis is my original research work.

Where contributions of others are involved, this has been clearly indicated in the thesis.

The copyright of this thesis rests with the author and no quotation from it or information derived from it may be published without the prior written consent of the author.

Acknowledgements

I would like to thank first of all my supervisor, Dr Stephanie Schorge, for her continuous care and support that went far beyond the duties of an ordinary supervisor and for which I'm truly grateful.

I would also like to thank my professors and colleagues, in my lab as well as in previous labs I've worked in, for sharing their time, knowledge, expertise as well as their everyday life with me, which has ended up in great partnerships and true friendships. A special thanks to Gabriele, my lab brother, (I'm gonna miss working together my friend!), the whole 808 gang, with all of which we came really close together (and not just because of lack of office space!), the Friday night pub crew (and Monday and Thursday sometimes...!) and especially Elodie, for being truly special to me.

A very big thank you also to my family, my brother Mathios and all my friends and beloved ones for always being there for me. It's their constant love and support through which I found the strength and courage to persist through the difficulties and finally reach the end of this big journey today.

Finally, I would also like to thank my examiners, Dr Martin Stocker and Prof Richard Baines, for finding the time to read and correct my thesis.

Abstract

Alternative splicing in voltage-gated sodium channels can affect pathophysiological conditions, including epilepsy and pain. A conserved alternative splicing event in sodium channel genes, including *SCN1A*, *SCN2A* and *SCN9A*, gives rise to the neonatal (5N) and adult (5A) isoforms. Differences in the ratio of 5A/5N in Na_v1.1 (encoded by *SCN1A*) in patients may lead to different predisposition to epilepsy or response to antiepileptic drugs (AED). Previous HEK293T whole-cell voltage-clamp recordings showed that Na_v1.1-5N channels recover more quickly from fast inactivation than 5A. However it was unknown whether this effect is conserved in Na_v1.2 (encoded by *SCN2A*) and Na_v1.7 (*SCN9A*) channels, or what the functional consequences of this splicing event are for neurons.

This project used whole-cell voltage-clamp recordings on heterologously expressed neonatal and adult channels to compare the biophysical properties of the splice isoforms for all three channel types and their modulation by AEDs. It also used current-clamp and dynamic-clamp recordings on transfected hippocampal cultured neurons to assess the effect of splicing on neuronal properties during epileptiform activity.

Biophysical analysis in HEK293T cells revealed that splicing profoundly regulates fast inactivation and channel availability during fast, repetitive stimulation, with neonatal channels showing higher availability compared to adult channels and this difference was conserved among Na_v1.1, Na_v1.2 and Na_v1.7. The change in inactivation imposed by splicing can be modeled as a modification of the stability of the inactivation state in resting channels. This change can be eradicated by administration of the AEDs phenytoin and carbamazepine. Current-clamp recordings in transfected neurons showed that the alternatively spliced variant modifies the rising phase of action potentials for Na_v1.1 and Na_v1.2 at high firing frequencies, implying a consistent splice-dependent modulation of channel availability. For Na_v1.1 in interneurons, this translated to higher firing frequency for the neonatal isoform, which also conferred a higher maximal firing rate during epileptiform events imposed under dynamic-clamp recordings.

Table of Contents

Chapter 1: Introduction.....	18
1.1 Voltage-gated sodium channel structure and function	18
1.1.1 Discovery and purification of the sodium channel protein.....	18
1.1.2 Na ⁺ channel structure: α -subunits.....	19
1.1.3 Sodium channel α -subunit genes: evolution and chromosomal location	22
1.1.4 β -subunits	24
1.1.5a Sodium channels subtypes have been appropriated to different locations and functions in neurons.	27
1.1.5b Non-canonical distribution of sodium channels	31
1.1.6 Molecular properties of VGSCs underlying function: Overview.....	31
1.1.7 Voltage Dependence of activation and gating	32
1.1.8 Ion selectivity	35
1.1.9 Inactivation	36
1.1.10 Persistent current	38
1.1.11 VGSC Pharmacology	40
1.2 VGSCs and Disease.....	44
1.2.1 Different Na ⁺ channels are associated with distinct diseases	44
1.2.2 <i>SCN9A</i> – Peripheral nerve sodium channelopathies.....	45
1.2.3 <i>SCN1A</i> & <i>SCN2A</i> – Brain sodium channelopathies	46
1.2.4 Epilepsy	46
1.2.5 Epilepsy and VGSCs	47
1.2.6 Dravet Syndrome	48
1.2.7 GEFS+	49
1.2.8 Epilepsy and <i>SCN1A</i>	49
1.2.9 <i>SCN2A</i> and Benign Familial Neonatal Infantile Seizures (BFNIS)	56
1.2.10 Epilepsy and <i>SCN3A</i> and <i>SCN8A</i>	57
1.2.11 Pain & Epilepsy and <i>SCN9A</i>	58
1.3 VGSCs and use-dependent blockers.....	61
1.3.1 Use-dependent blockers – AEDs	61
1.3.2 Phenytoin	61
1.3.3 The modulated receptor model	63

1.3.4 Molecular basis of phenytoin's action	64
1.3.5 Carbamazepine	66
1.4 VGSCs and splicing.....	68
1.4.1 Splicing	68
1.4.2 Alternative splicing in the <i>SCN1A</i> gene	69
1.4.3 <i>SCN1A</i> splicing and epilepsy.....	73
1.4.4 Possible reasons for differences between studies	76
1.4.5 5N overexpression in epilepsy.....	79
1.4.6 Functional studies for Na _v transcript variants.....	80
1.4.7 Dynamic-Clamp as a direct link to epileptiform bursts.....	85
1.5 Experimental aims	87

Chapter 2: General Materials and Methods..... 89

2.1 Molecular Biology.....	89
2.1.1 LB Broth, LB agar and Antibiotic solutions.....	89
2.1.2 DNA constructs and Cloning.....	90
2.1.3 Transformation of bacteria by heat shock and culture	90
2.1.4 DNA purification	91
2.1.5 DNA quantification	92
2.1.6 Mutagenesis of TTX binding site	92
2.1.7 Colony PCR.....	93
2.1.8 Agarose gel electrophoresis.....	94
2.2 Cell culture	95
2.2.1 Neuronal cultures.....	95
2.2.2 Preparation of coverslips for neuronal cultures	96
2.2.3 Preparation and expansion of cortical astroglial feeder layer.....	96
2.2.4 Freezing glial cells.....	97
2.2.5 Hippocampal neuronal culture preparation	97
2.2.6 Transfection of HEK293T cells using Lipofectamine.....	98
2.2.7 Transfection of hippocampal neurons using magnetofection.....	98
2.3 Electrophysiology	99
2.3.1 Electrophysiological recordings	99
2.3.2 Voltage clamp analysis	100
2.3.3 Voltage dependence of steady-state activation/inactivation.....	100

2.3.4 Recovery from fast inactivation	101
2.3.5 Current-clamp neuronal recordings	102
2.3.6 Single action potential parameters	103
2.3.7 Dynamic clamp recordings	104
2.4 Statistical analysis and modelling.....	105

Chapter 3: Functional dissection of the impact of splicing on onset and stability of inactivation in Na_v1.1 106

3.1 Hypothesis and Aims.....	106
3.2 Results: Probing the effects of splicing on fast inactivation	107
3.2.1 Validation of the constructs	107
3.2.2 Na _v 1.15N channels recover more quickly from fast inactivation than 5A channels ..	109
3.3 Results: Probing the ‘instantaneously available’ state with variable inactivating prepulses	114
3.3.1 The difference between splice isoforms is dependent on the length of the conditioning depolarisations	114
3.3.2 The difference in recovery from inactivation difference is masked by prolonged inactivating pre-pulses	120
3.4 Results: Probing the effects of voltage on inactivation recovery	122
3.4.1 The holding voltage can obscure the difference in inactivation recovery	122
3.5 Results: Probing the effects on rapid stimulation conditions	125
3.5.1 Recovery from inactivation difference is augmented during “high-activity”, “seizure-like” trains of depolarising steps	125
3.5.2 Splicing may have a specific effect on the affinity of the inactivation particle for the inner pore	127
3.5.3 No difference in inactivation recovery between variants with a simulated “interneuronal firing pattern”	132
3.6 Discussion:.....	134
3.6.1 Splicing affects a fast onset, short lived form of inactivation	134
3.6.2 The difference between variants is steeply dependent on voltage.....	136
3.6.3 A special role for the S4 in Domain 1 in stability of inactivation?	136
3.6.4 Could the difference between the variants be physiologically relevant? HEK293T cells show a potential for a difference – moving to neurons	137
3.7 Summary.....	140

Chapter 4: Conservation of a functional impact of alternative splicing in domain 1 of Na_v1.1 channels in neuronal sodium channels Na_v1.2 and Na_v1.7 141

4.1 Hypothesis and aims 141

4.2 Results: Comparing the functional properties of splice variants for Na_v1.2 and Na_v1.7 142

4.2.1 As in Na_v1.1, voltage dependence of activation/inactivation in Na_v1.2 & Na_v1.7 remains unaffected142

4.2.2 Preliminary investigation of recovery from fast inactivation in Na_v1.2 & Na_v1.7.....145

4.2.3 Recovery from fast inactivation difference is augmented in Na_v1.2 and Na_v1.7 with shorter depolarization conditions.....151

4.2.4 “High-activity, seizure-like” parameters maintain the difference between adult and neonatal channels for Na_v1.2 & Na_v1.7159

4.3 Summary of investigation of conservation 161

Chapter 5: Differential modulation of VGSC variants by the anti-epileptic drugs phenytoin and carbamazepine 165

5.1 Hypothesis and aims 165

5.2 Results: Comparing splice variant drug responses for Na_v1.1, Na_v1.2 & Na_v1.7 166

5.2.1 Addition of AEDs negates the inactivation recovery difference between Na_v1.1 5A and 5N variants.....166

5.2.2 Conservation of AED differences in Na_v1.2 and Na_v1.7 subtype isoforms167

5.3 Summary and discussion 169

Chapter 6: Altered sodium channel availability between neonatal and adult channels in neurons and effects on spike reliability in interneurons 171

6.1 Hypothesis and Aims 171

6.2 TTX resistance and transient expression of 5N and 5A constructs in interneuronal hippocampal cultures 172

6.3 Results: 173

6.3.1 Single AP parameters of Na_v1.1 neonatal and adult channels are similar in interneurons173

6.3.2 Na_v1.1 splicing controls spike reliability in interneurons.....175

6.3.3 Splicing in Na_v1.1 can modify sodium channel availability in interneurons during rapid trains178

6.3.4 Splicing in Na_v1.2 does not alter firing frequency fidelity in excitatory neurons180

6.3.5 Splicing in Na _v 1.2 has conserved effects on AP rise time in excitatory neurons.....	182
6.3.6 Effect of splicing on AP rise time is also conserved for Na _v 1.1 isoforms in excitatory neurons.....	185
6.4 Discussion.....	189
6.4.1 Splicing in Na _v 1.1 sets the maximal firing rate in interneurons.....	190
6.4.2 Molecular conservation suggests strong selection against neonatal Na _v 1.1 in mammals.....	190
6.5 Summary.....	195

Chapter 7: Effects of Na_v1.1 splicing on single cell response to network epileptic activity by Dynamic-Clamp..... 197

7.1 Hypothesis and Aims.....	197
7.2 Setup of a neuronal and interneuronal epileptic trace template.....	198
7.3 Magnitude of G _{th} – the conductance threshold.....	199
7.4 Results.....	202
7.4.1 In interneurons Na _v 1.1-5N channels confer higher firing ability under epileptic conditions.....	202
7.4.2 Na _v 1.1-5N channels also support higher availability during epileptic conditions in excitatory neurons.....	206
7.5 Discussion and summary of the results.....	208
Overview.....	210
Reference list.....	212

Appendix I: cDNA and amino acid sequence of all (TTX-sensitive and TTX-resistant) sodium channel splice variants used.....250

List of Tables

Table 1.1: Na _v β-subunits	27
Table 1.2: Na _v α-subunits	30
Table 2.1: Antibiotic concentrations for the preparation of agar plates and bacterial culture media	89
Table 3.1: V ₅₀ values and slopes for VD activation/inactivation of Na _v 1.1-5A and 5N from Fletcher et al., (2011), Thompson et al., (2011) and the current study in different recording conditions.....	109
Table 3.2: Na _v 1.1: Parameters of bi-exponential fits to recovery from long (100 ms) inactivating pre-pulses.....	113
Table 3.3: Na _v 1.1: Parameters of single exponential fits describing channel availability after 2 ms recovery from pre-pulses of different durations	119
Table 3.4: Na _v 1.1: Parameters of bi-exponential fits to recovery from long (100 ms) inactivating pre-pulses at -70 mV holding voltage.....	124
Table 3.5: Na _v 1.1: Parameters of bi-exponential fits to recovery from long (100 ms) inactivating pre-pulses at -100 mV holding voltage.....	124
Table 4.1: Na _v 1.7: Parameters of bi-exponential fits to recovery from long (100 ms) inactivating pre-pulses.....	147

Table 4.2: $Na_v1.2$: Parameters of bi-exponential fits to recovery from long (100 ms) inactivating pre-pulses	150
Table 4.3: $Na_v1.2$: Parameters of single exponential fits describing channel availability after 2 ms recovery from pre-pulses of different durations	154
Table 4.4: $Na_v1.7$: Parameters of single exponential fits describing channel availability after 2 ms recovery from pre-pulses of different durations	158

List of Figures

Figure 1.1: Three-dimensional structure of the VGSC.....	20
Figure 1.2: Three-dimensional structure of the sodium channel pore	21
Figure 1.3: Amino acid sequence similarity (A) and phylogenetic relationships (B) of VGSC α -subunits.....	23
Figure 1.4: Chromosomal location and arrangement of the 10 paralogous α -subunit human genes encoding the voltage-gated sodium channels.	24
Figure 1.5: Whole-cell sodium current from a patched Na _v 1.1-transfected HEK293T cell upon membrane depolarization	32
Figure 1.6: State-dependent interactions between the gating charge-carrying arginines in the S4 segment and negatively charged residues in neighboring transmembrane segments.....	34
Figure 1.7: Outward rotational sliding movement of S4 upon voltage changes leads to dilation and opening of the pore	35
Figure 1.8: The sodium channel pore, using the KcsA potassium channel α -helical fold (Doyle <i>et al.</i> , 1998) as a model.....	36
Figure 1.9: VGSC inactivation mechanism and structure	37
Figure 1.10: The persistent sodium current	39
Figure 1.11: The modulated receptor model	41
Figure 1.12: VGSC blocker binding and interaction	42
Figure 1.13: The unified loss-of-function hypothesis for Na _v 1.1 genetic epilepsies.	48
Figure 1.14: Mutations in Na _v 1.1 channel patients with epilepsy	50
Figure 1.15: Effects of epilepsy mutations on Na _v 1.1 current amplitude.....	52

Figure 1.16: Na_v1.1 is mainly found in interneurons53

Figure 1.17: VGSC blockade by phenytoin is both voltage- and activity dependent.62

Figure 1.18: The extended modulated receptor stochastic model64

Figure 1.19: Molecular model of sodium channel blocker to VGSC inner pore.....65

Figure 1.20: Structure and conservation of splicing in voltage-gated sodium channels70

Figure 1.21: Position of the *SCN1A* G>A (rs3812718) polymorphism at the intron between exons 5N and 5A.....72

Figure 1.22: Faster recovery from inactivation for Na_v1.1-5N channels.83

Figure 1.23: An overview of dynamic-clamp principles.....86

Figure 2.1: A representative action potential (A) and phase plot (B) used to analyse active properties of transfected neurons.....103

Figure 3.1: Na_v1.1: No difference in macroscopic properties and VD activation/inactivation between isoforms.109

Figure 3.2: Na_v1.1: Channels containing exon 5N recover more rapidly from inactivation after short recovery intervals.....111

Figure 3.3: Recovery from inactivation for isoforms of each channel comparing fits with all parameters free (green lines) and with τ_F and τ_S fixed (red lines)112

Figure 3.4: Na_v1.1: Pilot data indicating that shortening the prepulse duration increases the difference in recovery from inactivation between isoforms.....115

Figure 3.5: Na_v1.1: The neonatal isoform showed significantly more availability after a range of shorter pre-pulses under a brief interpulse gap duration (2ms).....117

Figure 3.6: Estimated channel availability for isoforms of each channel comparing quality of fits with all parameters free (green lines) and with Y_0 and τ fixed (red lines, behind green lines)...118

Figure 3.7: Na_v1.1: The difference in channel availability is also preserved in room temperature120

Figure 3.8: Na_v1.1: inactivation protocols bearing long inactivation pulses obscure any differences between 5A and 5N splice variants121

Figure 3.9: Na_v1.1: Changes in holding voltage eradicate the difference in inactivation recovery between the isoforms123

Figure 3.10: Na_v1.1: Trains of pulses mimicking a “seizure-like burst” retain the difference between the splice variants.126

Figure 3.11: A model of sodium channel gating shows that modification of a single gating step may be sufficient to alter stability of fast inactivation without altering other parameters128

Figure 3.12: The specific change in rates between states 12 and 1 replicates HEK293T cell findings for recovery from inactivation and availability130

Figure 3.13: Slow inactivation probably masks the predicted difference between isoforms on voltage dependence of inactivation recovery131

Figure 3.14: Na_v1.1: Simulation of an interneuronal firing pattern at -80mV does not reveal a difference between 5A and 5N splice variants133

Figure 3.15: Na_v1.1: Simulation of an interneuronal firing pattern at -70mV holding voltsge does not reveal a difference between 5A and 5N splice variants134

Figure 4.1: Na_v1.2: No difference in macroscopic properties and VD activation/inactivation between isoforms.143

Figure 4.2: Na_v1.7: No difference in macroscopic properties and VD activation/inactivation between isoforms.144

Figure 4.3: Na_v1.7: Channels containing exon 5N recover more rapidly from inactivation after short recovery intervals146

Figure 4.4: Recovery from inactivation for Na_v1.7 neonatal and adult isoforms, comparing fits with all parameters free (green lines) and with τ_F and τ_S fixed (red lines)146

Figure 4.5: Na_v1.2: Short recovery intervals at -80mV do not reveal a difference between splice variants as in Na_v1.1 (shown in inset) and Na_v1.7.....149

Figure 4.6: Recovery from inactivation for Na_v1.2 neonatal and adult isoforms, comparing fits with all parameters free (green lines) and with τ_F and τ_S fixed (red lines)149

Figure 4.7: Na_v1.2: The neonatal isoform showed significantly more availability after a range of shorter pre-pulses under a brief interpulse gap duration (2ms)152

Figure 4.8: Na_v1.2: Estimated channel availability for isoforms of each channel comparing quality of fits with all parameters free (green lines) and with Y_0 and τ fixed (red lines, behind green lines)153

Figure 4.9: Na_v1.7: The neonatal isoform showed significantly more availability after a range of shorter pre-pulses under a brief interpulse gap duration (2ms)156

Figure 4.10: Estimated channel availability for Na_v1.7 isoforms of each channel comparing quality of fits with all parameters free (green lines) and with Y_0 and τ fixed (red lines, behind green lines)157

Figure 4.11: Na_v1.2: Trains of pulses mimicking a “seizure-like burst” retain the difference between the splice variants160

Figure 4.12: Na_v1.7: Trains of pulses mimicking a “seizure-like burst” retain the difference between the splice variants161

Figure 5.1: Na_v1.1: Phenytoin and carbamazepine negate the inactivation recovery difference between neonatal and adult isoforms.....167

Figure 5.2: Na_v1.2: Phenytoin and carbamazepine negate the inactivation recovery difference between neonatal and adult isoforms.....168

Figure 5.3: Na_v1.7: Phenytoin and carbamazepine negate the inactivation recovery difference between neonatal and adult isoforms.....169

Figure 6.1: Stimulation conditions for establishing single AP parameters and firing frequency ability of transfected hippocampal neurons174

Figure 6.2: Intrinsic properties of interneurons expressing TTX-resistant splice isoforms of Na_v1.1175

Figure 6.3: Splicing in Na_v1.1 is sufficient to alter spike reliability of interneurons during rapid trains177

Figure 6.4: The increased failure rate in interneurons expressing the adult isoform is correlated with a slowing of the rise time of the action potentials during the series of depolarizing steps .179

Figure 6.5: Intrinsic properties of excitatory neurons transfected with splice isoforms of Na_v1.2181

Figure 6.6: Splicing in Na_v1.2 does not alter spike reliability in excitatory neurons during rapid trains, with neonatal-driven cells showing a non-significant trend to fire more at higher frequencies182

Figure 6.7: Expression of Na_v1.2 in excitatory neurons reveals conserved effect of splicing on rising phase of action potentials during fast trains184

Figure 6.8: Intrinsic properties of excitatory neurons transfected with splice isoforms of Na_v1.1 did not differ between neonatal and adult.....186

Figure 6.9: In excitatory neurons the neonatal isoform of $Na_v1.1$ does not confer greater spike reliability at higher firing frequency compared to the adult as in interneurons187

Figure 6.10: An effect of splicing on rising phase of action potentials during fast trains is also conserved when $Na_v1.1$ channel isoforms are expressed in excitatory neurons.....188

Figure 6.11: Molecular conservation of sodium channel splicing in domain 1. The neonatal exon has been destroyed in multiple mammalian copies of *SCN1A*194

Figure 6.12: The difference in channel availability between isoforms in HEK293T cells is translated to a difference in firing frequency fidelity in interneurons196

Figure 7.1: Dynamic clamp experimental procedure199

Figure 7.2: Calculation of the conductance magnitude used for both excitatory and inhibitory neurons and dynamic clamp experiments to set the magnitude of conductance threshold.201

Figure 7.3: Dynamic clamp experiments demonstrate that splicing in $Na_v1.1$ is sufficient to alter interneuron activity during epileptiform bursts203

Figure 7.4: Dynamic clamp experiments in inhibitory neurons showed two clusters of neuronal response to the same epileptic activity205

Figure 7.5: Dynamic clamp experiments in excitatory neurons demonstrate that splicing in $Na_v1.1$ is sufficient to alter only rising slope during epileptic activity207

Chapter 1: Introduction

1.1 Voltage-gated sodium channel structure and function

1.1.1 Discovery and purification of the sodium channel protein

Voltage-gated sodium channels (VGSCs) are critically important for the initiation and propagation of action potentials in excitable cells. As a consequence they play a central role in regulating neuronal and muscle fibre electrical excitability, enabling the coordination and communication of the body's higher processes.

The sodium channel protein was first discovered more than 30 years ago using neurotoxin-labelling methods (Agnew *et al.*, 1980; Beneski & Catterall, 1980) and was purified from rat brain in the early 1980s by Hartshorne and Catterall (Hartshorne & Catterall, 1981). Purification revealed a heterooligomeric polypeptide complex comprising of an alpha (α) (260kDa) subunit associated with one or two auxiliary beta (β) subunits, in this case β 1 (36kDa) and β 2 (33kDa), which will be discussed in more detail later on. Further studies on purified sodium channels revealed the existence of a functional pore within the channel that allows ion conduction (Talvenheimo *et al.*, 1982), while fusion within a planar lipid bilayer revealed gating in response to voltage changes (Hartshorne *et al.*, 1985; Furman *et. al.*, 1986). In parallel to that, successful cloning of the sodium channel cDNA from the electric organ of the eel *Electrophorus electricus* (Noda *et al.*, 1984) led to the heterologous expression and molecular manipulation of the channel. This, together with the parallel development of patch-clamp techniques, opened the way for more detailed functional and molecular analysis of the sodium channel protein, greatly expanding our knowledge and understanding about sodium channel structure and function.

1.1.2 Na⁺ channel structure: α -subunits

The sodium channel architecture is composed of a ~260kDa α -subunit in association with one or two regulatory β -subunits of 33 – 36kDa. Studies expressing sodium channel subunits in *Xenopus* oocytes (Noda *et al.*, 1986) and mammalian cell lines (West *et al.*, 1992) showed that the α -subunit alone is necessary and sufficient to give rise to a functional channel. The secondary structure of the α -subunit predicts that it is organised into four homologous domains (designated I – IV) connected to each other by cytoplasmic linkers, with each domain consisting of 6 α -helical transmembrane segments (S1 – S6) (Figure 1.1A). Segments 1 to 4 serve as the voltage domain of the channel, with S4 acting as the voltage sensor, while S5 and S6 together with their interconnecting re-entrant linker, called P-loop, form the pore region, which determines the ion selectivity and conductance properties of the channel (Guy & Seetharamulu, 1986). The four domains are folded into a square array within the plasma membrane, with the S5-S6 segments and their interconnecting P-loop located in the centre, forming the ion conducting aqueous pore. Recent studies have shown that the voltage sensing domain (VSD) of one of the four subunits is in closest proximity with the S5 – S6 domain of the next subunit (Namadurai *et al.*, 2015, Figure 1.1B).

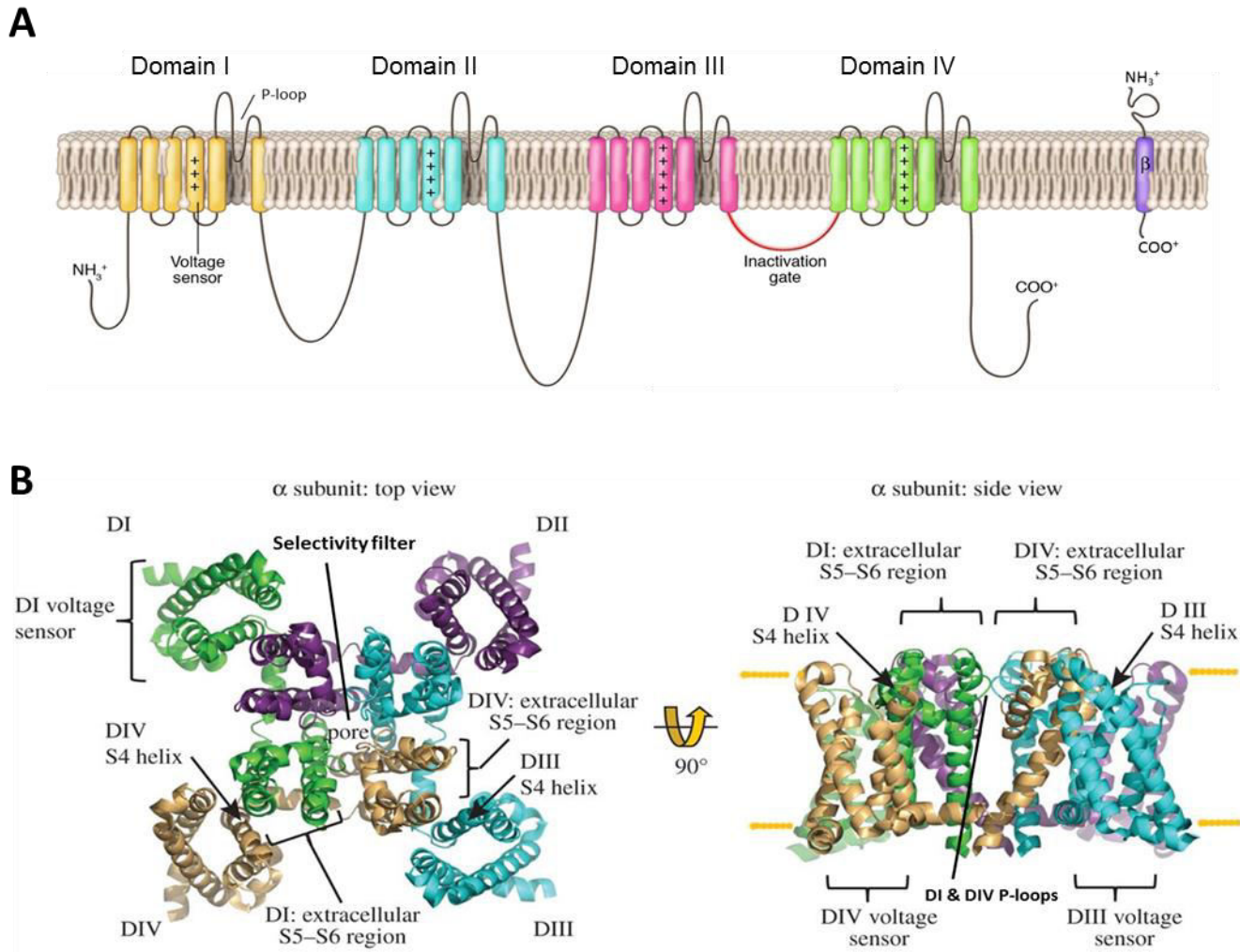


Figure 1.1: Three-dimensional structure of the VGSC

A. Schematic illustration of the Na^+ channel α - and β -subunit structure. The four homologous domains (I–IV) of the α -subunit are illustrated, with cylinders representing transmembrane α -helices ; S5 and S6 of each domain are the pore-lining segments of the channel and S4 acts as the voltage sensor. The β -subunit (violet, right) is a single transmembrane α -helix segment. β -subunits can interact with the α -subunit covalently or non-covalently, depending on the subtype. Figure redrawn from Meisler and Kearney, 2005. **B.** Putative transmembrane folding of the Na_v channel from the bacterium *Arcobacter butzeri* (Na_vAb) α -subunit from top view (left) and side view (right). Two of the four P-loops between S5–S6 lining the pore of the channel at side view are shown . Figure redrawn from Nanmadurai *et al.*, 2015.

The exact tertiary structure of sodium channels is still not fully determined. X-ray crystallography and Nuclear Magnetic Resonance (NMR) analysis of a distally related potassium channel (Doyle *et al.*, 1998) first gave some insight into the crystal structure and especially the pore region. Sato *et al.*, (2001) later used cryo-electron microscopy to create a 19 Å resolution image representation of a sodium channel. A 3D reconstruction based on Sato *et al.* (2001) images revealed a bell-shaped channel with a roughly symmetrical arrangement of the four channel domains around a cross-shaped central pore (Figure 1.2). More recently Payandeh *et al.*, (2011) captured a crystal structure of a bacterial sodium channel (Na_vAb) in the closed configuration, at a resolution limit of 2.7 Å. This work, together with many previous studies relating structure to function in VGSCs, has led to a growing understanding of how different regions of the α-subunit may contribute to the gating, activation, permeation and inactivation of the sodium channel, which will be discussed in more detail later on.

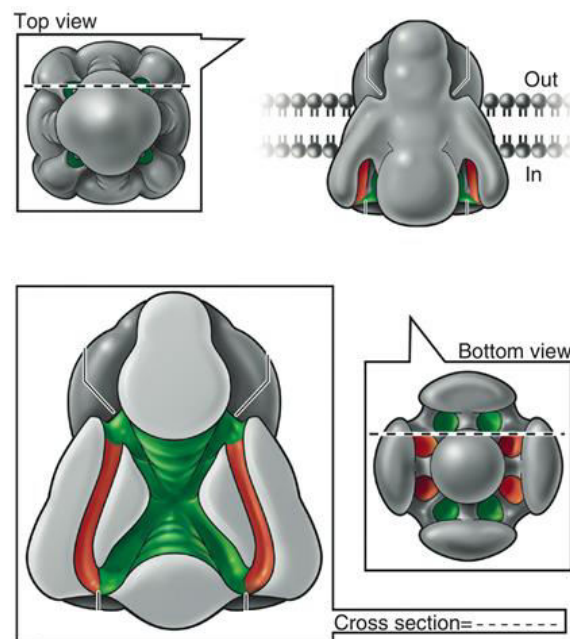


Figure 1.2: Three-dimensional structure of the sodium channel pore

The three-dimensional structure of the Na_v channel α-subunit at 19 Å resolution, compiled from electron micrograph reconstructions. Green color indicates the ion conducting pore and its connections to the intracellular and extracellular medium. Red color indicates gating pores, which will be discussed in more detail later on. Figure redrawn from Catterall, 2010.

1.1.3 Sodium channel α -subunit genes: evolution and chromosomal location

VGSCs are thought to be the last member among voltage-gated ion channels to have evolved, since they are not found in unicellular organisms, contrary to K^+ and Ca^{2+} channels (Marban *et al.*, 1998; Catterall, 2009). Na^+ channels are thought to have arisen from mutations in the primitive Ca^{2+} channel, which in turn evolved by gene duplication of the primordial 2TM K^+ channel, KcsA. KcsA is the prokaryotic potassium ion channel derived from *Streptomyces lividans* bacteria and each of its four identical subunits comprising the functional tetrameric channel is composed of only two transmembrane segments. This is because each subunit lacks the S1-S4 voltage sensing domain that sodium channels contain, instead KcsA is primarily activated by changes in pH (Schrempf *et al.*, 1995) The human genome contains 9 separate sodium channel genes (designated *SCN1A* – *SCN5A* and *SCN8A* – *SCN11A*), giving rise to an equal number of VGSC α -subunits (designated $Na_v1.1$ – $Na_v1.9$) expressed in excitable cells (Goldin *et al.*, 2000). All family members are quite closely related, sharing 50 – 85% amino acid sequence identity (Figure 1.3, Catterall *et al.*, 2005). This also translates to similar (yet not identical) functional properties and drug sensitivities for more closely related channels.

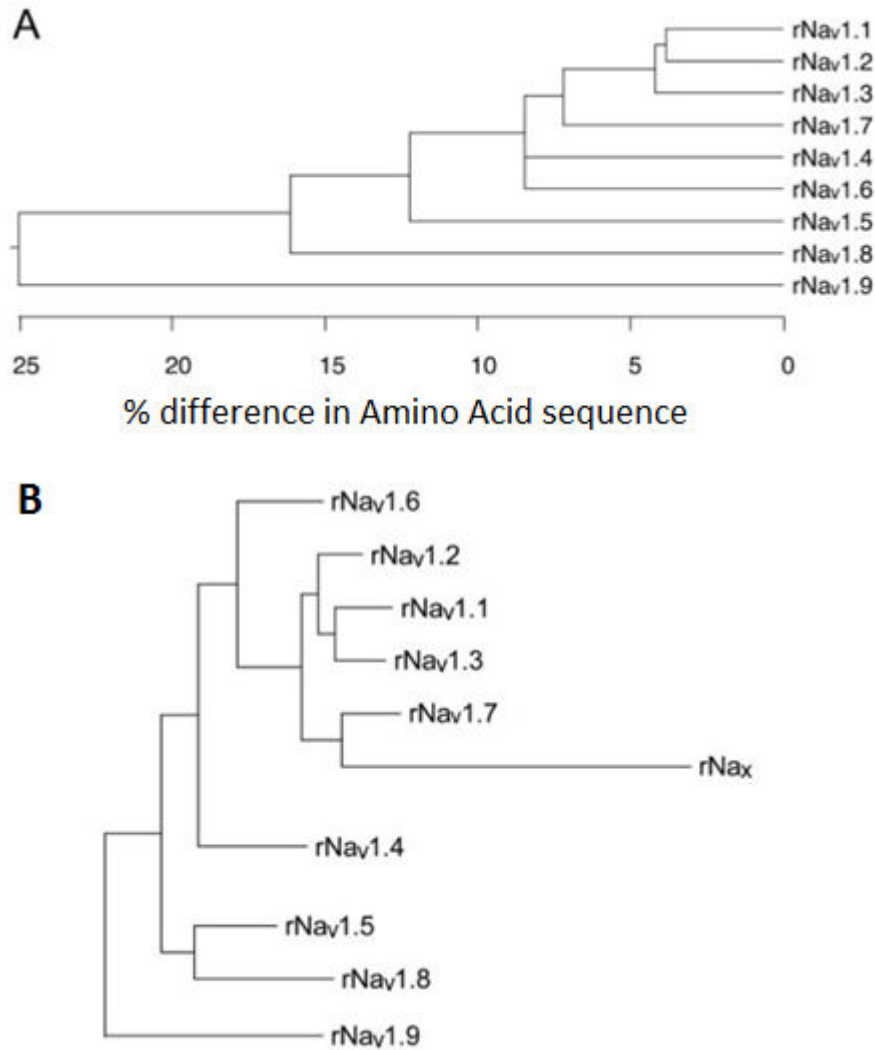


Figure 1.3: Amino acid sequence similarity (A) and phylogenetic relationships (B) of VGSC α -subunits

Analysis was performed by aligning the amino acid sequences for all isoforms. Even for most distantly related channels, the amino acid similarity is $>75\%$. Figure redrawn from Catterall *et al.*, 2005.

Four out of nine genes (*SCN1A*, *SCN2A*, *SCN3A* and *SCN9A*) are clustered in chromosomal position 2q24 in humans, while a second cluster in chromosome 3p21-24 includes *SCN5A*, *SCN10A* and *SCN11A*. *SCN4A* and *SCN8A* are isolated as single genes on chromosomal places 17q23 and 12q13 respectively (Figure 1.4, Meisler *et al.*, 2010).

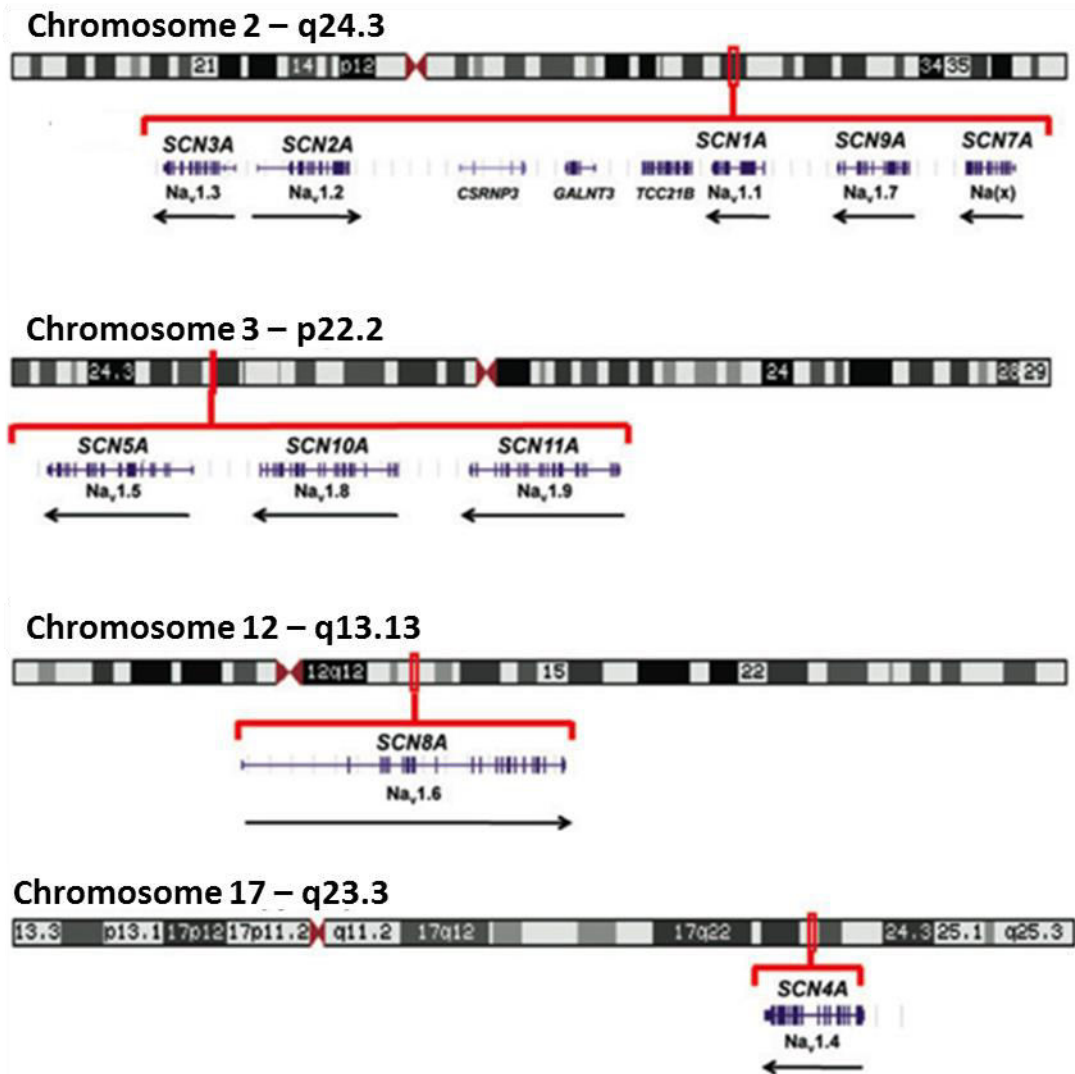


Figure 1.4: Chromosomal location and arrangement of the 10 paralogous α -subunit human genes encoding the voltage-gated sodium channels.

Figure redrawn from Meisler *et al.*, 2010.

1.1.4 β -subunits

β -subunits are not a requirement for sodium channels to be functional, but they are important for modulating the α -subunit's surface expression and biophysical properties. Hence, their expression

alongside with α -subunits is essential for proper channel function in vivo. β -subunits are encoded by four separate genes in mammals, giving rise to four different types (β 1- β 4). The β 1-encoding gene is located on chromosome 19q13, whereas the β 2 and β 4 genes are located next to each other alongside on chromosome 11q22-23, and β 3 is nearby at chromosome 11q24 (Catterall, 2009). β -subunits are expressed in both excitable and non-excitable (astrocytes, radial glia, Schwann cells) tissues within the nervous system and heart (Patino & Isom, 2010). There has also been evidence of expression of β -subunits in cells without the presence of any α -subunits (Patino & Isom, 2010). All four β -subunits are proteins with a single transmembrane-spanning segment containing a small intracellular carboxy-terminal domain and a large extracellular amino-domain (Figure 1.1A, right). The amino-domain is thought to fold in an immunoglobulin-like manner, a typical characteristic of cell adhesion molecules (Isom *et al.*, 1995).

β -subunits can associate with α -subunits in two ways, either non-covalently in the case of β 1 and β 3 subunits, or through disulphide bonds, for β 2 and β 4. One α -subunit can associate with one or more β -subunits, usually one covalently and one non-covalently linked (Catterall *et al.*, 2005; Patino & Isom, 2010).

Co-expression of β -subunits with the α -subunit of the sodium channel has at least two consequences. First of all, they can strongly modulate sodium channel kinetics, as seen in heterologous expression systems, ranging from voltage dependence of activation and inactivation to sodium current density. Isom *et al.*, (1995) reported an increase in current amplitude and membrane capacitance when β 2 was co-expressed with neuronal α -subunits in *Xenopus* oocytes. β -subunits also shifted the voltage dependence of activation and inactivation states towards hyperpolarisation in $\text{Na}_v1.6$ and $\text{Na}_v1.8$ channels stably expressed in a HEK293 cell line, while they also modulated current density (Zhao *et al.*, 2011). Overall, effects of β -subunits on sodium channel function appear to be variable and dependent on both the α - and β -subunit combination, as well as the cell type where the sodium channel is expressed (Savio-Galimberti *et al.*, 2012).

In addition to their role as functional modulators, β -subunits also act as cell adhesion molecules. They can interact with the extracellular matrix and other cell adhesion molecules as well as the cytoskeleton and intracellular regulatory and signalling proteins, like protein kinases and phosphatases (Isom, 2002; Brackenbury & Isom, 2011). Such β -subunit-dependent interactions are thought to mediate cell surface expression and trafficking of VGSCs, affecting both channel density (Isom *et al.*, 1995) as well as appropriate sub-cellular localization (Savio-Galimberti *et al.*,

2012). This can have a significant effect in cell responsiveness and has recently been suggested as a possible mediator affecting nociceptor excitability in vivo (Lopez-Santiago *et al.*, 2011). Apart from these roles, $\beta 2$ and $\beta 4$ intracellular domains have recently been suggested to function as potential transcriptional regulators of the *SCN1A* α -subunit, by translocating into the nucleus and enhancing gene expression (Savio-Galimberti *et al.*, 2012). Finally, there is growing evidence that β -subunits are involved in cellular migration and/or neurite outgrowth, linked also to cancer cell growth and metastasis (Eijkelkamp *et al.*, 2012).

The physiological importance of β -subunits becomes evident when looking at the effects of mutations in β -subunit genes in animals and humans or in knockout animal models. Heterozygous mutations in $\beta 1$ have been discovered in families with Generalized Epilepsy with Febrile Seizures plus (GEFS+), an epilepsy syndrome with usually an early life onset (Scheffer *et al.*, 2007). Also, mutations in $\beta 3$ and $\beta 4$ -subunits leading to reduced peak sodium current in $\text{Na}_v1.5$ have been linked to Sudden Infant Death Syndrome (SIDS) (Tan *et al.* 2010). Furthermore, whole $\beta 1$ and $\beta 2$ gene deletions in knockout experiments in mice reveal impairments in the myelination process and axonal conduction (Chen *et al.*, 2004), while they have also been linked to epileptic seizures, heart conditions, pain and premature death (Catterall, 2009; Patino & Isom, 2010). For an overview of mutant β -subunit-associated conditions, see table 1.1 (from Savio-Galimberti *et al.*, 2012).

Gene	Chromosome	β subunit	α subunit	Expression	Neurological Disease
<i>SCN1B</i>	19q13.1	$\beta 1$	Na _v 1.1–Na _v 1.7	Central and peripheral neurons, glia, skeletal, and cardiac muscles.	Seizures and epileptic syndromes: febrile seizures, Dravet syndrome, temporal lobe epilepsy
<i>SCN2B</i>	11q23	$\beta 2$	Na _v 1.1, Na _v 1.2, Na _v 1.5–Na _v 1.7	Central and Peripheral neurons, glia, cardiac muscle.	Traumatic nerve injury Multiple sclerosis, Neuropathic pain (post-trauma) Inflammatory pain, traumatic nerve injury
<i>SCN3B</i>	11q23.3	$\beta 3$	Na _v 1.1–Na _v 1.3, Na _v 1.5	Central and peripheral neurons, adrenal gland, kidney	Temporal epilepsy,
<i>SCN4B</i>	11q23.3	$\beta 4$	Na _v 1.1, Na 1.2, Na _v 1.5	Central and peripheral neurons, glia, skeletal and cardiac muscles.	Traumatic nerve injury Huntington's disease

Table 1.1: Na_v β -subunits

Summary of the different types of β -subunits associated with the different VGSC, and the related channelopathies associated with the mutations in the genes that encode them (modified from Patino and Isom, 2010).

1.1.5a Sodium channels subtypes have been appropriated to different locations and functions in neurons.

The various α -subunits have distinct regional, developmental and sub-cellular expression patterns that differ from each other, as well as between species. This expression is a highly dynamic process, depending on age, activity and pathophysiology. Because of the importance of sodium channels, many studies using antibody staining, RNA detection or a combination of these approaches have sought to clarify the distribution of different subtypes. Distinct expression and localization patterns suggest that different α -subunit channel subtypes play specialized roles in body physiology.

Na_v1.1, Na_v1.2, Na_v1.3 and Na_v1.6 are the prevalent α -subunits expressed in adult brain neurons in humans (Catterall, 2000; Goldin *et al.*, 2000; Goldin, 2001; Trimmer & Rhodes, 2004). Na_v1.1 and Na_v1.3 are primarily localized in neuronal somata, where they are believed to control neuronal excitability by setting the threshold for Action Potential (AP) generation in the axon initial segment (AIS) and further axonal propagation (Westenbroek *et al.*, 1989; 1992; Catterall, 2009). Na_v1.1 in particular is suggested to be preferentially expressed in the proximal part of the AIS of GABAergic interneurons, since it plays a predominant role in the excitability of fast-spiking parvalbumin-positive interneurons in the CNS (Yu *et al.*, 2006; Ogiwara *et al.*, 2007) and is also suggested to be expressed, at lower levels, in somatostatin-positive interneurons (Li *et al.*, 2014). In contrast, while highly conserved at the amino acid level, Na_v1.2 is primarily expressed in excitatory neurons, in unmyelinated or premyelinated fibres, usually early in development, before being replaced by Na_v1.6 in mature Nodes of Ranvier in myelinated axons and dendrites (Caldwell *et al.*, 2000; Jenkins & Bennett, 2001; Catterall *et al.*, 2010, Oliva *et al.*, 2012). Na_v1.6 channels are also found on the axon initial segment as well as on dendrites of projection neurons (Mantegazza *et al.*, 2010), while a recent study has also reported their presence at the distal part of the AIS in interneurons (Li *et al.*, 2014). Na_v1.2 and Na_v1.6 also show strong expression in the granule cells of the dentate gyrus as well as the hippocampal pyramidal cell layer, whereas the expression of Na_v1.1 and Na_v1.3 in these areas is moderate to low. On the contrary, all of these subtypes seem to be expressed in the cerebellar granular layer and in the cortical layers III, IV and VI, in comparison to layers I and II, which show low expression (Wood & Baker, 2001). Na_v1.3 brain levels are quite high in rodents during embryonic life and drop sharply soon after birth, with Na_v1.2 and Na_v1.6 taking over (Gordon *et al.*, 1987; Beckh *et al.*, 1989; Gazina *et al.*, 2010). In humans, expression of Na_v1.3 remains comparatively high in the adult brain (Chen *et al.*, 2000; Mantegazza *et al.*, 2010).

The rest of the neuronal sodium channels are Na_v1.7, Na_v1.8 and Na_v1.9, which are predominantly expressed in the peripheral nervous system (Ogata & Ohishi, 2002; Savio-Galimberti *et al.*, 2012). All three of these channels are suggested to play a key role in nociception. Na_v1.7 is localized mainly in sensory neuron axons, mediating AP initiation and propagation (Catterall, 2009; Black *et al.*, 2012). It is largely found in the PNS, and is particularly important for subthreshold signaling and nociception in small diameter neurons, which are anatomically distinct from the CNS neurons (Cox *et al.*, 2006; Yang *et al.*, 2004). Immunohistochemical analysis in rat DRG neurons showed a

wide $\text{Na}_v1.7$ expression, extending from the cell's soma to peripheral C-fibers in the skin and central dorsal horn up to the presynaptic terminal (Black *et al.*, 2012).

$\text{Na}_v1.8$ is thought to be the major contributor of nociceptor excitability especially at lower temperatures, since its kinetics appear to be cold-resistant (Zimmermann *et al.*, 2007). $\text{Na}_v1.9$, which was the last VGSC subtype to have been discovered (Dib-Hajj *et al.*, 2003), is also found in peripheral sensory neuron afferents. $\text{Na}_v1.9$ has much slower kinetic properties compared to $\text{Na}_v1.7$ and $\text{Na}_v1.8$, but it is activated near resting membrane potentials ($\sim -60\text{mV}$). As a result, $\text{Na}_v1.9$ acts more as a modulator of nociceptor membrane excitability rather than as a generator of APs in peripheral sensory neurons.

$\text{Na}_v1.4$ and $\text{Na}_v1.5$ are known as the non-neuronal VGSCs. $\text{Na}_v1.4$ is the primary VGSC in skeletal muscle, mediating myocyte excitability and muscle contraction. $\text{Na}_v1.5$ is the main sodium channel found in the heart. Reports have also suggested that $\text{Na}_v1.5$ is also transiently expressed in developing skeletal muscle, before being replaced by $\text{Na}_v1.4$ in later development (Catterall, 2009).

A tenth sodium channel subtype exists, Na_vx (Figure 1.3B), which is evolutionarily more distant from the VGSCs discussed so far. The *SCN7A* gene, which encodes Na_vx , is located in the cluster with *SCN1A*, *SCN2A*, *SCN3A* and *SCN9A* on the human chromosome 2. It has a widespread expression in many organs like the circumventricular organs of the brain, the heart, the uterus, the dorsal root ganglia and skeletal muscle (Savio-Galimberti *et al.*, 2012). Yet, Na_vx is not thought to work as a VGSC in the same way as the other Na_vs . Mouse knockout experiments have indicated that Na_vx may work as part of a mechanism sensing extracellular sodium levels in the brain and controlling the ionic balance (Hiyama *et al.*, 2002; Noda, 2006). For a summary of main temporal and spatial expression sites of the different sodium channel subtypes, see table 1.2.

For the purpose of this study, we focused on 3 distinct sodium channel subtypes, $\text{Na}_v1.1$, $\text{Na}_v1.2$ and $\text{Na}_v1.7$. All three channel subtypes share a conserved splicing event giving rise to two different splice isoforms, which are going to be compared in terms of their biophysical and functional properties, but are expressed in distinct types of neurons, thereby mediating different kinds of neuronal activity. Also, in terms of *both* the physiology of the neurons, and the macroscopic kinetics of gating, $\text{Na}_v1.7$ channels are more distant from the two channels in the CNS (Dib-Hajj *et al.*, 2013). Therefore, as part of this study it will be examined whether potential functional differences between splice isoforms are conserved among the three sodium channel

subtypes, despite their different macroscopic properties and areas of expression (described in detail in Chapters 6 & 7).

<u>Gene</u>	<u>Chromosome</u>	<u>Channel</u>	<u>Function</u>	<u>TTX sensitivity</u>	<u>Splicing at S3-S4?</u>
<i>SCN1A</i>	2q24.3	Na _v 1.1	inhibitory CNS	S	Yes
<i>SCN2A</i>	2q24.3	Na _v 1.2	excitatory CNS (early in development)	S	Yes
<i>SCN3A</i>	2q24.3	Na _v 1.3	excitatory/inhibitory CNS (embryonic)	S	Yes
<i>SCN4A</i>	17q23.3	Na _v 1.4	non-neuronal - skeletal muscle	S	No
<i>SCN5A</i>	3p22.2	Na _v 1.5	non-neuronal - cardiac myocytes	R	Yes
<i>SCN8A</i>	12q13.13	Na _v 1.6	excitatory CNS (later in development)	S	Yes
<i>SCN9A</i>	2q24.3	Na _v 1.7	fast PNS	S	Yes
<i>SCN10A</i>	3p22.2	Na _v 1.8	slow PNS	R	No
<i>SCN11A</i>	3p22.2	Na _v 1.9	slow PNS	R	No
<i>SCN7A</i>	2q24.3	Na(x)	salt-sensing	Unknown	unknown

Table 1.2: Na_v α-subunits

Summary of the different voltage-gated sodium channel α-subunit subtypes and general area of function. For tetrodotoxin (TTX) sensitivity, channels are separated to (S)ensitive and (R)esistant. Out of 10 sodium channel genes, 6 of them show a conserved splicing event at the S3-S4 linker of Domain I.

1.1.5b Non-canonical distribution of sodium channels

Lower levels of expression of some sodium channel subtypes in tissues beyond their major expression sites have also been detected. For example, transient expression of Na_v1.5 has been seen in some brain areas (Wang *et al.*, 2009), while the same has also been suggested for neuronal sodium channels, especially Na_v1.1, in the heart (Dar Malhotra *et al.*, 2001; Maier *et al.*, 2003). VGSC expression has also been detected in glial cells, despite the fact that glial cells are not thought to normally fire APs. Yet, AP-like events mediated by VGSCs have been reported in astrocytes and glial precursor cells in the past (Sontheimer *et al.*, 1996; Mantegazza, 2010). Moreover, an upregulation of Na-mediated currents in astrocytes has been detected in human tissues taken from epileptic patients, potentially linking Na-mediated glial defects to seizure spread (Steinhauser & Seifert, 2002). The exact roles of VGSC expression in glia are not yet fully understood. They have been suggested to involve regulation of cytoplasmic Na homeostasis (Sontheimer *et al.*, 1996) and phagocytosis (Black *et al.*, 2009). β -subunits also appear to have a regional and temporal spectrum of expression. For example, a splice variant of β 1 named β 1-A is highly expressed during embryonic development, with its levels falling sharply after birth while being replaced by β 1 (Wood & Baker, 2001). β 1 levels during early development are quite low, in contrast to β 2, which is expressed at high levels continuously from development to adulthood (Isom *et al.*, 1994). Furthermore, β 2 expression is only limited to neurons (Isom *et al.*, 1995), while β 1 is both expressed in neurons and muscle cells (Isom *et al.*, 1992).

1.1.6 Molecular properties of VGSCs underlying function: Overview

At resting membrane potentials (-65 to -75mV) sodium channels remain in a closed conformation in quiescent cells. Upon membrane depolarization above threshold levels, VGSCs are activated, that is to say, they shift into an open conformation within microseconds allowing Na⁺ ions to rush down their concentration gradient from the extracellular side to the cell interior. Concomitant Na⁺ flux through thousands of VGSCs gives rise to the classical transient macroscopic Na⁺ current traces seen in whole-cell patch clamp experiments (Figure 1.5). This inward Na⁺ current accounts

for the depolarizing phase of the AP in most excitable cells. Within 1 to 2 milliseconds after opening, sodium channels convert into a non-conducting, inactivated state so that Na^+ influx is ceased, irrespectively of prolonged depolarization.

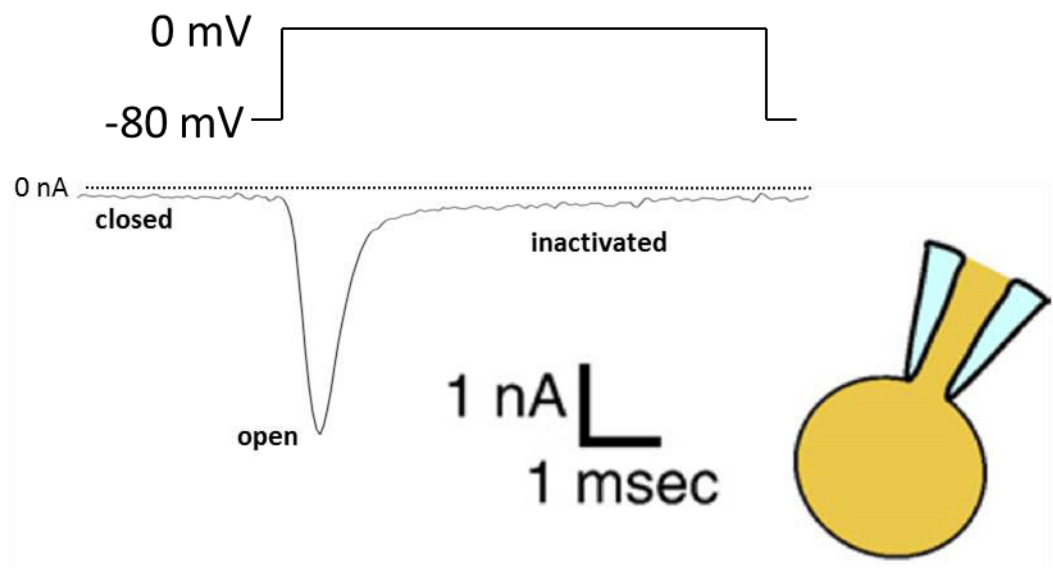


Figure 1.5: Whole-cell sodium current from a patched $\text{Na}_v1.1$ -transfected HEK293T cell upon membrane depolarization

Upon depolarization from -80mV to 0mV, voltage-gated sodium channels are passing from closed to open and then to inactivated state.

1.1.7 Voltage Dependence of activation and gating

The molecular mechanism that is suggested to lead to the opening of VGSCs upon depolarization is the movement of the S4 segments of the four domains of the channel, which act as voltage sensors for activation. Each S4 segment contains a repeated motif of positively charged amino acids (either an Arginine (R) or Lysine (K)) followed by two hydrophobic residues, creating a

transmembrane α -helix with positive charges pointing outwards (Figure 1.6A). The movement of the S4 segment creates a measurable electronic charge, known as the gating charge or gating current, which can be measured experimentally (Hodgkin & Huxley, 1952). At resting states the positively charged residues are in close proximity and interact with negatively charged amino acids mainly from segments 2 and 3 forming ion pairs. In this configuration, the negative resting membrane potential pulls the gating charge inwards, keeping the channel locked into a closed state (Figure 1.6, Resting). Upon depolarization, the change in the polarity of the membrane's electric field relieves the electrostatic force, so that the S4 segment is now moved outwards in a rotational manner, through a narrow gating pore, leading to opening of the channel since the gating charges are forming new pair partners with different negatively charged and polar residues than before at a more extracellular cluster, mainly from S1 and S2 segments (Miceli *et al.*, 2015; Figure 1.6, Activated). The movement detected by Miceli *et al.*, (2015) creates a conformational change of the S4 segment of 5 - 8Å relative to the membrane, and is consistent with electrophysiological measurements of the gating current, through small changes in charge movement across the S4 segment in response to voltage steps when pores are blocked. (Armstrong, 1974; Schneider, 1973; Ragsdale 1998). The S4 helix is suggested to slide through a narrow channel formed by segments 1, 2 and 3 while simultaneously rotating $\sim 30^\circ$ (Yarov-Yarovoy *et al.*, 2012), pulling the S4-S5 linker, (Catterall, 2010; Savio-Galimberti 2012) and consequently dilating the central pore of the channel by pivoting at its base (Payandeh *et al.*, 2011) (Figure 1.7). This mechanism was initially characterized as the “sliding helix” (Catterall, 1986) or “helical screw” model (Guy & Seetharamulu, 1986).

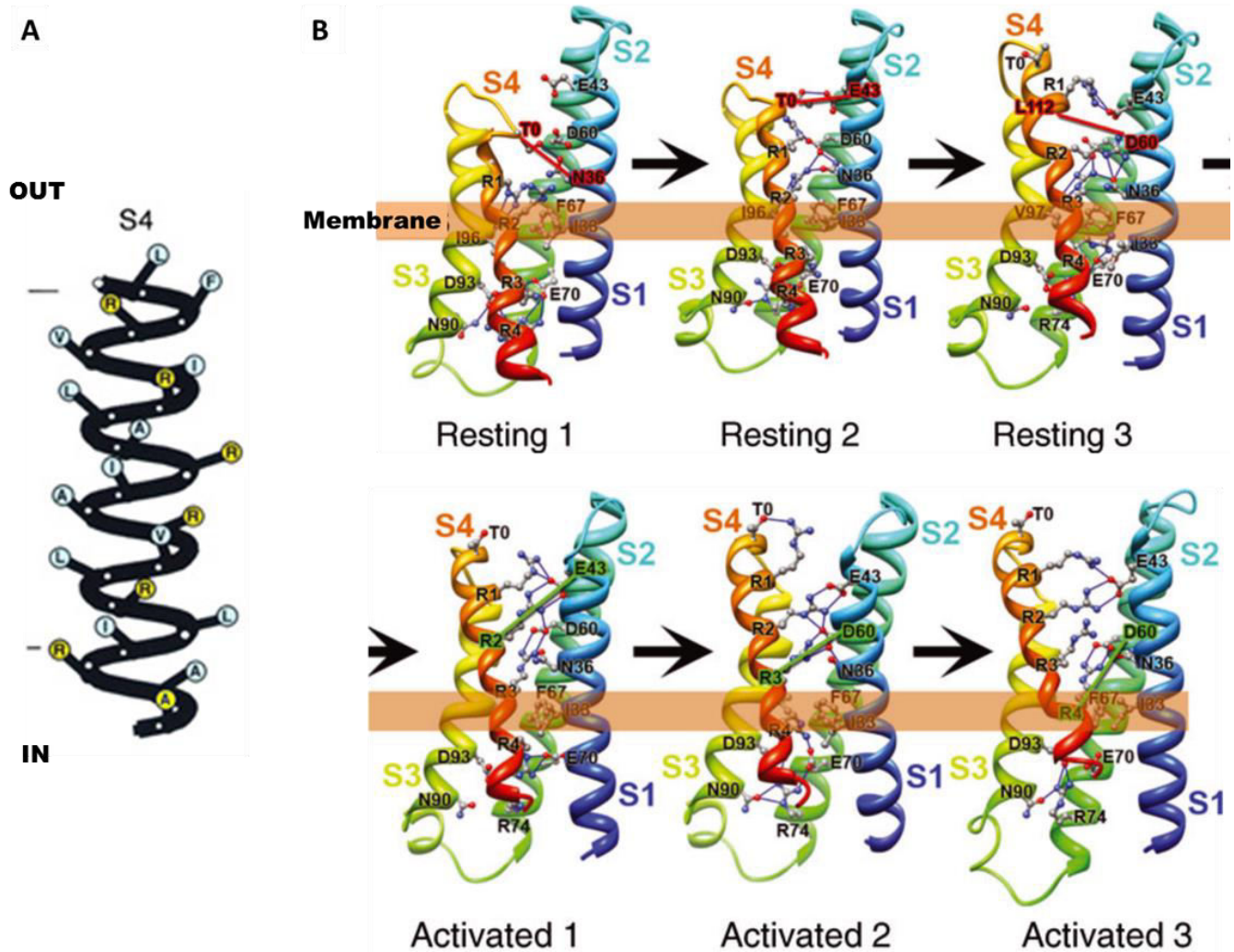


Figure 1.6: State-dependent interactions between the gating charge-carrying arginines in the S4 segment and negatively charged residues in neighboring transmembrane segments

A. amino acid orientation on the S4 segments of the sodium channel. Hydrophobic residues (in white) are flanked by positively charged arginine residues (in yellow) in every third position pointing outwards. Figure modified from Catterall, 2010. **B.** schematic representation of the gating model illustrating the rotational movement of the S4 segments through narrow channels in each domain of the sodium channel protein from resting to activation stages. A single (one of the four) Domain is illustrated here for clarity. The positively charged arginine residues (in blue) are stabilized by interacting with negatively charged and polar residues from the S1, S2 and S3 segments to keep the sensor locked at resting position. Upon depolarization, the S4 segment slides outward in a rotational way, transporting the gating charges from an inner aqueous vestibule to an extracellular aqueous vestibule, shifting the positively charged residues in more outward positions, yet still neutralized by interactions with negative residues in the upper transmembrane part of the protein. Figure redrawn from Catterall, 2012).

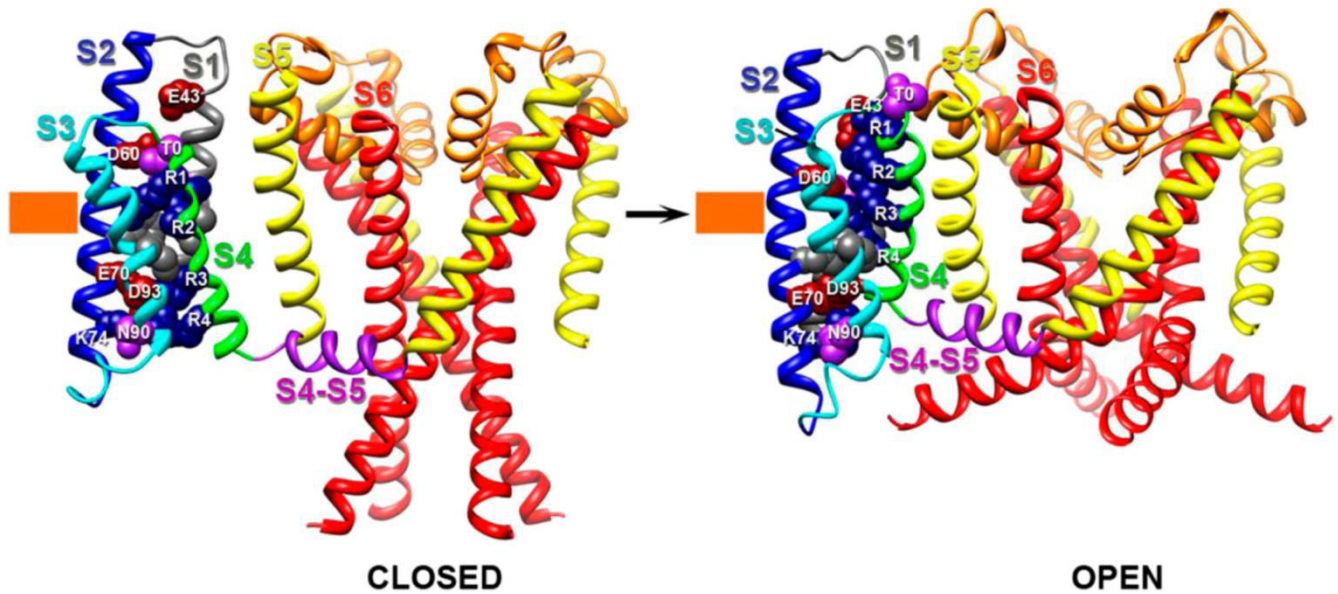


Figure 1.7: Outward rotational sliding movement of S4 upon voltage changes leads to dilation and opening of the pore

Cylinder representation model of the open and closed states for the bacterial sodium channel NaChBac upon voltage changes. Only one of the four voltage-sensing domains (S1 – S4) is shown here attached to the pore forming tetramer (S5 – S6) for clarity. R1 and R4 arginines on the S4 segment (in blue), negatively charged (in red), polar (in purple) and hydrophobic residues (in grey) on S1, S2 and S3 segments are represented as spheres. The S4 segment is tilted with respect to the S4-S5 linker from $\sim 100^\circ$ to $\sim 60^\circ$ as the pore passes from closed to open state. Figure taken from Yarov-Yorovoy *et al.*, 2012.

1.1.8 Ion selectivity

The central pore of the VGSC is lined by the four re-entrant S5-S6 linkers (P-loops), which come together at the centre to form the narrowest part of the channel. Different residues in each of these 4 loops come together to form an inner (DEKA) and outer (EEDD) ring within the folded channel. This confers an ion selectivity filter that makes the channel Na^+ -permeable upon activation (Figure 1.8, from Catterall 2000). Changing of the inner ring residues into all glutamates (EEEE) in

mutagenesis experiments can shift the ion selectivity to Ca^{2+} (Heinemann *et al.*, 1992; Ragsdale 1998). This indicates that the pore loops are the major determinants of ion selectivity in VGSCs.

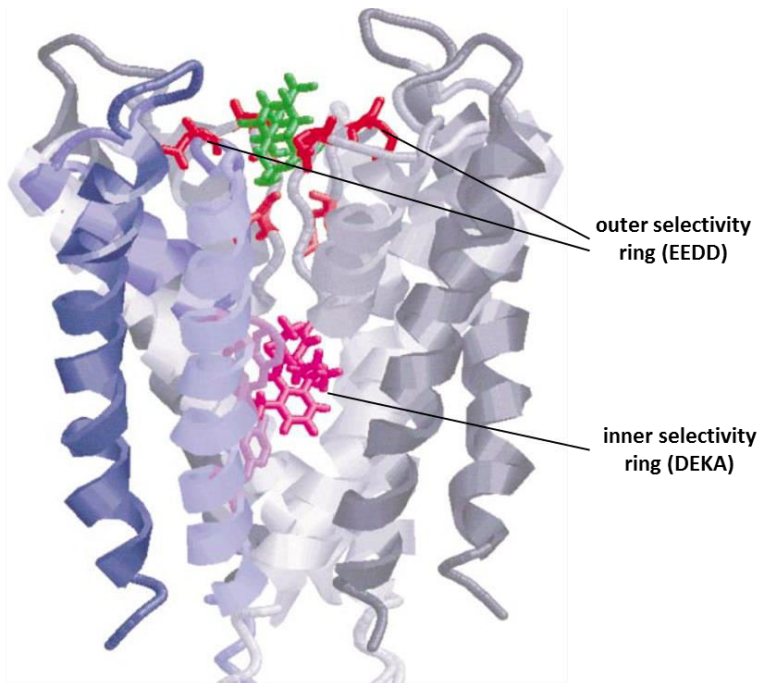


Figure 1.8: The sodium channel pore, using the KcsA potassium channel α -helical fold (Doyle *et al.*, 1998) as a model

Light gray or blue represent S5, while darker gray or blue S6 (M1 and M2 respectively in KcsA). Residues forming the outer ring of the selectivity filter (EEDD) are superimposed on the KcsA structure. Residues forming the inner selectivity ring (DEKA) are shown in red. Figure redrawn from Catterall, 2000.

1.1.9 Inactivation

The change in conformation of the VGSC from an open state to a non-conducting state within only 1-2 milliseconds from activation and upon maintained depolarization is known as inactivation. Inactivation is different from the closed and resting configuration of the channel. The classic, “fast” inactivation process involves the physical occlusion of the cytoplasmic end of the gating pore by the intracellular linker between domains III and IV. The main inactivation particle consists

of four consecutive amino acids, isoleucine, phenylalanine, methionine and threonine (IFMT) (Goldin, 2003; Savio-Galimberti *et al.*, 2012). This particle is suggested to block the channel pore in a “hinged-lid” or “ball-and-chain” mechanism (Figure 1.9). The inactivation gate receptor is thought to be partly formed by the S4-S5 cytoplasmic linker of domains III and IV (McPhee *et al.*, 1996; Marban *et al.*, 1998; Catterall, 2009) as well as the intracellular end of segment S6 in domain IV. More recent studies have also involved the C-terminus of the channel as part of the docking site as well (Mantegazza *et al.*, 2001; Motoike *et al.*, 2004).

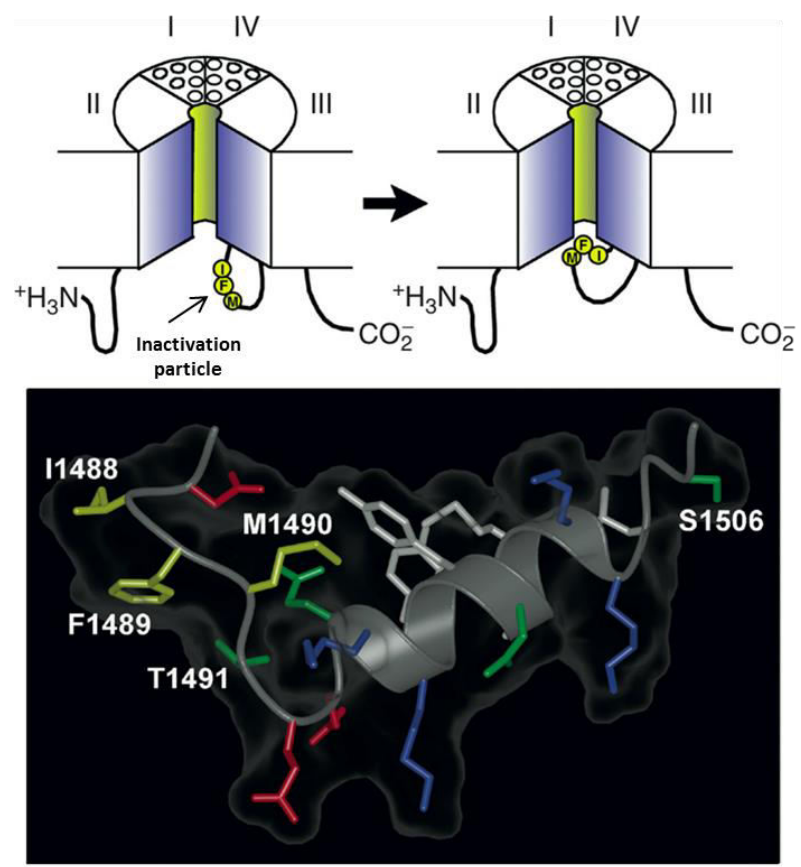


Figure 1.9: VGSC inactivation mechanism and structure

(Top) The hinged-lid mechanism of sodium channel fast inactivation. The IFM motif on the DIII – DIV intracellular loop of the channel is suggested to form a hinged lid, with the phenylalanine residue (F1489) physically occluding the mouth of the pore during inactivation. (Bottom) 3D structure of the inactivation gate by multidimensional NMR. The IFM motif is illustrated in yellow. Threonine 1491, which is also involved in inactivation and serine 1506, a major phosphorylation site, that can also be modulated by protein kinase C are also shown. Figure redrawn from Catterall, 2009.

Fast inactivation determines the refractoriness of the cell, setting a limit to how rapid repetitive firing it can sustain upon prolonged depolarization. Originally, Hodgkin & Huxley (1952) had characterized activation and inactivation as two independent processes. Following studies have suggested that the two processes are coupled, since inactivation derives its voltage dependence from the transmembrane movements of the four S4 voltage sensors, which also drive the activation process (Armstrong, 1981). Therefore, inactivation is suggested to be highly dependent on activation (Rudy & Silva, 2006). Recent studies have implicated the S4 segment of domain IV to play a principal role in this process (Capes *et al.*, 2013). The outward movement of the S4 segment of domain IV, which is intrinsically slower compared to the other three S4 segments (Bosmans *et al.*, 2008), is suggested to signal the starting of the fast inactivation process.

In contrast to fast inactivation, *slow* inactivation is a distinct process that does not involve the DIII – DIV intracellular IFMT linker. Slow inactivation involves conformational rearrangements of the channel pore, which restrict ion flow (Struyk & Cannon, 2002). Slow inactivation develops after prolonged depolarization or high frequency repetitive firing. Currents that are slowly inactivating take seconds to shut down (Ptak *et al.*, 2005). The exact mechanism and structural rearrangements through which slow inactivation occurs are not fully understood, yet they are thought to be independent of those driving fast inactivation.

1.1.10 Persistent current

A non-inactivating, “persistent” sodium current (INa_p) is a typical characteristic in many electrophysiological recordings from mammalian neurons. INa_p appears as “an intrinsic component of transient sodium currents” (Bean, 2007) (Figure 1.10). Its origin and mode of action are still not very well understood by electrophysiologists. The general notion is that it is derived from incomplete or defective fast inactivation. Taddese and Bean (2002) have described INa_p as a consequence of loose binding of the inactivation particle in partially activated channels, so that partial activation might play as much of a role as incomplete inactivation. INa_p accounts for 1 – 3% of the transient sodium current (Magistretti *et al.*, 1999; Mantegazza *et al.*, 2010). Nevertheless, INa_p has effects on neuronal function since it is suggested to have more

hyperpolarized voltage dependence of activation than the associated transient sodium current. For example, Taddese and Bean (2002) found that the I_{Na_p} of isolated tuberomammillary neurons had an activation midpoint of -55 mV, which was considerably hyperpolarized compared to that of the transient current (-28 mV). This allows the I_{Na_p} to operate as a modulator of neuronal subthreshold activity and fine-tune electrical excitability. Subthreshold persistent currents have been involved in facilitating repetitive firing (Mantegazza *et al.*, 2010), driving oscillations and spontaneous rhythmic firing in pacemaker neurons (Taddese & Bean, 2002). Conditions that affect I_{Na_p} magnitude and/or kinetics can therefore lead to pathophysiological conditions, as seen in neurological disorders. Even a small increase in I_{Na_p} (1 – 2%) is sufficient to increase spiking frequency (Kuo *et al.*, 2006) and to promote neuronal hyperexcitability, promoting setting a very favorable background for abnormal synchronous firing and, possibly, epileptogenesis (Scharfman, 2007). Mutations in the *SCN1A*, *SCN2A* and *SCN3A* genes associated with epilepsy can lead to an increase in I_{Na_p} amplitude (Meisler & Kearney, 2005). *SCN8A* mutations in mice affecting I_{Na_p} can also alter proper neuronal firing, leading to ataxia (Meisler *et al.*, 2002; 2004).

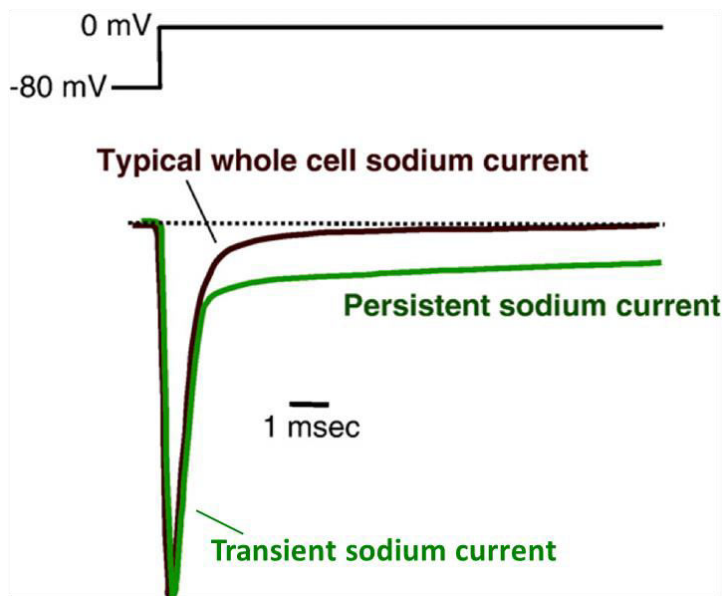


Figure 1.10: The persistent sodium current

Superimposition of a large persistent sodium current component (green trace) on top of a typical transient whole cell sodium current (black trace). Figure redrawn from Ragsdale, 2008.

Studying the persistent current properties in more depth is still a challenge for neuroscientists, since there is no known drug that can pharmacologically distinguish it from transient currents. As a result, INa_p cannot be studied in isolation. In addition, INa_p can vary considerably in different heterologous expression system studies, depending on the cell type and recording conditions. Its amplitude can be largely affected by temperature, G-protein activity and the major ion of the intracellular solution used (Fletcher *et al.*, 2011).

1.1.11 VGSC Pharmacology

Given the integral role that VGSCs play in excitable cell physiology as well as pathophysiological conditions, ranging from cardiac arrhythmias and neuropathic pain to muscle myotonia and epilepsy, it is not surprising that VGSCs have been the subject of extensive pharmacological study. Neurotoxin pore blockers like tetrodotoxin (TTX), interacting with P-loop residues at the extracellular side of the channel, have contributed to the greater understanding of VGSC structure and function. Among sodium channel subtypes, $Na_v1.1$, $Na_v1.2$, $Na_v1.3$, $Na_v1.4$, $Na_v1.6$ and $Na_v1.7$ are considered to be sensitive to TTX, i.e. they can be blocked by TTX in nanomolar concentrations, while $Na_v1.5$, $Na_v1.8$ and $Na_v1.9$ are TTX-resistant. (For a summary of TTX sensitivity of sodium channels, see table 1.2). TTX completely blocks Na^+ conductance of sensitive channels, and consequently is not therapeutically useful (as complete blockade of Na^+ current conductance in vivo would be lethal).

The mode of action of therapeutically used sodium channel blockers, such as local anesthetics, antiarrhythmics and antiepileptic drugs (AEDs), is through use-dependent inhibition. Such sodium channel blockers bind most efficiently when the channel is in an open or inactivated state. They are thought to have very little or no effect at rest when the channel is closed. Increased efficiency of drug action when the channel is open is probably a result of more efficient access to the binding site in the open/inactivated state. Thus, the drug will bind upon AP firing and dissociate after repolarization, relieving the channel from blockade (Figure 1.11). Yet, upon repetitive, high-frequency firing, as it occurs in many neurological pathological conditions, the association rate of the drug to its target surmounts the rate of dissociation. This creates a cumulative blocking effect

and consequently increases the steady-state channel block. Therefore, frequency-dependent blockers will only inhibit VGSCs in high activity areas, leaving normally active channels minimally affected. The optimal frequency at which drug blockade is strongest is determined by the pharmacokinetic properties of each compound, which will be different from drug to drug.

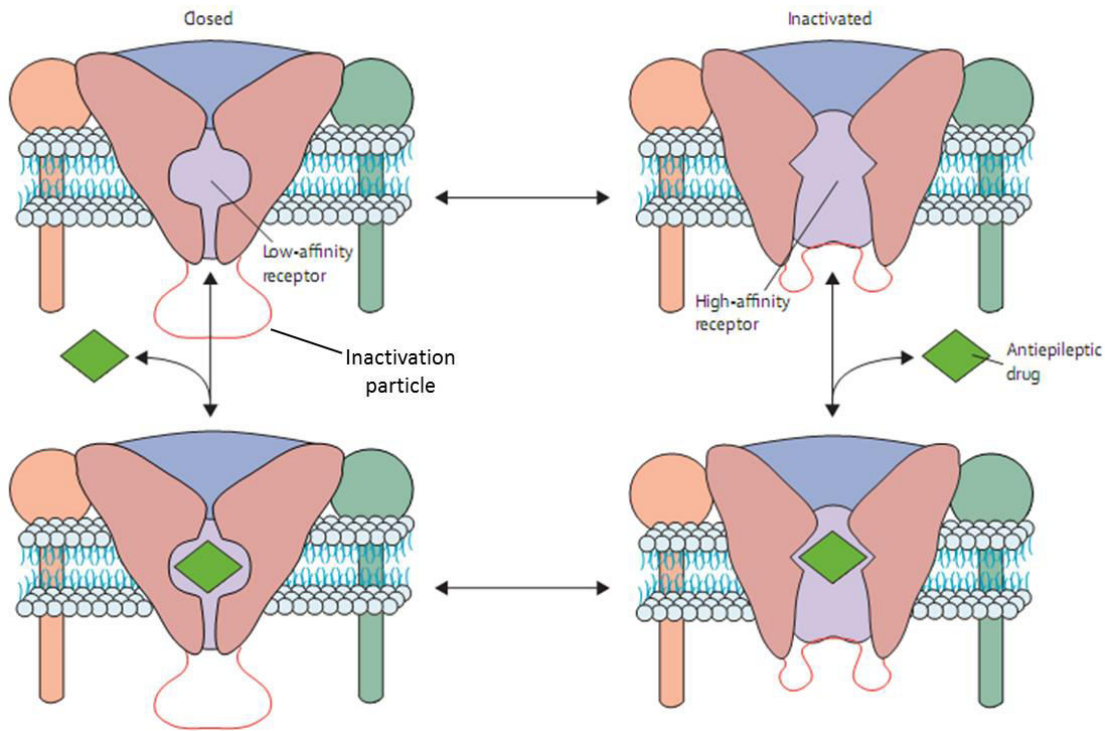


Figure 1.11: The modulated receptor model

Voltage-dependent or frequency-dependent inhibition of VGSCs by sodium channel blockers, such as many common AEDs (green diamond) are explained by the modulated receptor model. According to this model, the inactivated channel has a higher affinity for the drug to bind than the resting channel state. Figure redrawn from Mantegazza *et al.*, 2010.

Separate classes of sodium channel blockers are used in different pathophysiological conditions, depending on the nature of the condition and how it affects normal channel physiology. Local anesthetics, antiarrhythmics and AEDs all have slightly different binding sites, yet they share an

overlapping site of action located on a specific receptor pocket site. This pocket is formed by residues in the intracellular surface of the S6 segments of domains I, III and IV (Ragsdale *et al.*, 1994; 1996; Catterall, 2000; Catterall, 2009) (Figure 1.12A). The interaction of sodium channel blockers with specific amino acid residues at this site occludes the channel pore, hence impeding Na^+ conduction (Figure 1.12B). Of primary importance in determining the binding of such blockers is the electrostatic interaction between charged local anaesthetics and pi electrons of the aromatic ring of the Phe1579 residue, known as cation-pi interaction (Ahern *et al.*, 2008). This electrostatic attraction facilitates the interaction between the local anaesthetic and the sodium channel pore, thereby contributing to tonic channel inhibition.

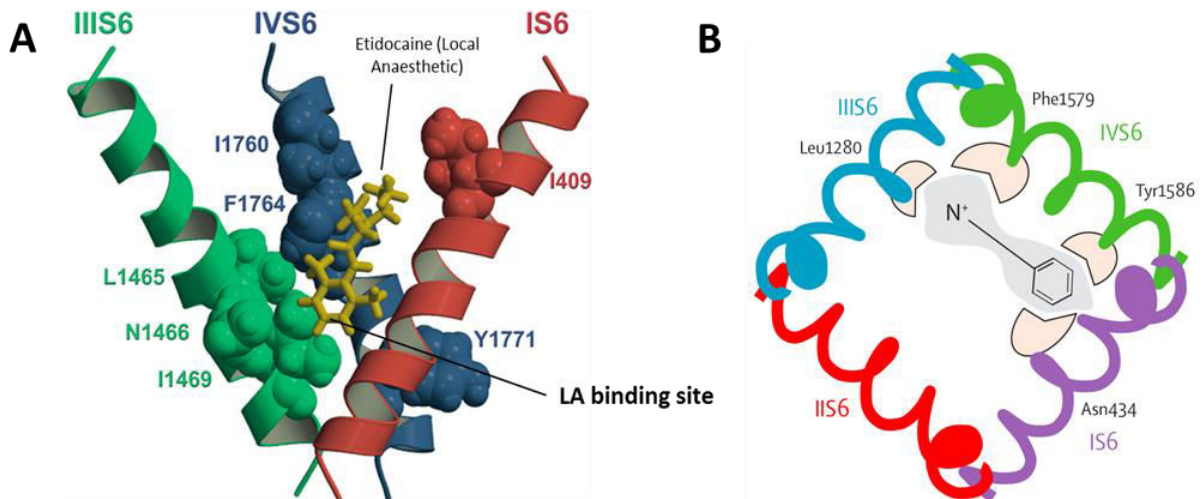


Figure 1.12: VGSC blocker binding and interaction

A. The IS6, IIIS6, and IVS6 transmembrane segments of the sodium channel form the Na^+ channel blocker binding site. Here is shown the 3D orientation of the amino acid residues and binding site of the local anaesthetic etidocaine (in yellow) that block the channel pore of $\text{Na}_v1.2$. Figure redrawn from Catterall, 2009. **B.** Illustration of a typical sodium channel blocker structure and interaction with the $\text{Na}_v1.4$ sodium channel: the positively charged nitrogen moiety in one end of the blocker interacts strongly with Phe1579 in S6 of domain IV and less with Leu1280 in S6 of domain III. At the other end of the blocker, an aromatic ring interacts with Tyr1586 and Asn434 in S6 of domains IV and I respectively. For other sodium channel subtypes, blockers interact with the same amino acid residues at the equivalent positions. Figure redrawn from Mantegazza *et al.*, 2010. A key problem with sodium channel blockers is that there is no or very little discrimination between different sodium channel subtypes.

This is mostly due to the high amino acid sequence conservation between VGSCs, which is greater than 85% for TTX-sensitive channels (Catterall *et al.*, 2005). Selective blockade of Na⁺ channels could suppress specific symptoms, such as pain or epilepsy, which can be due to defects on a particular channel subtype, with minimal side effects on the rest of VGSC function. In addition, even subtype-specific channel openers may prove useful therapeutically, for example in the case of Na_v1.1-specific openers in cases of epilepsy where these channels may be lost.

Compounds with some selectivity have started being developed, especially for pain-related disorders, targeting Na_v1.7 and Na_v1.8. For example, Abbott labs is currently developing an oral derivative of A-803467 (Jarvis *et al.*, 2007), a weakly-selective Na_v1.8 blocker that shows efficacy in alleviating neuropathic pain in mouse models (Drizin *et al.*, 2008). BZP (or else N-[(R)-1-((R)-7-chloro-1-isopropyl-2-oxo-2,3,4,5-tetrahydro-1H-benzo[b]azepin-3-ylcarbonyl)-2-(2-fluorophenyl)-ethyl]-4-fluoro-2-trifluoromethyl-benzamide), a suggested Na_v1.7-selective blocker, has partial selectivity conferred by poorly penetrating the brain, thereby having minimal CNS side-effects (McGowan *et al.*, 2009). An alternative way proposed to produce selectivity is the development of polyclonal antibodies against a channel's second and third extracellular loop (Chioni *et al.*, 2005). This approach has been used to selectively block TRP channels (Naylor *et al.*, 2008) as well as in voltage-gated calcium channels (Liao *et al.*, 2008).

1.2 VGSCs and Disease

1.2.1 Different Na⁺ channels are associated with distinct diseases

Mutations or other defects that can affect a channel's structure and its biophysical properties or surface expression can lead to neurological disorders, known as "channelopathies". Almost all of the conditions associated with sodium channel defects have an autosomal dominant mode of inheritance. From a clinical point of view, Na⁺ channels have been associated with different diseases that have in many cases lead to a better understanding of what roles these channels play in different tissues. Therefore, they have been separated depending on their principal target into four groups (George, 2005; Savio-Galimberti *et al.*, 2012): skeletal muscle sodium channelopathies (caused by mutations in Na_v1.4), cardiac sodium channelopathies (Na_v1.5), brain sodium channelopathies (Na_v1.1, Na_v1.2, Na_v1.3 & Na_v1.6) and peripheral nerve sodium channelopathies (Na_v1.7, Na_v1.8 & Na_v1.9). This project is focusing on three channels (Na_v1.1, Na_v1.2 & Na_v1.7) with different macroscopic properties, areas of expression, as well as distinct clinical manifestations. Therefore, the results found here are going to be relevant for more than one disease condition.

Hyperkalemic periodic paralysis (Ptacek *et al.*, 1991; Rajar *et al.*, 1991) and paramyotonia congenita (McClatchey *et al.*, 1992; Ptacek *et al.*, 1992) caused by mutations in the skeletal muscle Na_v1.4 channel subtype were the first sodium channelopathies to be described. To date, three more hereditary sodium channelopathies affecting skeletal muscles have been identified: hypokalemic periodic paralysis, potassium-aggravated myotonia and congenital myasthenic syndrome (Jurkat-Rott *et al.*, 2010). Many of the mutations in the *SCN4A* gene show a marked temperature dependence (Sugiura *et al.*, 2000; Wood & Baker, 2001). Temperature is important in Na⁺ channel function in disease as well as during electrophysiological recordings in heterologously expressed Na⁺ channels.

Cardiac sodium channelopathies mostly involve mutations in the *SCN5A* gene, which is predominant in the heart muscle, but the *SCN10A* gene has also recently been found to be expressed in the heart (Facer *et al.*, 2011; Verkerk *et al.*, 2012; Yang *et al.*, 2012). Heart syndromes associated with *SCN5A* mutations include long QT syndrome type 3 (Zimmer & Surber, 2008), Brugada syndrome (Kapplinger *et al.*, 2010), Atrial Fibrillation (Darbar *et al.*,

2008), progressive familial heart block type 1A (PFHB1A), familial atrial standstill, sinus node dysfunction (SND), sudden infant death syndrome (SIDS) and others. Most of these conditions are caused by gain-of-function effects on Na_v1.5 channels, except Brugada syndrome, which typically results from loss of function effects. This loss of function occurs via different mechanisms, ranging from expression of a non-functional channel (Valdivia *et al.*, 2004; Hsueh *et al.*, 2009) and decreased protein expression (Kyndt *et al.*, 2001) to defects in channel inactivation (Hsueh *et al.*, 2009). Interestingly enough, a novel *SCN5A* mutation that was identified recently in a patient with idiopathic epilepsy dying from SUDEP (Sudden Unexpected Death in Epilepsy) reveals a possible, previously unreported link between *SCN5A* mutations and epilepsy (Aurlien *et al.*, 2009). A possible explanation linking heart sodium channel mutations with epilepsy has come from rat studies, which have reported the localization of Na_v1.5 channels also in the rat limbic system apart from the cardiac muscle (Hartmann *et al.*, 1999).

1.2.2 *SCN9A* – Peripheral nerve sodium channelopathies

Peripheral nerve sodium channelopathies involve mutations in peripheral neuronal channel genes *SCN9A*, and to a lesser extent *SCN10A* and *SCN11A*. Such mutations are mainly associated with peripheral neuropathic and inflammatory related pain syndromes (Savio-Galimberti *et al.*, 2012). Na_v1.7, Na_v1.8 and Na_v1.9 are particularly important in peripheral DRG and nociceptive sensory neurons and, especially in the case of Na_v1.7, which is of primary focus here, they are considered primary mediators of neuropathic peripheral pain. Gain-of-function mutations in the *SCN9A* gene lead to different pain-related hypersensitivity disorders. Inherited primary erythromelalgia (Yang *et al.*, 2004) may be caused by a leftward shift in voltage dependence of activation (Cummins *et al.*, 2007). Paroxysmal extreme pain disorder (PEPD, Fertleman *et al.*, 2006) is caused by *SCN9A* mutations that slow fast inactivation in Na_v1.7 and result in increased persistent currents from these channels (Eijkelkamp *et al.*, 2012). In contrast, congenital insensitivity to pain (CIP), where pain perception is impaired in patients, is thought to be coupled with nonsense mutations in the *SCN9A* gene, leading to a truncated or non-functional channel (Cox *et al.*, 2006; Ahmad *et al.*, 2007).

1.2.3 *SCN1A* & *SCN2A* – Brain sodium channelopathies

Brain sodium channelopathies include mutations and defects in the sodium channel genes *SCN1A*, *SCN2A* and, to a smaller extent, *SCN3A* and *SCN8A*. For this project, focus will be given on *SCN1A* and *SCN2A*, which are thought to play distinct roles in the brain and are linked to different brain disorders.

The gene that is most associated with brain sodium channelopathies is *SCN1A*, with over 700 mutations to date giving rise to various forms of inherited and sporadic epilepsy syndromes. The most common of these syndromes are Generalized Epilepsy with Febrile Seizures plus (GEFS+) and Severe Myoclonic Epilepsy of Infancy (SMEI), also known as Dravet syndrome (Dravet *et al.*, 2005). Mutations in *SCN1A* have also been associated with autosomal dominant familial hemiplegic migraine type 3. Although originally this migraine syndrome was thought to be mediated through gain-of-function mutations (Cestele *et al.*, 2008), heterologous expression studies have suggested loss-of-function effects may be important (Kahlig *et al.*, 2008). Other types of epileptic disorders that have been associated with *SCN1A* mutations include intractable childhood epilepsy with generalized tonic-clonic (ICEGTC) seizures and familial febrile convulsions type 3A (FEB3A) (Savio-Galimberti *et al.*, 2012), although the former is now included in Dravet syndrome (Mullen & Scheffer, 2009; Savio-Galimberti *et al.*, 2012).

1.2.4 Epilepsy

Epilepsy is generally considered to be as a disorder of brain hyperexcitability, where parts or the whole of the brain undergoes abnormal excessive or synchronous neuronal activity. The basic hallmark of epilepsy is the occurrence of epileptic seizures, which are attacking events of hypersynchronous neuronal excitability. Epilepsy was actually defined as a disorder characterized by increased predisposition of generating seizures in the future (Fisher *et al.*, 2005). This definition has recently been extended by the International League Against Epilepsy (ILAE) in a more practical clinical version, defining epilepsy as a brain disorder with either 1. Minimum two unprovoked or reflex seizures with >24 h distance between them, or 2. A single unprovoked or

reflex seizure but with increased recurrence risk (>60%) according to the clinician, or 3. Being diagnosed with an epilepsy syndrome (Fisher *et al.*, 2014). Epilepsy affects more than 50 million people worldwide and people that experience an epileptic seizure at some point in their life have a 30 – 35% chance of experiencing a second one in the future (Berg, 2008).

The etiology of epilepsy can be a consequence of genetic abnormalities in multiple autosomal, X-linked or mitochondrial genes (Stafstorm, 2009) in about 50% of the cases (Pal *et al.*, 2010). Otherwise, epilepsy can develop as a result of head trauma or injury, or it can even arise as a secondary effect after, for example, a stroke or an infection. A large percentage of epilepsy events still remain idiopathic, i.e. of unknown origin (Berg *et al.*, 2010).

1.2.5 Epilepsy and VGSCs

There are a large and constantly increasing number of brain sodium channel mutations, especially in *SCN1A*, that are linked with a spectrum of epilepsy syndromes. These Syndromes range from the comparatively milder Generalized Epilepsy with Febrile Seizures plus (GEFS+) (Scheffer & Berkovic, 1997) to the more severe Dravet syndrome (Dravet *et al.*, 2005) (Figure 1.13). Related or subset epilepsy channelopathies include: borderline SMEI, Intractable Childhood Epilepsy with Generalized Tonic-Clonic seizures (ICE-GTC) and Severe Infantile Multifocal Epilepsy, which all lie along the GEFS+ – Dravet Syndrome spectrum (Singh *et al.*, 2001; Mulley *et al.*, 2005; Harkin *et al.*, 2007; Ragsdale 2008).

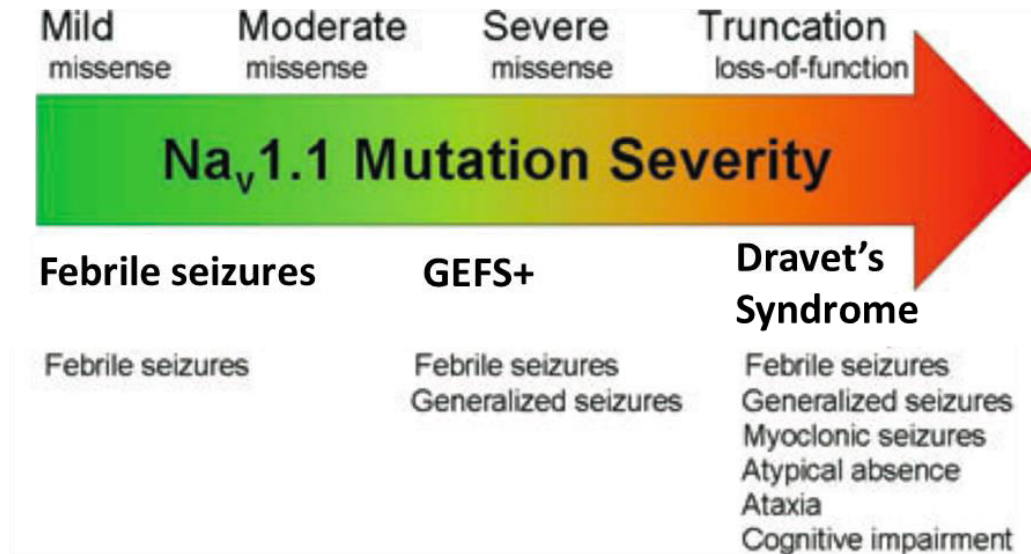


Figure 1.13: The unified loss-of-function hypothesis for Na_v1.1 genetic epilepsies.

The increase in mutation severity of Na_v1.1 loss-of-function mutations as indicated by the arrow, progressively leads to more severe forms of epilepsy syndromes, ranging from milder familial febrile seizures due to mild Na_v1.1 mutations to more severe GEFS+ and finally Dravet Syndrome, usually due to complete loss-of-function mutations. Symptoms of each epileptic syndrome are also given. Figure adapted from Catterall *et al.*, 2010.

1.2.6 Dravet Syndrome

SMEI, or else Dravet syndrome, after Dr. Charlotte Dravet who first described it in 1978, is a severe epileptic encephalopathy that usually begins in early infancy. The first seizure starts before the age of 1, mostly in association with fever (febrile seizures) (Scheffer *et al.*, 2009). With time, febrile seizures progress to a higher frequency and intensity. Seizure types include myoclonic (stiffening and jerking of muscles in arms, legs and head), complex partial and absence (fixed gaze with occasional eyelid flickering) seizures. Prolonged and clustered seizures may lead to status epilepticus (Dravet *et al.*, 1992; Engel, 2001; Catterall *et al.*, 2010), which can last for more than 30 minutes. After the age of 2, children start developing comorbidities, including ataxia, developmental delays and cognitive and intellectual impairments that progress to adulthood

(Jansen *et al.*, 2006). Post infancy seizures can usually become afebrile, occurring spontaneously even in the absence of fever. The etiology of Dravet has been primarily linked to mutations in the *SCN1A* gene (usually leading to a truncated or non-functional protein), but genetic mutations have also been found in *SCN9A*, *SCN2B*, *GABRG2* ($\gamma 2$ GABA_A receptor subunit), as well as a growing number of genes which do not encode ion channels (eg. *PCDH19*, a protein found in the extracellular matrix) (Depienne *et al.*, 2009). However, a significant number of Dravet syndrome cases still has no known genetic cause.

1.2.7 GEFS+

GEFS+ is a milder epilepsy syndrome compared than Dravet Syndrome. Febrile seizures begin from the age of 6months to 6 years. In some patients seizures may persist beyond 6 years of age (thus the “+” in these cases) and may become afebrile, including tonic-clonic, myotonic and absence seizures (Ragsdale *et al.*, 2008). Clinical symptoms are usually less severe than in Dravet patients, better controlled by AED treatment and with fewer or no cognitive impairments. Gene mutations associated with GEFS+ have been found primarily in *SCN1A*, but also in *SCN1B*, *SCN2A*, *GABRG2* and *GABRD*.

1.2.8 Epilepsy and *SCN1A*

A large (>700) and growing number of mutations discovered in the *SCN1A* gene is supposed to result in epilepsy syndromes of variable severity, ranging from GEFS+ to Dravet, linking Na_v1.1 function to these conditions. Mutations are widely distributed in the *SCN1A* gene, with no obvious hotspots or relation to domains of the channel that are linked to specific channel functions (Figure 1.14, Catterall 2010).

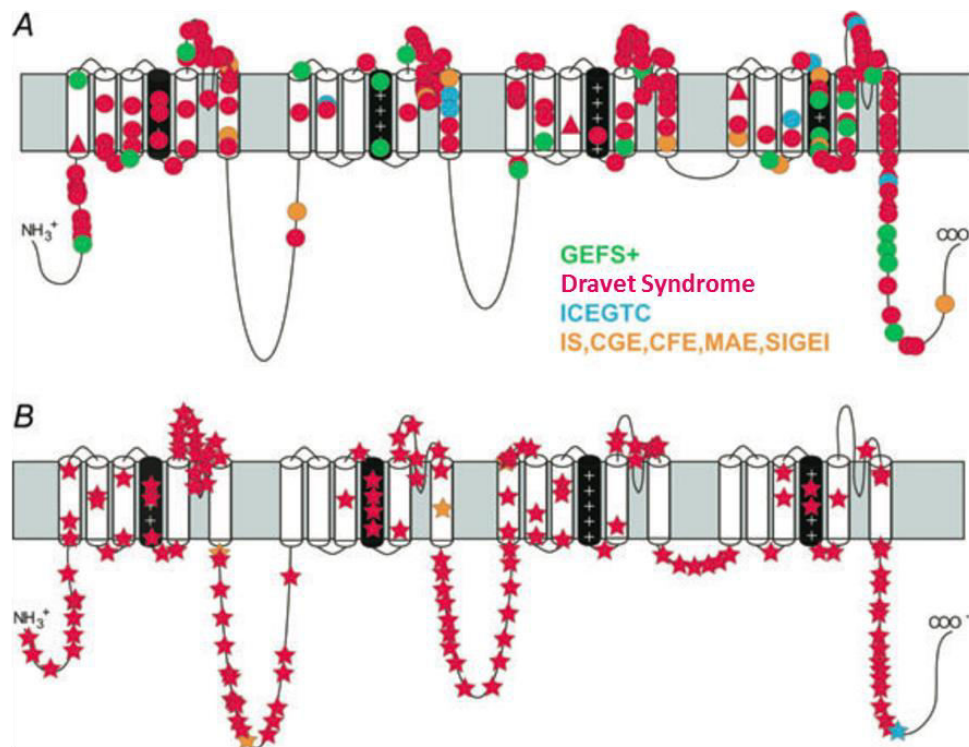


Figure 1.14: Mutations in Na_v1.1 channel patients with epilepsy

A. Circles indicate missense mutations while triangles represent in-frame deletions. **B.** Stars indicate truncation mutations mostly linked with Dravet Syndrome. Each epilepsy clinical type is indicated by color: GEFS+, generalized epilepsy with febrile seizures plus; ICEGTC, idiopathic childhood epilepsy with generalized tonic-clonic seizures; IS, infantile spasms; CGE, cryptogenic generalized epilepsy; CFE, cryptogenic focal epilepsy; MAE, myoclonic astatic epilepsy; SIGEI, severe idiopathic generalized epilepsy of infancy. Figure redrawn from Catterall *et al.*, 2010.

To understand the mechanisms through which Na_v1.1 mutations promote seizures, neuroscientists have developed *SCN1A*-knockout mouse models (Yu *et al.*, 2006) or mutant knock-in mice with various known GEFS+ or Dravet *SCN1A* mutations (Tang *et al.*, 2009; Martin *et al.*, 2010). In addition, the biophysical properties of cloned mutant channels have been extensively compared to their wild-type counterparts by electrophysiological recordings in heterologous expression systems including *Xenopus* oocytes and mammalian cell lines, using human channel isoforms, (Lossin *et*

al., 2002; 2003; Rhodes *et al.*, 2004; 2005; Mantegazza *et al.*, 2005; Ragsdale, 2008) or their rat or mouse orthologs (Spampanato *et al.*, 2001; 2003; 2004; Barela *et al.*, 2006, Ragsdale 2008).

Since epilepsy is a disorder linked with brain hyperexcitability, the original hypothesis was that proepileptic mutations in sodium channels causing GEFS+ and Dravet would result in gain-of-function effects that would increase excitability of the neurons affected. This was supported by several early studies. For example, Lossin *et al.*, (2002) has characterized several Na_v GEFS+ mutations in tsA201 cells that reduced channel inactivation and produced sustained “persistent” inward currents, which is consistent with a gain-of-function (hyperexcitability) effect in affected neurons. Similarly, a gain-of-function effect was also found by Cossette *et al.*, (2003) for the D188V *SCN1A* mutation, which impaired slow inactivation. Yet, on the other hand not all data fitted with this pattern. In contrast, later studies revealed many mutations that were mostly associated with loss-of-channel-function effects and likely decreased neuronal excitability. For example, the T875M mutation in *SCN1A* is suggested to lead to enhanced slow inactivation (Spampanato *et al.*, 2001), while the I1656M mutation caused a rightward shift in the voltage dependence of activation (Lossin *et al.*, 2003). Both changes are consistent with reduced neuronal excitability.

Ragsdale *et al.*, (2008) has reviewed the functional effects of a number of GEFS+ and Dravet related mutations, the vast majority of which leads to reduced Na⁺ currents (Figure 1.15). In addition, in the case of Dravet, which is a more severe condition to GEFS+, the majority of mutations are nonsense, resulting in a truncated or a completely non-functional channel (Mulley *et al.*, 2005; Ohmori *et al.*, 2006; Harkin *et al.*, 2007; Ragsdale 2008; De Jonghe, 2011).

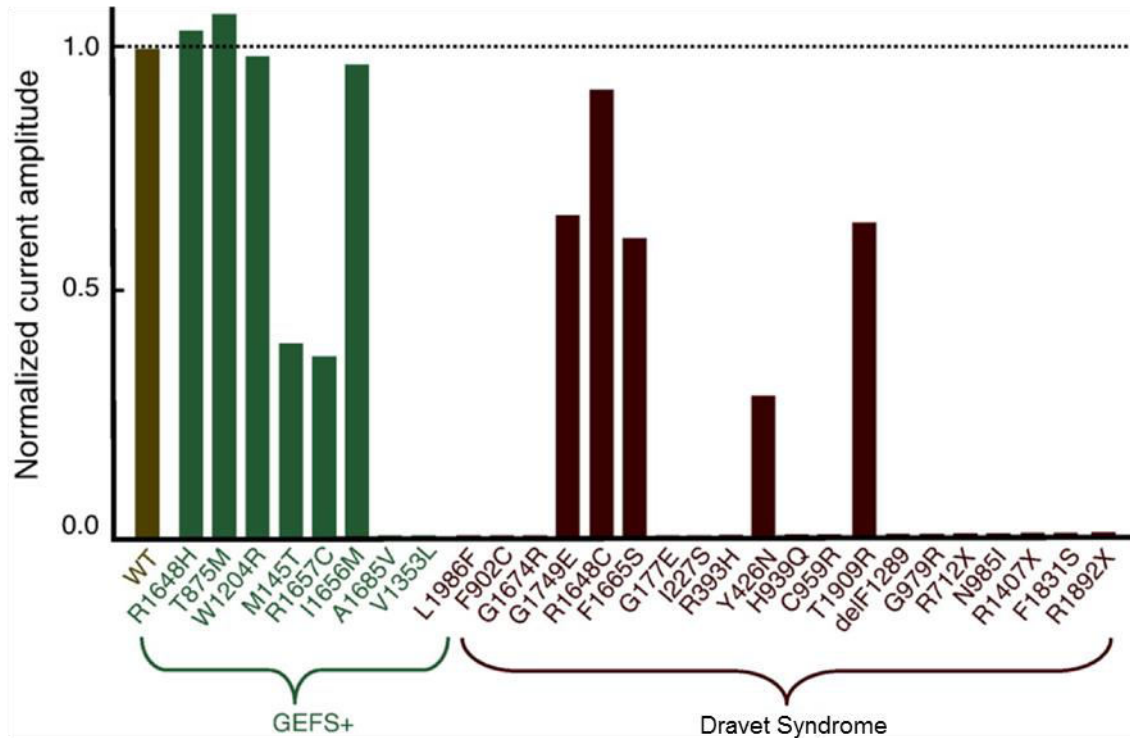


Figure 1.15: Effects of epilepsy mutations on Na_v1.1 current amplitude

Histogram of whole-cell Na max current recordings for several GEFS+ and Dravet Syndrome mutations, obtained from the following studies: Lossin *et al.*, 2002, 2003; Sugawara *et al.*, 2003; Rhodes *et al.*, 2004; Ohmori *et al.*, 2006; and Mantegazza *et al.*, 2005a. Current max amplitudes were normalized to the WT current obtained from each study. Most GEFS+ and all Dravet mutations result in partial or complete loss of sodium current. Figure redrawn from Ragsdale, 2008.

Another line of evidence linking epilepsy syndromes to loss-of-function mutations in *SCN1A* comes from mouse models. Homozygous *SCN1A* null mice, (*SCN1A*^{-/-}), experience severe, prolonged spontaneous seizures and die before 3 weeks after birth (Meisler *et al.*, 2010). Heterozygotes, (*SCN1A*^{+/-}), which had one functional and one mutant allele (similar to many Dravet patients), had less catastrophic effects than homozygotes, yet they also experienced spontaneous seizures. This indicates that the epileptic effects associated with many Dravet and GEFS+ cases in patients may have to do with *SCN1A* haploinsufficiency (Meisler & Kearney, 2005; Kearney & Meisler, 2009). *SCN1A* seems to be the only VGSC α -subunit gene in mice that

shows haploinsufficiency, since heterozygote (+/-) knockout mice for *SCN2A* (Planells-Cases *et al.*, 2000), *SCN3A* (Nassar *et al.*, 2006) and *SCN9A* (Nassar *et al.*, 2004) all have normal phenotypes.

An explanation for the unexpected finding that loss-of-function in sodium channels could result in epilepsy was proposed by Yu *et al.*, (2006), who used a $Na_v1.1$ knockout mouse, to show reduced excitability of GABAergic inhibitory neurons in the hippocampus as a result of reduced sodium current. This indicated for the first time that inhibitory interneurons were disproportionately sensitive to the loss of *SCN1A*, as summarised in Table 1.2. The same also applies for cerebellar GABAergic Purkinje neurons, as seen in a heterozygous *SCN1A*(+/-) mouse model (Kalume *et al.*, 2007). $Na_v1.1$ may account for a larger proportion of the total cell current in inhibitory interneurons than in excitatory neurons within the brain, meaning *SCN1A* loss-of-function mutations result in over-excitation, probably via reduced inhibition (Figure 1.16).

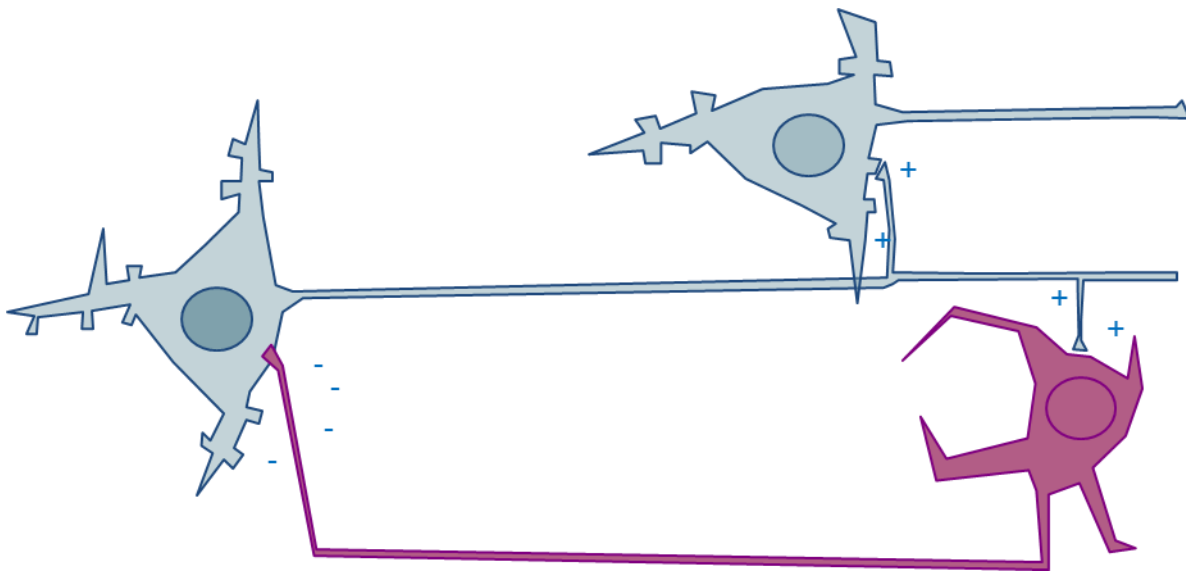


Figure 1.16: $Na_v1.1$ is mainly found in interneurons

GABAergic inhibitory interneurons are shown in red. Upon excitation via (mainly) *SCN1A* channel activation, interneurons project to hippocampal pyramidal neurons or Purkinje neurons (light blue) to inhibit their action. Loss of function of GABAergic interneurons due to *SCN1A* defects would result in hyperexcitability of primary neurons, probably through a classical “inhibition of an inhibitor” mechanism.

The finding that *SCN1A* may predominate in interneurons still does not fully explain why some mutations that are thought to be associated with gain of sodium channel function and electrical hyperexcitability in heterologous expression studies may also lead to epilepsy. There can be multiple reasons for this discrepancy and all of them have to be taken into account when evaluating results from such functional studies. First of all, a number of mutations may partly or solely result in channel trafficking defects, changing the abundance of functional channels on the cell surface. The biophysical properties of these mutants may not really differ from wild-type (or may even be opposite in functional effect), yet epilepsy could stem from fewer channels getting to the cell membrane. Secondly, the functional properties of a channel seem to be cell type-dependent and can also differ depending on whether a channel is studied in neurons or in heterologous expression systems. So, for example, Tang *et al.*, (2009) studied the properties of a GEFS+ mutation in neurons taken from transgenic mice and reported a loss of function, although the same mutation was characterized as a gain of channel function in previous studies carried out using heterologous expression systems. The same study also indicated that functional effects in neurons were dependent on the neuronal subtype expressing the mutant channel, therefore showing a subtype-specific functional effect (Tang *et al.*, 2009). Similarly, Rush *et al.*, (2006) working on an *SCN9A* mutant linked to a pain disorder known as Inherited Erythromelalgia (IE), showed that the same mutation (L858H) could cause hyperexcitability in DRG neurons, while it caused the opposite effect (hypoexcitability) in cultured superior cervical ganglion neurons. This clearly demonstrates that the outcome of the functional effect and consequent neuronal excitability of a proepileptic mutation in VGSCs does not only depend on the α -subunit sequence, but can be affected by neuronal background.

Modulation by protein kinases and phosphorylases can also play a role in the functional outcome, as well as association with accessory β -subunits, which have been shown to modulate the functional properties of VGSCs (Farmer *et al.*, 2012). α -subunits associate with different combinations of β -subunits in a subtype and cell-type specific manner, so that different regulation of Na_v1.1 by different β -subunits depending on the cell type may result in distinct functional properties. Also, the role of β -subunits on mediating targeted subcellular localization of the α -subunit can affect neuronal excitability as well and this localization process can again also be cell-type specific. Finally, channels expressed in heterologous systems are studied in isolation, whereas channels in neurons or from mouse *ex vivo* brain slices are found in a more complex cellular

milieu. Therefore, the functional contribution of an *SCN1A* mutation in a neuron will also rely on the balance of all the native, cell-specific currents that set the neuron's membrane potential, AP threshold and firing frequency.

A point of caution when extrapolating results of functional effects from heterologous systems to neurons and vice versa is possible compensatory mechanisms that neurons might exploit to minimize the effects of a mutation on excitability. Yu *et al.*, (2006) reporting a reduction in hippocampal GABAergic neuronal excitability in *SCN1A* null mice due to loss of Na_v1.1 channel expression, also reported an upregulation of Na_v1.3. This may represent a compensation mechanism in GABAergic neurons and probably accounted for a significant proportion of the residual sodium current seen in *SCN1A*(-/-) homozygotes, yet increased expression of Na_v1.3 was not enough to prevent seizures in mice. *SCN1A* missense mutations that cause a loss of function due to folding defects can sometimes be rescued and present a normal cell phenotype when interacting with accessory proteins or VGSC blockers (Rusconi *et al.*, 2007; 2009). Rescue could partly account for the phenotypic variability seen among GEFS+ patients who carry the same mutation. Similar variability was reported by Yu *et al.*, (2006), who found strain-dependent differences in the severity of *SCN1A* null phenotype between two strains of mice with different genetic backgrounds. Similarly in humans, a high level of clinical heterogeneity can be seen between patients carrying mutations in the same gene, even in cases where they carry the same gene mutation. Depienne *et al.*, (2010) has reported of an *SCN1A* mutation within a family, where the parent was described with a benign GEFS+ phenotype, while the severity of the phenotype on the child was much more neurologically devastating. This suggests that there are also other additional underlying factors, probably both environmental and epigenetic, that may modify the impact of a given mutation on clinical phenotype. Such finding may also partly account for population-specific differences in patients that show a wide range of GEFS+ phenotypes or different sensitivity to AED response, indicating that these may have an underlying genetic factor (Doty, 2010; Kobow *et al.*, 2013). These may include genetic variants, either on sodium channels themselves or in other genes. In sodium channels, one obvious contributor to variability in channel function is alternative splicing and the current study is focussed on dissecting how a conserved splicing event may affect channel function and drug response in three sodium channel subtypes, Na_v1.1, Na_v1.2 and Na_v1.7.

To re-evaluate, *SCN1A* mutations linked to epilepsy syndromes can either have a loss of channel function effect (in most cases) as well as gain-of-function effects. Yet, what sets the brain dysfunction is much more complex and multifactorial and results from widespread imbalance of whole brain network inhibition.

1.2.9 *SCN2A* and Benign Familial Neonatal Infantile Seizures (BFNIS)

Missense mutations in the *SCN2A* gene have been linked to different forms of epilepsy syndromes, the most common of which is benign familial neonatal infantile seizures (BFNIS). This is an autosomal dominant disorder that usually begins within 4 months of life in infants and is characterized by afebrile seizures that carry on spontaneously until about the first year, and then resolve without any residual neurological deficit. (Berkovic *et al.*, 2004). Seizures usually start focally, yet secondary generalization is not uncommon (Steinlein, 2014), yet they usually respond well to antiepileptic drug treatment (Miceli *et al.*, 2015). The temporal pattern of disease is consistent with the early life expression of Na_v1.2 in unmyelinated axons (Westenbroek *et al.*, 1989), which is replaced by Na_v1.6 later in postnatal development during axon myelination (Rasband 2010; Mantegazza *et al.*, 2010).

Similar to *SCN1A*, BFNIS mutations have been reported to have both gain and loss of function effects. Three BFNIS mutations in *SCN2A* studied by Misra *et al.*, (2008) show reduced current density due to either reduced expression within the plasma membrane or a depolarizing shift in voltage dependence of activation for the R1319Q mutant. Other mutations leading to BFNIS are suggested to result in gain of channel function in studies using transfected cell lines (Scalmani *et al.*, 2006; Liao *et al.*, 2010), which is consistent with primary expression of Na_v1.2 channels in excitatory brain nerves (Savio-Galimberti *et al.*, 2012).

Fewer cases of *SCN2A* mutations are linked to patients with GEFS+ (Sugawara *et al.*, 2001). More recently, patients also suffering from Dravet have also been found to carry *SCN2A* mutations (Ogiwara *et al.*, 2009; Shi *et al.*, 2009; Meisler *et al.*, 2010). In the case of Ogiwara *et al.*, (2009) the two de novo mutations studied (E1211K and I1473M) probably cause a gain-of-channel-function via a hyperpolarizing shift in voltage dependence of activation. A recent study has also

discovered a Na_v1.2 mutation linked with a more severe phenotype than BFNIS, including intractable seizures and brain and muscular developmental abnormalities (Baasch *et al.*, 2014). This suggests that in some cases the spectrum of epilepsies observed due to mutations in Na_v1.2 channels may overlap with that seen for Na_v1.1 mutations.

Furthermore, also in relation to the splicing event studied in this project, another missense mutation (L1563V at the S2 segment of DIV) specifically within the neonatal Na_v1.2 isoform has also been associated with epilepsy. The mutation is causing a positive shift to the voltage dependence of activation on neonatal channels specifically, leading to a gain-of-function effect and hyperexcitability. This proepileptic predisposition of the neonatal variant might also partly explain the disappearance of seizures postnatally in BFNIS patients, as a result of the developmental switch of Na_v1.2 channels in excitatory neurons (Liao *et al.*, 2010). This is further supported by recent finding from Gazina *et al.* (2014), where the genetic removal of the Na_v1.2 neonatal exon leads to a change in seizure threshold.

1.2.10 Epilepsy and *SCN3A* and *SCN8A*

There are very few cases of *SCN3A* or *SCN8A* mutations that are linked to epilepsy syndromes compared to *SCN1A* and *SCN2A*. Yet, in *SCN3A*, a missense (K354Q) mutation has been described in patients suffering from cryptogenic paediatric partial epilepsy (Eijkelkamp *et al.*, 2012). Study of this mutation in hippocampal neurons showed a hyperexcitability effect via increased persistent current and slowing of fast inactivation (Holland *et al.*, 2008; Estacion *et al.*, 2010). For *SCN8A*, missense mutations in this gene in some mouse models and in patients cause cognitive impairments, which are usually linked to ataxia (Trudeau *et al.*, 2006; Levin *et al.*, 2006), without any obvious association to seizures. Recently however, a *de novo* *SCN8A* mutation was been identified in a patient with infantile epileptic encephalopathy who died from SUDEP (Veermah *et al.*, 2012) and later on two new *de novo* *SCN8A* mutations (G214D and R1872Q) and one dominant mutation (L1331V), inherited from a parent with somatic mosaicism in patients with epileptic encephalopathy were also revealed (Carvill *et al.*, 2013). Three mouse model studies also suggest a role for *SCN8A* in epilepsy. Martin *et al.*, (2007) showed that mice with

haploinsufficiency for both Na_v1.1 and Na_v1.6 had a less severe seizure phenotype than *SCN1A*-only (+/-) heterozygotes. The mechanism suggested for this is that the Na_v1.6 mutation reduces excitability of excitatory neurons, thus partly offsetting the loss of Na_v1.1 in GABAergic inhibitory neurons and consequent reduced inhibition. Also, *SCN8A*(+/-) heterozygote mice are more resistant to chemically induced (Martin *et al.*, 2007) or electrically induced (Blumenfeld *et al.*, 2009) seizures, thereby indicating some possible degree of association between *SCN8A* and epilepsy.

1.2.11 Pain & Epilepsy and *SCN9A*

Due to its primary expression in the PNS rather than in the brain, *SCN9A* mutations are mostly associated with pain syndromes (Dib-Hajj *et al.*, 2009). Nevertheless, a missense mutation (N641Y) in the *SCN9A* gene has been identified within a family with febrile seizures (Singh *et al.*, 2009). Furthermore, Doty (2010) has reported that some mutations in *SCN9A* can act as modifiers of epilepsy severity on top of other mutations in other sodium channel subtypes or even lead to a mild seizure phenotype themselves.

Yet, most mutations on the *SCN9A* gene are usually associated with pain perception disorders, including primary erythralgia (PE), paroxysmal extreme pain disorder (PEPD), small-fiber neuropathy, as well as congenital insensitivity to pain (CIP). Depending on the effect of the mutation, the pain spectrum can vary from extreme sensitivity to complete insensitivity.

Paroxysmal extreme pain disorder (PEPD) is characterized by burning pain episodes, mostly in the rectum, eyes or jaw, often associated with skin redness, usually starting early in childhood and continuing throughout life (Fertleman *et al.*, 2007). There are currently 10 known missense mutations on the *SCN9A* gene giving rise to this particular disorder (Marcovic *et al.*, 2015), all of which are thought to work by affecting channel inactivation. Reduced or incomplete inactivation in mutant channels leads to prolonging of the AP and repetitive firing in DRG neurons (Dib-Hajj *et al.*, 2008).

On the other side of the spectrum, congenital insensitivity to pain (CIP) is a rare disorder characterized by the lack of any pain sensation from patients. This is mostly due to loss-of-

function mutations in the *SCN9A* gene, which can lead to impairment of AP firing in DRG neurons as it has been seen in CIP families (Cox *et al.*, 2006). Some of the known mutations in *SCN9A* gene leading to CIP phenotype include S459X, I767X, W897X, M899I, and M932L (Goldberg *et al.*, 2007; Yuan *et al.*, 2011; Marcovic *et al.*, 2015). Yuan *et al.* (2011) also indicated that for the mutations M899I and M932L, there was variation in pain sensitivity in the Chinese population which was partly related to a single nucleotide polymorphism (SNP) at exon 16 of the *SCN9A* gene (c3312G>T). This indicates that splicing can potentially play a crucial role in the outcome of *SCN9A* disorders, the mechanism of which is part of the current project here, where the biophysical profile of a conserved splicing event between *SCN1A*, *SCN2A* and *SCN9A* genes that has been related to epilepsy and pain disease states is going to be examined.

Similar to PEPD, primary erythralgia (PE) is an autosomal dominant pain disorder characterized by extreme neuropathic burning pain in response to heat or movement (Marcovic *et al.*, 2015). Therapy usually involves cooling of extremities at early stages, but soon becomes resistant to that and requires the usage of local anesthetics, such as lidocaine and mexiletine (Kuhnert *et al.*, 1999; Legroux-Crespel *et al.*, 2003), yet without much effect in many of the cases (Davis & Sandoroni, 2002). There are 19 mutations that are associated with PE to date, the vast majority of which are missense mutations leading to gain-of-function effects (Lampert *et al.*, 2006; Wu *et al.*, 2013; Marcovic *et al.*, 2015). For example, mutations I848T and L858H found at the S4-S5 linker of DII are suggested to cause a hyperpolarizing shift, probably due to a change at the VD of activation (Cummins *et al.*, 2004), which is linked to DRG hyperexcitability (Rush *et al.*, 2006). A similar biophysical effect was also found by Ahn *et al.* (2010) for the I234T mutant, which also showed slower deactivation and higher responses in current amplitude to depolarization stimuli due to a -18 mV shift in the voltage-dependence of activation and an accelerated time-to-peak. Furthermore, F1449V and A853P mutations can induce bursting of sensory neurons by lowering the action potential (AP) triggering threshold (Dib-Hajj *et al.*, 2005). Also, the substitution of serine to threonine in position 241 (S241T) is suggested to result to faster AP peak time, slower deactivation and increased sensitivity to lower depolarizations (Lampert *et al.*, 2006). Clinical symptoms of PE start in early childhood, around 5-6 years old, yet manifestation of the disease is thought to be partly dependent by a gene splicing event (Choi *et al.*, 2010) that will be studied in this project. This splicing event is also conserved in *SCN1A* and *SCN2A* genes and is also implicated in distinct disease manifestations (Kasperaviciute *et al.*, 2013; Kumari *et al.*, 2013;

Xu *et al.*, 2007; Gazina *et al.*, 2014). This indicates that this conserved splicing event in three functionally distinct channel types (Na_v1.1, Na_v1.2 & Na_v1.7) can modify the disease state of three phenotypically different disorders. Therefore, part of the current study is to reveal any potentially conserved biophysical mechanisms through which this splicing event is conferring different functional properties between the two splice isoforms of each channel type, which may account for the differences seen between them in distinct epilepsy and pain disease states.

1.3 VGSCs and use-dependent blockers

1.3.1 Use-dependent blockers – AEDs

As mentioned earlier, VGSCs are the targets of many kinds of drugs that can modulate their function in a use-dependent manner, such as local anaesthetics (Lidocaine), anticonvulsants and tricyclic antidepressants (Imipramine). Drugs that are mainly used in blocking the effects of sodium channels associated with epilepsy syndromes are called anti-epileptics or antiepileptic drugs (AEDs). However, these drugs have also been used for pain disorders, linked to *SCN9A* mutations, although without being able to discriminate specifically between channel subtypes (Lai *et al.*, 2004; Drenth & Waxman, 2007). Phenytoin, the prototypic VGSC blocker, and carbamazepine are front line AEDs used throughout the world for treating epilepsy.

1.3.2 Phenytoin

Phenytoin is suggested to be an effective treatment for partial and generalized tonic-clonic seizures in epileptic patients as well as in animal models (Perucca & Tomson 2011). However it is not effective in treating absence seizures (Dreifuss 1983; Mantegazza *et al.*, 2010). Phenytoin was the first antiepileptic to approach the ideal of suppressing epileptic activity, yet without affecting normal brain function. From very early on, Toman, (1949) doing experiments on the frog sciatic nerve noted that phenytoin did not have much effect on the initial AP caused by supramaximal current stimulation, but rather inhibited the following “rebound spike” generated (Ragsdale *et al.*, 1998). Intracellular microelectrode recordings from mouse spinal cord neurons by McLean & McDonald (1983) showed that phenytoin could prevent high frequency repetitive firing upon depolarizing current pulses, yet leaving spontaneous neuronal firing unaffected. The mechanism through which phenytoin could achieve that was still unknown, yet it was evident that phenytoin was selectively inhibiting high-frequency neuronal activity.

A greater insight into phenytoin’s mode of action was achieved from studies involving voltage-clamp recordings of VGSCs. These studies revealed that phenytoin is a very weak blocker of

sodium channels at hyperpolarized (less than -80 mV) membrane potentials, where sodium channels are suggested to be in a closed conformation. This indicated that phenytoin has a low affinity for VGSCs lying in resting states. However, with increased depolarization, phenytoin blocks VGSCs in a voltage-dependent manner, with greater blockade at progressively more depolarized potentials (Ragsdale *et al.*, 1998) (Figure 1.17A). The voltage dependence of phenytoin follows the same pattern as voltage dependence of channel fast inactivation (Figure 1.17B), indicating that phenytoin blocking action might be somehow related to the channel's inactivation process or state. Phenytoin blockade builds up in an activity-dependent manner upon high-frequency rates of stimulating pulses (Figure 1.17C).

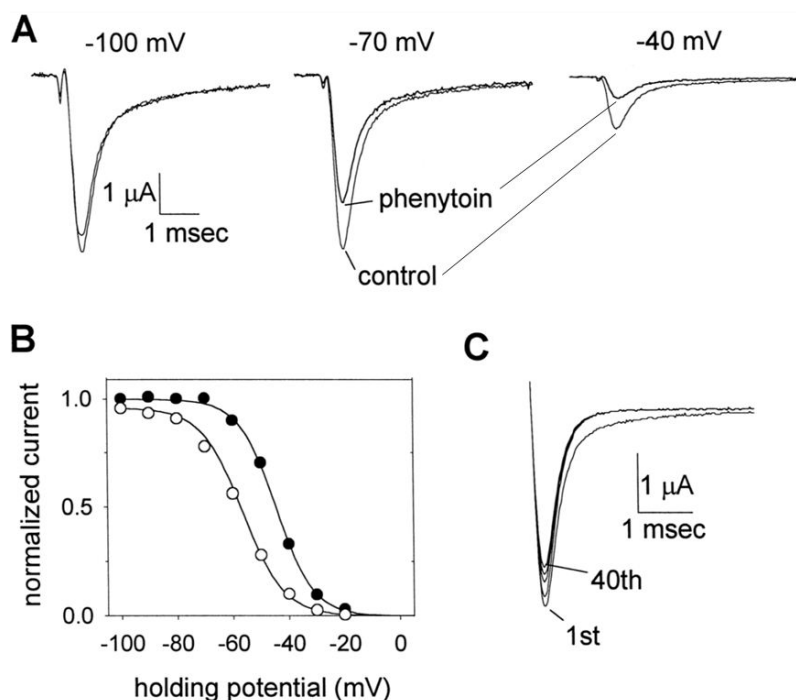


Figure 1.17: VGSC blockade by phenytoin is both voltage- and activity dependent.

A. Voltage-dependent block of phenytoin on $\text{Na}_v1.2\text{-}5\text{A}$ sodium channels: The level of inhibition on sodium currents from *Xenopus* oocytes after 100mM of phenytoin application increases at more depolarized holding potentials. Cells were held at -100, -70 and -40mV and currents were elicited by depolarization at 0mV. **B.** Phenytoin shifts the voltage dependence of inactivation of sodium channels to the left, i.e. to more negative potentials (control, black circles; phenytoin, open circles). **C.** Activity-dependent block of phenytoin in sodium channels. Giving a 10Hz train of stimuli in the presence of 100 μ M of phenytoin, the drug's blockade builds up from the 1st to the 40th pulse. Figure redrawn from Ragsdale *et al.*, 1998.

1.3.3 The modulated receptor model

As a conclusion from above, phenytoin is suggested to inhibit VGSC action in a voltage- and frequency-dependent manner. In order to understand this mechanism of action, the modulated receptor model was developed, firstly used to describe the mode of action of local anaesthetics (LAs), which work in a very similar mechanism to phenytoin. Site-directed mutagenesis studies suggest that LAs and AEDs share common or overlapping binding sites on VGSCs (Ragsdale *et al.*, 1998).

The modulated receptor model suggests that phenytoin has a low affinity for resting sodium channels but binds much more efficiently in the inactivated or open state. This reflects a modulation of the drug receptor site, which probably occurs through an allosteric mechanism as the channel changes conformation from a low affinity site in closed states to a high affinity site in inactivated or open states. Hence, the drug receptor site is in a low affinity conformation when the channel is resting, while converting into a high affinity state upon channel opening/inactivation. Given that sodium channel inactivation is more prevalent at more depolarized potentials and during high-frequency channel activation (Mantegazza *et al.*, 2010), this model accounts for phenytoin's voltage and activity dependence. The model also provides a mechanistic explanation of phenytoin's mode of action as an AED. During times of normal brain function between seizures most VGSCs are in resting state, since neurons would only fire single or short bursts of APs. Phenytoin would be a poor blocker in this state, hence only minimally affecting neuronal (and cognitive) functions. On the contrary, within a seizure, neurons experience "high frequency trains of APs, riding on prolonged depolarizing episodes" (Ragsdale *et al.*, 1998; Mantegazza *et al.*, 2010), the ideal condition for phenytoin to bind to high affinity sites in open and inactivated sodium channels and inhibit sodium current flow, hence suppressing seizures from developing.

The original modulated receptor model suggested only three VGSC conformational states: open, closed (resting) and inactivated. Kuo & Bean, (1994) suggested a more mechanistic gating scheme to characterize state-dependent binding of phenytoin in VGSCs. In this model the resting sodium channel can pass through five different closed transition states before opening, which are consistent with the outward movement towards activation of the four S4 segments that constitute the voltage sensors of the channel (Figure 1.18). Starting with all four S4 segments in closed state (C1), all four have to be activated (C5) before the actual channel opening can occur (O).

Phenytoin, or any other similar-acting drug (indicated as B (Blocker) at the bottom row), can bind to any transition state in the activation scheme with a binding strength that is proportional to the number of voltage sensors that are in open position (Kuo & Bean, 1994). This model version does not differ in principle from the original modulated receptor model, since it also predicts voltage and activity dependence of phenytoin binding, favouring blockade at more depolarized channel potentials.

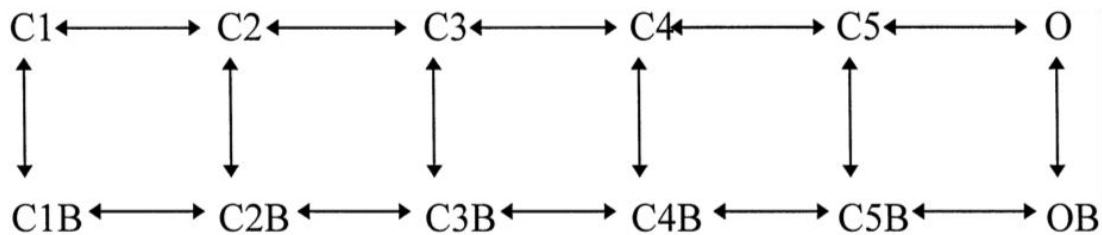


Figure 1.18: The extended modulated receptor stochastic model.

suggested by Kuo & Bean (1994) C1 – C5 represent closed states, free of drug blockade. C1B – C5B are closed states with the channel blocker bound. O and OB represent open channel states with blocker unbound and bound respectively.

1.3.4 Molecular basis of phenytoin's action

The intracellular part of the S6 segment in domain IV is thought to be crucial for drug binding in VGSCs, especially in the case of LAs and AEDs. Site-directed mutagenesis studies have revealed specific residues in IVS6 that contribute to the drug receptor site, which, when disrupted, decrease the drug's affinity for its binding site, with negligible effects in other channel functional properties. Two such residues of major importance for AED binding are a phenylalanine in position 1764 (F1764) and a tyrosine residue (Y1771) (Ragsdale *et al.*, 1994; Fizzard *et al.*, 2011). These two amino acids are thought to project towards the cytoplasmic vestibule of the VGSC pore to form a part of the drug binding site (Figure 1.19).

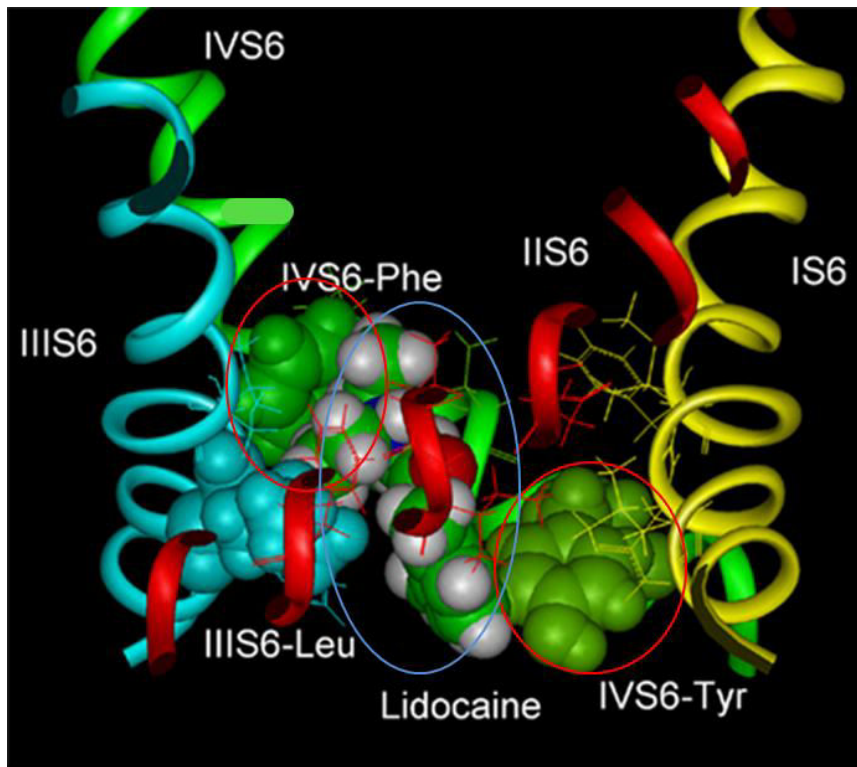


Figure 1.19: Molecular model of sodium channel blocker to VGSC inner pore

Model of interaction between the sodium channel blocker (here lidocaine, in blue circle) and the phenylalanine and tyrosine residues on the IVS6 segment of the sodium channel (in red circles), with the drug blocking the inner vestibule of the pore. Figure redrawn from Fozzard *et al.*, 2011.

The close relationship between AED blockade and inactivation of the sodium channel is what drove scientists to also study the inactivation particle (IFM) as a potential contributor to drug binding or of the drug's receptor site. After all, one of the functional effects of AEDs on VGSCs is to slow their recovery from fast inactivation, reducing in that way the channel availability for subsequent openings (Rogawski & Loscher, 2004). This happens because the rate of dissociation of AEDs in activated channels is much slower than their normal recovery from inactivation process, which occurs as the IFM linker is released from its intracellular site of binding. In search for such a relationship, Bennett *et al.*, (1995) disabled the inactivation linker (IFM) particle in

Na_v1.5 channels by substituting the three residues with glutamines (QQQ). Disruption of the inactivation gate greatly reduced the channel's blocking by lidocaine, a local anaesthetic with a similar mode of action to phenytoin. This indicated that drug binding in VGSCs in depolarized states may also involve residues present in the inactivation gate, in addition to those in IVS6. Alternatively, disruption of the inactivation process might act indirectly, by hindering the possible conformational changes that would be required to form a "high affinity drug binding site" (Ragsdale *et al.*, 1998).

1.3.5 Carbamazepine

Carbamazepine is another widely used AED, whose anticonvulsant profile is almost identical to phenytoin. Therefore, carbamazepine also exhibits voltage and activity-dependent inhibition of VGSCs, with minimal effects on normal brain function. However, compared to phenytoin, carbamazepine has a 3-fold lower affinity rate for depolarized channels so that it binds less effectively, yet its rate of binding is 5-times faster (Kuo *et al.*, 1997; Rogawski & Loscher, 2004). This could probably render carbamazepine more effective than phenytoin at blocking VGSCs during very high frequency firing. It could also partly explain why some different epilepsy patients with different VGSC mutations may be more responsive to treatment with one or the other drug.

Despite their wide usage as anticonvulsants, anaesthetics or pain killers, current use-dependent blockers, at their vast majority, cannot really discriminate between different sodium channel types. This limits their potential for efficiently tackling specific disease states without unwanted side-effects due to non-specific targeting. Therefore, any modification that could provide a pharmacological dissection between sodium channels would be of benefit for basic science and potentially clinically useful. Alternative splicing is a naturally occurring process that vastly increases the diversity of proteins and splice variants have sometimes been shown to have different pharmacological properties (Bruss *et al.*, 1999; Ryberg *et al.*, 2005; Song *et al.*, 2015).

In this study we compared the effect of both phenytoin and carbamazepine on recovery from fast inactivation in two splice variants of a conserved splicing event in Na_v1.1, Na_v1.2 and Na_v1.7

channels under conditions simulating very high, pathophysiological frequency firing. This was done in order to determine whether the functional effects that a conserved splicing event in VGSCs has can alter AED response in seizure-like conditions. Furthermore, potential differences in AED pharmacology between splice variants might be useful for pharmacologically discriminating between the different isoforms of sodium channels, which could potentially be of high clinical value for the development of more selective drugs.

1.4 VGSCs and splicing

1.4.1 Splicing

Alternative splicing of genes involves the processing of several possible mature mRNAs derived from a single gene transcript. In splicing introns (non-coding transcript regions of typically 200 – 1000 nucleotides) are removed (or “spliced-out”) and exons (coding transcript regions of 50 – 300 base pairs) come together in various ways (involving exon skipping, mutual exon exclusion etc.), resulting in subtly different final mature mRNA and protein combinations. It is an efficient way of increasing protein diversity from a single gene without the need of having to undergo gene duplication and mutation each time. Alternative splicing in neurons can therefore diversify protein function and widen neuronal responses within different neuronal subtypes (Bell *et al.*, 2004) or at different network activity levels (Mu *et al.*, 2003), thereby greatly expanding neuronal function and network structure. It is estimated that the vast majority of human genes are alternatively spliced, resulting in fine-tuning of physiological functions (Modrek & Lee, 2002; Pan *et al.*, 2008), with most of splice variants being expressed in the brain (Xu *et al.*, 2002).

As mentioned before, among sodium channels there are 10 different subtypes, thereby greatly expanding the range of possible responses upon activation according to the different spatial and temporal localization of each of them. Alternative splicing is yet another great source of increasing variability among sodium channels, while also holding potential advantages over the evolution of even more ion channel orthologs. First of all, different splice isoforms are likely to maintain the same expression pattern, which would be less likely to be kept with new channel subtypes. Furthermore, since splicing is carried out at the post-transcriptional level, it allows for finer and more precise modification of the ion channel properties and also on a much faster timescale than what would involve switching off the transcription of one gene and turning on another (Copley, 2004).

Among the multiple splicing events occurring in sodium channels, there is one event that is conserved among all neuronal TTX-sensitive sodium channel α -subunit genes (namely *SCN1A*, *SCN2A*, *SCN3A*, *SCN5A*, *SCN8A* & *SCN9A*). This involves the alternative splicing of two

mutually exclusive cassette exons which encode for part of the S3 and the entire S4 transmembrane segment of Domain I of the functioning channel (Figure 1.20C).

1.4.2 Alternative splicing in the *SCN1A* gene

The *SCN1A* gene has two alternately spliced variants of exon 5, denoted 5A and 5N (Figure 1.20A). A and N stand for Adult and Neonatal respectively, as when initially characterised in rat brain sodium channel mRNAs by Sarao *et al.*, 1991, the neonatal form is thought to preferentially be expressed in prenatal and early post-natal period and gradually being replaced by the adult form during development. Yet, 5N expression is still evident also in the adult brain. Amplified *SCN1A* mRNA taken from foetal brain contains >60% exon 5N, while in adult brains without a history of epilepsy 5N *SCN1A* levels were much lower (~9.5% to 30 – 40%) (Tate *et al.*, 2005; Heinzen *et al.*, 2007). Exons 5A and 5N are mutually exclusive, meaning that mature mRNAs will either retain one or the other exon. Despite several nucleotide differences between the two exons, following translation, 5A and 5N Na_v1.1 channels differ from each other only by three amino acid changes (adult to neonatal): Y203F, D207N and V211F (Tate *et al.*, 2005) (Figure 1.20B). When translated, exon 5 corresponds to the site of the channel spanning the extracellular loop between S3 and S4 in domain I and almost the entire S4 (Figure 1.20C). The differences between the two variants are all located on the S3 – S4 linker area. Since exon 5 spans a region of the channel that is important for voltage sensing, alternative splicing at this site was predicted to confer changes in channel (and consequently neuronal) behaviour.

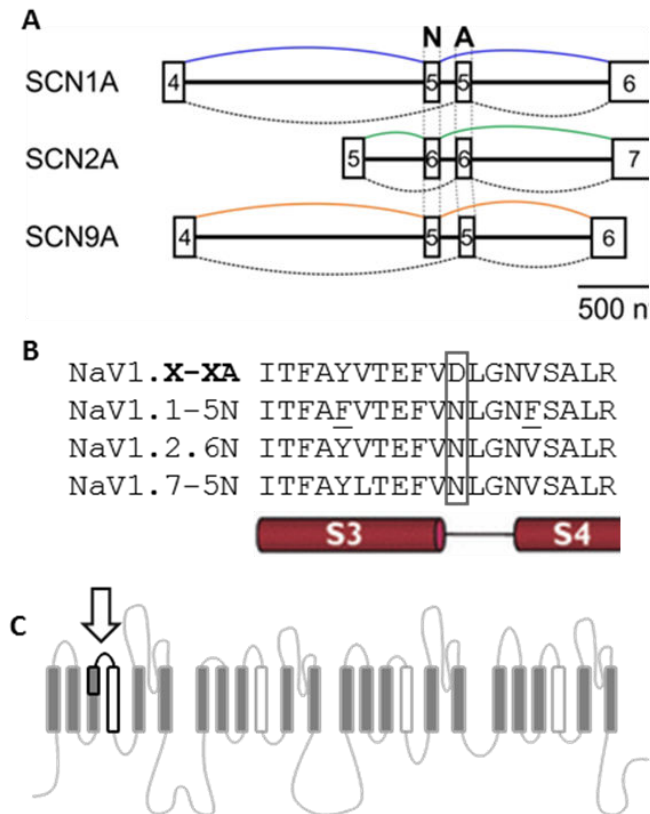


Figure 1.20: Structure and conservation of splicing in $Na_v1.1$, $Na_v1.2$ & $Na_v1.7$ voltage-gated sodium channels.

A. Conserved structure of the splicing motif in the first domain of $Na_v1.1$, $Na_v1.2$ & $Na_v1.7$ sodium channels. Introns (thin black lines) and exons (squares) are to scale. In all cases the neonatal exon (N) precedes the adult (A) exon and they are separated by a short intron. **B.** Conserved sequences encoded by the adult (top row) and neonatal versions (bottom 3 rows) of the conserved exons in sodium channels used in this study. The sequence encoded by the adult exons ($Na_v1.X-XA$) is invariant. The sequence encoded by the neonatal exons contains conservative amino acid substitutions. Only the part of the exon that differs between neonatal and adult sequences is shown here for clarity, since the rest of the exon sequence is identical between neonatal and adult genes. The sequence of the exons is aligned alongside with the S3 – S4 segment of Domain I of the α -subunit (shown in red). It has been previously shown that the two phenylalanine (F) substitutions in $Na_v1.1-5N$ do not alter channel properties (Fletcher *et al.*, 2011). The boxed site indicates where splicing toggles the negatively-charged aspartate (D) in the adult exon, and a neutral amino acid (asparagine, N, in these channels); the conserved replacement of a single amino acid in TTX-sensitive neuronal channels. **C.** Cartoon indicating the site of the single amino acid change in the short extracellular linker between the third and fourth transmembrane segments in domain I (DI S3-S4, arrow). The overall length of these channels is typically >2000 amino acids. The region outlined in black corresponds to the entire sequence encoded by the alternate exons, including the voltage sensor in the first domain.

This splicing event is conserved in all TTX-sensitive neuronal VGSCs, namely *SCN2A*, *SCN3A* (Sarao *et al.*, 1991; Gustafson *et al.*, 1993; Lu & Brown, 1998), *SCN8A* (Plummer *et al.*, 1997) and *SCN9A* (Belcher *et al.*, 1995) (Figure 1.20B). In the case of *SCN2A* and *SCN3A* it is exon 6 that is alternatively spliced, yet it corresponds to the same position in the channel sequence.

While humans have functional copies of both 5A and 5N in *SCN1A*, rodents contain a premature stop codon in the 5N exon of their *SCN1A* gene, leading to a non-functional protein (Fletcher *et al.*, 2011; Gazina *et al.*, 2010). Therefore, rodents only express 5A Na_v1.1 channels, but conserved alternative splicing in the other sodium channel subtypes is not affected. Studies estimating the relative proportions of adult and neonatal channels of different sodium channel types in rodents have revealed conflicting data that make the “adult” and “neonatal” nomenclature misleading in some cases. For example, Gazina *et al.*, (2010) found that the Na_v1.2-6N isoform was predominant in newborn mouse brains, but for *SCN3A* and *SCN8A* the A isoform was more abundant at the same time point. Higher abundance of the 5A isoform of *SCN8A* in newborn or early life rodent brains has also been found in other studies (Raymond *et al.*, 2004; Mechaly *et al.*, 2005). Gazina’s results were in accordance with Gustafson *et al.*, (1993) for *SCN2A*, but not for *SCN3A*, with the latter suggesting that Na_v1.3-6N levels are higher in newborn rats and get replaced by the adult isoform by P10. Yet, for all *SCN2A*, *SCN3A* and *SCN8A*, the 5N/5A ratio did gradually decrease with development.

Alternative splicing of exon 5 in *SCN1A* is partly modulated by the activity of the splice-modifier protein Nova 2. Overexpression of Nova 2 increased the proportion of 5N transcripts relative to 5A for *SCN1A* (Heinzen *et al.*, 2007). Similar developmental pattern expression for *SCN1A*, *SCN2A*, *SCN3A* and *SCN8A* in mice has suggested that Nova 2 or other splicing factors may be commonly involved in alternative splicing of all four genes (Gazina *et al.*, 2010). Nova 2 is thought to coordinate splicing in genes expressed in inhibitory neuronal synapses (Ule *et al.*, 2005), which is in line with a role of the *SCN1A* gene in inhibitory GABAergic interneurons.

For *SCN1A*, the relative proportion of 5A and 5N transcripts in humans can vary significantly from population to population and also between individuals. A major genetic cause that can modulate alternative splicing in exon 5 in humans is a single nucleotide polymorphism (SNP) located in the sequence encoding an intron of the *SCN1A* gene between exons 5A and 5N (Figure 1.21). A SNP is a common single nucleotide variation in the DNA sequence between individuals. It is different

from a mutation in the sense that SNPs occur in a much higher percentage of the population than mutations do, i.e. >1%. The particular SNP adjacent to exon 5N in the *SCN1A* gene (rs3812718) is located in the 5' splice donor site of the 5N exon (Figure 1.21, from Tate *et al.*, 2005). Individuals can either carry the ancestral G allele or the alternative A allele. The frequency of each allele in the population is fairly similar, i.e. about 0.45 for G and 0.55 for the A allele (Tate *et al.*, 2005). The major allele (A) is predicted to disrupt the consensus sequence of the 5N exon, thereby reducing its expression relative to the adult exon (5A) (Tate *et al.*, 2005; Heinzen *et al.*, 2007). On the other hand, the G allele is more “permissive”, i.e. allowing more efficient splicing of the 5N exon.

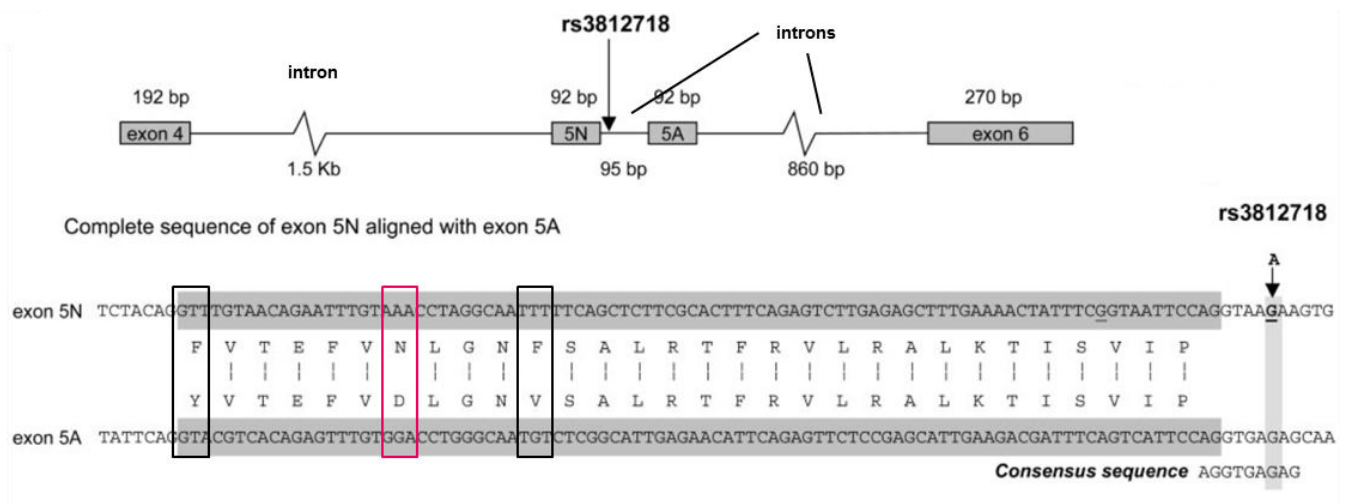


Figure 1.21: Position of the *SCN1A* G>A (rs3812718) polymorphism at the intron between exons 5N and 5A.

Genomic sequence of *SCN1A* between exons 5N and 5A, and exact location of the rs3812718 polymorphism at the consensus sequence. Amino acid changes between the Na_v1.1-5N and -5A exons are indicated in boxes. In red box is the conserved amino acid change across different channel subtypes. Figure redrawn from Tate *et al.*, 2005.

Studies quantifying the proportion of 5N splicing among different SNP genotypes (AA, AG and GG) have given different and sometimes conflicting results. Tate *et al.*, (2005) estimates 5N levels to be relatively low (~9.5%) in adult brains without a history of epilepsy, while there was no

significant difference between different genotypes. On the other hand, Heinzen *et al.*, (2007) used both quantitative PCR in human brain tissues as well as minigene assays to measure the effect of the SNP in relative exon proportions. Brain tissues showed a 5N splicing proportion of 0.7%, 28% and 41% for AA, AG and GG genotypes respectively. The minigene assay gave values of similar magnitude (7.5%, 40% and 51% respectively). Overall, the proportion of 5N splicing between studies was quite different. Furthermore, one of them also showed increased 5N splicing with increased G retention (AA<AG<GG) (Heinzen *et al.*, 2007), while in the other study 5N splicing was unaffected from genotype (Tate *et al.*, 2005). However, Tate *et al.*, (2005) used RT-PCR to determine the 5N percentage spliced, whereas Heinzen *et al.*, (2007) used quantitative PCR, which is more accurate, since it gives an absolute rather than a relative value. Therefore, an incremental increase in %N splicing occurring with increased G allele retention on the phenotype is likely to reflect an accurate measure. This project seeks to clarify the molecular mechanism linking a single amino acid in the extracellular loop to the voltage sensitivity and AED binding, by comparing the biophysical characteristics of three different channels that share the alternative splicing event in different conditions and modelling their behaviour.

1.4.3 SCN1A splicing and epilepsy

About 30% of epilepsy patients are resistant to one or more AEDs (Kwan & Brodie, 2000). Since VGSCs are considered to be the main targets of AED action, it has been suggested that pharmacoresistance in some patients may in part arise from genetic variations in sodium channels, which in turn may result in altered electrophysiological properties between individuals. Remy *et al.*, (2003) recorded sodium currents from hippocampal neurons derived from human brain tissues of both AED-resistant and AED-responsive patients. Neurons from AED-resistant patients showed loss of carbamazepine sensitivity to use-dependent block or in-vitro seizure activity, whereas neurons from responsive patients were sensitive to carbamazepine activity under the same conditions. The question that arose from this is: which mechanisms might influence a differential response of sodium channels between individuals? The evolutionary conserved alternative splicing of the voltage sensor spanning exon in VGSCs is an attractive candidate for such a mechanism.

This is because the voltage sensor region can affect the gating properties of the channel, as well as the channel's interaction with AEDs. Further supporting this, alternative splicing at the voltage sensor region in the insect sodium channel altered the sensitivity of the channel to pyrethroid insecticides (Tan *et al.*, 2002; Loscher *et al.*, 2009).

The splicing in domain I in the *SCN1A* gene is influenced by a G>A single nucleotide polymorphism (SNP) at the intron sequence between exons 5N and 5A. GG genotype individuals have a higher proportion of the 5N exon spliced compared to AA (Heinzen *et al.*, 2007), therefore they contain a higher proportion of 5N Na_v1.1 channels. A pharmacogenetic study compared patients' SNP genotypes with their maximal dosage of antiepileptics phenytoin and carbamazepine (Tate *et al.*, 2005). A significant association was found for people with the AA genotype correlated with a higher maximal dosage of carbamazepine compared to GG patients. A similar – albeit weaker – association was found for phenytoin. AG heterozygotes were in the middle, since they were prescribed with higher max doses of carbamazepine and phenytoin than GG patients and lower doses than AA homozygotes on average. This association was not replicated for phenytoin at maintenance doses in a second smaller study involving 71 Chinese patients (Tate *et al.*, 2006). Yet, within that patient group they found a marginally significant association when looking at phenytoin serum levels. Further supporting the link between the G>A SNP and altered drug response, Abe *et al.*, (2008) found, the percentage of AA genotype was significantly higher compared to AG and GG in a group of carbamazepine-resistant patients, while also insignificantly higher in (generally speaking) AED-resistant patients. More recently, a study performing transcranial magnetic stimulations (TMS) in healthy volunteers showed a significantly bigger increase in the cortical silent period (CSP) of GG compared to AA homozygous patients after carbamazepine administration, with no other difference at baseline (Menzler *et al.*, 2014). That is the first association study indicating that the polymorphism might affect carbamazepine response via specifically affecting GABAergic cortical interneurons.

However, these results should be dealt with caution, since this association has not always been replicated. Kwan *et al.*, (2008) and Haerian *et al.*, (2013) both failed to show any correlation between antiepileptic multidrug resistance in epilepsy and the SNP genotype. Another study involving 369 cases with pharmaco-resistant focal epilepsy syndromes did not find a correlation between the genotype and carbamazepine maintenance dosage (Zimprich *et al.*, 2008). Finally, an additional recent study found no association between the SNP genotype and AED responsiveness

(especially to carbamazepine) (Manna *et al.*, 2011), similar to an even more recent one that failed to show an association with carbamazepine response in North Indian epilepsy patients (Kumari *et al.*, 2013).

Apart from a potential role in altered AED response, the G>A SNP has also been linked with a possible predisposition to epilepsy and more specifically to febrile seizures. Buchner *et al.*, (2003) was the first to suggest that splicing differences and altered expression of sodium channel splice variants (in this case in Na_v1.6) can modify both the severity of inherited disorders, such as epilepsy, and also influence disease susceptibility. Concerning *SCN1A*, a study involving a cohort of Austrian and German patients suffering from febrile or afebrile seizures showed a significant association between febrile seizure incidence and the AA genotype, while epilepsy in general did not correlate with the SNP genotype (Schlachter *et al.*, 2009). However, this association was not replicated in a similar study in Australian patients (Petrovski *et al.*, 2009). Yet, in support of the first study, a newer study by Le Gal *et al.*, (2011) did find an association between the SNP in question and febrile seizures in a new cohort of patients. Statistical significance was also maintained when results from this study were combined with data from both previous studies, further supporting a correlation between the AA genotype and predisposition to febrile seizures. More recent studies also look in favour of an association of this polymorphism and epilepsy susceptibility (Kumari *et al.*, 2013). Baum *et al.*, (2014) has also reported a significant association between the G allele and decrease of epilepsy risk in Malay, Indian and Chinese patients, while also revealing an age component of that association, since at the Hong Kong subgroup of the study analysis revealed an association only in younger patients (<16 years old), but not in older ones. A meta-analysis done by the same group including this and previous reports still held that association, as also did a meta-analysis performed by Tang *et al.*, (2014), demonstrating an association between the polymorphism and susceptibility to febrile seizures. Interestingly enough though, at the same study, an association with epilepsy *without* febrile seizures was only seen in Caucasian patients, but not in Indian or Chinese.

1.4.4 Possible reasons for differences between studies

Taking all studies of this SNP mentioned above together, the link between the G>A SNP and altered AED dosage in epilepsy patients or febrile seizure predisposition remains controversial. Results between studies are usually mixed, even conflicting in many cases. A major issue that arises with AED response studies is that several of them look at the maximum or maintenance dosage in patients (Tate *et al.*, 2005; Zimprich *et al.*, 2008), but there is a number of factors that can affect AED pharmacokinetics/dosage other than the SNP in question. Genetic variations in drug-metabolizing enzymes (e.g. P450 CYP2C9, CYP2C19, CYP3A4) that are known to be involved in AED metabolism can affect drug pharmacokinetics, as shown in the case of phenytoin in multiple studies (Odani *et al.*, 1997; Mamiya *et al.*, 1998; Aynacioglu *et al.*, 1999; Hung *et al.*, 2004). Furthermore, genetic variability in metabolizing enzymes can also affect drug dosage requirements, as seen for both phenytoin (Steijns *et al.*, 2001) and carbamazepine (Tate *et al.*, 2005). An additional confound is the use of patients from different ethnic origins (Austrians/Germans, Australians, Chinese). Genetic differences between different ethnic backgrounds, like different polymorphisms in drug-metabolizing enzymes, might lead to differences in drug levels between subjects that could obscure a potential significant difference in AED responsiveness. Tate *et al.*, (2006) have actually reported a significant difference in allele frequency of the phenytoin-metabolizing enzyme CYP2C19 between a Chinese and European population, which is consistent with population-specific differences in drug metabolism. In further support to this notion, Lakhan *et al.*, (2009) also reported population-specific differences for the role of the multidrug transporter gene ABC1 in drug resistant epilepsy. Therefore, it is possible that observed discrepancies between association studies may be partly attributed to genetic factors other than the SNP in question, which can differ from population to population or even between individuals from the same ethnic background. In an effort to partly control for that, Tate *et al.*, (2006) tried to isolate the pharmacodynamic determinant of the G>A polymorphism from the AED pharmacokinetic factors by looking at serum drug levels instead of maximum or maintenance AED dose. This approach did reveal a marginally significant association with the G>A SNP genotype for phenytoin dosage, when previously it had failed to show a similar association when phenytoin maintenance doses were used.

An important additional reason for mixed results in association studies is that a single SNP will probably have little contribution on drug response on its own. Apart from influences from other genes discussed before, non-genetic factors can also influence the impact of the G>A polymorphism and possibly mask its effects. As suggested in Loscher *et al.*, (2009): “the inherited component of the response to drugs is typically polygenic”, with the G>A polymorphism having only a limited contribution to a polygenic inheritance. As a consequence, this makes it even harder for association studies to catch such correlations that do not correct also for non-genetic factors that may lack the power to find correlations for a weak genetic effect. For example, Tate *et al.*, (2006) looking for an association between the *SCN1A* G>A genotype and phenytoin maximum or maintenance dose, did not find a significant relationship, not even a trend as in their previous study (i.e. AA>AG>GG, Tate *et al.*, (2005)). Yet, when patient body mass was taken into account as an affecting parameter and was corrected for, a genotype trend was revealed, although it still did not reach statistical significance. This indicates that if the differences between genotypes are subtle then even small non-genetic parameters taken or not taken into account (like for e.g. body mass) can make a difference in revealing a trend or a significant correlation in association studies.

Furthermore, the G>A polymorphism in *SCN1A* only influences a single AED target, yet AEDs can also work through multiple targets. AEDs act similarly on sodium channel subtypes other than Na_v1.1. As a consequence, the contribution of an *SCN1A*-specific SNP on AED dosage might be smaller than expected and therefore more difficult to be detected in association studies. In addition, among other targets, carbamazepine may also bind acetylcholine receptors (Picard *et al.*, 1999). Genetic variations and mutations in the $\alpha 4$ and $\beta 2$ subunits of acetylcholine receptor channels have been linked to a rare form of epilepsy called named dominant nocturnal frontal lobe epilepsy (ADNFLE), as well as to altered sensitivity to carbamazepine compared to the wild-type channels (Picard *et al.*, 1999). This indicates that VGSCs constitute only a part of AED targets, not to mention that AEDs act also equally on sodium channel subtypes other than Na_v1.1. As a consequence, the contribution of an *SCN1A*-specific SNP on AED dosage might be smaller than expected and therefore more difficult to be detected in association studies.

Another point of caution in drug dosage association is whether AEDs are studied as one big group, for example in patients that receive a polytherapy treatment, or if drugs are assessed individually. Kwan *et al.*, (2008), who found no association between the G>A polymorphism and AED response, admits to have assessed AEDs as one big group rather than individually and this was

also the case in the Haerian *et al.*, (2013) study. This approach may have masked any potential associations between this SNP and individual drugs within these groups. In support to this argument, Abe *et al.*, (2008) found a significant correlation between the AA genotype and carbamazepine-resistant patients, but the correlation became insignificant when compared to generally AED-resistant patients. This finding leaves the potential for the correlation with AED response to be drug-specific. This is also further supported by the more significant association found for carbamazepine in comparison to phenytoin in Tate *et al.*, (2005). However, in opposition to that, a functional heterologous expression study on 5A and 5N Na_v1.1 channels showed a different sensitivity of the two variant channels to phenytoin but not to carbamazepine (Thompson *et al.*, 2011). This result, although it appears opposite to the previous association studies that suggest a higher difference between variants with carbamazepine treatment, is in principle in line with a drug-specific association of the SNP genotype and AED response.

As for Zimprich *et al.*, (2008), who failed to find an association between the SNP genotype and carbamazepine dosage, they used a cohort of patients that was suffering from focal epilepsy syndromes. Such syndromes may arise from completely different aetiology than one linked with the *SCN1A* gene and the SNP in question. Epilepsy is a heterogeneous disorder and aetiology will differ from patient to patient and – even more – from one group of patients to another. When studying a functional polymorphism on the *SCN1A* gene, the strongest correlations are likely those in epilepsy incidents and types that are influenced by one particular gene. These syndromes would probably include GEFS+ and SMEI, conditions that have directly been linked to *SCN1A* mutations/defects, so that an association of the G>A SNP with the severity of these disorders would benefit from a direct mechanistic link. This could be another important reason why some studies fail to show an association while some others do. Ideally, cohorts of patients should be chosen based on the aetiology (or at least “similarity”) of their epileptic syndromes, for example patients suffering from febrile seizures or SMEI patients etc. In fact, it is not too surprising that in the search for an association between the G>A polymorphism and seizure predisposition, it is primarily febrile seizure patients that show a correlation (Schlachter *et al.*, 2009; Le Gal *et al.*, 2011). As Schlachter *et al.*, (2009) states “the sodium channel gene *SCN1A* is arguably the most important gene found for Mendelian forms of febrile seizure syndromes so far”. Yet, this does not ignore the fact that febrile seizures can show complex inheritance beyond *SCN1A*, usually with a

polygenic basis, which may partly explain the lack of association between the G>A SNP and febrile seizure predisposition in Petrovski *et al.*, (2009).

Finally, it is worth noting that it seems unlikely for different proportions of 5A and 5N channels on their own, to confer febrile seizures in patients. The imposition of a proepileptic mutation on top of the SNP genotype might be processed differently, depending on whether this mutation is applied on a 5A or a 5N channel. Different *SCN1A* mutations may affect the channel's biophysical properties and AED response to different extents, which might be splice variant-specific. Thereby, proepileptic mutations in the *SCN1A* gene may result in a different functional effect, depending on whether they are expressed in a 5A or 5N context. Since different patients will probably have suffer from different mutations in the *SCN1A* gene and since each mutation may have different effects on the two *SCN1A* splice variants, this might as well account for some of the differences found between association studies, and between patients, even those carrying the same mutations.

1.4.5 5N overexpression in epilepsy

A separate link between relative proportions of alternatively spliced N and A channels and epilepsy has come from studies suggesting that N channel levels are upregulated after seizures, not only in the case of Na_v1.1, but also in other neuronal sodium channels where this splicing event is conserved. Gastaldi *et al.*, (1997) showed a transient upregulation for about 12 hours of the neonatal isoform in Na_v1.2 and Na_v1.3 channels in hippocampal neurons of a kainite-induced rat epilepsy model. A much longer-lasting increase of Na_v1.2-6N and Na_v1.3-6N levels compared to their adult isoforms was also seen in the dentate gyrus of a status epilepticus rodent model (Aronica *et al.*, 2001). These rodent models are not informative for *SCN1A* 5A/5N ratios, since rodents do not have a functional 5N copy (Tate *et al.*, 2005; Gazina *et al.*, 2010). A human study using brain tissues taken after surgery for refractory epilepsy showed an upregulation in Na_v1.1-5N levels in the temporal lobe relative to the hippocampus, which was significant only for patients with the “permissive” GG SNP genotype and not for AA or AG genotype patients (Tate *et al.*, 2005). A follow-up study (Heinzen *et al.*, 2007) did not find an association between increased Na_v1.1-5N levels and seizures in human brain tissues derived from mesial temporal lobe epilepsy

patients. On the contrary, neonatal transcripts showed a slight downward trend in relation to comparable tissues. A still unpublished human study within our lab comparing “epileptic” tissue samples taken out during surgery with non-age matched controls from the Parkinson’s brain bank showed a significant increase in N transcripts in epilepsy for all *SCN1A*, *SCN2A* and *SCN8A* genes. Therefore, although several studies suggest that neonatal channel levels are increased by seizures in most channels where this splicing event is conserved, results are still inconclusive. A study in *Drosophila* supports an activity-dependent regulation of this splicing event. Lin *et al.*, (2012), looked at alternative splicing of exons K and L in domain III of a *Drosophila* Na_v channel, at an equivalent position with the 5A/5N splicing event in domain I in humans. They found that increased synaptic activity promotes splicing towards exon L over exon K, which in turn may lead to seizure incidents. Therefore, in the same way that increased synaptic activity can bias a splicing decision in *Drosophila* Na_v channels, epilepsy could similarly result in more inclusion of the N transcript in human and rodent neuronal sodium channel subtypes.

1.4.6 Functional studies for Na_v transcript variants

Despite the high conservation of this splicing event among all neuronal TTX-sensitive sodium channel types, the importance of this splicing in neuronal functioning is still not clear. The conservation of this site is not only particularly striking but also uncommon. Gerstein *et al.*, (2014) has recently indicated that orthologous genes rarely share the same exon-intron structure or alternative splicing across three different species (humans, worms, flies), suggesting that alternative splicing is not generally well-conserved. In fact, apart from conservation, exon duplication and alternative splicing of this linker region has also been suggested to have arisen in other clades (for eg. insects) and related ion channels (eg. Ca²⁺ channels) as a means of repeated cases of convergent evolution, rather than pre-existing in a common ancestral gene (Copley, 2004).

The two different variants (neonatal and adult) have been suggested to differ when examined in individual Na⁺ channel subtypes in a variety of ways under particular recording conditions in non-

neuronal cells. In Na_v1.2 channels, which are preferentially expressed in CNS excitatory neurons early in life, splicing affects recovery from inactivation and voltage dependence of inactivation in HEK293T cells (Xu *et al.*, 2007), but that difference was not seen in another study, where β 2 subunits were co-expressed (Liao *et al.*, 2010). In Na_v1.7 channels, predominantly found in pain-mediating neurons in the PNS, splicing can modify the channel's association with β -subunits (Farmer *et al.*, 2012), while in tsa201 cells the adult variant showed slower development of inactivation as well as modifications in phosphorylation (Chatelier *et al.*, 2008). Another study using a different intracellular recording solution (CsCl instead of CsF) showed an increased rump current for the adult isoform compared to the neonatal as a result of a mutation at the inactivation gate (Jarecki *et al.*, 2009). Another human mutation in Na_v1.7 linked to erythromelalgia has been shown to differentially regulate inactivation in neurons between the two isoforms, thereby linking this splicing to differential disease course (Choi *et al.*, 2010).

In paralogue channels in other phyla, the homologous splicing event has been found to modify channel pharmacology in cockroaches (Tan *et al.*, 2002) and also to reduce fast inactivation in *Drosophila* (Lin *et al.*, 2012).

With relation to Na_v1.1 and epilepsy, the physiological purpose of a possible increase in N transcript levels in TTX-sensitive neuronal sodium channels is still unknown. No clear conclusion can still be drawn about whether this alternative splicing event leads to functional differences between neonatal and adult sodium channels that can make epilepsy worse, or whether it is a physiological response that may reduce future seizure occurrence. In order to answer this question and also try to understand what effect may this splicing have in epilepsy predisposition and in response to AEDs, the functional properties of the neonatal and adult channel variants need to be determined, not just for Na_v1.1 but also for all sodium channel subtypes where this splicing event is conserved. To date, very few studies have looked at the biophysical properties of 5A and 5N Na_v1.1 channels in order to delineate what is the effect of splicing at a functional level for this channel subtype. Thompson *et al.*, (2011) looked at functional properties and the AED response of wild-type Na_v1.1-5A and Na_v1.1-5N channels, transiently transfected in HEK293T cells at room temperature (20 – 22°C). In these conditions, there were no differences between the two isoforms in voltage dependence of activation and inactivation or recovery from inactivation. However 5N channels showed a higher sensitivity in blockade from phenytoin and lamotrigine compared to Na_v1.1-5A. In contrast, sensitivity to carbamazepine was the same for the two isoforms. A study

from our group looked at several functional features of Na_v1.1-5A and Na_v1.1-5N channels in HEK293T cells, while also comparing different recording conditions that could affect channel behaviour (Fletcher *et al.*, 2011). Na_v1.1 channel isoforms were compared at either room (20 - 22°C) or physiological (~37°C) temperatures, using a caesium fluoride (CsF) or a caesium chloride (CsCl) based intracellular solution, while also testing the effect of β-subunit co-transfection or G-protein activation. Results from this study revealed that recording conditions can significantly change the functional consequences of the two splice isoforms, with 5N channels appearing more sensitive than 5A to changes in temperature and major intracellular ion composition. The biophysical properties of the two splice variant isoforms were condition-dependent. For example, at room temperature and using a CsF-based intracellular solution, Na_v1.1-5N channels inactivated more rapidly than Na_v1.1-5A channels. On the other hand, substituting CsF for CsCl caused the opposite effect, with the 5N isoform channels now inactivating more slowly than 5A. When recording at physiological temperatures (37°C) with CsCl-based intracellular solution, the inactivation rate was exactly the same for both channel isoforms, as were their voltage dependence of activation and inactivation, current densities and proportion of persistent current. This finding indicates that there should be much caution when comparing electrophysiological data for Na_v1.1 splice isoforms in different conditions, since data may be skewed by experimental conditions.

Recordings at 37°C can maybe better recapitulate human body temperature conditions. Yet, these conditions are different to those most often used in electrophysiological recordings of heterologously expressed channels. Moreover, intracellular CsCl and HEK293T cells cannot precisely mimic the sodium channel's native environment within a neuron. VGSC α-subunits are suggested to interact with β-subunits in neurons, which can affect their membrane localization and/or modify their functional properties (Farmer *et al.*, 2012). Many functional studies of VGSCs co-transfect one or more β-subunits, usually β1 and β2, together with the α-subunit and results have been both condition and cell type-specific (Isom *et al.*, 1995; Meadows *et al.*, 2002; Qu *et al.*, 2001). In Fletcher *et al.*, (2011), at physiological temperature, β1 and β2 co-expression with the α-subunit did not reveal any differences between Na_v1.1-5A and Na_v1.1-5N channels. The same was also true for general G-protein activation within HEK293T cells using GTPγS, showing that, at physiological temperatures, modulation of the 5A and 5N isoforms by G-proteins is not significantly different.

Only one functional parameter was found to be significantly different between Na_v1.1-5A and Na_v1.1-5N channels under physiological temperature recording conditions with CsCl-based intracellular solution and that was recovery from fast inactivation. 5N channels were found to recover significantly more quickly from fast inactivation than their 5A counterparts (Figure 1.22, from Fletcher *et al.*, 2011). This difference was most pronounced for shorter recovery time intervals, and was lost at longer recovery intervals (200 ms onwards). This difference in rate of recovery was attributed to a single amino acid change between the two splice variants, which replaces a negatively charged aspartate residue into a neutrally charged asparagine, D207N. The other two flanking residues that differ between the two splice variants of Na_v1.1 do not seem to play a role in this recovery from inactivation difference. No difference in recovery from inactivation was found in Thompson *et al.*, (2011), however in that study recordings were made at room temperature (20 – 22°C) and using a CsF-based intracellular solutions. Therefore, the different recording conditions (which are also further away from physiological temperature) might have masked a potential difference.

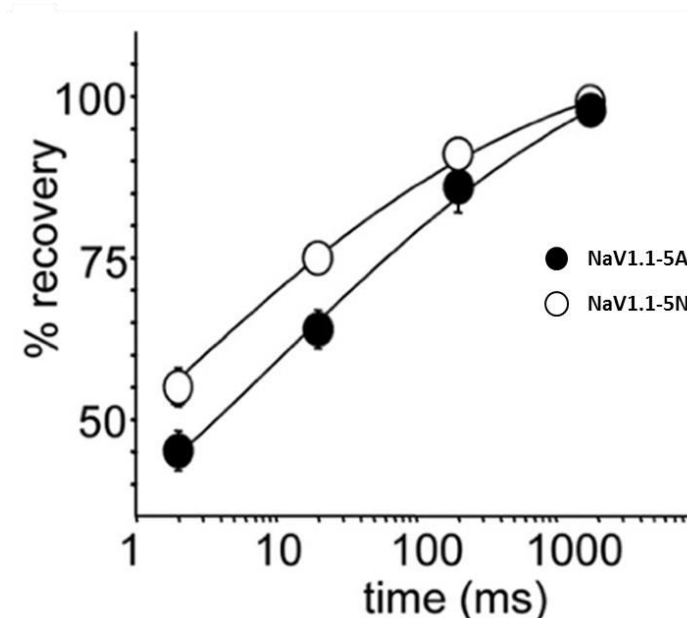


Figure 1.22: Faster recovery from inactivation for Na_v1.1-5N channels.

Na_v1.1-5N channels (open circles) recover more quickly from inactivation for shorter interpulse durations than Na_v1.1-5A channels (black circles) in whole-cell patch clamp recordings in HEK293T cells at 37°C. Figure modified from Fletcher *et al.*, 2011.

As seen from Fletcher *et al.*, (2011), electrophysiological recordings to characterize the biophysical properties of Na_v1.1-5A and Na_v1.1-5N channels and potential differences between them can be condition-dependent. The only difference detected in the CsCl-based intracellular solution and physiological temperature recording conditions was a faster recovery rate from inactivation for Na_v1.1-5N channels compared to 5A for shorter recovery time intervals. This difference was obscured under different recording conditions in another study (Thompson *et al.*, 2011). Since the differences between Na_v1.1 channel isoforms have been found to specific to recording conditions, we used the difference in recovery from inactivation found in Fletcher *et al.*, (2011) as a starting point in order to characterize the parameters that underlie this functional effect. Our aim was to illustrate how this difference between splice isoforms might be masked or augmented depending on recording conditions and stimulation parameters. We also aimed to investigate how the difference altered channel availability in conditions that mimic high-activity neuronal firing, for example, the kind of activity that occurs during an epileptic seizure. Any difference in these conditions might indicate that the biophysical properties of Na_v1.1-5A and 5N isoforms could contribute to physiological and pathophysiological differences. Such a finding could provide a mechanism on a biophysical/functional level, contributing to the difference in epilepsy predisposition that may be seen due to different 5A/5N relative proportions in some epilepsy patients.

Recovery from fast inactivation is a biophysical property of VGSCs that is directly affected by binding of AEDs, which make recovery significantly slower. Since Na_v1.1-5A and 5N channels have been linked with altered drug dosage to some AEDs (Tate *et al.*, 2005; 2006; Abe *et al.*, 2008; Thompson *et al.*, 2011), and since the biophysical property that distinguishes the two channel isoforms is directly affected by AED usage, another aim of this study is to determine whether recovery from inactivation is modulated differently between Na_v1.1-5A and Na_v1.1-5N channels in the presence of two widely used AEDs, phenytoin and carbamazepine. A potential differential modulation of a key functional property affected by AEDs between the two splice isoforms could provide a mechanistic explanation for association between AED dosage and the SNP in *SCN1A* that has been suggested by several pharmacogenetic studies.

Also, up to today and to our knowledge, no unifying functional impact of this splicing event has been suggested among the different sodium channel subtypes. Since the alternatively spliced linker region includes a voltage-sensing part of the channel, it seems possible that alternative splicing at

this site could have an adaptive significance, finely modulating the channel's gating properties and hence modifying the physiology of the neurons that the different isoforms are expressed in. On top of that, the fact that this exon duplication event seems to have arisen independently through convergent evolution between different kingdoms as well as between different ion channels (including subtypes of the same channel family as in VGSCs) could indicate a possible evolutionary drive for also a common functional impact between the alternatively spliced variants, perhaps slightly adapted to the predominant area of expression of each channel subtype. Actually, a parallel assessment of isoform functional properties across different sodium channel subtypes may reveal the evolutionary drive for the convergent nature of this splicing event by unmasking a possible unifying functional difference. Furthermore, extrapolation of this study from heterologous expression systems to each channels' native neuronal milieu might fill in the link between splicing in this area of the channel and effect on neuronal behavior. So, another aim is to ask whether the functional consequences of the conserved alternative splicing are also conserved in other neuronal sodium channels (in this case $Na_v1.2$ and $Na_v1.7$). By potentially extrapolating this effect in additional channels, this could provide evidence for this functional difference contributing to the conservation of alternative splicing in neuronal sodium channels.

1.4.7 Dynamic-Clamp as a direct link to epileptiform bursts

The biggest part of this study is characterizing the biophysical and functional differences between the neonatal and adult isoforms, initially in HEK293T cells and then in cultured neurons. Yet, voltage-clamp and current-clamp recordings, although quite informative as analysis tools, cannot feature the direct relevance of this splicing event to brain physiology and possible circuit pathology. The potential link of the G>A splicing event in *SCN1A* and possible differential predisposition to febrile seizures has already been discussed. In order for that association to be directly attributed to the activity of $Na_v1.1-5A$ and 5N variants, this would require the link of single cell response to a bigger brain network. Slice whole-cell or field recordings, where the relative expression of the two variants would be endogenously or exogenously manipulated, could potentially fill that gap. Yet, endogenous manipulation is impossible in rodents, since they do not

express the neonatal isoform, while on the other hand, exogenously transfecting the two variants in vivo in order to do slice recordings is an extremely difficult and challenging task. As a way to try to directly correlate single cell response of either $Na_v1.1-5A$ or $5N$ expressing cultured interneurons to broader network epileptic activity, dynamic-clamp recordings from single neurons can be used as a useful alternative. Dynamic-clamp is widely known as a way to simulate conductances in cells. Hence, it is also widely referred to as “conductance-clamp” (Yang *et al.*, 2015), since a command conductance is given initially on a cell and then the amplifier is injecting the appropriate current to the cell to keep the conductance steady (i.e. “clamped”) at the set value (Figure 1.23).

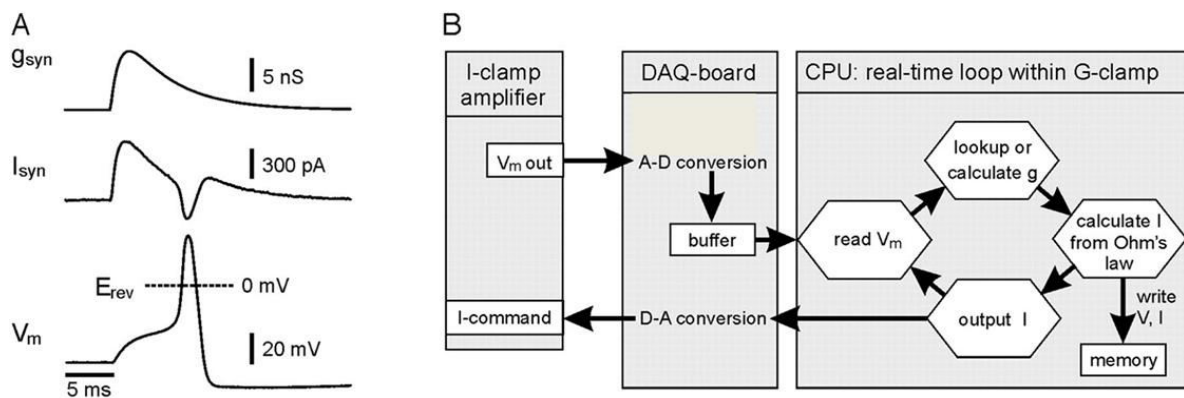


Figure 1.23: An overview of dynamic-clamp principles

A. building a dynamic clamp is based on the reciprocal interaction between the synaptic conductance command (g_{syn}), synaptic current injected (I_{syn}) to keep conductance clamped, and membrane potential of the cell (V_m). As current is injected into the cell to keep the conductance at the command value, the cell starts getting depolarized, so that less current is now needed to follow the g_{syn} . This is mostly evident when depolarization reaches threshold, so that an AP is fired, which vastly increases the cell’s conductance. Therefore, the I_{syn} needs to compensate for that sudden increased conductance due to the AP firing and actually inject negative current at this point in order to keep the g_{syn} steady (i.e. “clamped”). **B.** Schematic of hardware interactions and calculation of current injected from the amplifier through the real-time feedback loop within the G-clamp. The amplifier is recording the V_m output of the cell at a user-specified rate, which is then digitized and stored in an onboard buffer at the DAQ-board. The G-clamp system then continually reads the V_m , looks up or calculates the command conductance value (G), calculates the current (I) needed to keep G steady from Ohm’s law ($V=I R$) and then this value is written to memory and converted to a current command signal which is fed back to the cell through the amplifier. This process is then ongoing on a feedback loop, with the system injecting the appropriate current to keep conductance clamped. Figure redrawn from Kullmann *et al.*, 2004.

Dynamic-clamp can therefore be used to simulate the synaptic activity, in terms of changes in conductance, of a neuron's response under an epileptic network using in-vitro models of epilepsy, such as the zero Mg^{2+} (Deshpande *et al.*, 2007) or the 4-aminopyridine model (Gonzalez-Sulser *et al.*, 2012). This simulated epileptic conductance activity, which reflects synaptic response of a broad epileptic network, could then be used as an activity template for either neonatal or adult channels in neurons in order to validate how each of them affects neuronal behavior under broader epileptic network conditions.

1.5 Experimental aims

Delineating the difference between $Na_v1.1$ isoforms

To measure the difference in recovery from inactivation between $Na_v1.1$ 5A and 5N channels in HEK293T cells during shorter interpulse durations.

To assess the effect of inactivating prepulse length and voltage dependence on the difference in inactivation recovery between $Na_v1.1$ 5A and 5N channels.

To test if this difference can impact channel availability during high frequency activity, which may occur during epileptic events.

Identifying conserved differences in other channels

To evaluate if this difference in inactivation recovery is also conserved in closely related Na^+ channels bearing the same splicing event, namely $Na_v1.2$ and $Na_v1.7$.

To examine how fast inactivation recovery is affected in the presence of AEDs like phenytoin and carbamazepine between the two isoforms.

Testing the significance of splicing on neuronal physiology

To determine if this splicing event can affect neuronal properties when channels are expressed in their natural milieu (interneurons for Na_v1.1, excitatory neurons for Na_v1.2).

To examine if different neuronal backgrounds (Na_v1.1 in excitatory neurons, Na_v1.2 in interneurons) can affect the outcome of the splicing event.

To assess if the two Na_v1.1 isoforms can alter the way that interneurons respond during simulated epileptiform activity using Dynamic-Clamp.

Chapter 2: General Materials and Methods

2.1 Molecular Biology

2.1.1 LB Broth, LB agar and Antibiotic solutions

20g of LB Broth (Luria Bertani medium – Tryptone, 10 g; Yeast extract, 5 g; NaCl, 5 g, Sigma) was dissolved in 1L ddH₂O, autoclaved and stored at room temperature. 17.5g of LB agar (LB Broth to Agar ratio: 1.67 to 1, Sigma) were dissolved in 500 ml ddH₂O, autoclaved and stored at room temperature. For LB plate preparation, agar was melted and then cooled down below 40°C before addition of the proper antibiotic (ampicillin or ampicillin + tetracycline, see also table 2.1). Agar was poured into 10cm plates (VWR International), allowed to set and either used on the day, or stored at 4°C for up to 1 month.

<u>Antibiotic</u>	<u>Stock concentration</u>	<u>LB agar plate concentration</u>	<u>LB Broth culture concentration</u>
Ampicillin	10 mg/ml (in ddH ₂ O)	100 µg/ml	100 µg/ml
Tetracycline	5 mg/ml (in 100% EtOH)	5 µg/ml	5 µg/ml

Table 2.1: Antibiotic concentrations for the preparation of agar plates and bacterial culture media

2.1.2 DNA constructs and Cloning

Human sodium channel cDNAs are notoriously difficult to maintain in bacteria (Feldman & Lossin, 2014), so special care was taken in the growth and propagation of our clones. Human *SCN1A* transcript variant constructs, already incorporated into the pcDM8 vector, were transformed into TOP10/P3 *E.coli* cells (Life Technologies). These bacteria contain a low copy number plasmid, P3, with incorporated tetracycline- and ampicillin-resistance genes. During normal *E.coli* life cycle these genes carry amber mutations (stop codons), which render them inactive. Upon successful transformation, the pcDM8 vector encodes the supressorF gene, which can nullify these amber mutations, so that antibiotic-resistance genes are switched on, thereby inducing bacterial resistance to these antibiotics. The *SCN2A* and *SCN9A* transcript variant constructs are in pcDNA3 or pcDNA3-derived vectors. *SCN2A* and *SCN9A* transformants were grown under ampicillin selection only in One-Shot Stbl3 Chemically Competent *E.coli* cells (Invitrogen). *SCN1A*-transformed P3 cells were grown in ampicillin and tetracycline.

Even with Stbl3 cells (*SCN2A* and *SCN9A*), and low copy vectors (*SCN1A*), spontaneous mutagenesis of sodium channel gene constructs when propagated in bacterial cultures is not uncommon (Mantegazza *et al.*, 2005; Thompson *et al.*, 2011). To minimize this, the temperature during incubation of bacterial cultures was always kept below 30°C, and confluence of liquid cultures was not allowed to surpass an OD600nm value of 0.35.

2.1.3 Transformation of bacteria by heat shock and culture

50 µl of either TOP10/P3 *E.coli* cells or Stbl3 cells per transformation reaction were thawed on ice. 50 – 100 ng of supercoiled plasmid DNA was added and cells were incubated on ice for 30 mins. Bacteria were heat-shocked for 45 secs at 42°C (30 secs for TOP10/P3 cells) and then immediately put back on ice for 3 mins. 250 µl of pre-warmed S.O.C. medium (20 g/L Tryptone 5 g/L Yeast Extract, 4.8 g/L MgSO₄, 3.603 g/L dextrose, 0.5g/L NaCl, 0.186 g/L KCl, Sigma) was added to each transformation reaction and cells were then shaken (225rpm, IKA incubating

shaker) for 80 mins at 25°C. Bacteria were then spread on agar plates (2 plates per vial, one with 250 µl of cells and one with 50 µl of cells) containing the appropriate antibiotic selection and incubated for >24 hours at room temperature. Colony growth at this temperature is slower and it could take up to 5 days for colonies to appear. Sometimes, colonies were visible after having grown rapidly overnight even at this lower temperature. Usually these colonies carried corrupted or re-arranged plasmid DNA which was identified after sequencing. A bias towards slower-growing, more transparent, smaller colonies provided a higher rate for successful transformation of full length sodium channel cDNA constructs and a reduction in the number of false positive colonies selected. This is consistent with what is reported by other groups working on sodium channel cloning (Feldman & Lossin, 2014). It is possible that successful transformation of the Na_v-containing plasmid is toxic for bacteria, hence leading to a slow growth rate and, maybe, to a higher degree of damaged plasmid DNA.

After colonies of transformed bacteria had grown on agar plates, single colonies were inoculated in either 5 ml (Miniprep) or 1000 ml (Maxiprep) of LB Broth, containing the appropriate antibiotic concentration. Cultures were shaken at <30°C for >24 hours, until bacterial confluence (OD600nm) was near but not higher than 0.35.

2.1.4 DNA purification

DNAs were transformed and purified according to standard protocols (using QIAfilter Maxi Plasmid purification kit, Qiagen), excepting that bacteria were never incubated at higher than 30°C or to become more dense than OD600nm = 0.35. Keeping bacterial density relatively low was also important for increasing the ratio of supercoiled (sc) to open circular (oc) plasmid DNA at the end of the purification process. It has been reported that preserving a high degree of sc plasmid DNA can ameliorate plasmid transfection efficacy (Sousa *et al.*, 2009; Maucksch *et al.*, 2009). Since the purified plasmid DNA was to be used for transfection of HEK293T cells or cultured neurons, keeping a high degree of sc : oc plasmid DNA was important for supporting high transfection efficiency. Another study has also shown that to maximize the isolation of sc plasmid DNA from

QIAGENs purification kit, it necessary to conduct the whole process below 12°C (Carbone *et al.*, 2012). In contrast, performing the plasmid DNA isolation at temperatures higher than 30°C greatly increases the proportion of oc plasmid DNA compared to sc. Lower temperatures may markedly decrease the catalytic efficiency of nucleases and other enzymatic activities that can disrupt the DNA supercoiling, thereby introducing nicks that lead to an oc plasmid DNA secondary structure (Lee *et al.*, 1989; Osheroff *et al.*, 1983). Because all Na_v transcripts were maintained in low-copy number plasmids and bacterial confluence was kept relatively low in order to minimize spontaneous mutation rate, the volume inoculated was quite high (1L) in order to obtain a sufficient yield of high quantity of plasmid DNA. For Maxiprep purifications, 1000ml of LB Broth culture is more than what is recommended for a single purification, therefore each culture was split into two 500ml parallel reactions that were united in the final step. Plasmid DNA samples were resuspended in 100 µl Tris-EDTA (10 mM Tris, pH8.0; 1 mM EDTA, TE) Buffer and stored at -20°C.

2.1.5 DNA quantification

Plasmid DNA concentration was measured using a spectrophotometer (Nanodrop ND-1000, ThermoScientific). The 260/280nm absorbance ratio was used as a quality indicator, with samples < 1.6 being discarded. Proper sodium channel of the whole cDNA sequence was verified for all constructs by DNA sequencing every time after each Maxiprep preparation.

2.1.6 Mutagenesis of TTX binding site

Site-directed mutagenesis was performed in *SCN1A* 5A & 5N cDNA sequence to introduce a single amino acid change (F383S) in order to confer TTX resistance according to previous studies (Bechi *et al.*, 2012; Cestele *et al.*, 2013) using the QuikChange II XL kit according to

manufacturer's instructions (Stratagene, CA). For each reaction, the following was added: 5 µl of 10x reaction buffer, 10 ng of dsDNA template, 7.5 µl of forward and 7.5 µl of reverse primer (5 pmol/µl stock concentration), 1 µl of dNTP mix, 3 µl of QuikSolution, 1 µl of *PfuUltra* HF DNA polymerase (2.5 U/µl) and then ddH₂O to a final volume of 50 µl. The thermal cycling method was as follows: 95°C for 1 min, then 18 cycles of 95°C for 45 sec, 55°C for 45 sec, 72°C for 15 min and finally 72°C for 30 min. The homologous mutation was also performed in *SCN2A* 6A & 6N cDNA sequence (F385S) (Rush *et al.*, 2005) as well as in *SCN9A* 5A & 5N sequence (Y362S) (Choi *et al.*, 2010). The mutagenesis primers used for *SCN1A* were (in red is the nucleotide that is different from the wild-type sequence):

CTAATGACTCAGGACTCCTGGGAAAATCTTTATC (forward) and
GATAAAGATTTTCCCAGGAGTCCTGAGTCATTAG (reverse).

The mutagenesis primers used for *SCN2A* were:

CTCATGACTCAAGACTCCTGGGAAAACCTTTATC (forward) and
GATAAAGGTTTTCCCAGGAGTCTTGAGTCATGAG (reverse).

In the case of *SCN9A*, the mutagenesis primers were:

CTAATGACCCAAGATTCCTGGGAAAACCTTTAC (forward) and
GTAAAGGTTTTCCCAGGAATCTTGGGTCATTAG (reverse).

All mutagenesis primers were designed and characterized using the PrimerX online software (http://www.bioinformatics.org/primerx/cgi-bin/DNA_1.cgi).

Transformation of the mutated constructs was performed in TOP10/P3 *E.coli* cells for *SCN1A* and Stbl3 cells for *SCN2A* and *SCN9A*. Successful mutagenesis was confirmed by DNA sequencing.

2.1.7 Colony PCR

Due to the relatively high occurrence of false positive colonies and low success rate during both cloning and mutagenesis of the Na_v-carrying plasmid, colony PCR followed by agarose gel electrophoresis was routinely used to screen a large number of colonies at once. In colony PCR

bacterial colonies are directly used as the DNA template using an initial denaturation step before the PCR reaction to lyse the bacteria and allow the primers to gain access to the cells interior and therefore to the plasmid DNA. This was the most efficient method to quickly screen most, if not all, colonies that had grown and therefore to maximize the chances of achieving a successful mutagenesis or cloning. It should be made clear that colony PCR was not used to directly identify point mutations, but rather as an initial screening method to identify whether a bacterial colony truly contained a sodium channel plasmid instead of empty plasmid. To do this, a specific part of the sodium channel cDNA was cloned using primers that were complementary to the two ends of that part of the channel's cDNA sequence, which was then amplified by PCR. If the colony contains a sodium channel insert, then the PCR reaction gives a product that runs as a clear band and at a predicted length on agarose gel electrophoresis. Colonies that were positive for insert are then grown on LB medium, minipreped and then sequenced for verification of successful mutagenesis. If the colony contains just empty plasmid (e.g. sodium channel insert lost), then no band is seen on the agarose gel and the colony is then discarded. For colony PCR, each colony to be screened was picked and dissolved in 4 μ l LB medium. Each PCR reaction then contained: 1 μ l of the dissolved colony, 2 μ l of forward recognition primer (5 pmol/ μ l), 2 μ l of reverse recognition primer (5 pmol/ μ l) and 5 μ l of HotStar Taq Mastermix (2x) (Qiagen). The thermal cycling reaction was then as follows: 95°C for 15 mins, then 24 cycles of 95°C for 30 sec, 57°C for 30 sec, 72°C for 1kb/min and finally 72°C for 10 min. After the PCR reaction, 2 μ l of 5x gel blue loading dye (Qiagen) was added on each sample and then all samples were loaded on a 1% agarose gel.

2.1.8 Agarose gel electrophoresis

Gel electrophoresis using 1% (w/v) agarose gels was used to separate and identify DNA fragments of predicted size in order to select the final candidates for DNA sequencing and verification. 1g of Agarose (Sigma) was dissolved in 100 ml x1 TAE solution (40 mM Tris, 20 mM acetic acid, and 1 mM EDTA) and boiled. After cooling down, 1 μ l of 10000x Gel Red Nucleic Acid Gel Stain (Biotium) was added and the mixture was poured into a gel electrophoresis tray with combs already loaded and was allowed to set. Before loading, the DNA samples were mixed with one

fifth total volume of 5x gel blue loading dye (Qiagen). The DNA amount loaded in each sample was 100 ng. Depending on the predicted fragment size loaded, 100 bp or 1 kb DNA ladders (NEB) were always loaded on the first loading chamber as molecular weight markers. Gels were usually run for 50 min at 90 Volts and then fragments were visualized with the use of a UV-light transilluminator.

2.2 Cell culture

All animal procedures were carried out according to the Animals (Scientific Procedures) Act 1986 on PPL 70-7684 (S.Schorge).

2.2.1 Neuronal cultures

Neuronal cultures were isolated from P0 glutamic acid decarboxylase-green fluorescence protein (GAD67-GFP) mouse pups. GAD67-GFP mice selectively express enhanced green fluorescent protein (EGFP) at the axons, soma and dendrites of parvalbumin (Pv) calretinin (CR) and somatostatin (SS)-expressing interneurons (Tamamaki *et al.*, 2003). They therefore provide a very useful tool for the identification and distinction of interneurons specifically, by simple visualization of cells under UV light. Mice that are homozygous for the GAD67-GFP transgene die before birth, while hemizygous mice are viable and fertile. Therefore, during crossbreeding, GAD-67-GFP mice were paired with wild-type mice, resulting in a 50% chance of giving a transgenic offspring. At any given litter, GAD67-GFP P0 pups have skulls that are transparent enough for the brain interneuronal fluorescence to be visible under UV-light illumination. Therefore, GAD67-GFP P0 pups were identified from wild-type ones by shedding UV light on their skull surface and monitoring fluorescent illumination by using UV goggles.

2.2.2 Preparation of coverslips for neuronal cultures

13-mm glass coverslips (VWR) were placed in ceramic racks and incubated in concentrated nitric acid (65% w/w) for at least 24 hours. Coverslips were then rinsed four times for 2 hours with distilled water and then baked overnight at 225°C to sterilize. The next day, coverslips were placed into 24-well plates and 60µl of poly L-lysine (PLL, Sigma-Aldrich, P2636) solution (1 mg/ml in borate buffer, Sigma) were applied on each coverslip and coverslips were then incubated overnight at 37°C. The following day, coverslips were washed from PLL with distilled water three times, 2 hours each. After the last wash, 1ml of Glial Medium (minimal essential medium (MEM, Sigma, M2279), supplemented with 0.6% (w/v) D-glucose (Sigma, G8769, 45% solution), 1% (w/v) Penicillin-Streptomycin (Invitrogen, 15140-122, 100x), 200 mM L-glutamine (Sigma, G7513) and 10% (v/v) horse serum (Invitrogen, 16050-122)) was added on each well and plates were placed in the incubator for up to one week until ready to use.

2.2.3 Preparation and expansion of cortical astroglial feeder layer

Hippocampal neurons were cultured on top of a mouse astroglial monolayer, in order to provide neurons with the trophic support for proper neuronal growth and survival (Kaech & Banker, 2006). There are several protocols for culturing hippocampal neurons, with or without the use of a supporting glial feed layer (Kaech & Banker, 2006), the reason this one was chosen was that it is a standardized protocol already being used routinely in the lab for culturing mouse hippocampal neurons and for electrophysiological recordings. The protocol used for isolating and expanding cortical astroglial cells from P0 mice was exactly the same as the one used in Kaech & Banker, 2006 for rats. Once flasks reached a 90 – 95% confluence, glial cells were plated on sterilized coverslips pre-treated with PLL one week before neuronal plating, with the glial medium being replaced every 2-3 days.

2.2.4 Freezing glial cells

If glial cells were not used immediately for plating, they were frozen down for later use. 90 – 95% confluent flasks were rinsed with 10 ml CMF-HBSS (Calcium-, magnesium- and bicarbonate-free Hank's balanced salt solution (HBSS, Sigma, H9394) and 10 mM HEPES buffer, pH 7.3 (Invitrogen, 15630056)). Cells were incubated for 2 min with 2 ml of 0.05% Trypsin-EDTA (1x) (Gibco/Invitrogen, 25300054) and trypsin activity was stopped by adding 8 ml of Glial Medium. Cells were centrifuged for 5 min at 2000 rpm and then resuspended in 0.5 ml Glial Medium + 0.5 ml 2x Cell-Freezing Medium (20% DMSO (Sigma, D2650) + 80% Fetal Bovine Serum (FBS, Invitrogen, 10082147) before being aliquoted in 2 ml cryotubes. These were frozen at -20°C for 2 hours and then moved to -80°C until needed for plating. After defrosting and culturing into T75 flasks for about one week, glial cells were treated as before freezing down.

2.2.5 Hippocampal neuronal culture preparation

P0 mice were decapitated and heads were washed in 3x25 ml of Wash buffer (Hank's Balanced Salt Solution (HBSS, Sigma, H9394) + 5 mM HEPES (1M, pH 7.3, Invitrogen, 15630056)). The brain was removed and hippocampi were isolated with the use of fine tweezers. Isolated hippocampi were rinsed 5 times with 5 ml Wash buffer and were then digested with trypsin type XI (1 mg/ml; Sigma, T1005) and 1% (w/v) DNase I (Sigma, D5025-150 KU) for 10 min at 37°C. Trypsinisation was stopped by adding 5 ml of Dissection solution (Wash buffer + 20% Fetal Bovine Serum (FBS, Invitrogen, 10082147)). Cells were mechanically dissociated using a series of fine Pasteur pipettes. Dissociated neurons were plated in 24-well plates at a density of 100,000 cells/well upon a glial feed layer in Neurobasal A culture medium (Invitrogen, 10888022) with B27 supplement (1x; Invitrogen, 17504044) and glutamine (25 µM; Invitrogen, 35050038) and cultured at 37°C and in 5% CO₂. Next day, a 1 µM araC (Sigma, C6645) was added to stop further glial proliferation.

2.2.6 Transfection of HEK293T cells using Lipofectamine

Heterologous expression of Na_v1.1, Na_v1.2 and Na_v1.7 (N and A) splice variants was performed in HEK293T cells (Human Embryonic Kidney cells stably expressing the SV40 large T antigen, also known as tsA201 cells) widely used in in-vitro sodium channel function studies (Thompson *et al.*, 2011, Chatelier *et al.*, 2008, Fletcher *et al.*, 2011). HEK293T cells were grown in Dulbecco modified Eagle's medium (DMEM + Glutamax, Sigma) supplemented with fetal bovine serum (10%) and maintained in a humidified 5% CO₂ atmosphere at 37°C for up to 20 passages.

One day before transfection, cells were plated in 4 well plates (Nunc, Denmark) at 20 – 30% confluence. The next day cells were transiently transfected with 0.5 µg of the sodium channel plasmid using 1.6 µl of Lipofectamine 2000 (Invitrogen) per well. An eGFP-containing plasmid was cotransfected in a 3:1 eGFP-to-sodium channel plasmid concentration ratio as a marker of successful transfection. 24 hours after transfection, cells were trypsinised using 0.05% Trypsin-EDTA (1x) (Gibco/Invitrogen) and split into 35 mm petri dishes (Nunc, Denmark) containing sterilized 13 mm borosilicate glass coverslips (VWR International) at 20 – 30% confluence for electrophysiological analysis on the next day.

2.2.7 Transfection of hippocampal neurons using magnetofection

The pcDM8-hNa_v1.1 5A/5N or pcDNA3-hNa_v1.2 6A/6N DNA vector was co-transfected with a reporter Red Fluorescent Protein (RFP)-carrying plasmid under a beta-actin promoter in a 5 : 1 molar ratio. The cultured neurons were transfected on day 4 after plating by magnetofection with NeuroMag according to manufacturer's instructions (OZ biosciences). Briefly, the cell medium was replaced 1 hour prior to transfection with serum-free Neurobasal A medium. Plasmid DNA (0.5 µg) was incubated with 1 µl of NeuroMag beads per well in 100 µl Opti-MEM for 15 minutes at RT and added dropwise on each well. Cells were incubated for 15 minutes at 37°C on top of the magnetic plate; the plate was then removed and original culture medium was restored after 45 minutes. Recordings were performed 4-6 days after transfection to ensure maximal expression of the transfected gene. For interneuronal recordings, cells patched showed co-localization of both

green (indicating interneurons) and red (indicating successful transfection with the sodium channel plasmid).

2.3 Electrophysiology

2.3.1 Electrophysiological recordings

Macroscopic currents from transiently transfected channels in HEK293T cells were recorded using voltage clamp in the whole cell patch-clamp configuration. Recordings were carried out 48 – 72 hours after transfection. Cell-attached coverslips were placed on the chamber of a fluorescence-inverted microscope (Olympus). Extracellular solution (in mM: 135 NaCl, 10 HEPES, 2 MgCl₂, 1.8 CaCl₂, 4 KCl, pH 7.35) was continuously perfused using a gravity-driven heated perfusion tube system for at least 10 minutes before recordings started. All HEK293T cell recordings were carried out at physiological temperature (37°C +/- 2°C). Filamented borosilicate glass pipettes (GC150-F; Warner Instruments) were pulled using a model P-97 Flaming/Brown micropipette puller (Sutter Instrument, Novato, CA) to a final resistance of 1 – 3 MΩ. Whole-cell and pipette capacitance were corrected prior to recordings by using a +10 mV voltage step to integrate capacitive transients. The +10 mV seal test was also used to determine the access resistance of the pipette. Series resistance was monitored, but not compensated. At physiological temperatures series resistance compensation on the Axonclamp 700B would often result to the introduction of large transients, even at compensations <50%. Therefore, in voltage-clamp recordings compensation was avoided and series resistance was routinely kept <2 MΩ. Therefore, in the worst case scenario, a patched cell with a 2 MΩ series resistance producing a current of 5 nA (largest current magnitude allowed) would result in a voltage-clamp error of 10 mV. Recordings started within 1 min of establishment of the whole cell configuration. Cells with a capacitance >35 pF, or a series resistance >3 MΩ were discarded from the analysis to avoid space-clamp errors. Recordings were acquired using a Multiclamp 700B amplifier (Molecular Devices) using in house

software for Labview 8.0 (D Kullmann), together with an analogue-to-digital converter (BNC-2090A, National Instruments) for generating voltage command pulses. Data were leak-subtracted using a P/4 protocol and sodium currents were low-pass Bessel filtered at 10 kHz and digitized at 50 kHz. Peak currents <600 pA were discarded from the analysis to avoid distortion by endogenous current. Cells that produced currents >5 nA were excluded to avoid large series resistance errors.

2.3.2 Voltage clamp analysis

The design and control of voltage protocols as well as acquisition and analysis of recorded current traces were performed using Labview 8.0 (National Instruments). Raw data was exported and subsequently analyzed (curve fitting – statistical analysis) using the Origin 8.0 software. The liquid junction potential for intracellular CsCl solution (in mM: 145 CsCl, 5 NaCl, 10 HEPES, 10 EGTA, pH 7.35) was calculated to be -4.4 mV but was not corrected.

2.3.3 Voltage dependence of steady-state activation/inactivation

Starting from a holding potential of -80 mV, cells were stepped to a range of potentials (-120 mV to +60 mV) in 10mV increments for 300 ms, with 2 sec stimulus intervals between steps to allow full recovery of channels from the inactivated state. The four leak subtraction (-P/4) steps run after each stimulus pulse and before the next stimulus step. Voltage dependence of activation was determined as a function of relative membrane conductance against potential, using the equation $G = I / (V - V_{rev})$, where G is peak conductance (pSiemens), I is the peak sodium current (in pA) at any given membrane potential (V, in mV) and V_{rev} is the reversal potential of the sodium current calculated by the Nernst equation. The resulting conductance during each potential was normalized to the maximum conductance for each cell. Normalized conductance values against membrane potential were fitted in Origin 8.0 with a Boltzmann equation, $G/G_{max} = 1 / (1 + \exp((V_{50} - V) /$

k)) to determine the half-maximal channel activation voltage (V_{50}) and the slope factor (k). G/G_{max} is the normalized conductance value at any given potential (V).

The voltage dependence of fast inactivation was determined by measuring the peak sodium current during a 30 ms test pulse to -10 mV, after a 100ms prepulse between -120 to +40 mV with 10 mV increment in each step, starting from a holding potential of -80mV. Peak currents from each step were normalized to the maximum response for each cell. Normalized current-to-voltage data were fit with a Boltzmann equation, $I_{Na} = (A + (B - A)) / (1 + \exp ((V_{50} - V) / k))$, where I_{Na} is the fraction of sodium current that is available at any given membrane potential (V), while A and B are the lower (bottom) and higher (top) values of the curve respectively.

2.3.4 Recovery from fast inactivation

Recovery from inactivation was analyzed using a two-pulse protocol with varying time intervals (0.5 ms to 2000 ms) between pulses to allow different levels of recovery. The first pulse (P1) occurred as a voltage step to -10 mV (from a holding membrane potential of -80 mV) lasting for 100 ms, followed by incrementally increased interpulse gaps with each cycle (0.5 ms to 2000 ms), returning back to holding potential. A second pulse (P2) at -10 mV was then applied for 25 ms, with the sodium current generated normalized to the first current peak and then plotted against the interpulse time (recovery period). Several modified versions of the original protocol template were used throughout the study, affecting small parameters of the protocol like the holding voltage or the duration of the first pulse. Deviations from the original protocol are illustrated in insets in the results section.

2.3.5 Current-clamp neuronal recordings

Current-clamp recordings of transfected neurons were obtained using the whole-cell patch clamp technique. The internal pipette solution contained (in mM): 126 K-gluconate, 4 NaCl, 1 MgSO₄, 0.02 CaCl₂, 0.1 BAPTA, 15 Glucose, 5 HEPES, 3 ATP-Na₂, 0.1 GTP-Na, pH 7.3. The extracellular (bath) solution contained (in mM): 2 CaCl₂, 140 NaCl, 1 MgCl₂, 10 HEPES, 4 KCl, 10 glucose, pH 7.3. D-(-)-2-amino-5-phosphonopentanoic acid (D-AP5; 50 μM), 6-cyano-7-nitroquinoxaline-2,3-dione (CNQX; 10 μM) and picrotoxin (PTX; 30 μM) were added to block NMDA, non-NMDA, and GABAA receptors, respectively. Tetrodotoxin (TTX; 1 μM) was also added to block all native voltage-gated sodium channels, allowing recordings only from the transfected TTX-resistant ones. Patch pipette resistance was between 5 and 7 MΩ. Series resistance was between 7 and 15 MΩ. Experiments were performed at room temperature (22-24°C), since stability of transfected neurons at physiological temperature was too low for full-length recordings to be performed (should more time were available, this would be a reasonable extension of this study). Neurons with unstable resting potential and/or bridge-balance >15 MΩ were discarded. The gigaohm seal and whole cell configuration were obtained in voltage-clamp mode and then the amplifier was switched to current-clamp. Bridge balance compensation was applied and the resting membrane potential was held at -70 mV. Action potential firing was recorded by injecting 10 ms long depolarizing current steps of increasing 20 pA amplitude. For the firing frequency reliability protocol, a 110% value of the neuron's threshold current was used (i.e. a supra-threshold stimulus), given in 11 consecutive pulses with increasing frequency in each step (30 – 90 Hz). Cells were allowed to recover for 4 seconds between successive trains of pulses. Current-clamp recordings were acquired at 10 kHz and performed using a multiclamp 700B amplifier (Axon Instruments, Molecular Devices, Sunnyvale, CA, USA), a National Instruments digitizer (NI) and a Labview acquisition software homemade by Dimitri Kullmann. An inverted IX71 microscope (Olympus, Japan) equipped with a 120-watt mercury lamp (X-cite series 120, Exfo) that allowed visualization of red (RFP) and green (EGFP) fluorescence was used. (EGFP filter: Excitation, Blue; Cube, U-MWB; Excitation Filter, 450 – 480 nm; Dichroic Mirror, 500 nm; Barrier Filter, 515 nm ; RFP filter: Excitation, Green; Cube, U-MWG; Excitation Filter, 510 – 550 nm; Dichroic Mirror, 570 nm; Barrier Filter, 590 nm).

2.3.6 Single action potential parameters

The single action potential shape parameters were derived using the pClamp software (Molecular Devices) and analyzed with the Prism software (GraphPad Software, Inc.). A phase-plane plot of the first action potential elicited after sufficient depolarization with current steps was obtained for each cell by plotting the time derivative of voltage (dV/dt) versus the voltage. This allowed identification of the AP voltage threshold, peak and amplitude as well as the maximum rising and depolarizing slopes (Figure 2.1) (Bean, 2007). The action potential threshold was defined as being the voltage at which dV/dt exceeded 10 mV/ms, similar to other studies (Pozzi *et al.*, 2013).

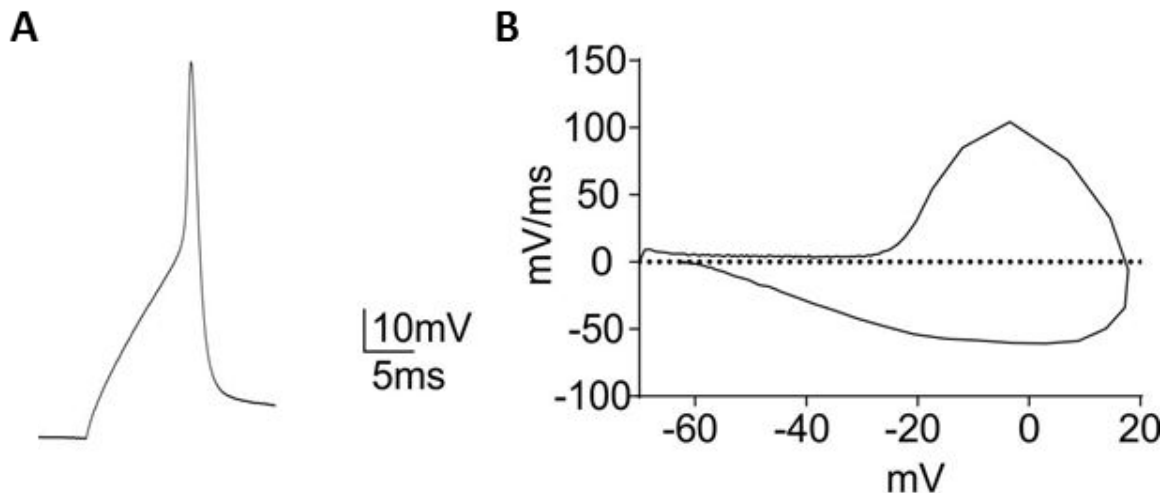


Figure 2.1: A representative action potential (A) and phase plot (B) used to analyse active properties of transfected neurons.

The highest and lowest points on the y axis are a measurement of the maximum rising and repolarizing slopes of the AP respectively. The highest x axis point (furthest at the right) is a measurement of the AP peak voltage. The AP threshold is the voltage at which the y axis exceeds 10mV/ms. The AP amplitude is the difference between the AP peak and the AP threshold voltage.

2.3.7 Dynamic clamp recordings

For voltage-clamp spontaneous excitatory synaptic activity of the neuronal and interneuronal epileptic traces (4AP, 100 μM) and current-clamp recordings in dynamic clamp configuration the internal and the extracellular solutions were the same described before for neuronal whole cell patch clamp recordings. For voltage-clamp recordings, D-AP5 (50 μM) and PTX (30 μM) were added in the extracellular solution to block NMDA and GABAA receptors respectively. For current-clamp recordings TTX (1 μM), D-AP5 (50 μM), CNQX (10 μM) and PTX (30 μM) were added to block endogenous sodium channels (allowing isolation of transfected TTX-resistant sodium currents), NMDA receptors, AMPA receptors and GABAA receptors, respectively. Experiments were performed at room temperature (22-24°C). For voltage-clamp recordings, neurons were clamped at -70 mV and cells with unstable resting potential and/or a leak current >100 pA were discarded. For current-clamp recordings, neurons with unstable resting potential and/or bridge-balance >15 M Ω were discarded. Bridge balance compensation was applied and the resting membrane potential was held at -70 mV. Dynamic clamp experiments were performed as followed: neuronal or interneuronal current traces were recorded in voltage-clamp configuration holding neurons at -70 mV in the presence of 4AP. The resulting current traces were then converted into conductance ($G=I/V$). Using a dynamic clamp software, the conductance traces were used to dynamically inject currents in Na_v1.1-5A or 5N transfected neurons (in the presence of TTX) in current-clamp configuration, the resulting response voltages were recorded and AP elicited were analyzed. Dynamic clamp software in real-time read the voltage of the patched neurons and calculated the current to be injected from the conductance trace ($I=G*V$). In order to normalize for the conductance magnitude used in each cell and to be able to compare different cells, the conductance threshold of each patched neuron was calculated, before the dynamic clamp experiments with the epileptic conductance trace. An AMPA conductance step protocol ($E_{\text{rev}}=0\text{mV}$; $\tau=1\text{ms}$; $\Delta G=1\text{nS}$) was used to find the conductance threshold that elicited an AP and then the epileptic conductance trace was scaled to the 15% of the conductance threshold. The sampling frequencies in voltage and in current clamp configurations were set at 20 kHz to accurately overlap the conductance traces with the software voltage reading. An event was selected as AP if its peak crossed 0 mV. All recordings and analysis for neurons were carried blinded to isoform expressed. Recordings were acquired using a Multiclamp 700A amplifier

(Axon Instruments, Molecular Devices, Sunnyvale, CA, USA) and Signal dynamic clamp software in conjunction with CED Power 1401-3 (CED, Cambridge Electronic Design Limited), filtered at 10 kHz and digitized at 50 kHz.

2.4 Statistical analysis and modelling

Results are shown as mean \pm s.e.m., with n = sample size. Normally distributed two sample groups were compared by Student's unpaired two-tailed t -test, at a significance level of $P < 0.05$. Sample groups without a normal distribution were compared using Mann-Whitney's non-parametric U test. For comparisons of more than two sample groups, two-way ANOVA was used, followed by either the Bonferroni's or the Dunnett's test. Fitting used the Levenberg-Marquardt algorithm to minimize the χ^2 value, with the amplitudes of rates constrained to give positive values. To analyze cumulative frequency in dynamic clamp experiments, Mann-Whitney test was used instead of the Kolmogorov-Smirnov test because the events were dependent within groups (an AP depends on the stimulus pattern as well as the previous AP history). Statistical analysis was carried out using the Prism software (GraphPad Software, Inc.) or Origin (OriginLab). All modeling was carried out using IonChannelLab (Santiago-Castillo *et al.*, 2010).

Chapter 3: Functional dissection of the impact of splicing on onset and stability of inactivation in Na_v1.1

3.1 Hypothesis and Aims

A different relative proportion of 5A and 5N channels in epileptic patients has been associated with altered febrile seizure predisposition (Schlachter *et al.*, 2009, Le Gal *et al.*, 2011) as well as a difference in AED response (Tate *et al.*, 2005; 2006; Abe *et al.*, 2008) between individuals, although these associations have not always been replicated (Kwan *et al.*, 2008; Manna *et al.*, 2011; Haerian *et al.*, 2013). A recent functional study has partly attributed this to a difference in recovery from fast inactivation between the two isoforms under physiological temperature conditions (37°C) and a CsCl-based intracellular solution, with neonatal channels recovering relatively faster than adult ones for shorter interpulse durations (Fletcher *et al.*, 2011). The same study has also shown that recording conditions can affect channel behaviour and either mask or reveal differences between the two splice variants, as also indicated by another group, using different recording conditions (25°C, CsF- based intracellular solution) (Thompson *et al.*, 2011). The overall hypothesis is that splicing has a specific effect on the inactivation of Na_v1.1 sodium channels, and this chapter describes systematic investigations of how splicing modifies the onset, stability and recovery from fast inactivation.

Aims:

1. Confirm and expand previous findings on the effect on recovery from inactivation.
2. Investigate time dependence of onset of the effect.
3. Investigate the voltage dependence of the effect.
4. Determine whether splicing could have an effect on channel availability during fast depolarization trains.

These findings will serve as a potential guideline to reveal what effects of splicing might be conserved in other sodium channels. Furthermore, detailed analysis of how splicing modifies inactivation, will allow a prediction of how splicing affects channel availability under conditions that can actually mimic interneuronal firing patterns or fast neuronal activity that occurs during a seizure.

3.2 Results: Probing the effects of splicing on fast inactivation

3.2.1 Validation of the constructs

We first confirmed that both splice variants generated sodium currents that were comparable to earlier studies of these channels (Fletcher *et al.*, 2011; Thompson *et al.*, 2011). Voltage dependence of activation and inactivation were compared for 5A and 5N Na_v1.1 channels under conditions used previously (CsCl-based intracellular, 37°C), where both splice variants showed similar macroscopic kinetics (e.g. onset of inactivation, Figure 3.1A,B), and voltage dependence of activation and steady state inactivation (Boltzmann non-linear curve fits, P>0.05, two-way ANOVA, Figure 3.1C). This comes in agreement with Fletcher *et al.*, (2011), who also did not find a difference between splice variants under the same conditions (Table 3.1). In the same study, changing the recording conditions (CsF-based intracellular, room temperature) still did not reveal any voltage dependence differences between splice variants, although V_{1/2} of activation and inactivation did shift between conditions (Table 3.1). The latter conditions were also used at an independent study (Thompson *et al.*, 2011), which also did not reveal any difference in voltage dependent properties or macroscopic kinetics between the two Na_v1.1 isoforms (Table 3.1). Thus, as with previous studies, we confirmed that splicing did not have diffused effects on multiple voltage dependent parameters or on the overall shape of currents in response to individual voltage steps.

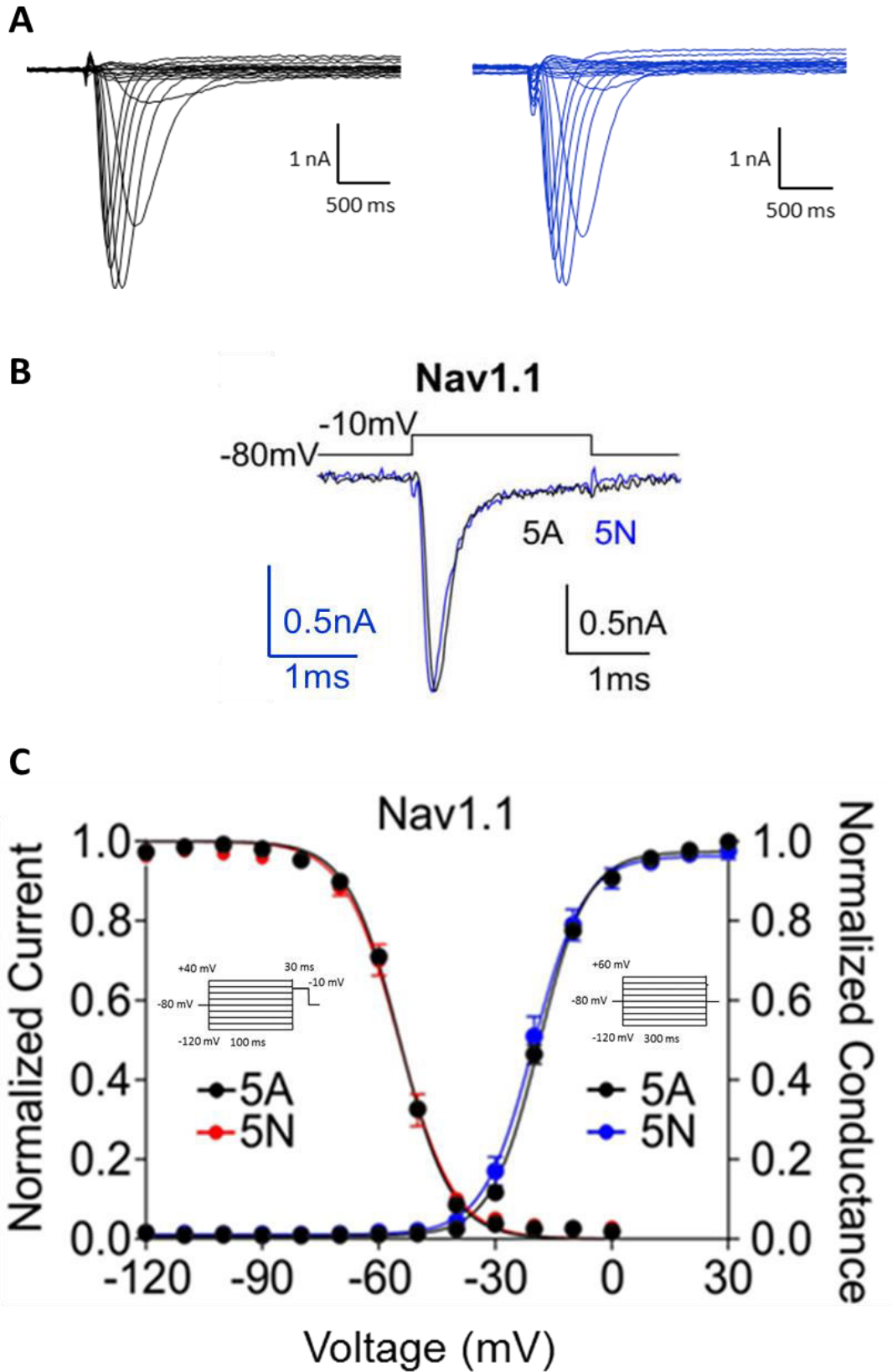


Figure 3.1: Na_v1.1: No difference in macroscopic properties and VD activation/inactivation between isoforms.

A. Representative traces from HEK293T cells expressing adult (black) and neonatal (blue) isoforms evoked by a 2 ms step to -10 mV. **B.** Macroscopic properties of the currents were largely indistinguishable for an individual pulse (-80 to -10 mV). **B.** Voltage Dependence of activation & inactivation – no difference is seen between 5A and 5N variants. Numbers of cells (5A n = 6; 5N n = 6)

	Fletcher <i>et al.</i> (37°, CsCl)		Fletcher <i>et al.</i> (RT, CsF)		Fletcher <i>et al.</i> (RT, CsCl)		Thompson <i>et al.</i> (CsF, RT)		Liavas (37°, CsCl)	
Nav1.1 variant	5A	5N	5A	5N	5A	5N	5A	5N	5A	5N
V ₅₀ activation (mV)	-18.5 ± 0.9	-18.8 ± 0.8	-21.2 ± 1.7	-22.6 ± 1.2	-15.4 ± 1.1	-17.3 ± 1.3	-15.8 ± 0.8	-17.8 ± 0.6	-16.5 ± 1.4	-17.9 ± 1.9
slope	6.7 ± 0.4	6.5 ± 0.3	6.0 ± 0.4	5.4 ± 0.2	6.2 ± 0.4	5.8 ± 0.4	7.7 ± 0.1	7.8 ± 0.1	7.2 ± 0.6	8.6 ± 0.8
n	15	18	9	14	18	13	22	24	6	6
V ₅₀ inactivation (mV)	-53.7 ± 1.2	-53.1 ± 1.3	-58.4 ± 1.4	-60.1 ± 0.7	-54.1 ± 1.6	-58.0 ± 2.0	-64.0 ± 0.6	-65.7 ± 0.8	-55.4 ± 1.1	-55.1 ± 2.4
slope	6.3 ± 0.3	5.9 ± 0.7	8.1 ± 0.9	6.7 ± 0.4	6.2 ± 0.5	6.9 ± 0.3	-5.9 ± 0.2	-5.9 ± 0.2	-7.4 ± 0.6	-8.2 ± 1.1
n	15	11	8	12	14	9	19	21	6	6

Table 3.1: V₅₀ values and slopes for VD activation/inactivation of Na_v1.1-5A and 5N from Fletcher *et al.*, (2011), Thompson *et al.*, (2011) and the current study in different recording conditions.

RT refers to room temperature. At any given condition, there was no difference in VD of activation /inactivation or slope between Na_v1.1-5A and 5N channels (P>0.05, two-way ANOVA). n number at each study is given in the table.

3.2.2 Na_v1.15N channels recover more quickly from fast inactivation than 5A channels

The main difference between neonatal and adult Na_v1.1 channels found by Fletcher *et al.*, (2011) was a faster recovery rate from fast inactivation for 5N channels compared to 5A at physiological temperature. This experiment was repeated here under the same conditions but including additional interpulse time points, from 0.5ms to 2000ms, in order to improve the description of the time course, which in Fletcher *et al.*, (2011) was limited to a single exponential because of the smaller number of time points. By increasing the number of time points describing the recovery, it will be possible to separate fast and slow components of the exponential time course. The nomenclature that will be used for this and later protocols in this chapter is given in Figure 3.2A for clarity. The increased resolution revealed that both neonatal and adult channels recovered from long inactivating prepulses (100 ms) with a bi-exponential timecourse. Similar to Fletcher *et al.*,

(2011), 5N channels recovered faster compared to 5A, but with the additional points used here, it was clear that this difference was most pronounced for shorter recovery intervals (Figure 3.2B,C). The recovery timecourse was well fit by two exponentials [$Y_0 + A_F \cdot (1 - \exp(-t/\tau_F)) + A_S \cdot (1 - \exp(-t/\tau_S))$], consistent with a fast (τ_F : 1.1 = 1.7 ms), and a slow (τ_S : 1.1 = 220 ms) component of recovery from inactivation. Y_0 is the y-axis intercept, while A_F and A_S are the relative amplitudes of the fast and slow component respectively. The τ_F and τ_S components were similar for both splice variants, suggesting that splicing was not altering the *rate* of either component, but the *proportion* of fast or slow component in the recovery. To probe this relationship, the number of free parameters was reduced by comparing splice variants with both rates (τ_F and τ_S) fixed and only the relative amplitudes of the fast (A_F) and slow (A_S) components allowed to vary. These constraints allowed good fits ($r^2 > 0.98$ for both fits with these restrictions, Table 3.2), however even with the rates fixed, A_F and A_S values did not significantly vary between the two fits. Instead, the main difference between the fits was the Y_0 parameter, which sets the starting point of the fits (i.e. the theoretical ‘instantaneous availability’ after no recovery interval). Hence, by comparing the relative proportion of fast and slow components of recovery and a component of instantaneous availability, these data revealed that the major difference between the variants was a contribution of approximately 7.6% of 5N channels, which according to the fit have not inactivated or they recovered from inactivation even faster than 0.5 ms. For 5A channels, no contribution from this parameter was needed for the fits (i.e. 0% of 5A channels were in the ‘instantaneously available’ state). This initial difference in offset established the difference in availability between the two splice variants, which remained until obscured by much longer interpulse recovery intervals and was sufficient to describe the difference between the neonatal and adult $Na_v1.1$ isoforms (Figure 3.2 and Table 3.2).

In order to exclude the possibility of bias during the data fitting, the analysis was again repeated, this time with all parameters free to fluctuate (Figure 3.3, green lines). The data still produced good fits ($r^2 > 0.98$, Table 3.2), yet the deviation from the values obtained with fixed parameter fits were negligible, with all the free fit values over. Taken together, these findings are consistent with splicing altering an inactive state that is extremely rapid in recovery, with longer, slower inactivated states remaining insensitive to splicing.

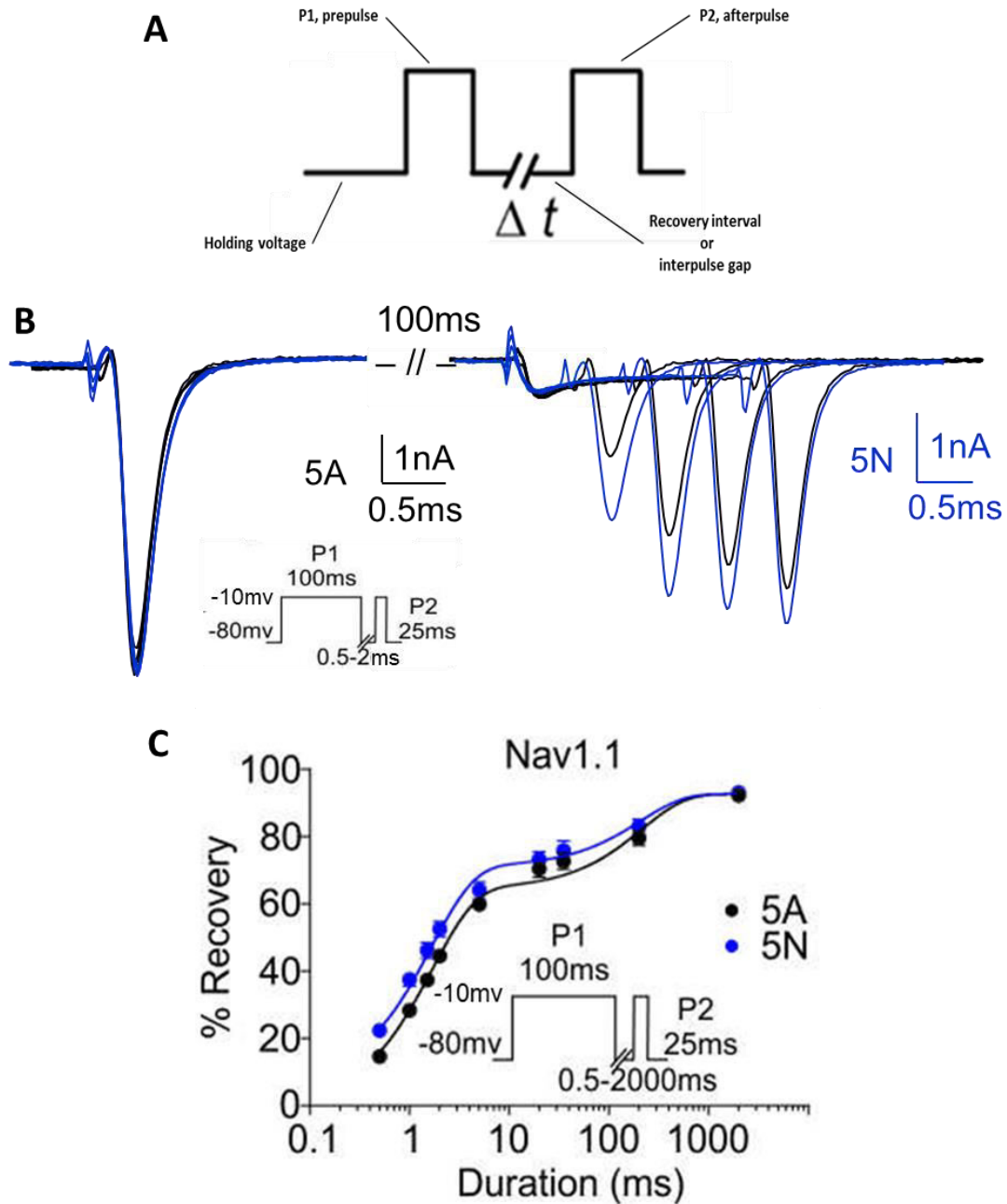


Figure 3.2: $Na_v1.1$: Channels containing exon 5N recover more rapidly from inactivation after short recovery intervals

A. Nomenclature used for each component of the protocols used throughout the chapter. **B.** Raw traces for recovery from inactivation after 0.5, 1.0, 1.5 & 2.0 ms recovery interval for $Na_v1.1$ neonatal (blue) and adult (black) channels.

C. $Na_v1.1$: Short recovery intervals at -80mV reveal a difference between splice variants with 5N recovering more quickly than 5A, which is lost as intervals get longer. (5A, n = 10; 5N, n = 9). Note that additional time points prior to 2 ms confirm and extend the difference seen in Fletcher *et al.*, (see Figure 1.22).

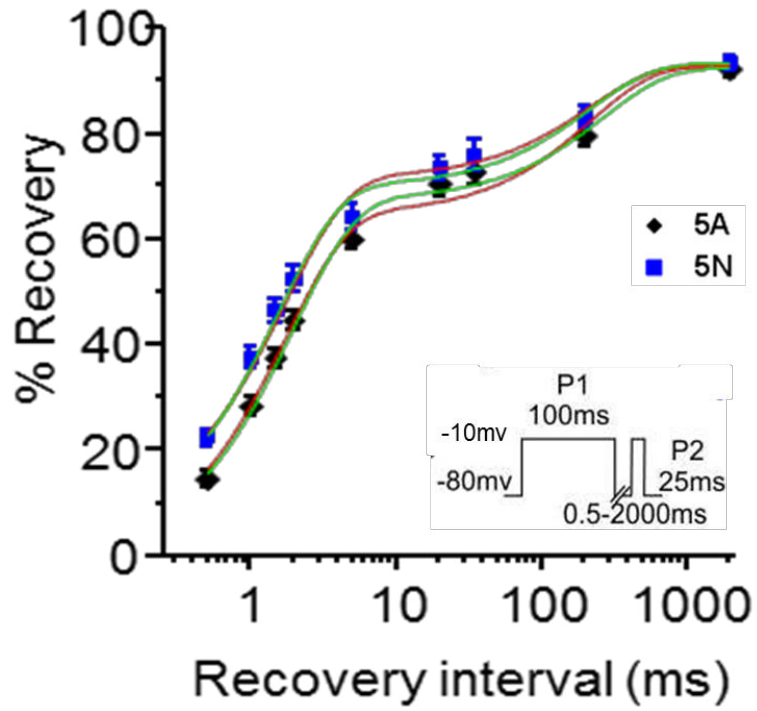


Figure 3.3: Recovery from inactivation for isoforms of each channel comparing fits with all parameters free (green lines) and with τ_f and τ_s fixed (red lines)

Values and standard errors of the fit values are in table 3.1.

Table 3.2: Na_v1.1: Parameters of bi-exponential fits to recovery from long (100 ms) inactivating pre-pulses.

Top panel: Optimized fitting parameters with τ_F and τ_S constrained (red lines in Figure 3.3, rates with n/a standard error (s.e.) were fixed). *Bottom panel:* Free fits with all parameters allowed to vary (green lines in Figure 3.3). R^2 is the adjusted R-square statistic used to improve comparison of fits with different degrees of freedom.

Parameters from constrained fits (red lines in Figure 3.3)

	Na _v 1.1-5N		Na _v 1.1-5A	
	Value	s.e.	Value	s.e.
Y_0	0.076	0.018	0	0.027
A_F	0.63	0.03	0.66	0.04
τ_F (ms)	1.7	n/a	1.7	n/a
A_S	0.23	0.02	0.27	0.03
τ_S (ms)	220	n/a	220	n/a
R^2	0.996		0.995	

Parameters from free fits (green lines in Figure 3.3)

	Na _v 1.1-5N		Na _v 1.15A	
	Value	s.e.	Value	s.e.
Y_0	0.044	0.040	0.003	0.036
A_F	0.65	0.04	0.67	0.36
τ_F (ms)	1.5	0.2	1.9	0.2
A_S	0.23	0.03	0.25	0.03
τ_S (ms)	218	69	272	95
R^2	0.994		0.994	

3.3 Results: Probing the ‘instantaneously available’ state with variable inactivating prepulses

3.3.1 The difference between splice isoforms is dependent on the length of the conditioning depolarisations

According to the previous section, the main effect of splicing in $\text{Na}_v1.1$ is on the earliest component of availability after inactivation, with the difference potentially being due to a difference in the *onset* of recovery from fast inactivation. Thus, the next question asked was whether a briefer inactivating first pulse (i.e. shorter P1 duration), would increase the difference in the availability between 5A and 5N channels. Since neurons are usually depolarized for only a couple of milliseconds during an action potential (AP), a difference present after short depolarisations may be physiologically more relevant than a difference that requires prolonged depolarisation to develop. Reducing P1 duration from 100 ms to 20 ms did augment the difference between $\text{Na}_v1.1$ 5A and 5N for shorter interpulse gaps (2, 12 and 22 ms) (Figure 3.4). As a result, with a shorter P1 duration, 12 ms and 22 ms interpulse gaps now showed a significant difference in terms of inactivation recovery between 5A and 5N ($P < 0.001$, two-way ANOVA with Bonferroni’s post-hoc tests, Figure 3.4B), a difference that was lost when a longer P1 duration was applied (100 ms, Figure 3.4A).

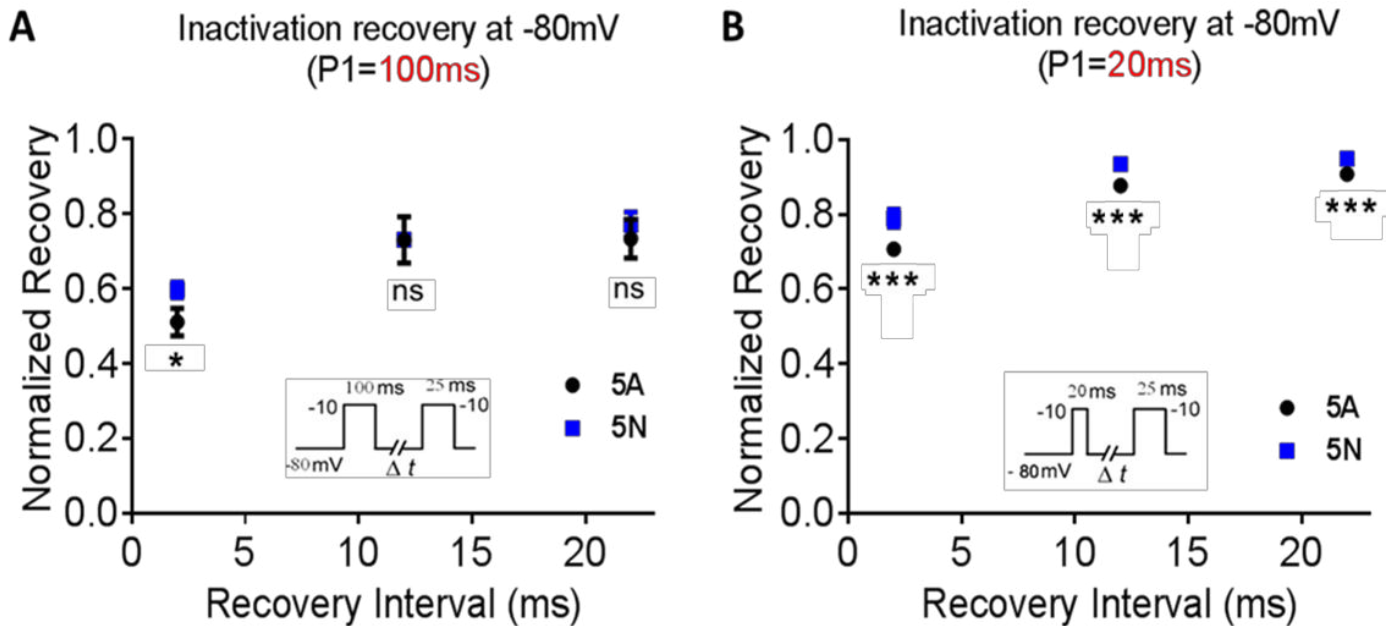


Figure 3.4: Na_v1.1: Pilot data indicating that shortening the prepulse duration increases the difference in recovery from inactivation between isoforms.

short recovery intervals at -80mV (5A n=3; 5N n=4) reveal a difference between splice variants, which is masked as intervals get longer (5A, 0.52 ± 0.04 , 0.73 ± 0.06 , 0.73 ± 0.05 ; 5N, 0.60 ± 0.02 , 0.73 ± 0.01 , 0.77 ± 0.03 for recovery intervals of 2, 12 and 22 ms respectively). **B.** a shorter P1 duration (20ms) (5A n=7; 5N n=6) appears to augment that difference (5A, 0.71 ± 0.02 , 0.88 ± 0.01 , 0.91 ± 0.01 ; 5N, 0.79 ± 0.02 , 0.93 ± 0.01 , 0.95 ± 0.01 for recovery intervals of 2, 12 and 22 ms respectively). Error bars are included, but are obscured by symbols.

In order to analyse in further detail the effect of P1 duration on inactivation recovery, a protocol was designed to probe channel availability after increasing P1 intervals, from very short (2 ms) to very long (500 ms). The interpulse gap duration was fixed to 2 ms, a value that had been shown from previous experiments to reveal a difference between the variants (Figure 3.2). In principle, the ideal P1 duration for probing a difference in Y_0 would be ~ 0 ms (to test the instantaneous availability of channels), however 2 ms was the shortest P1 duration that could be reliably stepped in voltage clamp configuration. In these conditions, the availability for both neonatal and adult

isoforms were most suitably fit as a first order exponential decay [$Y_0 + A \cdot \exp(-t/\tau)$]. Initial fits were carried out with all parameters free to vary (Figure 3.6, green lines). In this instance, the confidence intervals of both Y_0 and τ overlapped for the fits of the two isoforms, suggesting no real difference in time course and offset between neonatal and adult $Na_v1.1$ channels. Note, however that because this fit is an exponential decay, Y_0 is no longer the starting offset but the final offset (i.e. the value of predicted channel availability after a 2 ms recovery from a prepulse of infinite duration). In contrast, the amplitude (A) did differ significantly between the two isoforms (5A, 0.533 ± 0.006 ; 5N, 0.662 ± 0.004 , $P < 0.05$, two-way ANOVA). As A represents the proportion of channels available after the shortest possible pre-pulses, this suggests the difference between variants is not just in the fastest component of recovery (i.e. the instantaneously available from previous section) but also in the fastest component of onset of inactivation, in spite of the lack of difference in the rate of inactivation during the depolarising pulses (Fletcher *et al.*, 2011).

In order to test the hypothesis that only the amount (denoted by the amplitude, A, in the equation) but not the timecourse of availability after 2 ms was changed (i.e. that the difference between isoforms could be explained by a change in a single parameter) the data were fit with the τ and Y_0 fixed to be the same for the adult and neonatal isoforms, and only the amplitude (A) allowed to vary (τ : 1.1 = 159 ms; $Y_0 = 0.2$; Figure 3.6 red line and Table 3.3). Data fits were again acceptable ($r^2 > 0.94$) and almost identical to the totally free fits, keeping a significant and robust difference between the two isoforms concerning the amplitude. Testing 5A and 5N channels under this protocol revealed that shorter P1 durations increased the difference between splice variants (Figure 3.5 & 3.6). Direct comparison of the fits of each isoform for all data points with two-way ANOVA indicated that neonatal $Na_v1.1$ channels showed significantly more recovery from inactivation after a range of shorter pre-pulses compared to adult ones ($P < 0.001$). The difference started waning off as the P1 duration got longer so that at P1 values > 200 ms it was completely masked (Figure 3.5A). The experiment was repeated just for the initial shorter P1 durations (2 – 10 ms) where the difference is most evident, with 5N channels significantly more available than 5A under these conditions ($P < 0.001$; Figure 3.5B). Therefore, the neonatal isoform here shows significantly increased availability after short inactivating pre-pulses compared to the adult isoform.

To test if this difference is dependent on temperature, we repeated the same experiment, this time at 25°C. In spite of the fact that the recovery of both neonatal and adult channels decreased at lower temperature, we saw for $Na_v1.1$ isoforms that the difference in availability persisted at room

temperature ($P < 0.001$, two-way ANOVA, Figure 3.7). These findings are consistent with splicing altering an inactive state which is both rapid in onset and rapid in recovery, with longer, slower inactivated states remaining insensitive to splicing.

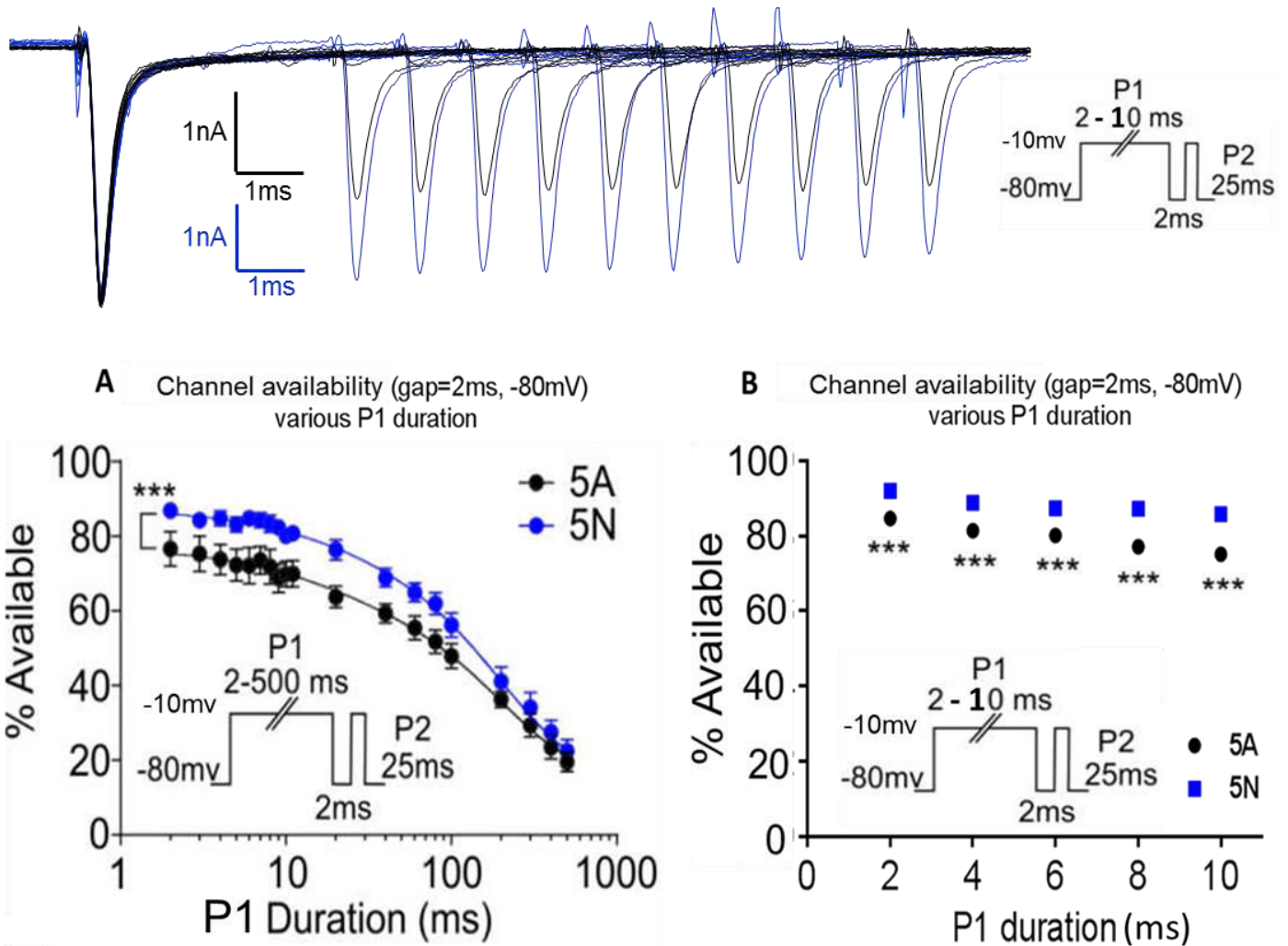


Figure 3.5: Na_v1.1: The neonatal isoform showed significantly more availability after a range of shorter pre-pulses under a brief interpulse gap duration (2ms)

Raw traces are given for P1 duration of 2, 3, 4, 5, 6, 7, 8, 9 & 10 ms for Na_v1.1 neonatal (blue) and adult (black) channels. Curves in **A** and **B** are fit with single exponentials as described in the text. **A**. P1 duration = 2 – 500ms (5A n=6; 5N n=6). **B**. P1 duration = 2 – 10ms (5A n=10; 5N n=5). The error bars in **B** are masked by the data points. The different duration of the protocol used in **B** means that these cells cannot be directly compared to cells in **A**.

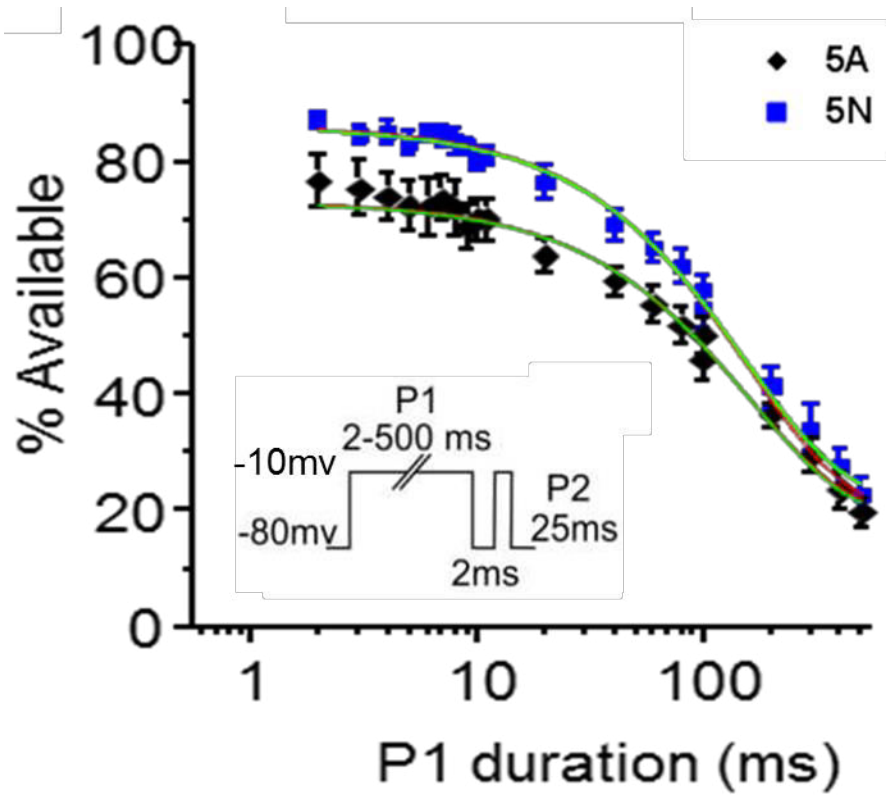


Figure 3.6: Estimated channel availability for isoforms of each channel comparing quality of fits with all parameters free (green lines) and with Y_0 and τ fixed (red lines, behind green lines)

The green fits were seeded with the same values for both isoforms. Note that from the free fits only the non-overlapping errors for parameter A are consistent with this value being different between the isoforms (see table 3.2, bottom panel).

Table 3.3: Na_v1.1: Parameters of single exponential fits describing channel availability after 2 ms recovery from pre-pulses of different durations

Top panel: optimized fitting parameters with inactivation time constant τ and the offset (Y_0) fixed. The parameters with n/a standard error (s.e.) were fixed at values similar to those found for free fits to both isoforms of the channel (as described in Figure 3.9). *Bottom panel:* Fits with all parameters allowed to vary. To better compare the goodness of fits with the different degrees of freedom the adjusted R-square statistic (R^2) is given.

Parameters from constrained fits (red lines in Figure 3.9)

	Na _v 1.1-5N		Na _v 1.1-5A	
	Value	s.e.	Value	s.e.
Y_0	0.2	n/a	0.2	n/a
A	0.662	0.004	0.533	0.006
τ (ms)	159	n/a	159	n/a
R^2	0.991		0.989	

Parameters from free fits (green lines in Figure 3.9)

	Na _v 1.1-5N		Na _v 1.1-5A	
	Value	s.e.	Value	s.e.
Y_0	0.22	0.02	0.19	0.02
A	0.640	0.022	0.547	0.018
τ (ms)	155	13	164	15
R^2	0.991		0.989	

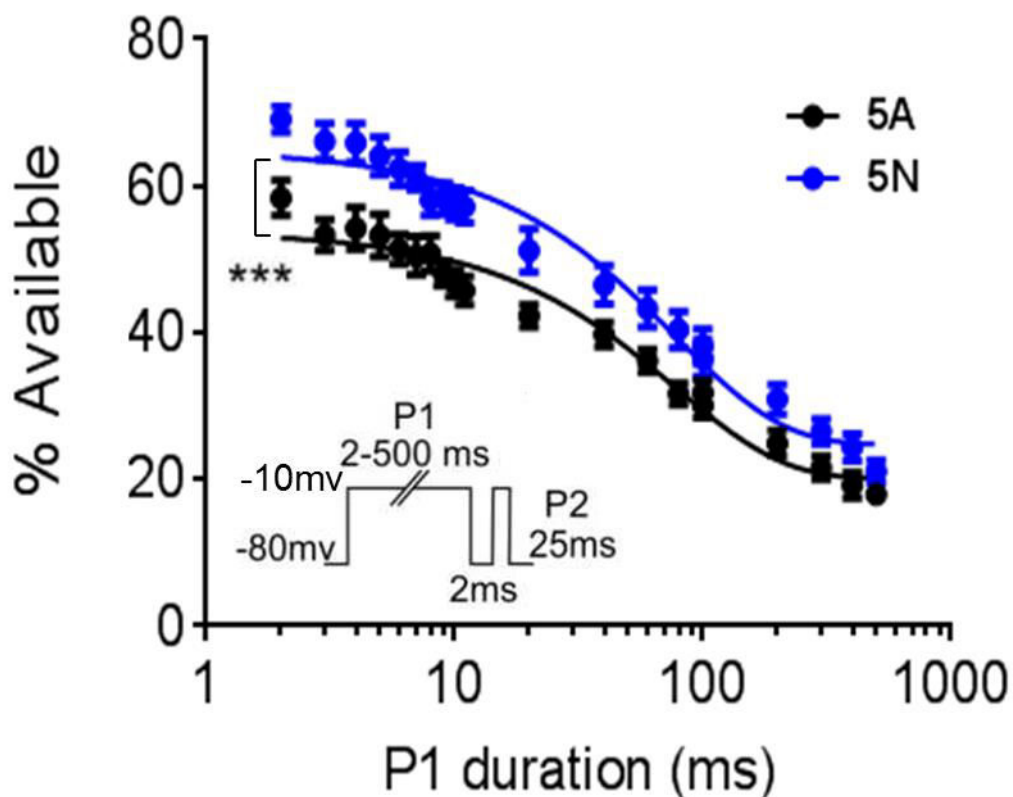


Figure 3.7: Na_v1.1: The difference in channel availability is also preserved in room temperature

The effect of splicing on channel availability after short depolarising prepulses is preserved in room temperature recordings. Recordings are for variants of Na_v1.1 (5A n = 7; 5N n = 10).

3.3.2 The difference in recovery from inactivation difference is masked by prolonged inactivating pre-pulses

Since briefer inactivation pulses (<10 ms) increased the difference in availability between 5A and 5N variants, it was hypothesized that longer inactivating steps, using a prolonged P1 duration, would have an opposite effect, i.e. eradicate the difference in the recovery rate between 5A and 5N variants. Therefore, the duration of the first depolarizing pulse (P1) was increased from 100 ms to

300 ms to induce more inactivation, and availability was assessed after variable recovery intervals. Data points in this situation were most appropriately fitted with a single rather than a double-exponential, likely because the prolonged depolarizing pulse has pushed the channels more into slow inactivated states than before, where a fast component was much more evident. As a result of that prolonged inactivating pulse, recovery from inactivation was decreased for both variants. As expected, these longer pulses also obscured the difference between the isoforms with both the fitting curves as well as each time point over laying for the two isoforms (two-way ANOVA, $P>0.05$) (Figure 3.8).

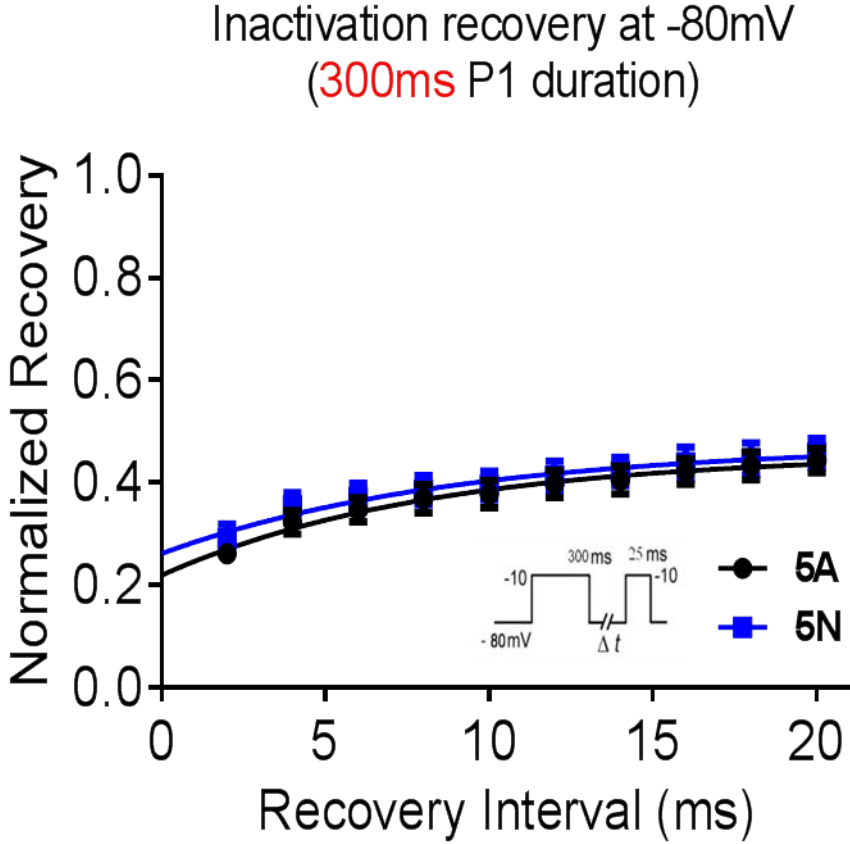


Figure 3.8: $Na_v1.1$: inactivation protocols bearing long inactivation pulses obscure any differences between 5A and 5N splice variants
(5A n=7; 5N n=9).

3.4 Results: Probing the effects of voltage on inactivation recovery

3.4.1 The holding voltage can obscure the difference in inactivation recovery

Fast recovery from inactivation is dependent on voltage as well as time. This suggests that the difference seen here in fast inactivation recovery might be sensitive to the potential at which cells are held before stimulation and during the recovery interval. Different holding potentials, however, also may alter the distribution of channels in deactivated and inactivated states. In the case of neurons, the steady state amount of inactivation would be set by the resting membrane potential (RMP) of each cell, while in voltage-clamped HEK293T cells it is defined by the holding voltage. In order to examine how this voltage affects the inactivated states and consequently the difference between $\text{Na}_v1.1\text{-5A}$ and 5N channels, the original experiment probing recovery from inactivation was repeated (i.e. $P1 = 100$ ms, gap $0.5 - 2000$ ms), this time holding the cell at -70 mV, and using -70 mV during the recovery gap (this is approximately -75 mV, taking into account the liquid junction potential, or LJP, of the CsCl internal solution, which was not corrected during recordings). Changing to a -75 mV holding potential completely eradicated the difference in recovery between the splice isoforms ($P > 0.05$, two-way ANOVA, Figure 3.9A). Two-exponential fit analysis of the data points for both $\text{Na}_v1.1\text{-5A}$ and 5N indicated that the difference seen before at -80 mV holding voltage in the Y_0 parameter (the theoretical “instantaneous availability”) was now eradicated, while none of the other equation parameters varied between isoforms (see values on Table 3.4, $P > 0.05$, two-way ANOVA). Absolute membrane potential is a difficult parameter to measure, and it is possible that -75 mV is more representative of the membrane potential of GABAergic interneurons, which were measured at -65 mV (Lamsa *et al.*, 2007), however the Allen Brain Atlas online database of cortical interneurons suggests a significantly more negative resting potential (-70 to -80 mV with an uncorrected -14 mV LJP, <http://celltypes.brain-map.org/>). In order to test the possibility of more negative potentials generating greater differences between variants, the experiment was repeated using a *hyperpolarized* holding potential (-100 mV, or approximately -105 mV after subtracting the LJP). Although both variants recovered more rapidly at this hyperpolarised potential, there was again no difference in recovery between variants at any given interpulse interval, nor in any of the parameters from the two-exponential fit analysis of the curves ($P > 0.05$, two-way ANOVA, Figure 3.9B and Table 3.5).

Thus the difference between the variants was steeply dependent on the voltage used to maintain cells, however given the difficulties of comparing membrane potentials between cells held in different conditions, it is difficult to extrapolate from the HEK293T voltage clamp data to the situation in neurons. Furthermore, the resting membrane potential of an excitable cell such as a neuron is not constant, but fluctuates depending on the signal input that constantly receives from neighbour cells. In order to directly assess the impact of splicing on neuronal activity, the variants must be compared in neurons where current clamp recordings may allow direct comparison of the channel availability in more physiological conditions (see chapters 6 & 7).

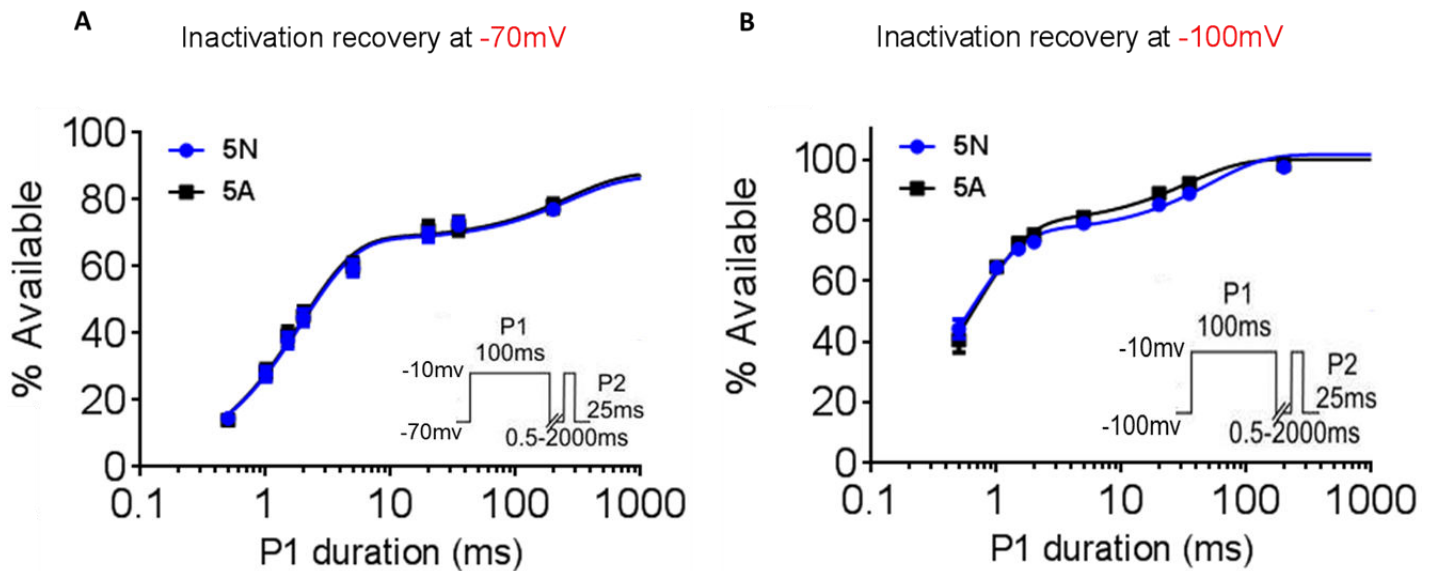


Figure 3.9: $\text{Na}_v1.1$: Changes in holding voltage eradicate the difference in inactivation recovery between the isoforms

Inactivation recovery protocols performed at **A.** more depolarized (-70 mV) (5A $n=7$; 5N $n=8$) or **B.** strongly hyperpolarized (-100 mV) potentials (5A $n=5$; 5N $n=6$) obscure any differences between 5A and 5N splice variants (0.5 ms – 2000 ms interpulse recovery intervals)

Table 3.4: Na_v1.1: Parameters of bi-exponential fits to recovery from long (100 ms) inactivating pre-pulses at -70 mV holding voltage.

	Na _v 1.1-5N		Na _v 1.1-5A	
	Value	S.E.	Value	S.E.
Y₀	0.004	0.037	0	0.031
A_F	0.69	0.03	0.71	0.03
t_F (ms)	1.9	0.2	1.8	0.2
A_S	0.19	0.02	0.2	0.03
t_S (ms)	286	114	262	97
R²	0.995		0.995	

Table 3.5: Na_v1.1: Parameters of bi-exponential fits to recovery from long (100 ms) inactivating pre-pulses at -100 mV holding voltage.

	Na _v 1.1-5N		Na _v 1.1-5A	
	Value	S.E.	Value	S.E.
Y₀	0.016	0.127	0.001	0.044
A_F	0.58	0.13	0.85	0.25
t_F (ms)	0.91	0.22	0.76	0.12
A_S	0.24	0.03	0.22	0.02
t_S (ms)	123	53	125	4
R²	0.971		0.991	

3.5 Results: Probing the effects on rapid stimulation conditions

3.5.1 Recovery from inactivation difference is augmented during “high-activity”, “seizure-like” trains of depolarising steps

Our initial data suggest the difference between the splice variants is greatest after short depolarising steps with short intervals for recovery. This raises the possibility that the difference between the variance is exacerbated in pathophysiological fast firing bursts of action potentials – such as seizures. The next aim was to model a situation mimicking this sort of burst like behaviour – a series of fast, relatively short depolarisations – to test whether these burst-like events could evoke different responses from the splice variants. The protocol alternated short depolarising P1 pulses (to -10 mV for 10 ms) with even shorter recovery intervals than the previous protocol (1 ms) and holding at -80 mV. Hippocampal interneurons have been found to fire at a physiological frequency range of 40 to 80Hz, with some cells reaching 100Hz during high frequency oscillations (Quilichini *et al.*, 2012). The recovery gap duration between depolarisations here is shorter compared to physiological interpulse gaps between interneuronal spikes. Therefore, this protocol may mimic very fast, “pathophysiological” neuronal firing, or even the kind of activity that would be evident during a seizure event.

As seen in Figure 3.10, there was a gap in channel availability that emerged after the first pulse, and which remained for all consecutive pulses, with the two Na_v1.1 variants, as 5A and 5N peaks, decaying more or less in parallel through the train. Comparing the two isoform populations as a group, the difference between the two splice variants under these “seizure-like” or “high-activity” conditions was highly significant (two-way ANOVA, P<0.001) throughout the train of pulses, with 5N channels always more available and remaining approximately 10% more available compared to 5A channels (Figure 3.10). This indicated that 5N channels do have the potential to respond differently to 5A as far as their availability is concerned under conditions mimicking fast interneuronal spiking or an epileptic event. Such a distinct response at these conditions lays a functional biophysical basis for the differential predisposition for febrile seizures that occurs in patients with different 5A/5N relative proportions argued by several studies (Schlachter *et al.*, 2009, Le Gal *et al.*, 2011). However, as noted above, these findings predict a difference between

the variants, which must be confirmed in neurons, ideally in interneurons where $Na_v1.1$ channels are thought to dominate (see chapter 7).

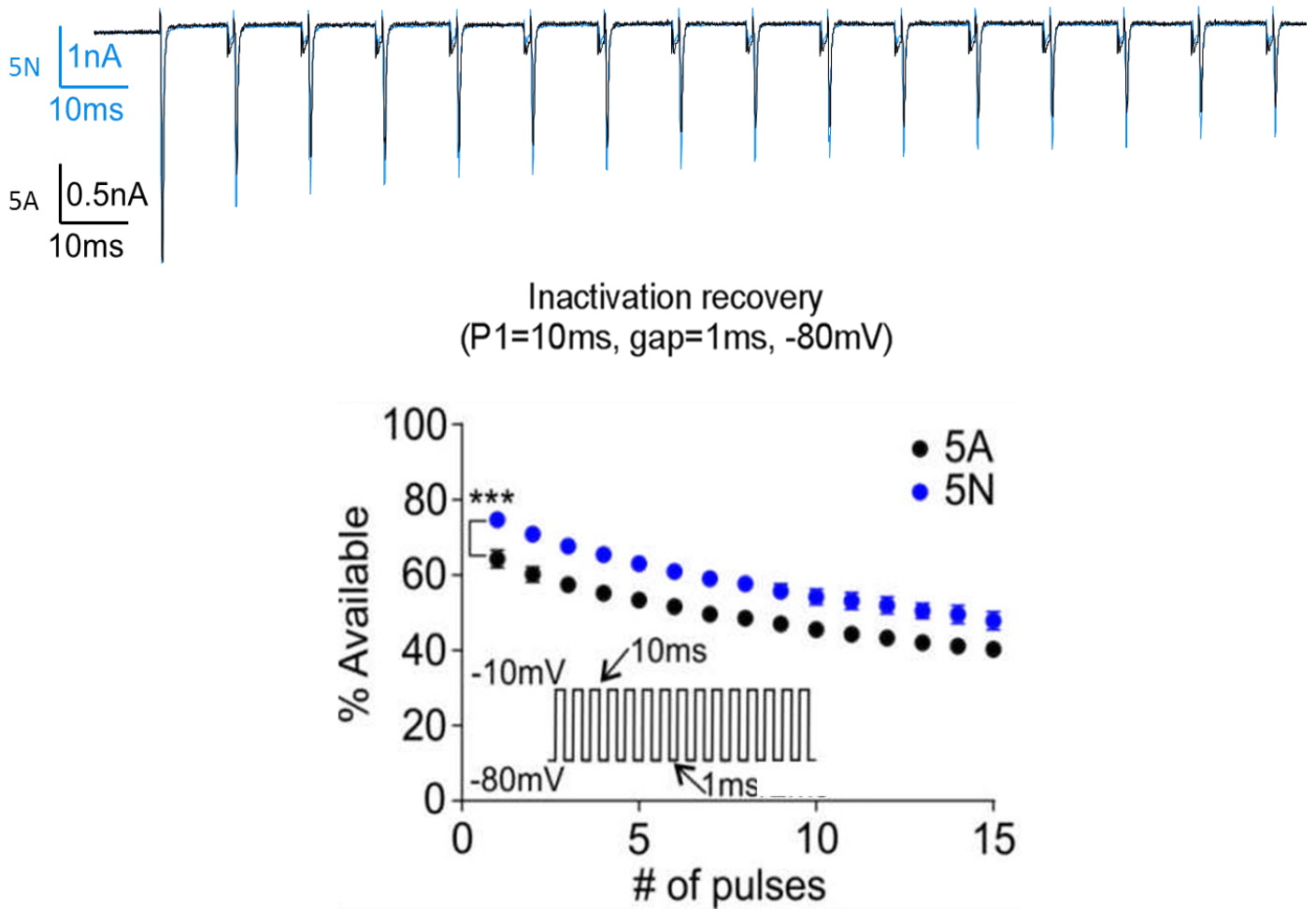


Figure 3.10: $Na_v1.1$: Trains of pulses mimicking a “seizure-like burst” retain the difference between the splice variants.

Raw traces are given on top for $Na_v1.1$ neonatal (blue) and adult (black) channels (5A n=8; 5N n=8)

3.5.2 Splicing may have a specific effect on the affinity of the inactivation particle for the inner pore

The modelling in this section was largely carried out by my supervisor, S. Schorge, using my data.

HEK293T cell data suggest that splicing can change the fastest component of recovery from inactivation (i.e. the instantaneous recovery, section 3.2.2), without altering voltage-dependence of activation and inactivation or macroscopic kinetics of the channels. In order to determine if in principle this is biophysically possible, a recently reported model of Na_v channels (Carter *et al.*, 2012) was fitted to Na_v1.1 currents recorded in HEK293T cells. In order to match data collected in our conditions, the rates used to fit the base model were adjusted to match the voltage sensitivity of activation, possibly because Carter *et al.*, (2012) were using neurons likely to be expressing a mix of Na_v channels with a small amount of Na_v1.1. This initial model (Figure 3.11.D) was then used to examine if it is possible to change the stability of inactivation without altering its voltage dependence, or macroscopic kinetics of currents in response to voltage steps. The model (thick grey line overlay) accurately predicts macroscopic currents produced by either splice isoform of Na_v1.1. 5A (thin black line) and 5N (thin blue line) (Figure 3.11B). Macroscopic currents predicted by the model for both isoforms for a single step were identical, as also were the predicted voltage dependence of activation (right side) and inactivation (left side) of both isoforms of Na_v1.1 model (Figure 3.11C). Because this model only includes active and fast-inactivated states (there are no slow inactivated states), there was a deviation from the steepness of the voltage-dependence of activation curve (Figure 3.11C) which is likely due to contamination by slow inactivated states at different potentials in HEK293T cells.

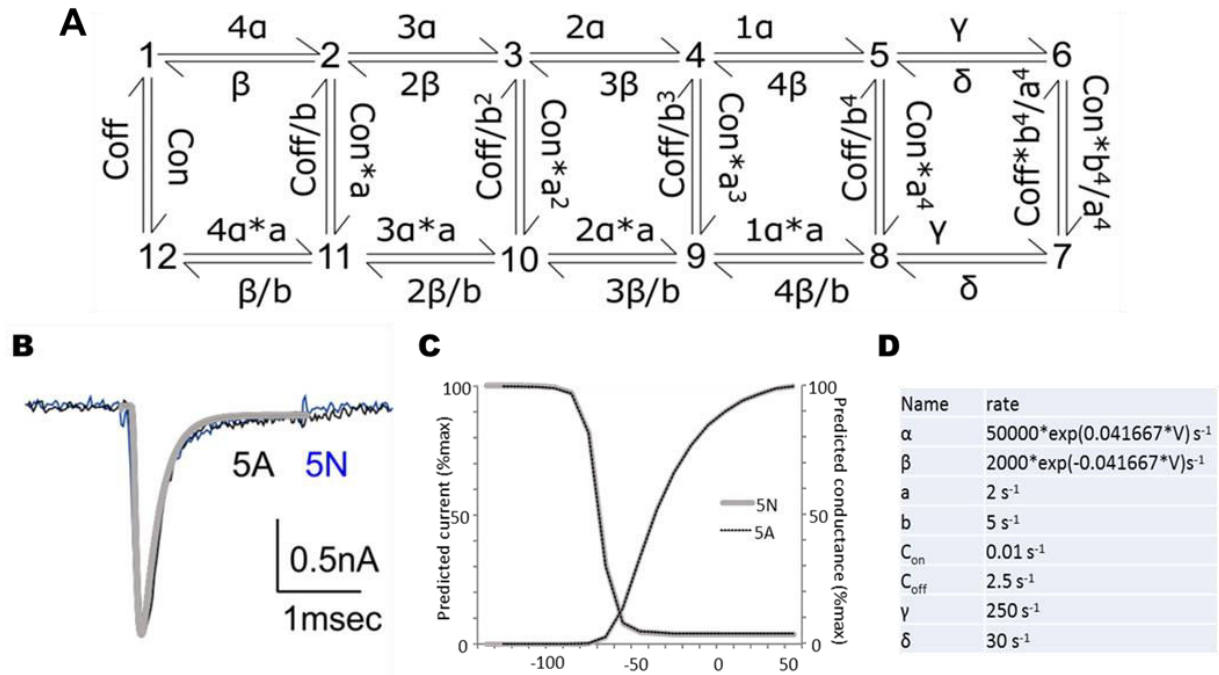


Figure 3.11: A model of sodium channel gating shows that modification of a single gating step may be sufficient to alter stability of fast inactivation without altering other parameters

A. The scheme, as adapted from Carter *et al.*, (2012) and used for our hNa_v1.1 channels in HEK293T cells at 37°C. The top left position (#1) corresponds to resting, closed channels with all four voltage sensors down (de-activated) and the inactivation particle off (i.e. channels are not inactivated, or are de-inactivated). At rest at -80 mV 87% of channels are in this state, and 11% of channels have a single voltage sensor up (state #2). The only state which passes current is state #6 (top right), which channels briefly visit upon depolarization. The bottom row of states (#7-12) all have the inactivation particle bound ('on'). During a typical step to -10 mV, approximately 1 ms after the step >85% of channels are in state #7 (where the pore is open, but no current passes because the inactivation particle is bound). The two splice isoforms of Na_v1.1 were modelled by changing the rate at which channels move between states #1 and #12 (i.e. the rate at which the inactivation particle binds to or comes off the inner pore of channels with all four voltage sensors in the resting, 'down', configuration). The transitions for adult isoforms are 0.35 times the rates for transitions between these states for the neonatal isoforms (exact values: Adult (1-12) = $0.01 \cdot 350 \text{ s}^{-1}$; Neonate (1-12) = $0.01 \cdot 1000 \text{ s}^{-1}$; Adult (12-1) = $2.5 \cdot 350 \text{ s}^{-1}$; Neonate (12-1) = $2.5 \cdot 1000 \text{ s}^{-1}$). **B.** The model can predict macroscopic currents produced by either splice isoform of Na_v1.1. 5A = thin black line, 5N = thin blue line, model = thick grey line overlay, however, as this is a simplified model, it does not replicate all aspects of channel behaviour (e.g. no slow inactivation). Macroscopic currents predicted by the model for both isoforms for a single step from -80 mV to -10 mV were identical. **C.** Predicted voltage dependence of activation (right side) and inactivation (left side) of both isoforms of Na_v1.1 model. The data from 5N are behind data from 5A, but the line is thick to show complete overlay. **D.** Values used in model for 5N. The only difference for 5A was a slowing of rates between states 1 and 12 by 0.35.

The scheme is composed of 12 different states where a Na_v channel may be at any given time. The top left position (#1) corresponds to resting, closed channels with all four voltage sensors down (de-activated) and the inactivation particle off (i.e. channels are not-inactivated, or they are de-inactivated). The four positions to the right of that (#2 - #5) are still in resting, de-inactivated states with an increasing number of S4 voltage sensors shifting to “up” positions as the channel moves to the right. Even channels in position #5, where all four S4 segments are in up positions, are still in a non-conducting state. The only state which passes current is state #6 (top right), which channels briefly visit upon depolarization. The states in the bottom row (#7 - #12) all have the inactivation particle bound (‘on’), so they are all in non-conducting states.

At rest at -80 mV 87% of channels are in state #1, and 11% of channels have a single voltage sensor up (state #2). During a typical step to -10 mV, approximately 1 ms after the step >85% of channels are in state #7 (where the pore is open, but no current passes because the inactivation particle is bound).

It was first systematically probed whether it is possible to uncouple recovery from fast inactivation from other aspects of channel activity, such as production of persistent current, or voltage dependence. Not surprisingly, changes made to most of transition rates altered both the voltage-dependence and the rates of onset of inactivation. However, one of the main parameters determining the recovery from fast inactivation is the return of the fully deactivated channel from the inactivated state (bottom left state #12 in Figure 3.11A), back to the state which is fully deactivated and non-inactivated (top left state #1 in Figure 3.11A). It was found that changing the rate of the transitions between these two states (by a factor of 0.35) was sufficient to change the rate of recovery with little or no impact on other parameters (Figure 3.12A). This change was also sufficient to reproduce the difference in availability during trains of short stimuli (Figure 3.12B).

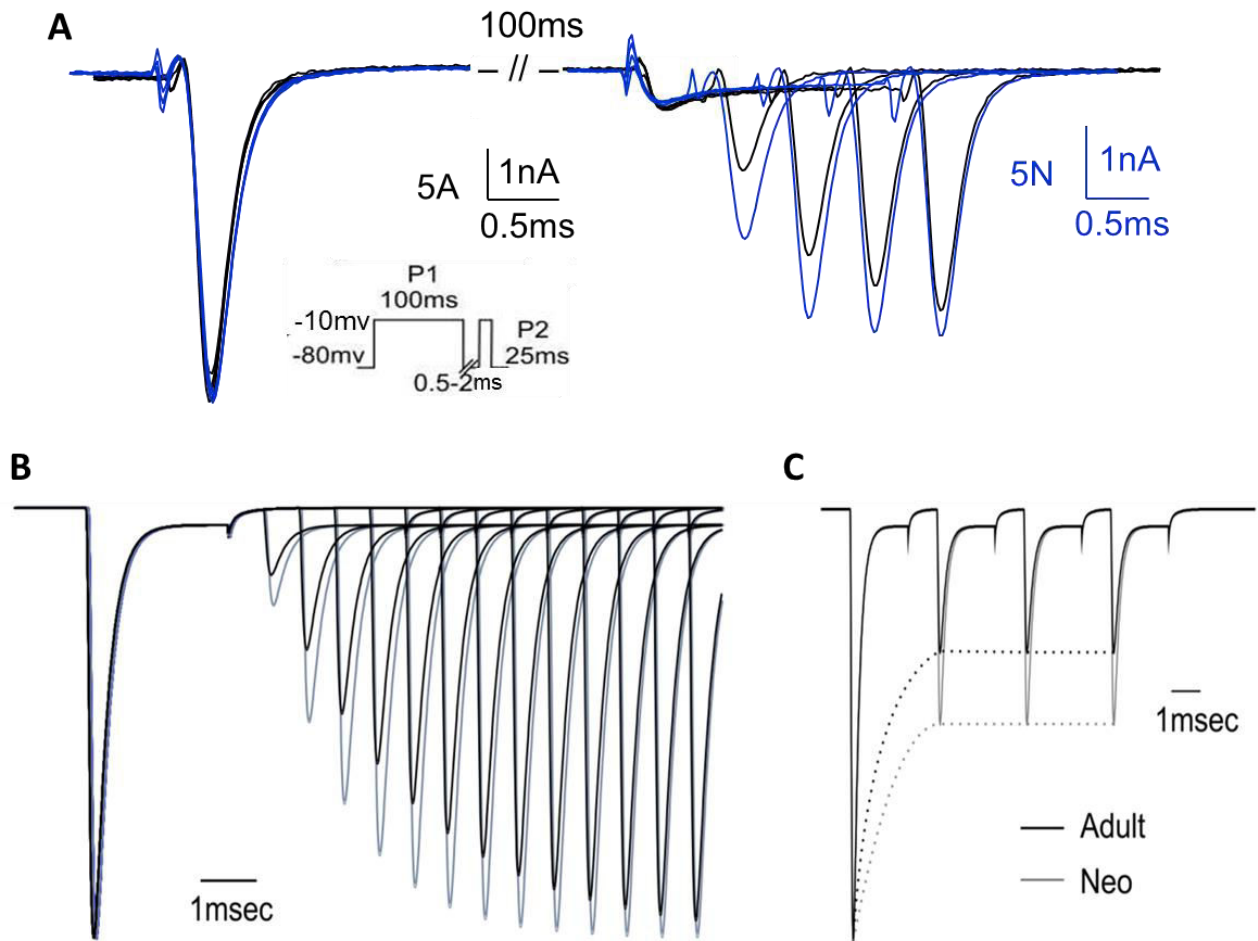


Figure 3.12: The specific change in rates between states 12 and 1 replicates HEK293T cell findings for recovery from inactivation and availability

A. Raw traces for recovery from fast inactivation after 0.5, 1, 1.5 and 2 ms for adult (black) and neonatal (blue) $\text{Na}_v1.1$ channels. **(B. C.)** Slowing the transitions between states 12 and 1 (grey traces, faster rates $1-12 = 0.01 \cdot 1000 \text{ s}^{-1}$; $12-1 = 2.5 \cdot 1000 \text{ s}^{-1}$ black traces, slower rates, both = grey rate $\cdot 0.35$) is sufficient to increase the rate of recovery **(B)**, and the availability of channels during a train of short steps **(C)**, without modifying the kinetics of the currents during steps (both predicted currents are overlaid in the first steps of A and B). Voltage dependence of activation and steady state inactivation were also unchanged by this manipulation (Figure 3.11C).

There was one additional change in the voltage dependence of recovery from inactivation (Figure 3.13A) that was predicted by the model, which was not seen in HEK293T cells (Figure 3.13B). This is a difference in how the voltage during the recovery step affected the rate of recovery, where the model predicted the neonatal channels to be more sensitive to hyperpolarising recovery intervals. The difference could be possibly attributed to the lack of slow inactivation in our model, as it may be that contamination by slow inactivated states in HEK293T cells obscures the difference between the two isoforms.

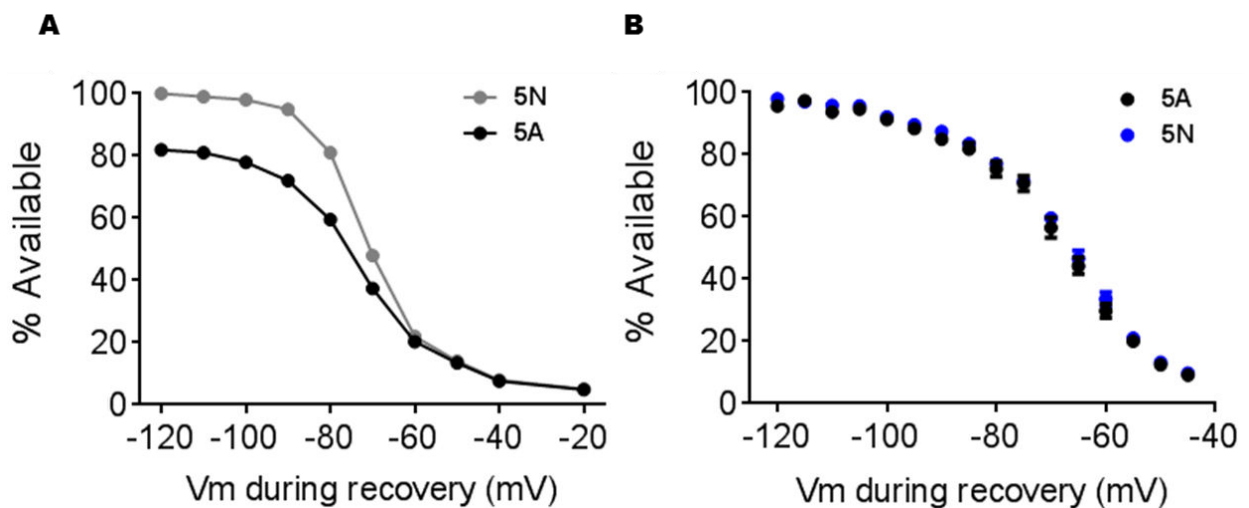


Figure 3.13: Slow inactivation probably masks the predicted difference between isoforms on voltage dependence of inactivation recovery

A. According to the model, changing the rate of transition between states 12 and 1 alters the voltage dependence of recovery from inactivation at strongly hyperpolarized potentials. **B.** For Na_v1.1, the holding voltage during short (2ms) recovery intervals does not change the amount of channel availability (5A n = 13; 5N n = 17).

Because this model is based on a structural scheme of the channel, these data suggest that splicing which affects the linker before the voltage sensor in domain I may have an impact on the affinity of the inactivation particle for fully de-activated channels.

3.5.3 No difference in inactivation recovery between variants with a simulated “interneuronal firing pattern”

Up to now, experiments have suggested that the combination of short P1 intervals, short interpulse gap durations and a resting membrane potential of approximately -80 mV are the conditions that can hold a robust difference in recovery from inactivation between Na_v1.1 5A and 5N channels, with 5N channels always recovering more quickly. As a simplified alternative, in order to partially simulate a “physiological interneuronal firing pattern”, a recovery protocol was designed with “interneuronal-like” parameters. Hence, the holding membrane voltage was set at -80 mV (i.e. approximately -85 mV after junction potential), while depolarizing pulses were given at 100Hz frequency, a rate consistent with published reports of a rapid, yet still physiological, interneuronal firing rate (Quilichini *et al.*, 2012). Pulses went from -80 mV to +20 mV (not -10 mV as in all previous protocols) in order to simulate depolarization during an AP, while for the same reason depolarization (i.e. P1 duration) was kept as short as possible (2 ms). The firing rate here was lower than the frequency rate used in the previous “seizure-like” protocol (e.g. 10 ms step, 1 ms recovery).

Under these conditions, no difference was seen between the 5A and 5N variants, as they recovered from inactivation at exactly the same rate throughout the pulse train (two-way ANOVA, $P > 0.05$; Figure 3.14A). Pushing the system further in order to again try and mimic a pathophysiological, “seizure-like” firing rate, the firing frequency was doubled to 200Hz by reducing the interpulse gap duration. Again, 5A and 5N variants appeared to recover from inactivation in an identical way under these conditions (two-way ANOVA, $P > 0.05$; Figure 3.14B).

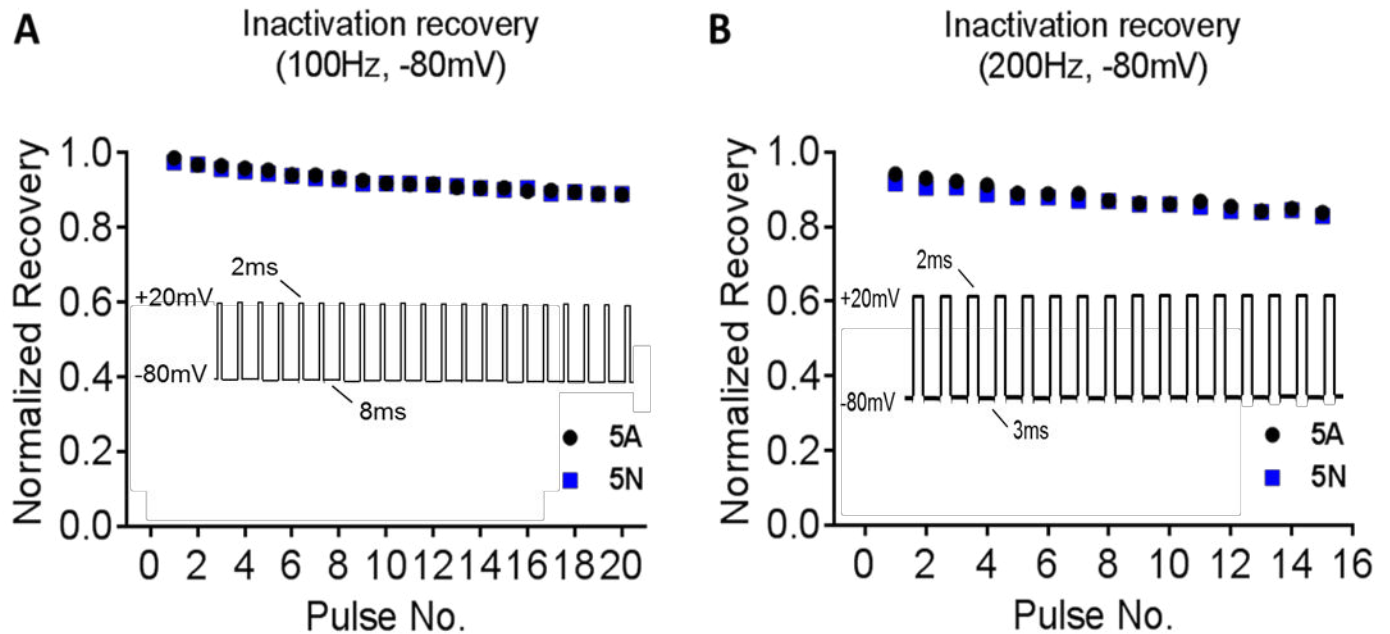


Figure 3.14: Na_v1.1: Simulation of an interneuronal firing pattern at -80mV does not reveal a difference between 5A and 5N splice variants

neither at A. 100Hz firing frequency (5A n=11; 5N n=6), nor at B. 200Hz firing frequency (5A n=6; 5N n=3).

One possibility is that the relative lack of inactivation (in the 100Hz train only ~10% of channels inactivate) obscures any differences between the variants. To test whether slightly depolarising the resting membrane potential could reveal a difference between the two isoforms, the experiments were repeated with a holding potential of -70 mV. In these conditions the splice variants again remained indistinguishable, at 100Hz (two-way ANOVA, $P > 0.05$; Figure 3.15A), and at 200Hz firing frequency (two-way ANOVA, $P > 0.05$; Figure 3.15B). It may be that the stronger depolarisation in the steps was sufficient to obscure the difference between the variants, or that the relatively small amount of inactivation (~ 20%) meant that the differences were not big enough to be seen. Thus, while much of our data indicate that splicing will change channel availability, to test the physiological significance, it is necessary to confirm that conditions in neurons are within the range that generates the difference.

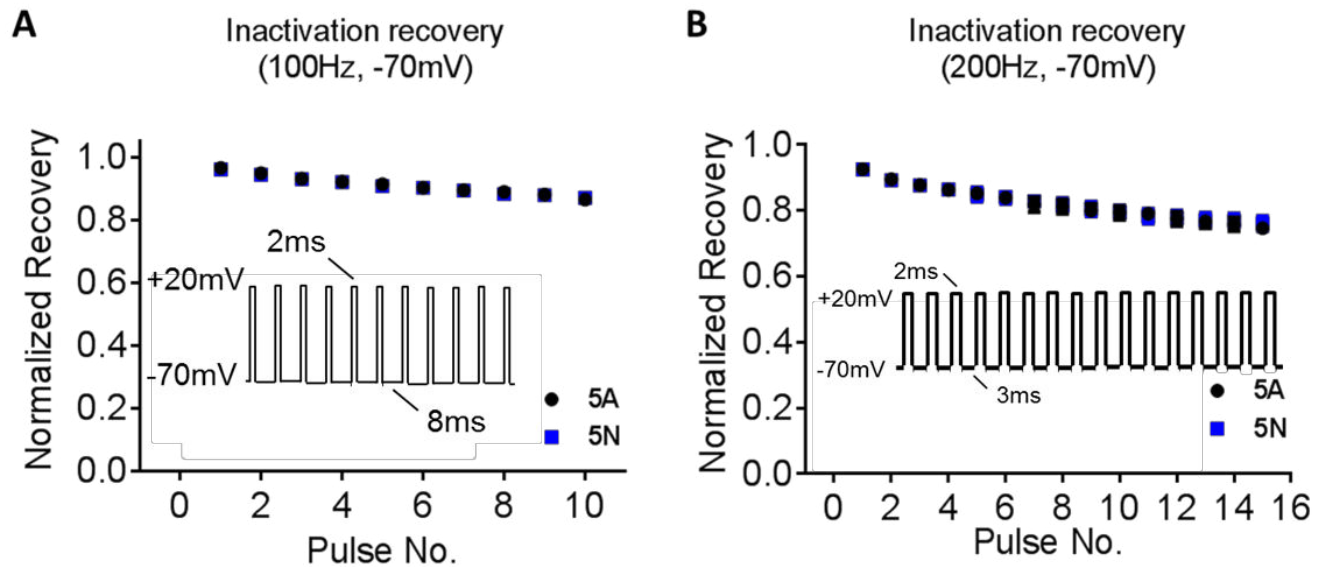


Figure 3.15: Na_v1.1: Simulation of an interneuronal firing pattern at -70mV holding voltage does not reveal a difference between 5A and 5N splice variants

neither at **A**. 100Hz firing frequency (5A n=11; 5N n=14), nor at **B**. 200Hz firing frequency (5A n=6; 5N n=8)

3.6 Discussion:

3.6.1 Splicing affects a fast onset, short lived form of inactivation

Results here indicate that the difference between the two isoforms is strongest for short-lived inactivated states, achieved by brief depolarisations. Such states also tend to be rapid in onset (Ulbricht, 2005), therefore the original relatively long prepulse (100 ms) used may mask a difference of availability between isoforms by shifting channels out of the short lived inactivated states and into slow inactivated states. This is likely to be the case in Figure 3.8, where the prolonged depolarization pulse (300 ms) has probably shifted cells much more towards slower inactivation, a state that does not appear to be affected by the splicing difference, as was seen in

the analysis before. Shifting towards a slower inactivated state is also suggested by the loss of the double exponential recovery relationship, indicative of a fast and a slow component of inactivation as seen before for a P1 duration of 100 ms (Figures 3.2 & 3.3) and satisfactory fitting of the data with a single exponential, thereby implying that a single, slower inactivated state almost exclusively determines the recovery of the channels after prolonged depolarisations. The shortest P1 durations (2 – 10 ms, Figure 3.5) prevented cells from entering into slow inactivated states and allowed for the difference in availability between the two isoforms to be revealed under a fixed short (2 ms) recovery interval. At longer time points slow inactivation is now probably determining the recovery rate and therefore availability and becomes the rate limiting step at that time and masks the effect of the splicing on channel availability. Therefore, it is a matter of further study to investigate how the distribution of channels in different inactivated states prior to activation might affect their availability at recovery. This initial distribution is going to be heavily dependent on the original holding voltage where cells are held and how changing voltage may affect splice variant behaviour is described in results section 3.4.

Briefer pre-pulses that favour short-lived inactivated states are also suggested to be more representative of action potentials (AP) firing in neurons, when depolarisation lasts usually for 1, or at most only a few, milliseconds and prolonged depolarisations are not likely physiological. Therefore, the ability of the splice isoforms to respond differently after short depolarisations may mean splicing changes the ability of sodium channels to open repeatedly during trains of fast stimuli, such as bursts of action potentials. This would also be in line with this splicing event playing a potential role in epilepsy, where neurons are suggested to undergo very rapid burst firings. Therefore, another major matter of study was to assess isoform availability under conditions of repetitive short depolarisations, mimicking AP bursts in neurons during high-frequency, “seizure-like” stimulations (Results section 3.5).

3.6.2 The difference between variants is steeply dependent on voltage

The difference in fast inactivation recovery between Na_v1.1 5A and 5N channels is confined to a specific membrane holding potential of -80 mV, while it is lost at more depolarized (-70 mV) or more hyperpolarized (-100 mV) potentials. It is not clear what membrane potential in HEK293T cells is most relevant to neurons. One report may suggest -60 to -65 mV as a physiological resting potential seen in brain interneurons (Lamsa *et al.*, 2007), which are the principal areas of expression of Na_v1.1 channels (Yu *et al.*, 2006). In comparison, the recently published online database of cells from the Allen brain atlas predicts a more negative potential between -70 and -80 mV for most interneurons (<http://celltypes.brain-map.org/>). However, the absolute potential depends on the liquid junction potentials, and recording setup (e.g. ground connection), which makes direct comparison between recordings carried out with different solutions or equipment notoriously unreliable. The most direct approach is to test whether the behaviour of the variants in neurons reflects the difference in availability as predicted in HEK293T cells. According to the results here, the balance of channel inactivation states set by the holding voltage, can obscure the difference in inactivation recovery seen between the two Na_v1.1 channel isoforms, however, in HEK293T cells it is not clear how the holding voltage interacts with the fast inactivation recovery process in Na_vs. Hence, in order to determine if the biophysical differences observed between variants may have physiological relevance, variants will need to be compared in neurons, using protocols designed to probe the differences seen here (see chapters 6 & 7).

3.6.3 A special role for the S4 in Domain 1 in stability of inactivation?

At the molecular level, the modelling suggests that inclusion of a negatively charged amino acid (in the adult exon) in the D1S3-S4 linker stabilizes the inactivation particle in the inner side of the channel pore when all four S4 sensors are down. In crystal studies of voltage-gated channels the S3-S4 linkers are notably disorganized compared to the helices (Payandeh *et al.*, 2011), and consequently at this time the exact position of the conserved amino acid change is not known. Previous studies of gating currents have suggested that the voltage sensor in the fourth domain

(D4S4) is most important for limiting the rate of *onset* of inactivation (Capes *et al.*, 2013), and this S3-S4 linker is already implicated in drug binding (Yang *et al.*, 2009). Here, it is proposed that the S4 segment in the first domain (D1S4) may have a relatively more important role in *release* from inactivation. A possible mechanistic explanation is that, while the S4 in the fourth domain is the last to activate and to initiate inactivation (Capes *et al.*, 2013; Chanda and Bezanilla, 2002), the S4 in DI may be the last to dissociate from the inactivation particle, thereby being the rate limiting step in recovery from fast inactivation.

The model used here, which is adapted from Carter *et al.* (2012), is designed to only contain the fast inactivated states. One reason for this is that the physical basis of slow inactivated states, although important for some types of drugs, is not well characterized (Karoly *et al.*, 2010).

3.6.4 Could the difference between the variants be physiologically relevant? HEK293T cells show a potential for a difference – moving to neurons

It has already been previously reported that, under physiological temperature conditions using a CsCl-based intracellular solution, neonatal *SCN1A* channels show faster inactivation recovery compared to adults for shorter, but not for longer recovery intervals after long depolarization steps (P1=100 ms) (Fletcher *et al.*, 2011). By widening the number and range of recovery interval data points gathered in our study – hence allowing appropriate data fit and analysis – as well as manipulating the different parameters that can affect the inactivation recovery relation, has revealed new insights about the relationship between this splicing event and sodium channel biophysics and behaviour.

Our data in Figures 3.2 & 3.3 show increased recovery of neonatal channels from fast inactivation for recovery intervals ≤ 10 ms, which comes in line with the main findings in Fletcher *et al.*, 2011. A double exponential relationship such as the one that best fits the data here usually implies the existence of two distinct molecular events occurring. With the significant difference in inactivation recovery between splice variants being confined at the initial part of the curve while being lost on the second part, it could be argued that the molecular component that confers this difference between 5A and 5N channels occurs on a very rapid scale. This component gets masked by a

second molecular event occurring later on in the inactivation recovery process, which may act as a rate-limiting step making the two channels behaving similarly from that point and on. Therefore, these findings are consistent with splicing altering an inactive state that is both rapid in onset and rapid in recovery, with longer, slower inactivated states remaining insensitive to splicing.

All components of the equation characterizing the two fits were comparable, irrespectively of the level of constraint of the constants (red VS green lines), apart from the Y_0 parameter, which defined each fit's starting point. In this case, Y_0 represents a very fast, almost instantaneous component of inactivation that was established even before the first interpulse gap time point of 0.5ms measured here. Therefore, Y_0 defined the difference between the two fits throughout the fast and slow components of recovery from inactivation described by the double exponential decay equation, until convergence of the fits at later time points, most probably due to a common rate limiting step. To experimentally validate whether Y_0 constitutes an inactivation component that occurred even earlier than the first 0.5ms recovery interval examined here, even shorter time points should be taken. This though is next to impossible, given the limitations of the equipment and the time constant of the cell membrane itself. Our model predicts that after 0.10 ms 3% of neonatal channels have returned to the top row of states (de-inactivated) while for adult channels at this (very fast) time point 2% will have left the inactivated states. By 0.50 ms, the neonatal channels have 20% de-inactivated (18% in state #1 and 2% in state #2), while adult have only 14% (12% in state #1 and 2% in state #2). Thus the model predicts that the difference in variants would occur as soon as 100 microseconds after returning to -80 mV, and clearly outside the time points accessible to experimental whole cell voltage clamp. This is because the charging time constant of the cell is a function of its capacitance times the access resistance. Given that the average access resistance that was achieved during voltage clamp recordings was about 1.5 – 2 M Ω and the average HEK293T cell capacitance was around 16 – 20 pF, this gives an average charging time constant of around 240 – 400 μ s, therefore any voltage change below that timeframe is impossible to be accurately clamped.

From the experimental data, we could not exclude the possibility that the Y_0 difference between the two fits is due to a bigger percentage of neonatal channels compared to adult ones having remained at the closed, non-inactivated state during the initial depolarisation phase (#5). This would imply that upon shortest repolarizations after P1 and consequent very fast re-depolarisation there is a bigger pool of neonatal channels at the closed non-inactivated (#5) state that can transit

into the open state compared to adult channels at these shortest recovery intervals, where the vast majority of channels still did not have enough time to recover from inactivation and reactivate. Yet, according to the channel modelling, there are no channels for either isoform remaining at that stage during the P1 depolarization at -10 mV in order to support that notion. Actually, from the very first microseconds of repolarization to -80 mV they pass extremely fast to the bottom left states, without any vertical transactions to the top, non-inactivated states (including #5). The only vertical transaction that occurs in the model is from state #12 to #1, which is where it is suggested here that the difference between the two splice variants lies. Therefore, according to the model, the difference in Y_0 cannot actually occur due to a different proportion of neonatal channels compared to adults in state #5 immediately after repolarisation, but instead is due to the different rate at which channels return from state 12 to 1.

As a conclusion of this analysis, the distinct neonatal and adult Y_0 values found here are defining the difference between the two fits right from their origin, so that after that they run distinctively and in parallel, at least until a common rate limiting component makes them converge at longer recovery interval time points. This distinct, parallel movement between the isoforms during fast recovery is in line with the short train depolarization data in Figure 3.11, where the difference in channel availability is defined from the very first depolarization and then the two lines run in parallel.

HEK293T expression is an oversimplified simulated system and not a real neuron firing APs. Neuronal firing involves many other voltage-gated channels from sodium channels, and after-hyperpolarization events not taken into account here as well as different depolarization rates, especially during trains of APs, which may alter the response of the sodium channels. Therefore, extensive additional characterisation of parameters in HEK293T cells may not be the most informative way forward, as this may not reflect the impact on neuronal activity. Furthermore, the inactivation recovery when cells were held at -80 mV and together with the recording conditions that were set, might had been too close to 1 (i.e. full recovery) for recovery curves to have enough space potential to be separated. It cannot be ruled out that under more appropriate physiological conditions (β -subunit co-expression, channel phosphorylation etc.) inactivation recovery might had been less complete, thereby allowing potential differences between 5A and 5N channels to be better revealed.

Therefore, HEK293T cells have been used here as a means to reveal that the two isoforms have indeed the potential to respond differently under fast stimulating conditions, and to make predictions for how splicing may alter neuronal behaviour. Yet, in order to explore the neuronal effect of the two isoforms in their native environment, it is important to move to a more physiologically relevant system than HEK293T cells. Two lines forward might be useful for determining what aspects of splicing are physiologically important. Firstly, what differences are conserved in other channels (see chapter 4) and secondly, what differences are imposed on neuronal behaviour when splicing is manipulated (see chapter 6 & 7).

3.7 Summary

Summarizing the results for Na_v1.1 5A and 5N splice variants and their difference in recovery from fast inactivation, it has been suggested here that the difference between splice variants seems to be most robust at a resting membrane potential of approximately -80 mV (or -85 mV corrected for LJP), with short P1 intervals, and short interpulse gap durations (≤ 2 ms). Interestingly enough, the difference between splice variants is completely masked by prolonged depolarizing P1 steps, resting membrane potentials other than -80 mV and by recovery intervals longer than 20 ms. Finally, the difference is robust in consecutive rapid pulse protocols that are consistent with the sort of fast neuronal activity that might occur during epileptic events. This indicates that splicing may have its biggest impact on inactivation in conditions that could mimic interneuronal firing patterns or fast activity during a seizure. Given the sensitivity of splice variants to changes in voltage and duration of stimuli, it is important to confirm the difference observed can translate to effects which can have physiological relevance. The remaining chapters explore this by addressing some further questions: Does splicing have conserved effects on other channels? (Chapter 4) Can manipulating splice variants change the firing of neurons? (Chapter 6) Does splicing have the potential to change how neurons respond during epileptiform events? (Chapter 7)

Chapter 4: Conservation of a functional impact of alternative splicing in domain 1 of Na_v1.1 channels in neuronal sodium channels Na_v1.2 and Na_v1.7

4.1 Hypothesis and aims

The alternative splicing motif in domain 1 of Na_v1.1 channels is conserved in all five TTX-sensitive neuronal Na⁺ channels: Na_v1.1, Na_v1.2, Na_v1.3, Na_v1.6 and Na_v1.7. The conservation of this site is particularly striking given recent data suggesting that alternative splicing is not, in general, well-conserved (Gerstein *et al.*, 2014). In Na_v1.1, channels containing exon 5N recover more quickly from fast inactivation in several stimulation paradigms explored here already. Fletcher *et al.*, (2011) attributed the functional difference to a single amino acid change between the Na_v1.1 5A and 5N exons (D207 to N). This change is conserved in Na_v1.1, Na_v1.2, Na_v1.6 and Na_v1.7 channels. This observation prompts the question whether there is a conserved functional impact imposed by alternative splicing in neuronal sodium channels, which may indicate an evolutionary drive that supports its molecular conservation (Copley, 2004). Up to now, there has been no functional study comparing adult and neonatal transcript variants that compares multiple related sodium channel subtypes bearing the same splicing event. Therefore, this study asked whether a molecular conservation of splicing in different channel subtypes could lead to a conserved functional change. Does the difference in inactivation recovery between variants found in Na_v1.1 channels also occur in closely (Na_v1.2) and more distally related (Na_v1.7) sodium channel subtypes? Of all sodium channels Na_v1.2 has the closest sequence similarity to Na_v1.1, while Na_v1.7 although still quite similar in sequence is more distantly related, (Catterall, 2005). An additional difference is that Na_v1.7 is largely found in peripheral neurons, and is particularly important for subthreshold signaling and nociception in small diameter neurons, while Na_v1.1 and Na_v1.2 are preferentially expressed in the central nervous system. Nav1.1 plays a predominant role in the excitability of fast-spiking parvalbumin-positive interneurons in the CNS (Yu *et al.*, 2006). In contrast, Nav1.2 is primarily expressed in excitatory neurons, and is particularly important early

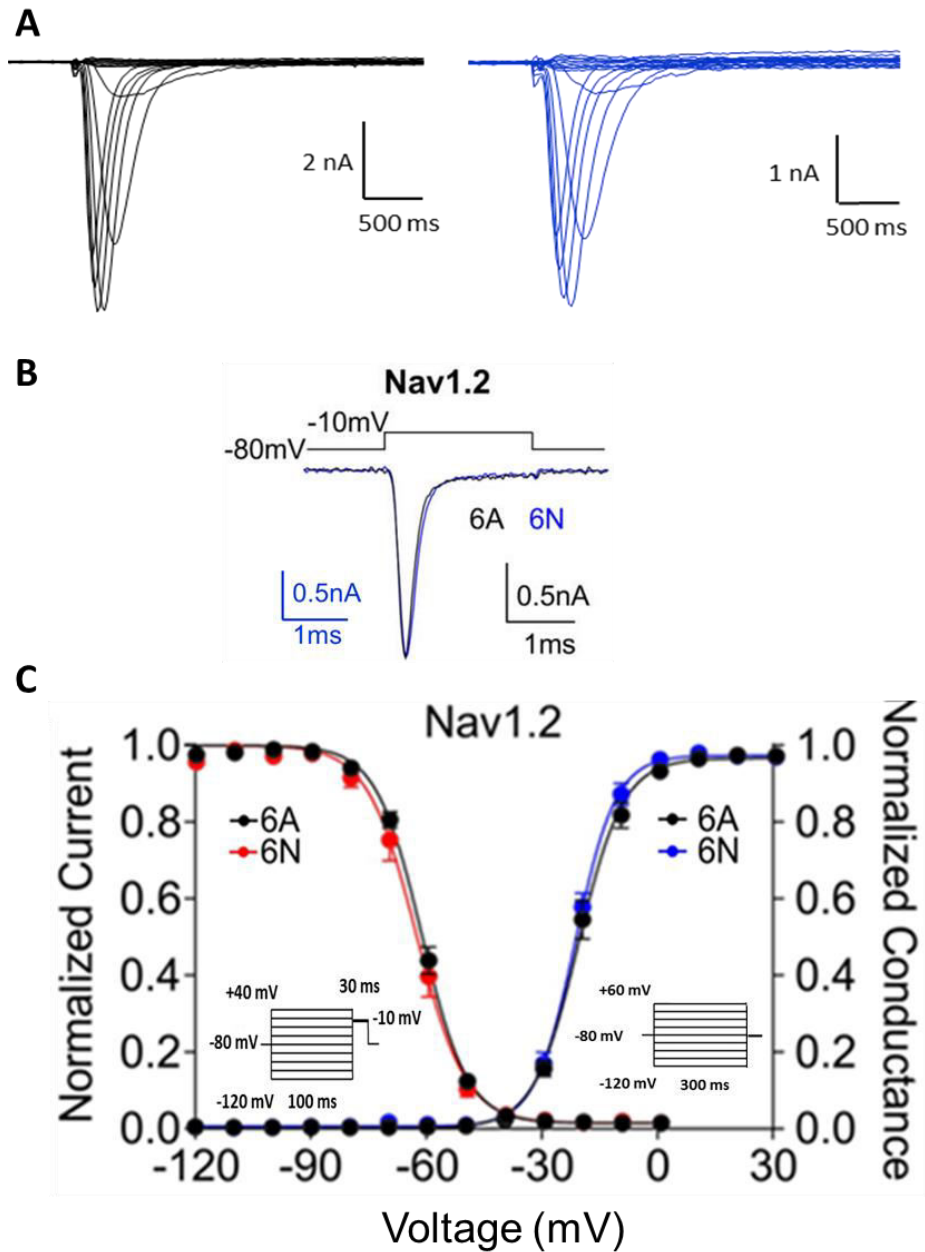
in development (Oliva *et al.*, 2012). In terms of both the physiology of the neurons, and the macroscopic kinetics of gating, Na_v1.7 channels are more distant from the two channels in the CNS (Dib-Hajj *et al.*, 2013). Nevertheless the site of splicing is conserved across all three channels.

Both Na_v1.2 and Na_v1.7 neonatal variants have the conserved asparagine residue at an equivalent position to N207 in Na_v1.1 5N, which was sufficient and necessary to confer a higher rate of inactivation recovery compared to the adult isoform (Fletcher *et al.*, 2011). As a result it was hypothesized that the same splicing event in Na_v1.2 and Na_v1.7 channels will confer a conserved functional difference in fast inactivation recovery as for Na_v1.1, in spite of the different functional roles and spatial distributions of the channels.

4.2 Results: Comparing the functional properties of splice variants for Na_v1.2 and Na_v1.7

4.2.1 As in Na_v1.1, voltage dependence of activation/inactivation in Na_v1.2 & Na_v1.7 remains unaffected

The first step in the study of Na_v1.2 and Na_v1.7 channels was to compare voltage dependence properties between the adult and neonatal isoforms. Voltage dependencies of activation and inactivation did not differ between variants for Na_v1.2 (Figure 4.1, A & B) or Na_v1.7 (Figure 4.2, A & B) (Boltzmann non-linear curve fits, $P > 0.05$, two-way ANOVA). Consistent with other publications, Na_v1.7 channels showed a -17 mV more hyperpolarized $V_{1/2}$ of inactivation compared to Na_v1.1 and around -10 mV more hyperpolarized $V_{1/2}$ of inactivation compared to Na_v1.2 (Chatelier *et al.*, 2008; Farmer *et al.*, 2012). However, as for Na_v1.1, in these recording conditions, there were no differences in voltage dependence properties between transcript variants for Na_v1.2 and Na_v1.7 channels (see Figure 4.1 & 4.2).



$$6A: V_{1/2\text{activation}} = -21.5 \pm 3.7 \text{ mV}$$

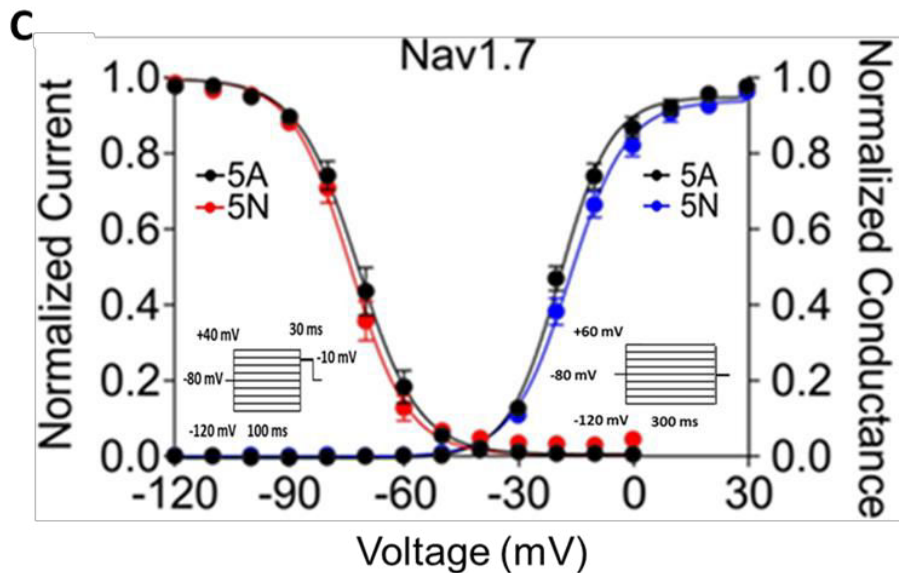
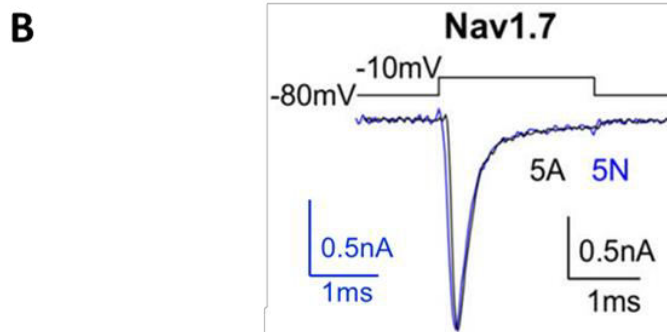
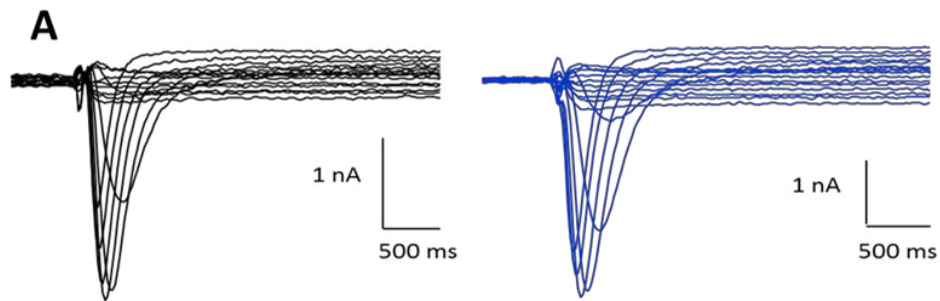
$$6A: V_{1/2\text{inactivation}} = -61.3 \pm 1.4 \text{ mV}$$

$$6N: V_{1/2\text{activation}} = -21.2 \pm 1.6 \text{ mV}$$

$$6N: V_{1/2\text{inactivation}} = -62.9 \pm 2.4 \text{ mV}$$

Figure 4.1: Nav1.2: No difference in macroscopic properties and VD activation/inactivation between isoforms.

A. Representative traces from HEK293T cells expressing adult (black) and neonatal (blue) isoforms evoked by a 2 ms step to -10 mV. Macroscopic properties of the currents were largely indistinguishable for individual pulses. **B.** Voltage Dependence of activation & inactivation – no difference is seen between 6A and 6N variants (6A n = 9; 6N n = 7).



$$5A: V_{1/2\text{activation}} = -15.9 \pm 2.5 \text{ mV}$$

$$5A: V_{1/2\text{inactivation}} = -71.8 \pm 3.6 \text{ mV}$$

$$5N: V_{1/2\text{activation}} = -16.2 \pm 3.0 \text{ mV}$$

$$5N: V_{1/2\text{inactivation}} = -74.3 \pm 3.9 \text{ mV}$$

Figure 4.2: Nav1.7: No difference in macroscopic properties and VD activation/inactivation between isoforms.

A. Representative traces from HEK293T cells expressing adult (black) and neonatal (blue) isoforms evoked by a 2 ms step to -10 mV. Macroscopic properties of the currents were largely indistinguishable for individual pulses. **B.** Voltage Dependence of activation & inactivation – no difference is seen between 5A and 5N variants (5A n = 6; 5N n = 7).

4.2.2 Preliminary investigation of recovery from fast inactivation in Na_v1.2 & Na_v1.7

Using the original inactivation recovery stimulating parameters described in Fletcher *et al.*, (2011), Na_v1.7 showed a difference in fast inactivation recovery rate between 5A and 5N splice variants (Figure 4.3). As for Na_v1.1, the data were fit with a double-exponential decay ($Y_0 + A_F \cdot (1 - \exp(-t/\tau_F)) + A_S \cdot (1 - \exp(-t/\tau_S))$), consistent with a fast (τ_F), and a slow (τ_S) component of recovery from inactivation. Parameters were allowed to both freely fluctuate (Figure 4.4, green line fits) or rate constants were fixed (τ_F : 1.7 = 9.2 ms; τ_S : 1.7 = 312 ms), thus allowing only the relative amplitudes of the fast (A_F) and slow (A_S) components to vary (Figure 4.4, red line fits). Both conditions allowed good fits ($r^2 > 0.99$ for all fits; Table 4.1) with negligible difference between the two levels of constraint (green vs red lines). Fits revealed a difference between neonatal and adult isoforms. This difference was similar to the one previously seen for Na_v1.1, with 5N channels recovering more than 5A after shorter recovery intervals, indicated also by a significant difference on the Y_0 parameter between Na_v1.7-5A and 5N (0.079 vs 0.012 for free fits, $P < 0.05$, two-way ANOVA), which was in accordance to what was seen for Na_v1.1 isoforms. Similar to Na_v1.1, the difference started attenuating at longer interpulse time intervals. Therefore, Na_v1.7 appears to behave in a similar way to Na_v1.1, as far as the inactivation recovery rate of its transcript variants is concerned. The difference might even be more robust for Na_v1.7 channels, since 5N channels recover more quickly than 5A for longer interpulse gap durations for Na_v1.7 than for Na_v1.1.

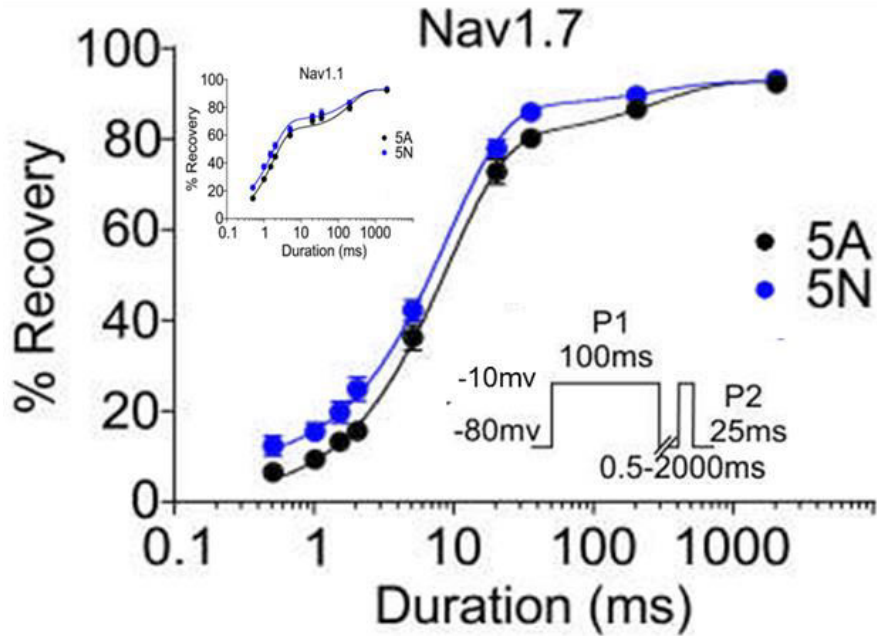


Figure 4.3: $\text{Na}_v1.7$: Channels containing exon 5N recover more rapidly from inactivation after short recovery intervals

Short recovery intervals at -80mV reveal a difference between splice variants with 5N recovering more quickly than 5A, which is masked as intervals get longer, similar to $\text{Na}_v1.1$ (shown in inset). (5A n=5; 5N n=8).

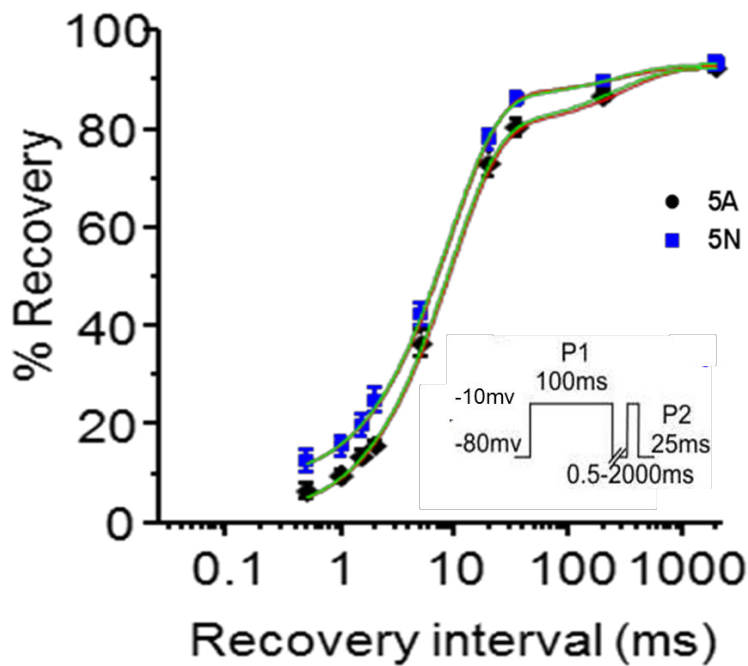


Figure 4.4: Recovery from inactivation for $\text{Na}_v1.7$ neonatal and adult isoforms, comparing fits with all parameters free (green lines) and with τ_f and τ_s fixed (red lines)

Values and standard errors of the fit values are in table 4.1.

Table 4.1: Na_v1.7: Parameters of bi-exponential fits to recovery from long (100 ms) inactivating pre-pulses.

Top panel: Optimized fitting parameters with τ_F and τ_S constrained (red lines in Figure 4.4, rates with n/a standard error (s.e.) were fixed). *Bottom panel:* Free fits with all parameters allowed to vary (green lines in Figure 4.4). R^2 is the adjusted R-square statistic used to improve comparison of fits with different degrees of freedom. Compare to values for Na_v1.1 given in Table 3.2.

Parameters from constrained fits (red lines in Figure 4.4)

	Na _v 1.7-5N		Na _v 1.7-5A	
	Value	s.e.	Value	s.e.
Y_0	0.084	0.004	0.015	0.005
A_F	0.79	0.01	0.80	0.01
τ_F (ms)	9.2	n/a	9.2	n/a
A_S	0.06	0.01	0.11	0.01
τ_S (ms)	312	n/a	312	n/a
R^2	0.999		0.999	

Parameters from free fits (green lines in Figure 4.4)

	Na _v 1.7-5N		Na _v 1.7-5A	
	Value	s.e.	Value	s.e.
Y_0	0.079	0.007	0.012	0.009
A_F	0.78	0.01	0.79	0.02
τ_F (ms)	8.7	0.4	8.9	0.6
A_S	0.07	0.01	0.12	0.02
τ_S (ms)	273	139	265	100
R^2	0.999		0.999	

When the same protocol was applied to Na_v1.2 6A and 6N channels, short recovery intervals failed to reveal a difference between splice variants, despite showing a small trend for 6N channels to recover more quickly (Figure 4.5). The recovery timecourse for Na_v1.2 channel isoforms was again well fit by two exponentials ($Y_0 + A_F \cdot (1 - \exp(-t/\tau_F)) + A_S \cdot (1 - \exp(-t/\tau_S))$), consistent with a fast (τ_F Na_v1.2 = 1.1 ms), and a slow (τ_S Na_v1.2 = 406 ms) component of recovery from inactivation. Contrary to what was seen for Na_v1.1 and Na_v1.7 variants, the instantaneous availability of both Na_v1.2-6A and 6N channels (Y_0 parameter) was similar (0 for both isoforms). To compare splice variants we fixed both rate constants (τ_F and τ_S) and only allowed the relative amplitudes of the fast (A_F) and slow (A_S) components to vary ($r^2 > 0.98$ for fits with these restrictions, Table 4.2), similar to what was done for Na_v1.1 and Na_v1.7 isoforms (Figure 4.5 & 4.6; Table 4.2). The lack of difference in Na_v1.2 was unexpected, especially considering that the more distally related Na_v1.7 channel did show a conserved functional change similar to Na_v1.1. Yet, since differences found under these conditions are quite subtle, even for Na_v1.1 and Na_v1.7, it is possible that differences for Na_v1.2 here are masked (note that only a relatively small proportion of Na_v1.2 channels have recovered after 2 – 10 ms at -80 mV) and can be revealed under the protocols used to maximise the difference between Na_v1.1 variants, and which reduce the amount of slow inactivation.

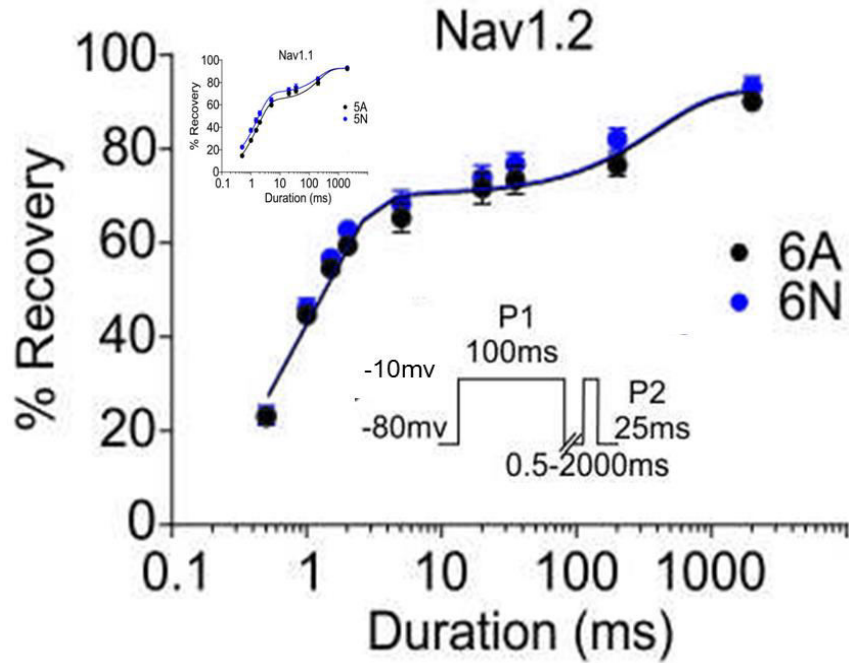


Figure 4.5: $Na_v1.2$: Short recovery intervals at $-80mV$ do not reveal a difference between splice variants as in $Na_v1.1$ (shown in inset) and $Na_v1.7$ (6A n=7; 6N n=6).

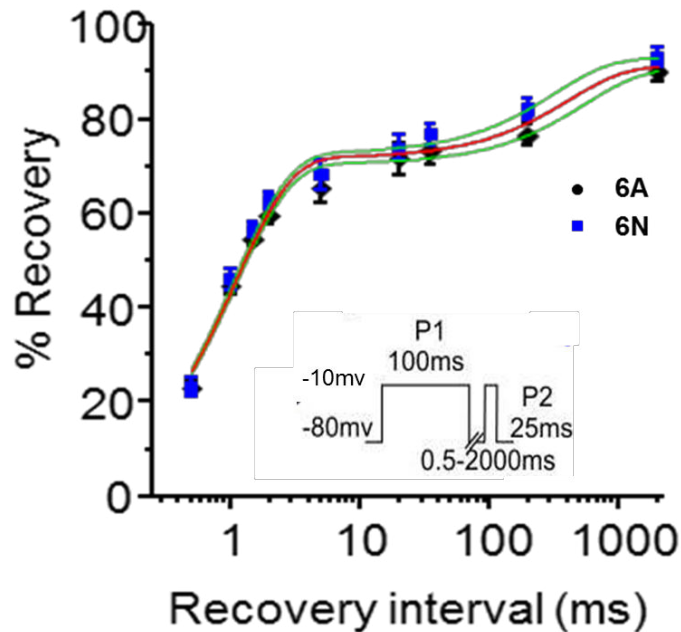


Figure 4.6: Recovery from inactivation for $Na_v1.2$ neonatal and adult isoforms, comparing fits with all parameters free (green lines) and with τ_f and τ_s fixed (red lines)

Values and standard errors of the fit values are in table 4.2.

Table 4.2: Na_v1.2: Parameters of bi-exponential fits to recovery from long (100 ms) inactivating pre-pulses.

Top panel: Optimized fitting parameters with τ_F and τ_S constrained (red lines in Figure 4.6, rates with n/a standard error (s.e.) were fixed). *Bottom panel:* Free fits with all parameters allowed to vary (green lines in Figure 4.6). Note that for the constrained fits, all rates for Na_v1.2-6N and Na_v1.2-6A were fit as a group as there were no differences between the data from individual fits. R^2 is the adjusted R-square statistic used to improve comparison of fits with different degrees of freedom.

Parameters from constrained fits (red lines in Figure 4.6)

	Na _v 1.2-6N		Na _v 1.2-6A	
	Value	s.e.	Value	s.e.
Y_0			0.000	0.049
A_F			0.72	0.05
τ_F (ms)			1.1	0.1
A_S			0.20	0.03
τ_S (ms)			406	219
R^2	n/a		0.981	

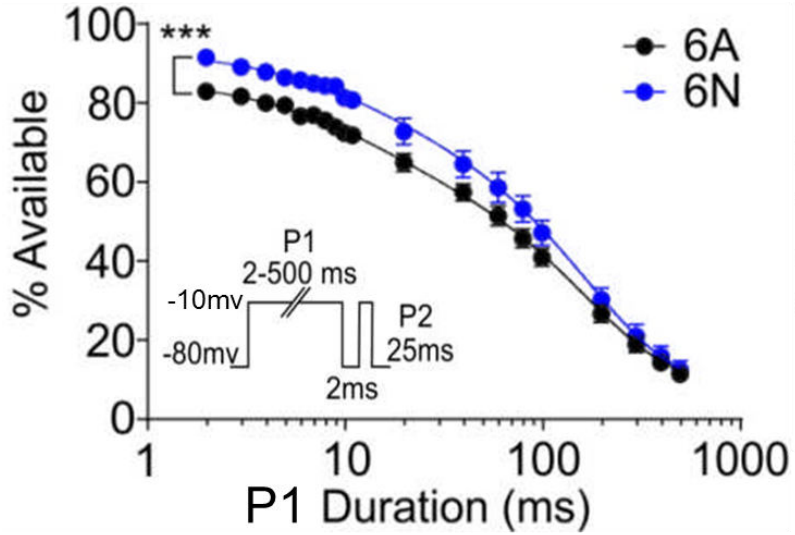
Parameters from free fits (green lines in Figure 4.6)

	Na _v 1.2-6N		Na _v 1.2-6A	
	Value	s.e.	Value	s.e.
Y_0	0	0.081	0	0.069
A_F	0.73	0.08	0.71	0.06
τ_F (ms)	1.1	0.2	1.0	0.2
A_S	0.20	0.04	0.20	0.04
τ_S (ms)	315	202	541	559
R^2	0.978		0.981	

4.2.3 Recovery from fast inactivation difference is augmented in Na_v1.2 and Na_v1.7 with shorter depolarization conditions

Because action potentials and depolarizations due to EPSCs in neurons are typically much shorter than the 100 ms depolarizing steps used in the protocol above, the difference in response to shorter pre-pulses seen for Na_v1.1 isoforms in Chapter 3 is likely to be more relevant to physiological temperature conditions. Furthermore, an inactivation recovery protocol using variable P1 durations for Na_v1.1-5A and 5N channels previously revealed that shorter P1 durations allowed 5N channels to recover considerably more than 5A, with the difference gradually attenuating as P1 intervals increased in duration. Applying the same protocol on Na_v1.2-6A and 6N channels this time revealed a difference in inactivation recovery between the two splice variants in the same direction and of a similar magnitude as for Na_v1.1 under these conditions ($P < 0.001$, two-way ANOVA; Figure 4.7A). As seen in an independent experiment in Figure 4.7B, it is the shortest P1 durations that generate the biggest difference in availability for Na_v1.2-6A and 6N variants. Results here also partly explain why a significant difference was not seen for Na_v1.2 6A and 6N channels using the original recovery from inactivation protocol (Figure 4.5), since using a P1 duration over ~50 ms in Na_v1.2 channels is sufficient to mask the difference between the 6A and 6N variants.

A Channel availability (gap=2ms, -80mV) various P1 duration



B Channel availability (gap=2ms, -80mV) various P1 duration

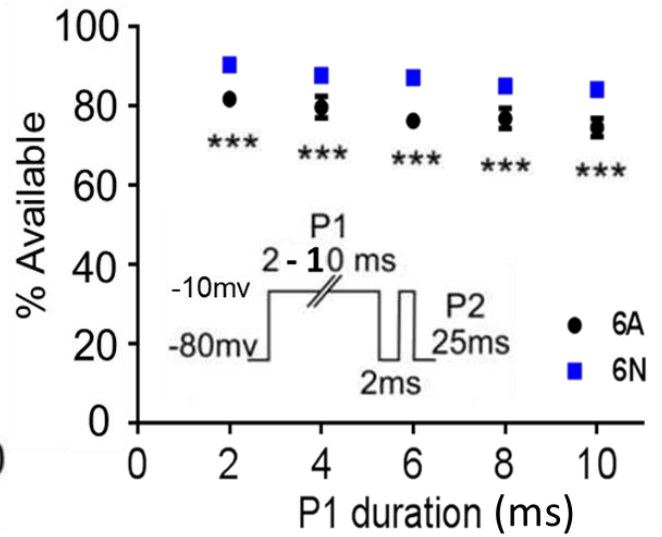


Figure 4.7: $Na_v1.2$: The neonatal isoform showed significantly more availability after a range of shorter pre-pulses under a brief interpulse gap duration (2ms)

Curves are fit with single exponentials as described in the text.. **A.** P1 duration = 2 – 500ms (6A n=10; 6N n=9). **B.** P1 duration = 2 – 10ms (6A n=6; 6N n=6)

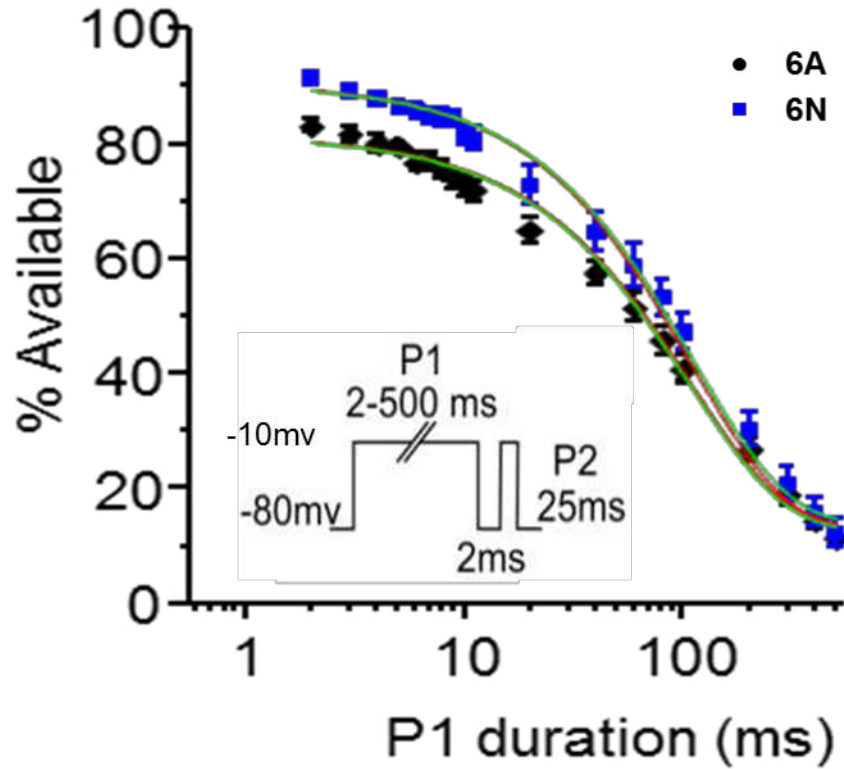


Figure 4.8: Na_v1.2: Estimated channel availability for isoforms of each channel comparing quality of fits with all parameters free (green lines) and with Y_0 and τ fixed (red lines, behind green lines)

The green fits were seeded with the same values for both isoforms. Note that from the free fits only the non-overlapping errors for parameter A are consistent with this value being different between the isoforms (see table 4.3, bottom panel).

Table 4.3: Na_v1.2: Parameters of single exponential fits describing channel availability after 2 ms recovery from pre-pulses of different durations

Top panel: optimized fitting parameters with inactivation time constant τ and the offset (Y_0) fixed. The parameters with n/a standard error (s.e.) were fixed at values similar to those found for free fits to both isoforms of that channel (as described in Figure 4.8). *Bottom panel:* Fits with all parameters allowed to vary. To better compare the goodness of fits with the different degrees of freedom the adjusted R-square statistic (R^2) is given.

Parameters from constrained fits (red lines in Figure 4.8)

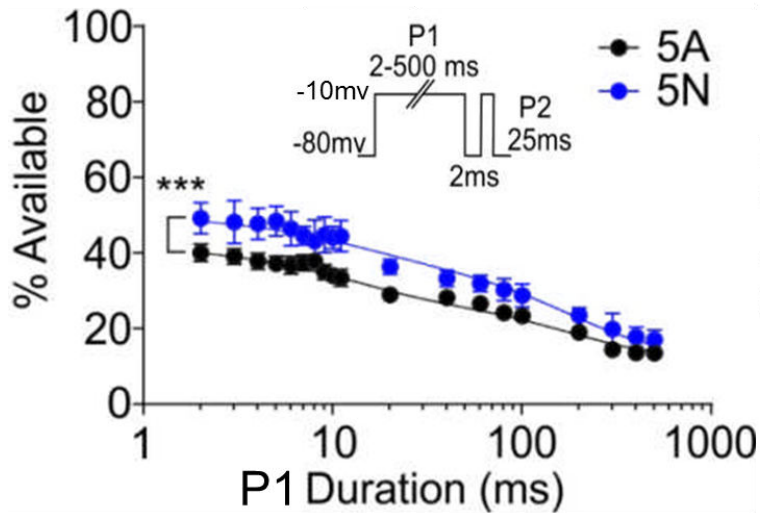
	Na _v 1.2-6N		Na _v 1.2-6A	
	Value	s.e.	Value	s.e.
Y_0	0.13	n/a	0.13	n/a
A	0.775	0.004	0.684	0.006
τ (ms)	108	n/a	108	n/a
R^2	0.993		0.994	

Parameters from free fits (green lines in Figure 4.8)

	Na _v 1.2-6N		Na _v 1.2-6A	
	Value	s.e.	Value	s.e.
Y_0	0.13	0.02	0.13	0.01
A	0.764	0.012	0.689	0.014
τ (ms)	111	10	106	8
R^2	0.992		0.993	

In the case of Na_v1.7, using the same variable P1 duration protocol, the difference in recovery between 5A and 5N variants was once again repeated (Figure 4.9A). Similar to both Na_v1.1 and Na_v1.2, the difference was most robust at earlier time points (note the overall increase in inactivation for Na_v1.7 variants compared to the CNS channels; Figure 4.9B). Na_v1.7 5N channels maintained their increased availability compared to 5A even at longer P1 durations (up to 300 ms). Data for the neonatal and adult isoforms for both channel subtypes were fit as a first order exponential decay [$Y_0 + A \cdot \exp(-t/\tau)$]. When all parameters were free to vary (Figures 4.8 & 4.10, green lines and tables 4.3 & 4.4 for Na_v1.2 and Na_v1.7 respectively) the difference between the two isoforms was once again mostly described by the amplitude (A). As for Na_v1.1, in order to test the hypothesis that the amount of availability changed, but not the timecourse of onset was changed by splicing, the data were fit with the τ fixed to be the same for the adult and neonatal isoforms, and only the amplitude (A) was allowed to vary (τ : Na_v1.2 = 108 ms; 1.7 = 95 ms; $r^2 > 0.94$ for both fits; Figures 4.8 & 4.10, red lines and tables 4.3 & 4.4 respectively). For both Na_v1.2 and Na_v1.7, direct comparison of either free or fixed fits of the two isoforms for all data points with two-way ANOVA indicated that neonatal channels showed significantly more availability after a range of shorter pre-pulses compared to adult ones ($P < 0.001$). The difference started waning off as the P1 duration got longer so that at longest P1 values it was completely masked. Therefore, the neonatal isoform here shows significantly increased availability after short inactivating pre-pulses compared to the adult one for all three channels: Na_v1.2, Na_v1.7, as well as Na_v1.1.

A Channel availability (gap=2ms, -80mV) various P1 duration



B Channel availability (gap=2ms, -80mV) various P1 duration

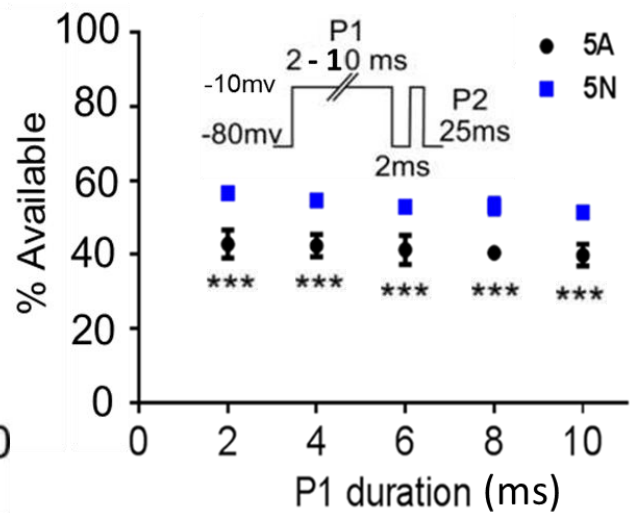


Figure 4.9: Na_v1.7: The neonatal isoform showed significantly more availability after a range of shorter pre-pulses under a brief interpulse gap duration (2ms)

Curves are fit with single exponentials as described in the text. **A.** P1 duration = 2 – 500ms (5A n=7; 5N n=10). **B.** P1 duration = 2 – 10ms (5A n=5; 5N n=5)

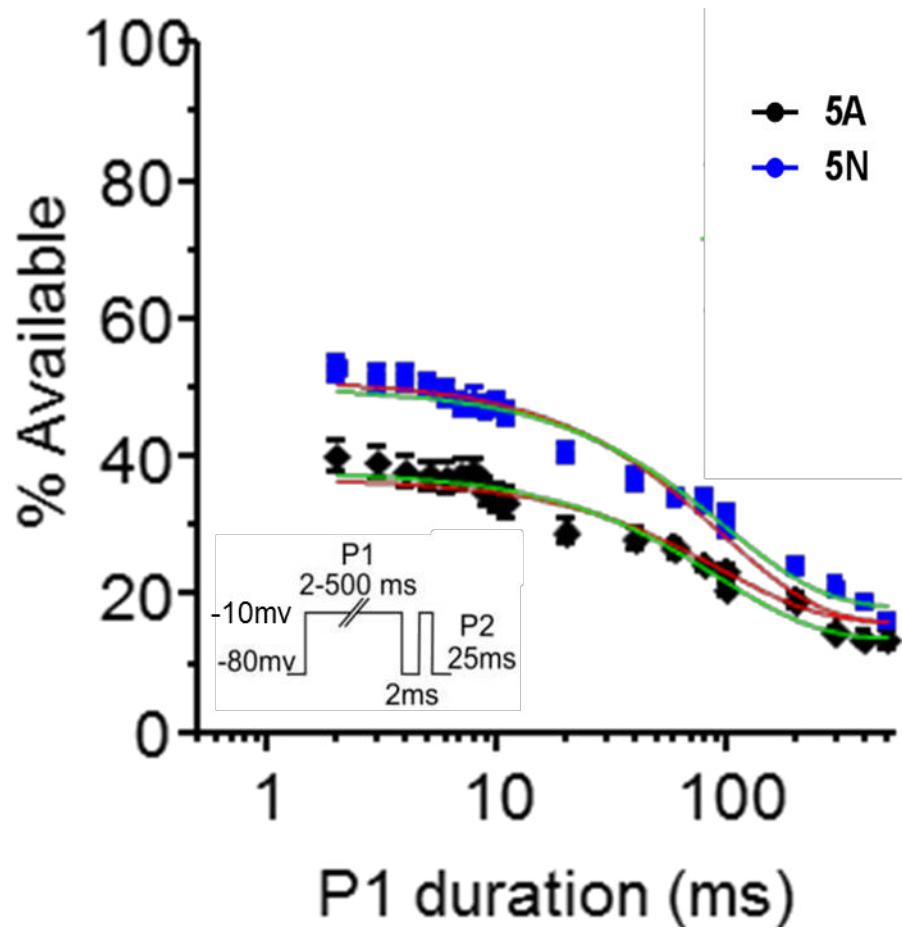


Figure 4.10: Estimated channel availability for $Na_v1.7$ isoforms of each channel comparing quality of fits with all parameters free (green lines) and with Y_0 and τ fixed (red lines, behind green lines)

The green fits were seeded with the same values for both isoforms. Note that from the free fits only the non-overlapping errors for parameter A are consistent with this value being different between the isoforms (see table 4.4, bottom panel).

Table 4.4: Na_v1.7: Parameters of single exponential fits describing channel availability after 2 ms recovery from pre-pulses of different durations

Top panel: optimized fitting parameters with inactivation time constant τ and the offset (Y_0) fixed. The parameters with n/a standard error (s.e.) were fixed at values similar to those found for free fits to both isoforms of that channel (as described in Figure 4.10). *Bottom panel:* Fits with all parameters allowed to vary. To better compare the goodness of fits with the different degrees of freedom the adjusted R-square statistic (R^2) is given.

Parameters from constrained fits (red lines in Figure 4.10)

	Na _v 1.7-5N		Na _v 1.7-5A	
	Value	s.e.	Value	s.e.
Y_0	0.16	n/a	0.16	n/a
A	0.351	0.008	0.208	0.009
τ (ms)	95	n/a	95	n/a
R^2	0.967		0.942	

Parameters from free fits (green lines in Figure 4.10)

	Na _v 1.7-5N		Na _v 1.7-5A	
	Value	s.e.	Value	s.e.
Y_0	0.18	0.01	0.14	0.01
A	0.323	0.012	0.243	0.010
τ (ms)	98	10	92	9
R^2	0.977		0.972	

4.2.4 “High-activity, seizure-like” parameters maintain the difference between adult and neonatal channels for Na_v1.2 & Na_v1.7

Protocols mimicking “high-activity” or “seizure-like” conditions, which combine parameters used to assess the difference in inactivation recovery between Na_v1.1 5A and 5N channels, were applied to both Na_v1.2 and Na_v1.7 adult and neonatal channels. Therefore, we delivered trains of short (10 ms) depolarizing steps and compared channel availability between isoforms of Na_v1.2 in HEK293T cells, as it was done for Na_v1.1 channel isoforms before (Figure 4.11). Under these conditions, the difference between availability of splice isoforms was evident (P<0.001, two-way ANOVA) after the first step and was sustained for the entire train, with the adult isoforms remaining approximately 10% less available than the neonatal isoform. We repeated experiments with Na_v1.7, which exhibits relatively more inactivation after short steps (Figure 4.12). Trains with 1 ms recovery between steps produced complete inactivation in both isoforms of Na_v1.7 (data not shown) and consequently to allow these channels to produce measurable currents we used a 2 ms recovery period between steps (Figure 4.12). In these conditions the Na_v1.7 isoforms replicated the differences seen in Na_v1.1 and 1.2 with an immediate onset and sustained increase in availability of the neonatal isoform throughout the train duration (P<0.001, two-way ANOVA). Therefore, under these conditions, adult and neonatal transcript variants from three different sodium channel genes are behaving in a biophysically consistent manner with the same functional difference across all three channel subtypes.

Inactivation recovery
(P1=10ms, gap=1ms, -80mV)

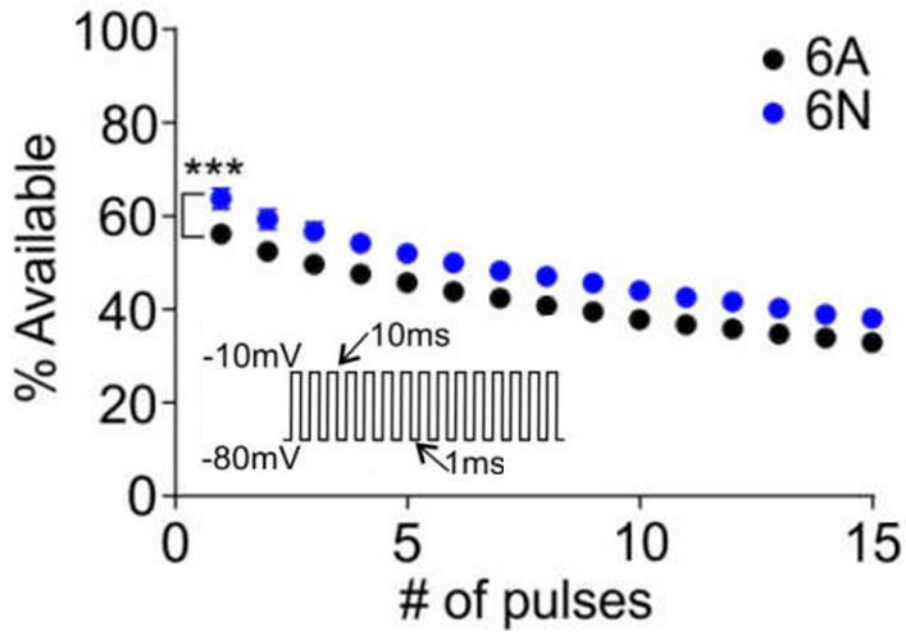


Figure 4.11: Na_v1.2: Trains of pulses mimicking a “seizure-like burst” retain the difference between the splice variants similar to Na_v1.1 (6A n=11; 6N n=9).

Inactivation recovery (P1=10ms, gap=2ms, -80mV)

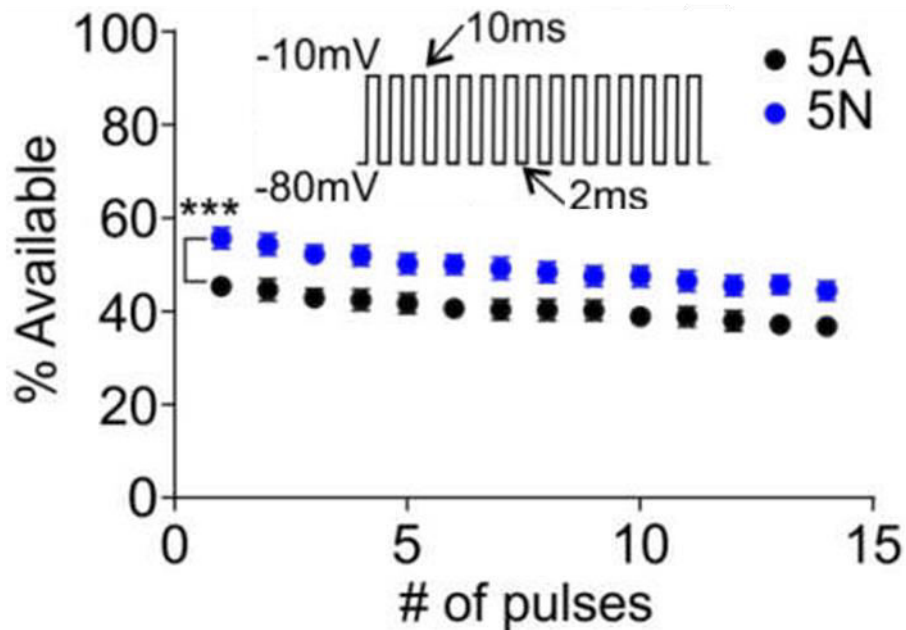


Figure 4.12: Na_v1.7: Trains of pulses mimicking a “seizure-like burst” retain the difference between the splice variants

similar to Na_v1.1 and Na_v1.2, but with a slightly different protocol (2 ms gap between steps, 5A n=6; 5N n=8).

4.3 Summary of investigation of conservation

This chapter has demonstrated that a conserved molecular splicing event between sodium channel subtypes can lead to a conserved functional change in channel availability. After shorter depolarisations that favour fast inactivated states the neonatal isoforms for all three sodium channel subtypes, Na_v1.1, Na_v1.2 and Na_v1.7, show more availability than their adult counterparts. This is true using identical recording conditions (physiological temperature, CsCl-based intracellular, no β-subunits), and identical, or in one case similar voltage protocols (short P1

intervals, short interpulse gap durations, RMP of -80 mV). Therefore it appears that the intrinsic effect of this alternative splicing event on early recovery from inactivation is evolutionarily conserved across these three distinct sodium channel subtypes. This suggests this feature may be imposing an evolutionarily important effect on channel activity.

The evolutionary conservation of alternative splicing in sodium channels is especially striking because the different channel types support divergent functions. Na_v1.1 plays a predominant role in the excitability of fast-spiking parvalbumin-positive interneurons in the CNS (Yu *et al.*, 2006). In contrast, while highly conserved at the amino acid level, Na_v1.2 is primarily expressed in excitatory neurons, and is particularly important early in development (Oliva *et al.*, 2012). Na_v1.7 is largely found in peripheral neurons, and is particularly important for subthreshold signaling and nociception in small diameter neurons, which are anatomically distinct from the CNS neurons where Na_v1.1 and Na_v1.2 predominate (Cox *et al.*, 2006; Yang *et al.*, 2004). In terms of *both* the physiology of the neurons, and the macroscopic kinetics of gating, Na_v1.7 channels are more distant from the two channels in the CNS (Dib-Hajj *et al.*, 2013). Nevertheless the site of splicing is conserved across all three channels and, furthermore, it has been implicated in disease states for all three subtypes.

One of the most direct indications that this splicing may be important in human disease comes from studies of Na_v1.2 where mutations within the neonatal exon are associated with epilepsy (Xu *et al.*, 2007), and where genetic removal of the neonatal exon leads to a change in seizure threshold (Gazina *et al.*, 2014). In the case of Na_v1.2, development of seizures is associated with a gain-of-function effect of the channel, and may be due to a developmental change in excitatory neurons (Liao *et al.*, 2010; Gazina *et al.*, 2014). In Na_v1.7, a mutation associated with adult-onset inherited erythromelalgia (erythermalgia) was shown to modify the inactivation of the adult isoform only, consistent with delayed onset of symptoms (Choi *et al.*, 2010). For *SCN1A*, the G>A polymorphism disrupts the inclusion of the neonatal exon in Na_v1.1 channels and has been associated with altered dosage of AEDs in people with epilepsy (Tate *et al.*, 2005; Zhou *et al.*, 2012) as well as possibly modifying the likelihood of developing epilepsy (Abe *et al.*, 2008; Kumari *et al.*, 2013), but this finding also has not been replicated universally (Manna *et al.*, 2011). These different findings are consistent with the polymorphism interacting with other genetic differences that may differ among different populations. Results shown here in HEK293T cell recordings provide a conserved functional effect between neonatal and adult isoforms across

channel types that may contribute to the development of disease state linked with this splicing event for each channel type.

We have focused on identifying conserved effects of splicing on channel activity; however splicing may also act by changing how isoforms interact with other proteins, and this may contribute to the different effects in different neuronal backgrounds. In Na_v1.7, splicing has been shown to modify phosphorylation (Chatelier *et al.*, 2008) as well as how these channels associate with β -subunits (Farmer *et al.*, 2012). Additional insight into the conserved impact of splicing, includes studies showing that in flies a homologous splicing event in the third domain, which appears to have arrived through convergent evolution, hyperpolarizes voltage dependence of activation and creates a persistent current (Lin *et al.*, 2009), which has pronounced effects on neuronal excitability (Lin *et al.*, 2012). This splicing event, giving rise to exons K or L, is also linked to epilepsy occurrence in *Drosophila* (Lin *et al.*, 2012), since its manipulation can lead to seizure suppression (Lin *et al.*, 2015), which is reminiscent of how the homologous event in human Na_v1.1 is associated with epilepsy predisposition. Another major correlation between the two homologous splicing events is that splicing of the L exon in *Drosophila* is activity-dependent and is promoted by increased synaptic activity, which may, in turn, promote seizures (Lin *et al.*, 2012). In parallel to that, epilepsy in humans has been shown to promote splicing towards the neonatal variant (Heizen *et al.*, 2007, Fletcher *et al.*, 2011), possibly as a result of increased neuronal activity. In addition, increased inclusion of exon L in *Drosophila* is regulated by the RNA-binding protein *Pasilla* (Lin *et al.*, 2012), whose mammalian homologues are *Nova1* and *Nova2* and these splicing factors have been involved in regulating the mammalian Na_v1.1 splicing event (Heinzen *et al.*, 2007; Gazina *et al.*, 2010). Finally, in cockroaches a similar splicing motif has been shown to modify channel pharmacology (Tan *et al.*, 2002). A link between this splicing event in human Na_v1.1 and altered anti-epileptic drug response has been also suggested before (Tate *et al.*, 2005; 2006; Abe *et al.*, 2008; Zhou *et al.*, 2012; Menzler *et al.*, 2014) and is examined in more detail in Chapter 5.

Our data demonstrate that after brief depolarizations, a conserved site of alternative splicing imparts a conserved impact on channel availability in HEK293T cells, most likely by manipulating inactivation recovery. To our knowledge this is the first time a site of alternative splicing has been shown to have conserved function on three separate ion channels.

At a physical level the data from the model indicate that the inclusion of a negatively charged amino acid (in the adult exon) in the D1S3-S4 segment is sufficient to stabilize the inactivation particle in the inner side of the channel pore. As the neonatal exon does not contain a charged amino acid at that position, it is tempting to speculate that the interaction of the charged arginine with the potential across the membrane is sufficient to alter the ‘down’ position of the attached voltage-sensor. Data found here are consistent with the splicing in the first domain destabilizing the inactivation particle after all four voltage sensors have returned to the ‘down’ position. It is proposed here that the S4 segment in the first domain may have a predominantly important role in stabilizing inactivation, and this is why splicing in DI has specific effects on this parameter. Consistent with this link between the S4 targeted by splicing and the biophysical effect, a paralogous splicing motif in DIII of *Drosophila* has been shown to have robust effects on the amount of persistent current produced by channels (Lin *et al.*, 2009; 2012; 2015), a property that is also linked with the inactivation process and the motility of the inactivation particle. This is consistent with splicing in the S3-S4 linker affecting the motility of the inactivation particle in a way that is determined by which domain the splicing event occurs. In *Drosophila* such splicing in DIII results in generation of a persistent current possibly as a result of altered binding of the inactivation particle leading to incomplete inactivation (Stafstrom, 2007; Kiss, 2008). In the human paralog, we show here that splicing in the first domain affects channel availability by having an effect on release from inactivation, as it is modelled in Chapter 3. This reinforces the notion that even across different species, the conservation of splicing at the S3-S4 linker, even if in different domains, has specific effects on the inactivation particle and can be linked with seizure occurrence both in humans and flies.

However, as all this work was carried out in HEK293T cells, we still cannot rule out other roles for this splicing in regulating interactions with other proteins, or contributing to neuronal functions. Future work exploring these possibilities, ideally in neuronal backgrounds will be necessary to test those possibilities. A first look of the two splice isoforms in their native neuronal milieu is further explored in Chapter 6.

Chapter 5: Differential modulation of VGSC variants by the anti-epileptic drugs phenytoin and carbamazepine

5.1 Hypothesis and aims

Previous reports have suggested that splicing in Na_v1.1 may contribute to an altered maximum or maintenance dosage of AEDs prescribed in epileptic patients (Tate *et al.*, 2005; 2006; Abe *et al.*, 2008; Zhou *et al.*, 2012; Kasperaviciute *et al.*, 2013) or alter pharmacoresponse to AEDs such as carbamazepine (Menzler *et al.*, 2014), however these findings are not always reproduced (Kwan *et al.*, 2008; Manna *et al.*, 2011; Haerian *et al.*, 2013; Kumari *et al.*, 2013). It has been shown here and elsewhere (Fletcher *et al.*, 2011) that Na_v1.1-5A and 5N variants have an innate difference in their early inactivation recovery rates, a property that is directly affected by AED action. Preliminary work in that report had indicated that phenytoin, a first line AED, might obscure the difference between Na_v1.1-5A and 5N channels, but these preliminary data did not explicitly measure differences between the variants. In addition Thompson *et al.*, (2011) previously reported a differential modulation of Na_v1.1-5A and 5N recovery rates with phenytoin and lamotrigine, but not with carbamazepine. However, this study was carried out in conditions where the intrinsic difference in inactivation was obscured, and did not investigate the impact of the drugs on the functional difference which has been identified here as being conserved among channels. As yet, no study has investigated the impact of AEDs on splice variants of multiple sodium channels. Association studies between the *SCN1A* genotype and drug dosage – primarily phenytoin and carbamazepine – give mixed conclusions for both anti-epileptics. Results become even more dubious since some of these studies treat AEDs as one unit (Kwan *et al.*, 2008; Haerian *et al.*, 2013), ignoring potential differences between AEDs. In order to clarify the relationship between splicing and AED inhibition, we compared channel availability using the same high-frequency stimulation conditions that produced robust differences between the variants from all three channels, this time in the presence of either phenytoin or carbamazepine, in order to allow the development of a use-dependent block. Results were extended to both Na_v1.2 and Na_v1.7 adult and

neonatal transcript variants, in order to see whether a functional conservation between sodium channel subtypes also applies for AED pharmacology of the adult and neonatal isoforms.

5.2 Results: Comparing splice variant drug responses for Na_v1.1, Na_v1.2 & Na_v1.7

5.2.1 Addition of AEDs negates the inactivation recovery difference between Na_v1.1 5A and 5N variants.

Recovery from inactivation under “seizure-like” stimulation trains allows a higher recovery rate for neonatal over adult channels throughout the protocol in the absence of any AED (Figure 5.1, pale blue and grey). Repeating the same protocol for Na_v1.1 transcript variants in the presence of phenytoin (50 μM in DMSO, 1 : 1000 dilution, 0.1% DMSO concentration in the extracellular solution) reduced the amount availability for both 5A and 5N channels (Figure 5.1A). This reduction became more evident with increased pulse numbers in comparison to the drug-free protocol. In addition, the 5N channels underwent a greater relative reduction in recovery, so that the difference between the two channel variants was obscured ($P > 0.05$, two-way ANOVA). So, the effect of phenytoin on the neonatal isoform was strong enough to reduce the availability to a level similar to that of the adult isoform, and the difference between the isoforms was eradicated for the duration of the train. Similarly, the difference between Na_v1.1 5A and 5N channels were also obscured in the presence of 50 μM carbamazepine (in DMSO, 1 : 1000 dilution, 0.1% DMSO concentration in the extracellular solution) ($P > 0.05$, two-way ANOVA; Figure 5.1B). It has been shown before that DMSO concentrations of 0.1% and below in the external solution has no measurable effect on I_{Na} (Ilyin *et al.*, 2005), therefore any effect seen in the presence of either phenytoin or carbamazepine is suggested to be a result of the drugs activity and not due to the DMSO. It should also be noted that reversibility of the effect by washing out either phenytoin or carbamazepine was not performed, due to high variability of current rundown after prolonged recordings, which made current measurements unreliable. However, both splice variants were compared under the same conditions.

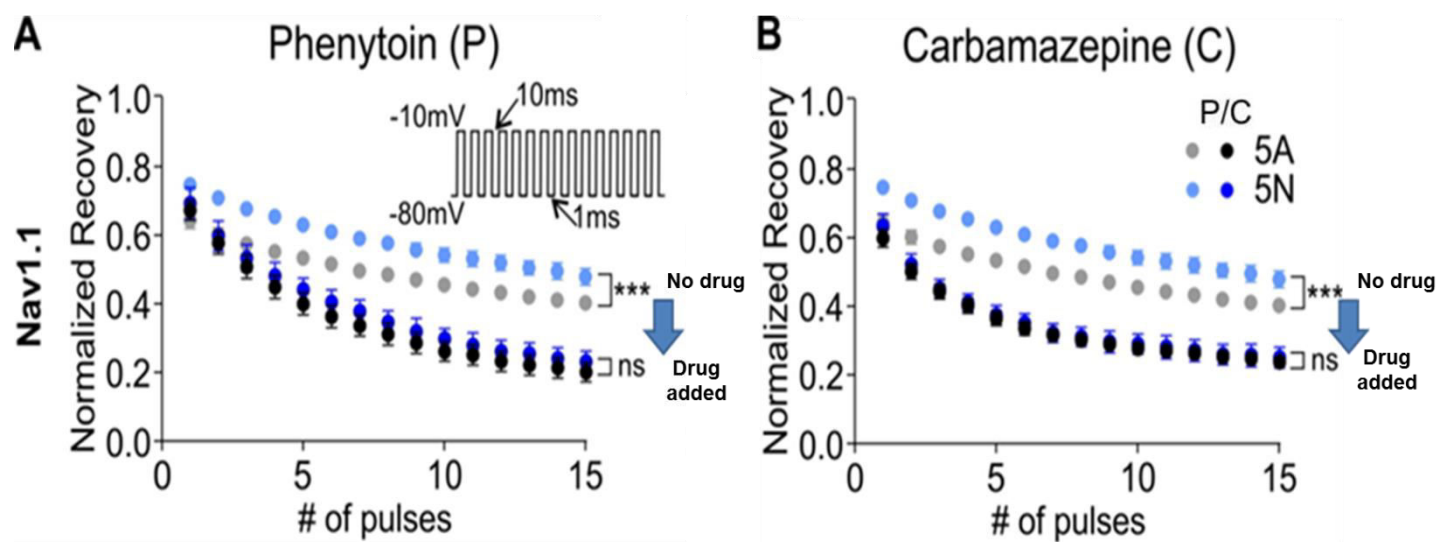


Figure 5.1: Na_v1.1: Phenytoin and carbamazepine negate the inactivation recovery difference between neonatal and adult isoforms

Addition of AEDs (phenytoin & carbamazepine) reduces channel availability after the first step, and obscures the difference between Na_v1.1 neonatal and adult isoforms during a series of fast pulses (two-way ANOVA $p > 0.05$). The increased inhibition of the neonatal isoform means that the presence of either drug entirely removes the difference between the isoforms during the series of pulses. **A.** +50 μ M phenytoin (5A $n=10$, 5N $n=7$). **B.** +50 μ M carbamazepine (5A $n=7$, 5N $n=5$). Pale blue and grey data are from using the same protocol in the absence of drugs, dark blue and black data indicate the presence of drugs. Drug concentrations approximate half maximal inhibition in RT recordings (Thompson *et al.*, 2011).

5.2.2 Conservation of AED differences in Na_v1.2 and Na_v1.7 subtype isoforms

Experiments done in the presence of phenytoin or carbamazepine for Na_v1.1 transcript variants were now repeated for Na_v1.2 and Na_v1.7 channel subtypes. This would indicate whether the pharmacological difference between adult and neonatal isoforms is conserved across different channel types, in the same way as the intrinsic differences in inactivation. Indeed, similar to Na_v1.1, addition of either phenytoin (Figure 5.2A) or carbamazepine (Figure 5.2B) obscured the difference between Na_v1.2-6A and 6N channel variants, so that their initial difference under drug-free conditions ($P > 0.05$, two-way ANOVA; Figure 5.2 pale blue and grey) was now lost.

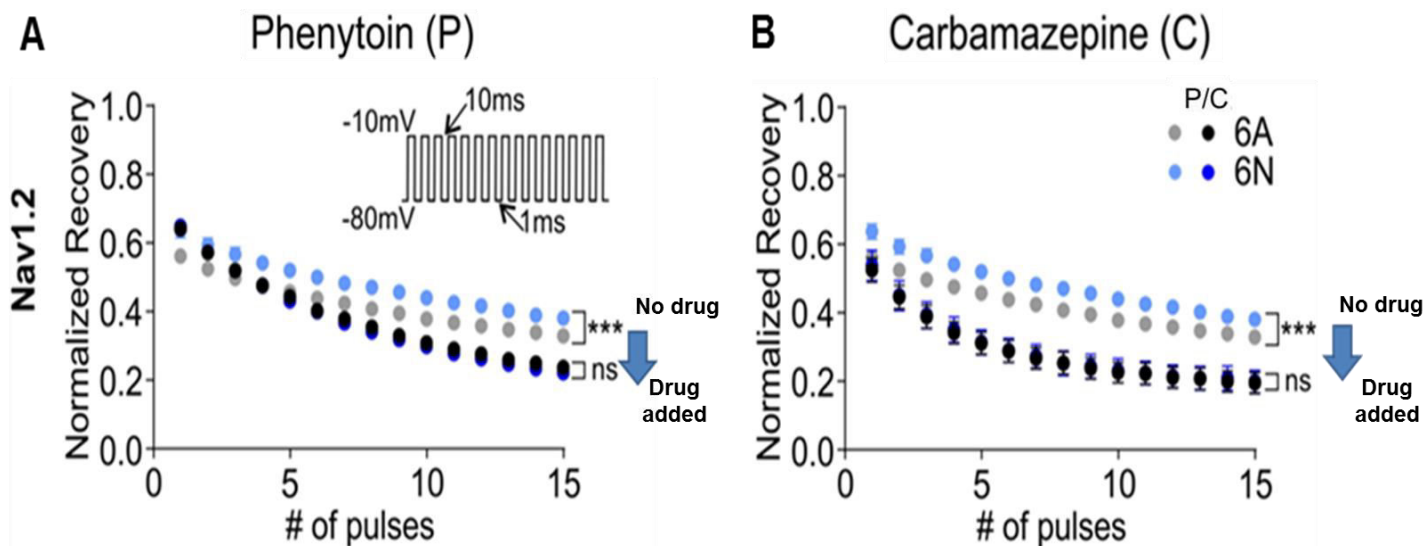


Figure 5.2: $Na_v1.2$: Phenytoin and carbamazepine negate the inactivation recovery difference between neonatal and adult isoforms

Similar to $Na_v1.1$, addition of AEDs (phenytoin & carbamazepine) reduces channel availability after the first step, and obscures the difference between $Na_v1.2$ neonatal and adult isoforms during a series of fast pulses (two-way ANOVA $p > 0.05$). The increased inhibition of the neonatal isoform means that the presence of either drug entirely removes the difference between the isoforms during the series of pulses. **A.** +50 μ M phenytoin (6A n=7, 6N n=6). **B.** +50 μ M carbamazepine (6A n=15, 6N n=15). Pale blue and grey data are from using the same protocol in the absence of drugs, dark blue and black data indicate the presence of drugs. Drug concentrations approximate half maximal inhibition in RT recordings (Thompson *et al.*, 2011).

The slightly adapted protocol that allowed 2 ms recovery (to allow channels to produce measureable currents) was used to reveal the same situation applied for the more distally related $Na_v1.7$ channel subtype, both in the presence of phenytoin (Figure 5.3A) as well as carbamazepine (Figure 5.3B). Therefore, the addition of either phenytoin or carbamazepine negates any difference in channel availability between adult and neonatal transcript variants that was previously evident in drug-free conditions ($P > 0.05$, two-way ANOVA; Figure 5.3 pale blue and grey), and this effect is conserved across at least three sodium channels.

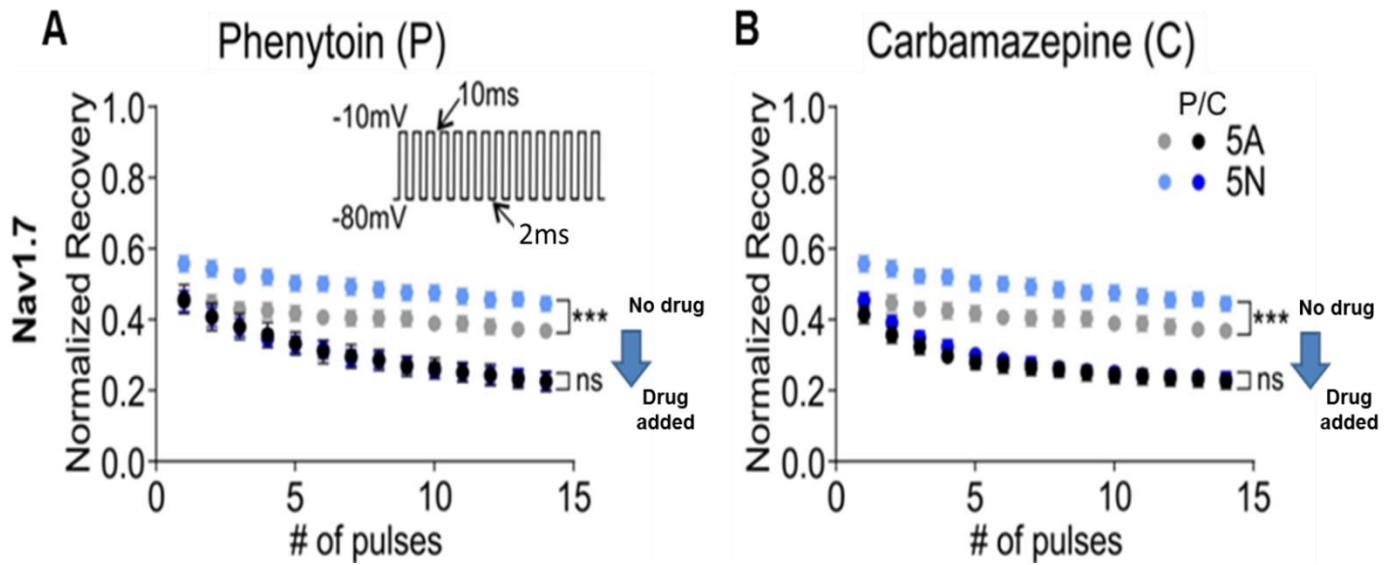


Figure 5.3: $Na_v1.7$: Phenytoin and carbamazepine negate the inactivation recovery difference between neonatal and adult isoforms

Similar to both $Na_v1.1$ and $Na_v1.2$, addition of AEDs (phenytoin & carbamazepine) reduces channel availability after the first step, and obscures the difference between $Na_v1.7$ neonatal and adult isoforms during a series of fast pulses (two-way ANOVA $p > 0.05$). The increased inhibition of the neonatal isoform means that the presence of either drug entirely removes the difference between the isoforms during the series of pulses. **A.** +50 μ M phenytoin (5A $n=12$, 5N $n=11$). **B.** +50 μ M carbamazepine (5A $n=7$, 5N $n=8$). Pale blue and grey data are from using the same protocol in the absence of drugs, dark blue and black data indicate the presence of drugs. Drug concentrations approximate half maximal inhibition in RT recordings (Thompson *et al.*, 2011).

5.3 Summary and discussion

In $Na_v1.1$, the rs3812718 polymorphism that alters splicing of the neonatal isoform in humans, and was initially associated with altered dosage of phenytoin and carbamazepine in patients (Tate *et al.*, 2005). These drugs are thought to work by binding to and stabilizing the inactivated states (Kuo and Bean, 1994), which our data in Chapter 3 have indicated may be specifically targeted by

splicing. From the results here, it can be concluded that in the presence of phenytoin or carbamazepine, adult and neonatal transcript variants show comparable activity, and this change is conserved also in $\text{Na}_v1.2$ and $\text{Na}_v1.7$ channel subtypes. This highlights the similarity in mechanism between the drugs, and indicates that treatment may have distinct effects on different splice isoforms of different types of channels beyond $\text{Na}_v1.1$, and that any neurological disorder that alters splicing at this site in a neuronal channel may alter the mechanism of drug response.

On a first glance, the difference between isoforms found here could be attributed to a different binding of the drug between the two channel isoforms, such that the neonatal variant has a higher affinity, making it more sensitive to the action of the AEDs since this variant shows a higher relative change in inactivation recovery compared to adult channels. Yet, the possibility cannot be excluded that the binding of either AED upon neonatal or adult channels could be similar and the AED may simply be slowing down the rate of inactivation recovery to levels where a different – probably common – molecular event acts as a rate limiting step that defines the recovery rate. In that case, the action of either AED may be masking the difference between splice variants in the same way that long interpulse intervals or prolonged P1 durations do in the protocols described in chapter 3, essentially by driving the channels into slow inactivated states, or states where the first, fastest recovery is no longer the limit for re-opening.

The conserved differences in response to AEDs may provide more insight into how these drugs work. One key challenge is that the drugs are likely to have increased effects on neonatal isoforms of multiple sodium channels in different types of neurons. This could be particularly relevant to epilepsy, as several studies have suggested that the inclusion of the neonatal exon in different sodium channels is increased in models of epilepsy (Gastaldi *et al.*, 1997), or in patients with epilepsy (Heinzen *et al.*, 2007; Tate *et al.*, 2005). Thus, splicing may alter the efficacy of drugs on both excitatory and inhibitory neurons, and the effects in non-epileptic tissue may be different than in epileptic tissue, where increased neonatal exon inclusion may increase the impact of AEDs on recovery from inactivation. Our results highlight the importance of the same parameter that is sensitive to splicing in the response to antiepileptic drugs.

Chapter 6: Altered sodium channel availability between neonatal and adult channels in neurons and effects on spike reliability in interneurons

6.1 Hypothesis and Aims

Results from the previous chapters have revealed up to now that under our conditions (37°C, CsCl-based intracellular solution) Na_v1.1 neonatal channels are able to recover more quickly from fast inactivation than adults – and hence are more available to be activated during a following stimulation – specifically under conditions of high-frequency, repetitive stimulation. Moreover, this effect was also conserved among other sodium channels bearing this splicing event, namely in this study Na_v1.2 and Na_v1.7 splice variants.

A major limitation of this study up to now, as well as most studies on these splice variant properties (Xu *et al.*, 2012, Fletcher *et al.*, 2011, Thompson *et al.*, 2011, Farmer *et al.*, 2012), is that characterization is performed on heterologous expression systems (mostly HEK293T cells). Cell lines typically used to express these channels for voltage-clamp recordings and consequent characterization of their biophysical properties, cannot recapitulate the whole anatomy of sodium channels or their regulation. Differences in accessory β -subunits, G-proteins and subcellular localization of channels may modify the impact of splicing on neuronal behavior (Fletcher *et al.*, 2011; Farmer *et al.*, 2012), especially since different sodium channel types are expressed on different types of neurons. This calls for the need to investigate sodium channel variants under their native physiological neuronal context, to evaluate their behavior and see how they may modify actual neuronal firing and properties. In the cases of Na_v1.1 and Na_v1.2, these channel types are suggested to primarily be expressed in interneurons and excitatory neurons respectively, in the CNS (Yu *et al.*, 2006; Oliva *et al.*, 2012). Therefore, the aim here was to investigate how splice variants of either Na_v1.1 or Na_v1.2 affect neuronal frequency firing and neuronal properties in interneurons and excitatory neurons respectively. Furthermore, this also allows direct assessment of whether potential differences found between neonatal and adult variants in their

physiological context are altered when these are expressed on a different neuronal background, by evaluating neonatal and adult Na_v1.1 properties in excitatory hippocampal neurons as well as inhibitory neurons.

6.2 TTX resistance and transient expression of 5N and 5A constructs in interneuronal hippocampal cultures

The most direct approach to current-clamp studies of Na_v1.1 neonatal and adult variants in neurons involves the manipulation of splice variant levels in mice by using variant-specific shRNAs to lower neonatal or adult expression and evaluate the effects on neuronal firing. However, this approach was not possible, since rodents have lost the ability to express the neonatal variant and only express adult Na_v1.1 channels (Fletcher *et al.*, 2011, Gazina *et al.*, 2010). Furthermore, this would not allow us to study the channel's effect in isolation, since the currents from the Na_v1.1 isoform would be blended with the contribution of all the native sodium channel types that are also expressed in these neurons.

To address these issues, site-directed mutagenesis was used on the *SCN1A*-5A & 5N constructs to introduce the F383S mutation. The phenylalanine residue at this position is integral for the binding of tetrodotoxin (TTX) on the outer mouth of the channel, thereby blocking sodium conductance through the pore (Heinemann *et al.*, 1992). The F383S mutation modifies the binding pocket of TTX on the channel so that it can no longer bind, thereby conferring TTX resistance, as also seen in previous studies (Bechi *et al.*, 2012; Cestele *et al.*, 2013). The homologous mutation was also performed on the *SCN2A* 6A & 6N cDNA constructs (Rush *et al.*, 2005).

After conferring TTX resistance transient transfections were attempted in hippocampal neuronal cultures from P0 mice as a means to express the neonatal Na_v1.1 variant in neurons. This approach is difficult, especially due to the very low transfection efficiency rate of most neuronal transfection reagents, which is usually about 1 – 5% (Wanisch *et al.*, 2013). Many different lipid-based transfection reagents were tested for efficiency of transient transfection in neurons with either the neonatal or adult construct. All of these reagents resulted into either very poor transfection efficiencies (~1% for Lipofectamine 2000, Effectene, calcium phosphate) or too high cell toxicity

and cell death (poly-jetPEI). Eventually, a transfection technique called magnetofection was tested, using the Neuromag reagent (OZ Biosciences), which is reported to have specific high efficiency for transfecting neurons. Magnetofection is based on the mixture and pair formation of the nucleic acid with magnetic beads, which are introduced in the neuronal cell medium and then dragged into the neurons with the use of a magnetic plate that is placed underneath the cultures.

In order to discriminate interneurons from excitatory neurons in the cultures, the GAD67-GFP mouse strain was used (Tamamaki *et al.*, 2003). In this strain the GFP protein is expressed under the GAD67 promoter, so that it is only present in interneurons. In this way, interneurons can be identified by the emission of green light under fluorescence. The percentage of interneurons on every coverslip was around 10 – 15%. As a marker of successful transfection, a red fluorescent protein (RFP) under the β -actin promoter was co-transfected together with either the neonatal or adult sodium channel construct. Transfection efficiency with magnetofection usually reached around 10%, which resulted on average in 1 – 1.5% of neurons in the culture being interneurons successfully transfected. These could now be selected by the concurrent expression of GFP and RFP for current-clamp recordings. Excitatory neurons were selected by the absence of GFP expression (GFP negative). Current-clamp recordings were performed in the presence of 1 μ M TTX in order to block the native sodium channel current and to measure the firing of purely adult- or neonatal-driven activity.

6.3 Results:

6.3.1 Single AP parameters of Na_v1.1 neonatal and adult channels are similar in interneurons

The effect of splicing in Na_v1.1 channels was examined first in interneurons. Interneurons expressing either isoform of Na_v1.1 were able to elicit APs upon brief depolarizing current steps of 10 ms (Figure 6.1A). Both 5A- and 5N-transfected interneurons showed similar passive membrane properties (resting membrane potential, input resistance, Figure 6.2A), as well as similar threshold current (i.e. amount of current injected to reach threshold – Figure 6.2C). Phase plot analysis of

single APs elicited by $\text{Na}_v1.1\text{-5A}$ and 5N channels was used to analyze the active properties of transfected interneurons (Figure 6.2B). No significant difference was found between channel variants in terms of threshold voltage, maximum rising and repolarizing slopes, AP amplitude or 50% AP width ($P>0.05$, unpaired two-tailed Student's T test; Figure 6.2C). So, at the single AP level, $\text{Na}_v1.1\text{-5A}$ and 5N channels appeared to have similar properties in interneurons.

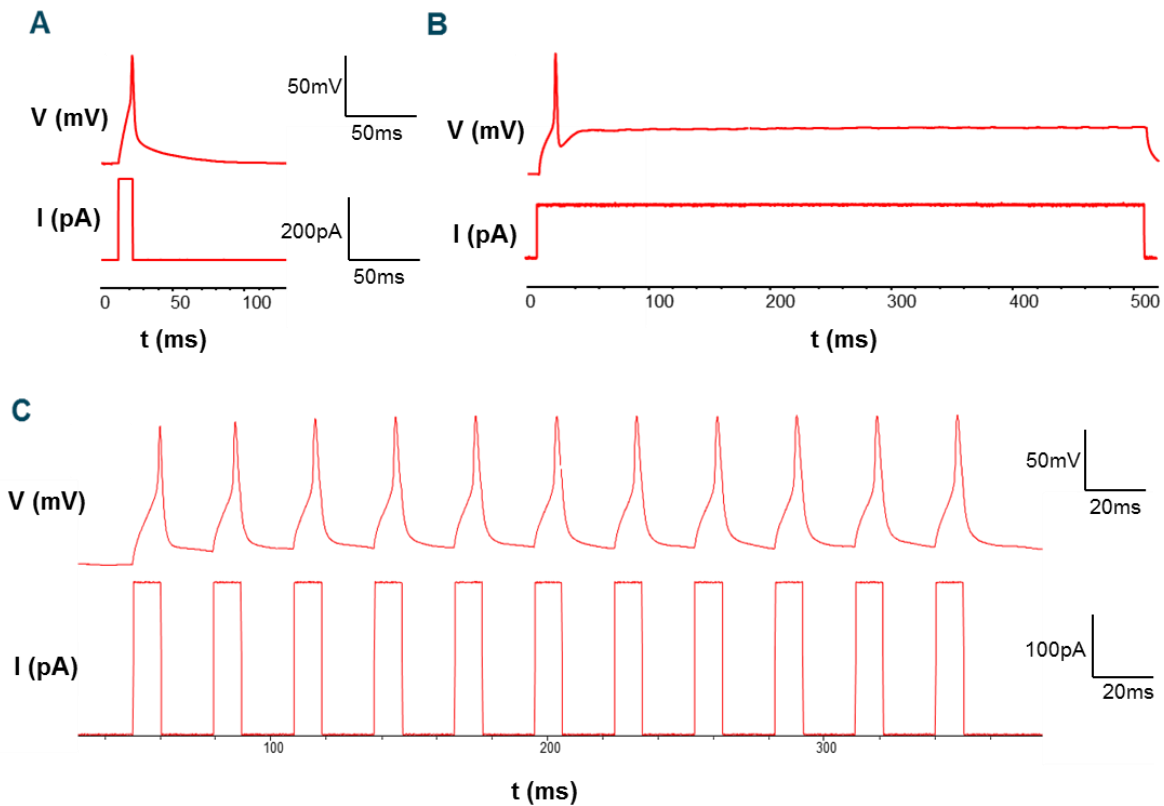


Figure 6.1: Stimulation conditions for establishing single AP parameters and firing frequency ability of transfected hippocampal neurons

A. A 10ms depolarizing current pulse was given at increasing amplitudes up to the threshold current where an AP fired. **B.** Prolonged depolarization (500ms) often generated just a single spike for both neonatal and adult isoforms. **C.** Firing frequency reliability was assessed by giving a 110% of the threshold current in (A) – i.e. a suprathreshold stimulus – in successive pulses, with intervals between pulses getting shorter with each step to increase the firing frequency (33 – 90Hz).

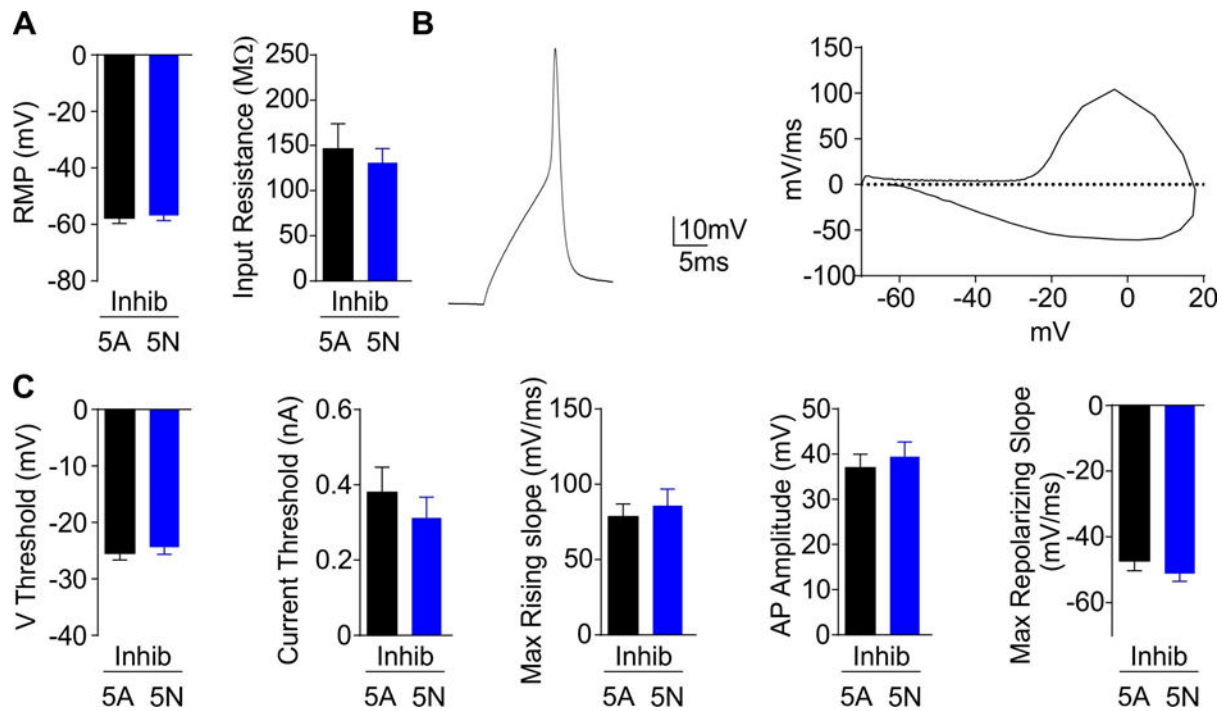


Figure 6.2: Intrinsic properties of interneurons expressing TTX-resistant splice isoforms of Na_v1.1

A. Neither resting membrane potential (RMP, left, 5A, -57.8 ± 1.8 ; 5N, -56.7 ± 1.8) nor input resistance (5A, 146.2 ± 27.8 ; 5N, 131.0 ± 15.6) was affected by changing the splice isoform of Na_v1.1. **B.** A representative action potential (left) and phase plot used to analyse active properties of transfected neurons. **C.** Parameters describing individual action potentials were not altered by changing the splice isoform of Na_v1.1. V Threshold: 5A, -25.5 ± 1.2 ; 5N, -24.4 ± 1.3 , Current Threshold: 5A, 0.380 ± 0.067 ; 5N, 0.312 ± 0.055 , Max Rising slope: 5A, 82.8 ± 9.3 ; 5N, 94.1 ± 10.0 , AP Amplitude: 5A, 37.0 ± 3.0 ; 5N, 39.5 ± 3.2 , Max Repolarizing slope: 5A, -47.4 ± 3.0 ; 5N, -51.2 ± 2.3 . (5A n=14; 5N n=13, cells were patched from three independent transfection preparations on three separate days).

6.3.2 Na_v1.1 splicing controls spike reliability in interneurons

In order to test the firing frequency of transfected interneurons, a prolonged depolarizing current of 500 ms was initially used. However, prolonged depolarization frequently evoked just a single AP (Figure 6.1B), while in the cases it evoked trains of APs, firing rates seemed to be dependent more on transfection efficiency (channel density) rather than on the use-dependence properties of the

two variants. In order to test the impact of splicing on repetitive firing in a controlled and normalized manner, interneurons were depolarized using trains of short, successive 10 ms current steps at increasing frequencies (33 – 90 Hz), with a magnitude of 110% of the threshold current that was required to elicit a single AP in 10 ms, i.e. meaning a supra-threshold stimulus (Figure 6.1C). This protocol, therefore, was used to assess firing reliability of each variant channel by evaluating at which level and at what frequency each variant would fail to fire, despite being given a supra-threshold stimulus. Furthermore, this protocol is thought to be better than prolonged depolarizing steps for reflecting the intermittent nature of excitatory inputs *in vivo* and also allows the controlled assessment of the frequency limits of AP firing.

Recordings in interneurons revealed that the neonatal Na_v1.1 isoform was able to support a higher fidelity of APs than adult channels in response to faster trains of current injections of 60 Hz and on (P<0.001, two-way ANOVA; Figure 6.3A,B). At lower frequencies the two variants could elicit APs equally reliably, with no failures in firing reliability for any variant. Yet, adult-driven interneurons start showing AP failures at lower frequencies compared to “neonatal” interneurons. The average frequency of 50% reliability for 5N-expressing interneurons (~83 Hz) was significantly higher than the equivalent for adult-driven interneurons (~69 Hz; P<0.001, unpaired two-tailed Student’s T test), while there is no difference of the AP decay rate as the stimulation frequency increases between the two variants (P>0.05, unpaired two-tailed Student’s T test) (Figure 6.3C). Therefore, this indicates that at a *high* frequency rate, interneurons can sustain AP firing more reliably when expressing all neonatal than when expressing all adult channels.

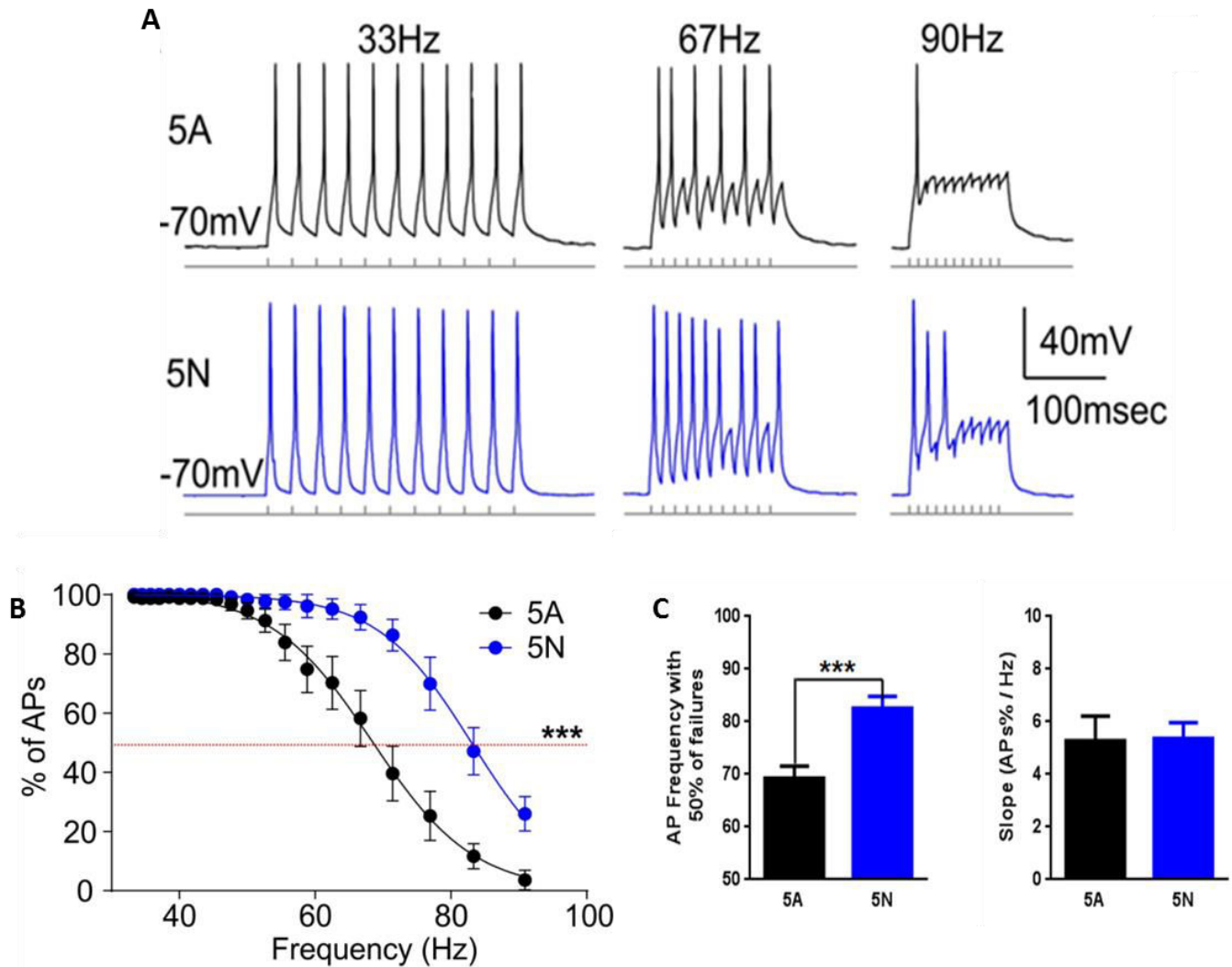


Figure 6.3: Splicing in Na_v1.1 is sufficient to alter spike reliability of interneurons during rapid trains

A. Representative traces from interneurons transfected with Na_v1.1-5A (top, black) and Na_v1.1-5N (bottom, blue) showing reduced ability of the adult isoform to support action potentials at higher frequencies. Neurons were subjected to trains of 10 ms depolarizing current steps at 110% of their threshold currents in the presence of 1 μ M TTX to block endogenous channels. Neurons were cultured from GAD67-GFP mice, and interneurons were identified by co-localization of GFP and RFP. **B,C.** Interneurons expressing the neonatal isoform of Na_v1.1 are able to sustain significantly higher rates of firing. The rate at which neurons fired action potentials at 50% of stimuli (dashed red line) was significantly higher for neurons expressing neonatal channels (5N 82.55 \pm 2.27, n = 12; 5A 69.27 \pm 2.33, n = 12; ***p = 0.0005, unpaired two-tailed Student's T test). Recordings and analysis of failure rates were carried out while investigator was blinded to isoform expressed. **C.** The slope of the AP decay rate with increased stimulation frequency was similar between Na_v1.1-5A and 5N-driven interneurons.

6.3.3 Splicing in Na_v1.1 can modify sodium channel availability in interneurons during rapid trains

Potential differences in neonatal and adult channel availability, which were suggested to occur also in HEK293T cell recordings at higher frequency stimulations as seen in Chapter 3, may possibly account for the difference in firing frequency reliability found between neonatal- and adult-transfected interneurons. In order to test this, the rising slope of APs was used as an indicator of sodium channel availability, by monitoring how this slowed during repetitive firing. The slowing of the AP rising slope is consistent with reduced sodium channel availability, as suggested by Scott *et al.* (2014), where a decrease in sodium channel activation in hippocampal slices is reflected by a decay in the AP rising phase during repetitive firing.

As a first test, a frequency of 44 Hz was taken, at which all pulses still generate an AP in both variants, so, *phenotypically*, there is no difference between the variants in terms of their firing reliability. The rising slope of each successive pulse was then normalized to the initial AP to monitor how it slows with successive pulses (Figure 6.4A). At this frequency, rising slopes of APs supported by the “adult” isoform of Na_v1.1 showed marked slowing as trains of stimuli progressed, while for neonatal-driven interneurons the rising slope decay rate was less profound and significantly higher than the adult at the later part of the train stimulation (Figure 6.4B). So, even at frequencies without AP failures, and therefore no firing differences between the variants (44 Hz), the neonatal isoform of Na_v1.1 was associated with a more constant AP rising slope during the train compared to the adult, with the difference AP rising slopes broadening during the train and becoming significant from the 7th stimulus on ($P < 0.05$, two-way ANOVA). If the stimulation frequency was increased to 56 and 67 Hz (i.e. frequencies at which the neonatal-driven interneurons start firing more reliably than adult ones), the difference in rising slope was evident after a single AP and increased even further as the stimulation frequency increased ($P < 0.001$, two-way ANOVA; Figure 6.4C). This suggests that for a stimuli arriving in rapid succession, splicing may change sodium channel availability after a single AP.

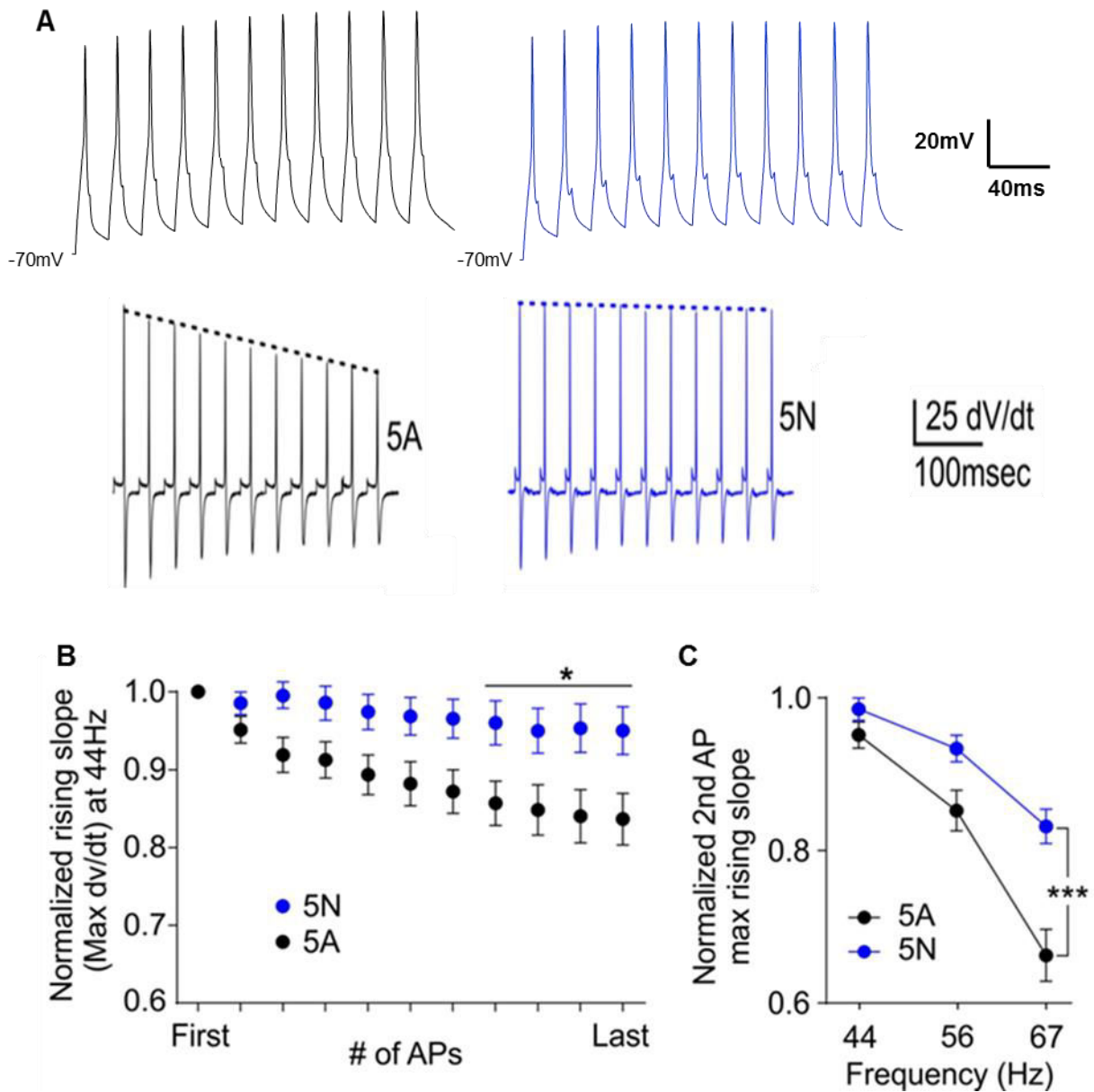


Figure 6.4: The increased failure rate in interneurons expressing the adult isoform is correlated with a slowing of the rise time of the action potentials during the series of depolarizing steps

A. Representative AP traces at 44 Hz frequency stimulation (top panel) and first derivatives of the action potentials (bottom panel) evoked by a series of steps from an interneuron expressing $Na_v1.1$ -5A (left, black), and $Na_v1.1$ -5N (right, blue). The height of the peak, as indicated by the dotted lines, corresponds to the steepest part of the rising slope (i.e. where the change in voltage per unit time is largest). Traces from a stimuli of 44 Hz is the fastest rate of stimuli where interneurons expressing adult isoforms were able to support action potentials for all steps. **B.** Adult isoforms show reduced ability compared to neonatal isoforms to maintain fast rising slopes of action potentials

during trains of stimuli. As the series of steps progressed, in cells expressing Na_v1.1-5A there was a marked slowing of the rising phase (the peak of the first derivative as in A), consistent with decreasing availability of these channels. There was no correlating decrease in rate of uptick of action potentials carried by Na_v1.1-5N, indicating that unlike adult isoforms the availability of neonatal channels was not reduced during trains of action potentials. By the end of the series the action potentials supported by the adult isoforms were significantly slower than those supported by neonatal isoforms (*p<0.05; two-way ANOVA followed by Bonferroni correction for multiple comparisons, 5A n=12; 5N n = 13). **C.** At higher rates of firing the reduction in rising slope for adult isoforms is evident after a single action potential. Data show the change in rising slope as measured from the first derivative for those interneurons that fired in response to both the first and second stimuli at higher frequencies. Cells which failed to fire action potentials were excluded (5A n = 12; 5N n = 13). At 66 Hz the difference became strongly significant (p<0.001; two-way ANOVA followed by Bonferroni correction for multiple comparisons).

6.3.4 Splicing in Na_v1.2 does not alter firing frequency fidelity in excitatory neurons

To test whether splicing in Na_v1.2 shared a conserved effect on neuronal behavior with splicing in Na_v1.1, we compared APs supported by isoforms of Na_v1.2 in excitatory (i.e. GFP negative) neurons and asked whether there were similar effects on rise time. Similar to what was seen for Na_v1.1, there were no real differences in the passive properties of neurons transfected with either Na_v1.2-6A or 6N or on most single AP parameters (P>0.05, unpaired two-tailed Student's T test; Figure 6.5A,B). A small difference was only found at the 50% half-width of the single AP (P<0.05, unpaired two-tailed Student's T test; Figure 6.5C), with the Na_v1.2-6A channels generating APs with shorter half-widths. This effect was not seen in Na_v1.1 isoforms, but was in accordance to what was found recently in more immature neurons expressing only Na_v1.2-6A or 6N in slice recordings (Gazina *et al.*, 2014).

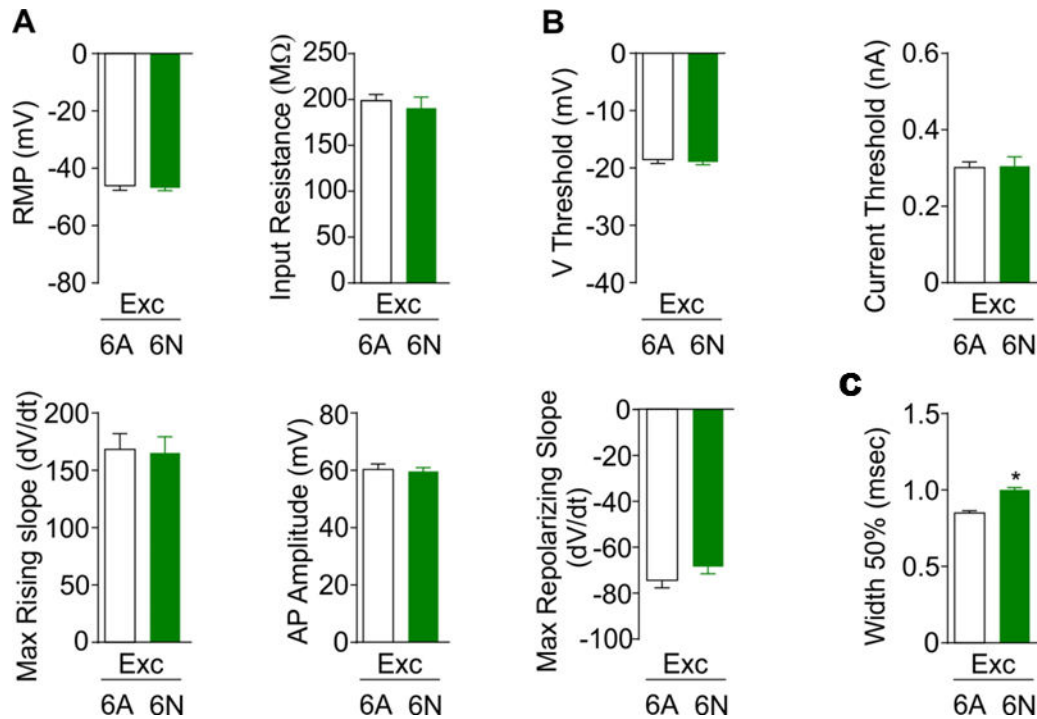


Figure 6.5: Intrinsic properties of excitatory neurons transfected with splice isoforms of Na_v1.2

A. Passive properties of neurons and **B.** of most single action potentials are not altered by transfection of different splice isoforms of Na_v1.2. RMP = resting membrane potential. **C.** Expression of the adult isoform of Na_v1.2 reduces the half width of APs in excitatory neurons. The mean half width was shorter for neurons expressing Na_v1.2-6A (0.86 ± 0.02 ms) compared to Na_v1.2-6N (0.99 ± 0.04 ms; * $p=0.01$; unpaired two-tailed Student's T test).

In terms of firing reliability at higher stimulation frequency, the two Na_v1.2 channel variants showed equal reliability, since the difference in frequency at which 50% of APs failed was not significantly different between neonatal and adult isoforms ($P>0.05$, two-way ANOVA; Figure 6.6A,B). There was a trend for the neonatal isoform to support firing more reliably at higher frequency rates, but this did not reach significance.

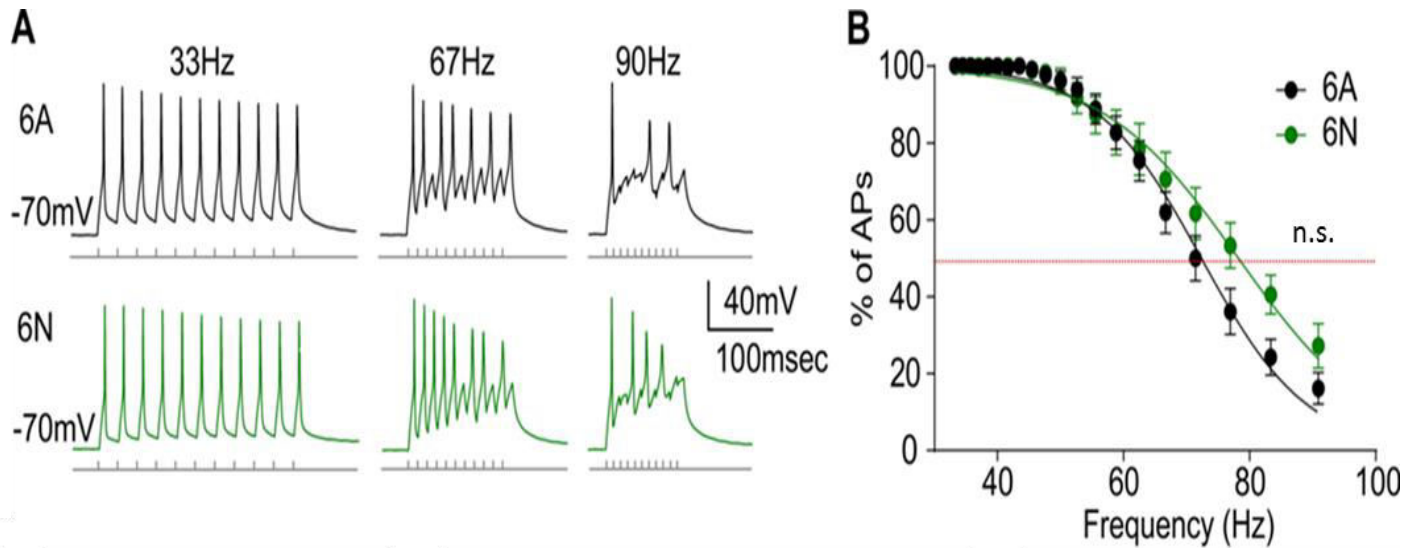


Figure 6.6: Splicing in Na_v1.2 does not alter spike reliability in excitatory neurons during rapid trains, with neonatal-driven cells showing a non-significant trend to fire more at higher frequencies

A. Representative traces from excitatory neurons transfected with Na_v1.2-6A (top, black) and Na_v1.2-6N (bottom, green). Recordings were carried out in 1 μ M TTX to block endogenous channels. **B.** Excitatory neurons expressing the neonatal isoform of Na_v1.2 are able to sustain slightly, but not significantly, higher rates of firing than those expressing the adult isoform. The rate at which excitatory neurons fired action potentials for 50% of stimuli, as calculated by average of exponential fits to individual cells, was not different ($p > 0.05$). Recordings and analysis of failure rates were carried out while investigator was blinded to isoform expressed.

6.3.5 Splicing in Na_v1.2 has conserved effects on AP rise time in excitatory neurons

Comparing the decay of the rising slope during AP trains for the two isoforms as done before for Na_v1.1 at 44 Hz, both neonatal and adult isoforms of Na_v1.2 showed a similar, pronounced slowing of AP rise times during trains ($P > 0.05$, two-way ANOVA; Figure 6.7A,B). This indicated that in excitatory neurons, inactivation accumulated for both Na_v1.2-6A and 6N channels to a similar degree, and this degree was more similar to that of the adult Na_v1.1 channels in interneurons, than the neonatal (Figure 6.4A). When neurons were pushed to fire at higher firing

frequencies (56 and 67 Hz), the neonatal isoform supported faster rise times for APs even after a single firing during shorter inter-stimulus intervals ($P < 0.05$, two-way ANOVA; Figure 6.7C), similar to what was seen for $Na_v1.1$ -5A and 5N constructs in interneurons. This suggests that, again, at higher stimulation frequencies, the availability of the neonatal $Na_v1.2$ channel is higher compared to the adult, although, in this case, this does not directly translate to a significantly higher firing fidelity in excitatory neurons. Thus, for depolarizations in rapid trains, splicing in both *SCN1A* and *SCN2A* genes in their natural milieu has conserved effects on the AP rising phase after a single action potential in two different cell types.

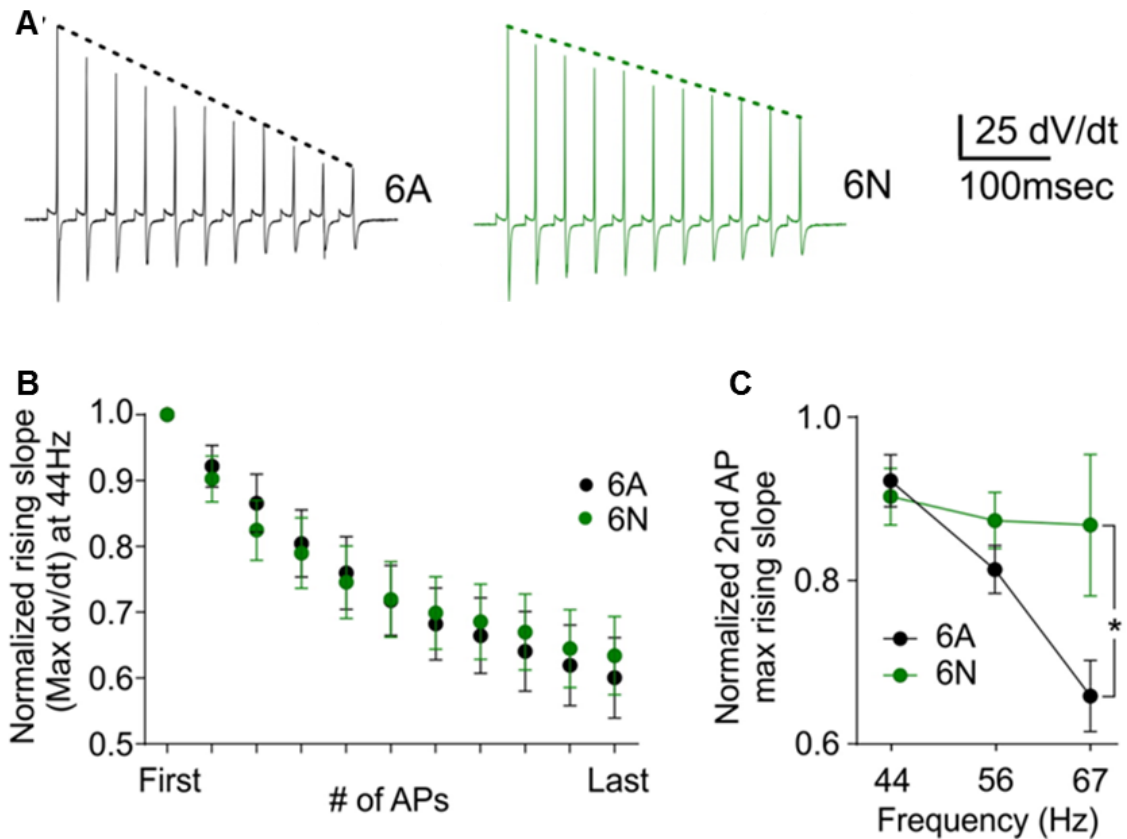


Figure 6.7: Expression of Na_v1.2 in excitatory neurons reveals conserved effect of splicing on rising phase of action potentials during fast trains

A. The second differential of the action potentials evoked by representative series of steps from an excitatory neuron expressing Na_v1.2-6A (left, black), and Na_v1.2-6N (right, green), showing marked drop in the speed of the rising slope for both isoforms. Traces are from stimuli at 44 Hz. **B.** During trains of stimuli neither isoform is able to maintain rapid rising phases of action potentials in excitatory neurons. As with Na_v1.1, both isoforms show similar slowing during the trains. **C.** At higher rates of firing the reduction in rising slope for adult isoforms is evident after a single action potential. Despite the smaller intrinsic differences in isoforms of Na_v1.2 compared to Na_v1.1, the Na_v1.2 isoforms confirm that for short interpulse intervals, the neonatal channels are more able to support fast rising phases. Data show the change in rising slope as measured from the second derivative for those excitatory neurons that fired in response to both the first and second stimuli. Cells which failed to fire action potentials were excluded (6A n =10; 6N n=9). At 67 Hz the difference was significant ($p < 0.05$; two-way ANOVA followed by Bonferroni's multiple comparisons test).

6.3.6 Effect of splicing on AP rise time is also conserved for Na_v1.1 isoforms in excitatory neurons

To further explore the conservation of the splicing effect on neuronal behavior, it is important to validate whether the same channel isoforms have conserved effects on different types of neurons. This could give an indication of whether channel isoforms may behave differently when expressed in a neuronal environment other than their native one and validate whether the differences they produce are cell type-specific. Therefore, it was asked whether neonatal isoforms of Na_v1.1 were also able to support increased channel availability, this time in excitatory neurons, as opposed to interneurons as seen before. Interneurons have different membrane dynamics, frequently supporting faster trains of APs than pyramidal neurons. It is unknown whether Na_v1.1 expression in excitatory neurons would confer a firing frequency high enough for any potential difference between the isoforms in reliability to be revealed, yet channel availability will be a more robust index of functional conservation of the splicing event in this neuronal milieu.

Na_v1.1-5A and 5N channels expressed in excitatory neurons did not confer any different passive properties in the cells in terms of their RMP, input resistance or cell capacitance, or on their current threshold ($P > 0.05$, unpaired two-tailed Student's T test; Figure 6.8A). As for single AP properties, neonatal and adult Na_v1.1 channels showed similar properties for threshold voltage, max rising and repolarizing slopes, AP amplitude and 50% AP width, similar to interneurons ($P > 0.05$, unpaired two-tailed Student's T test; Figure 6.8B).

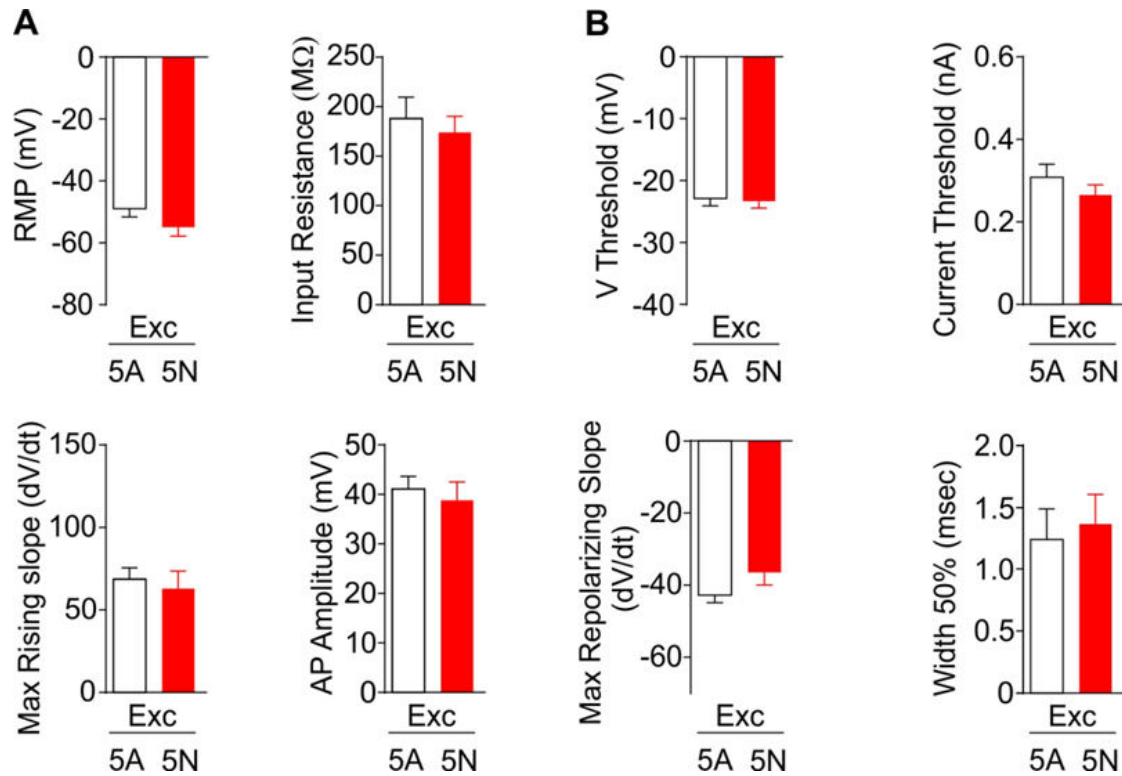


Figure 6.8: Intrinsic properties of excitatory neurons transfected with splice isoforms of Na_v1.1 did not differ between neonatal and adult

A. Passive properties of neurons and **B.** of single action potentials are not altered by transfection of different splice isoforms of Na_v1.1. RMP = resting membrane potential.

In terms of firing frequency, neonatal and adult-driven neurons fired equally reliably during the whole range of stimulation frequencies tested (33 – 90 Hz, $P > 0.05$, two-way ANOVA; Figure 6.9A,B). In excitatory neurons the recombinant neonatal isoform of Na_v1.1 did not confer interneuron-like fast firing, indicating that membrane properties other than sodium channel availability set the maximal firing rate in these cells. In contrast to interneurons, the rising phase of APs carried by both isoforms slowed to a similar extent during trains of APs at 44 Hz ($P > 0.05$, two-way ANOVA; Figure 6.10A,B), and again this was similar to the decay seen for adult channels in interneurons. However, similar to the case in interneurons as well as Na_v1.2 in excitatory neurons, when pushed to higher frequencies splicing did impose a significant difference

in rise time after a single AP at the highest (67 Hz) firing frequency tested ($P < 0.05$, two-way ANOVA; Figure 6.10C).

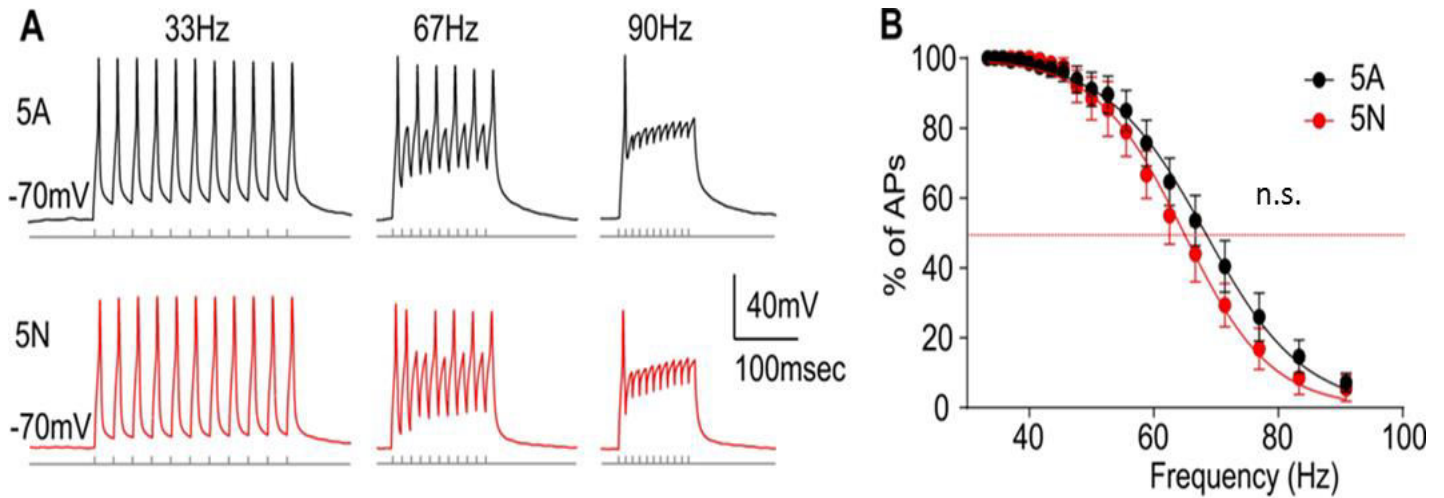


Figure 6.9: In excitatory neurons the neonatal isoform of Na_v1.1 does not confer greater spike reliability at higher firing frequency compared to the adult as in interneurons

A. Representative traces from excitatory neurons transfected with Na_v1.1-5A (top, black) and Na_v1.1-5N (bottom, red). Recordings were carried out in 1 μM TTX to block endogenous channels. **B.** Transfected excitatory neurons are not able to sustain high rates of firing with either isoform of Na_v1.1. The rate at which neurons fired action potentials at 50% of stimuli, as calculated by the average of exponential fits to individual cells, were not different. Recordings and analysis of failure rates were carried out while investigator was blinded to isoform expressed.

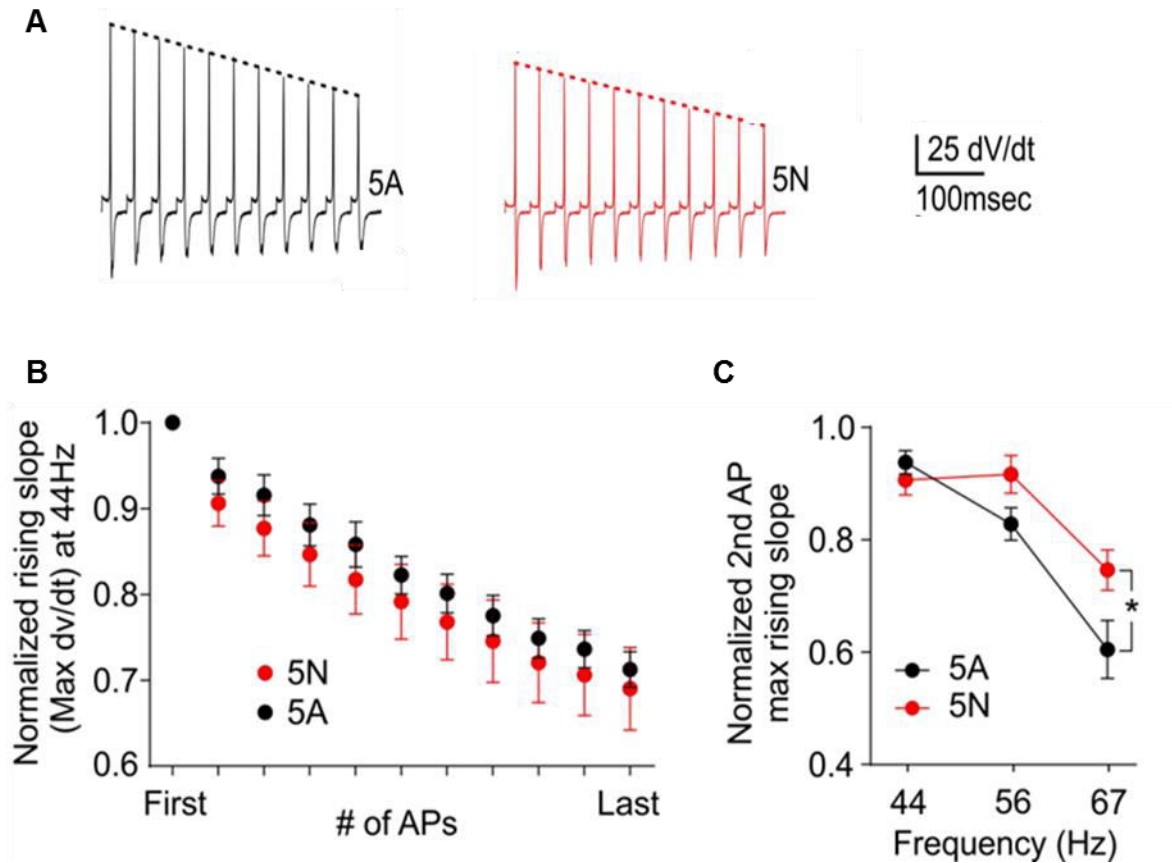


Figure 6.10: An effect of splicing on rising phase of action potentials during fast trains is also conserved when $Na_v1.1$ channel isoforms are expressed in excitatory neurons

A. The second differentials of action potentials evoked by a representative series of steps from an excitatory neuron expressing $Na_v1.1$ -5A (left, black), and $Na_v1.1$ -5N (right, red). Traces are from stimuli at 44 Hz, which is the fastest rate of stimuli where excitatory neurons were able to support action potentials for all steps. **B.** During trains of stimuli both adult and neonatal isoforms show marked slowing of the rising phases of the action potentials. In contrast to interneurons, where neonatal isoforms maintained rapid rising slopes, excitatory neurons showed slowing for both isoforms, indicating trains of action potentials reduced the availability of these channels. Adult and neonatal rising slopes were similar throughout the trains. **C.** At high firing frequencies the adult isoforms show reduced rising slope after a single AP. The difference is consistent with that seen for interneurons expressing the same isoforms. Data show the change in rising slope as measured from the second derivative for excitatory neurons that fired in response to both the first and second stimuli. Cells which failed to fire action potentials were excluded (Adult $n = 10$; Neonate $n = 6$). At 67 Hz the difference was significant ($p < 0.05$; two-way ANOVA followed by Bonferroni's multiple comparisons test).

Therefore, in excitatory cells, splicing in *SCN1A* can still modify sodium channel availability in response to stimuli arriving with short inter-stimuli intervals, such as bursts of APs, similar to the situation in interneurons or $\text{Na}_v1.2$ isoforms in excitatory neurons as well.

6.4 Discussion

Recordings in transfected neurons reveal that alternative splicing in sodium channels affects the fidelity of action potentials during trains of stimuli in interneurons, most likely by altering the stability of the fast component of inactivation. While the effects of splicing are most pronounced in interneurons, consistent effects are seen in excitatory neurons where the adult isoforms appear to reduce channel availability after a single action potential. This effect is conferred by isoforms of at least two different channels ($\text{Na}_v1.1$ and $\text{Na}_v1.2$), and is consistent with a conserved effect of splicing on the inactivation of TTX-sensitive sodium channels, as it was seen before in HEK293T cell recordings (Chapter 3). Although $\text{Na}_v1.1$ channels are most associated with interneurons that can fire rapid trains, in excitatory cells these channels had a trend towards firing less reliably than $\text{Na}_v1.2$, which highlights the importance of cellular background in determining the firing parameters. Both $\text{Na}_v1.1$ and $\text{Na}_v1.2$ isoform pairs showed a difference in channel availability after high stimulation frequency, irrespectively of the cellular background, hence revealing a conserved functional effect of the splicing event. Yet, it is only in interneurons, where this is translated into a change in firing reliability for the $\text{Na}_v1.1$ isoforms, indicating that the native neuronal background of $\text{Na}_v1.1$ channels is permissive to maximizing the functional difference between variants.

Our finding that splicing is able to impose conserved functional consequences in different channels with different distributions in the nervous system, suggests that the impact of splicing on inactivation may be the key functional consequence that has led to the conservation of this molecular event. However we cannot rule out other roles for this splicing in regulating interactions with other proteins, or contributing to distinct functions in different neuronal populations or during development of the nervous system.

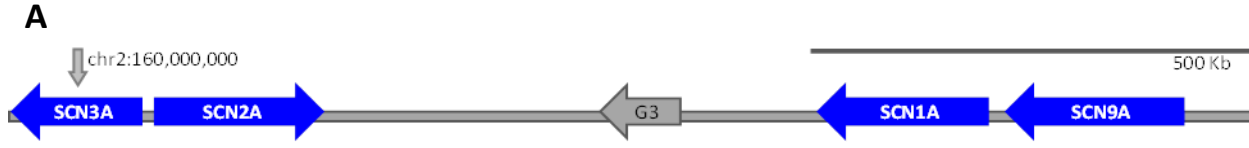
6.4.1 Splicing in Na_v1.1 sets the maximal firing rate in interneurons

Changing the splice isoform of Na_v1.1 was sufficient to change the ability of interneurons to fire action potentials in response to fast trains of depolarizing current steps. The slowing of the rising phase of the action potentials conveyed by the adult isoform strongly suggests that the reduced ability to fire rapidly is due to a steady reduction in availability of channels during longer trains, likely due to their sequestration in the fast inactivated states. Similarly, the effects of splicing in both Na_v1.1 and Na_v1.2 in excitatory neurons indicate that reliance on the adult isoform can reduce the availability of channels after a single action potential. These data are consistent with splicing having a relatively modest effect on neuronal behavior, imposing a small reduction in channel availability when the adult exon is included. Recently accumulation of sodium channel inactivation was shown to be important for setting spike timing (Scott *et al.*, 2014), thus splicing may have a role in detecting synchronous inputs. However, further work in preparations with intact synaptic inputs would be necessary to determine whether individual EPSPs are sufficient to reduce adult isoform availability relative to neonatal availability during bursts of synaptic activity.

6.4.2 Molecular conservation suggests strong selection against neonatal Na_v1.1 in mammals

Despite the fact that the functional effect of this splicing event in sodium channel availability is conserved among Na_v1.1 and Na_v1.2 isoforms in two different kinds of neurons, it is only for Na_v1.1 in interneurons that this is translated to a difference in firing ability. Therefore, Na_v1.1 isoforms expressed in their physiological milieu can set a difference in interneuron firing at high frequencies, which are considered physiological for an interneuron (60 – 90 Hz). On the contrary, Na_v1.2 isoforms in excitatory neurons do not support that difference. Even at higher frequencies, where there is a trend for neonatal Na_v1.2 channels to confer higher reliability, this stimulation frequency is beyond the typical physiological firing range of excitatory neurons. This means that, even though the effect on sodium channel availability is conserved, it is only the Na_v1.1 isoforms that can have a phenotypic effect in neurons under physiological conditions, at least with the

stimulation protocol used here. Although such an effect of the neonatal isoform could be considered as a positive consequence in epileptic conditions (also partly supported by association studies, e.g. Schlachter *et al.*, 2009; Le Gal *et al.*, 2011; Kumari *et al.*, 2013; Tang *et al.*, 2014), its overall effects in normal brain physiology as well as pathophysiology remain unclear. It has been noted before (Fletcher *et al.*, 2011; Gazina *et al.*, 2010) that along evolution the rodent copy of exon 5N in *SCN1A* has acquired stop codons that render it non-functional. In humans, the single nucleotide polymorphism (SNP) rs3812718 significantly reduces the expression of this exon during early development (Heinzen *et al.*, 2007). Interestingly, this SNP occurs with a roughly 50% prevalence in human chromosomes, suggestive of an ongoing evolutionary selection for a SNP that reduces levels of exon 5N. This selective pressure to reduce 5N in *SCN1A* may not be specific to rodents and humans. Analysis of 22 mammalian genomes where exon 5N could be identified in *SCN1A* using the location of this gene in the conserved cluster of five sodium channel genes (Figure 6.11A) showed frameshifts and stop codons in seven copies of 5N (Figure 6.11D,E, in red), and removal of positively charged arginines from the S4 segment in a further seven copies (Figure 6.11C,E in purple), a substitution likely to be damaging for channel function. As an example of damage, rabbit 5N harbors 11 amino acid substitutions out of 30 possible in this normally highly-conserved voltage-sensing module (Figure 6.11C, Oc, in yellow). Altogether, looking down at the single base pair level, only 8 of the 22 copies of *SCN1A* identified did not contain likely deleterious amino acid substitutions (Figure 6.11C). Further evidence for negative selection of 5N comes from the finding that a splice site polymorphism homologous with rs3812718 has apparently independently arisen in giant panda (*Ailuropoda melanoleuca*; in light blue, Figure 6.11E).



B

1.2 YVTEFVN LGNVSALRTFRVLRALKTISVIP
 1.9 YLTEFVN LGNVSALRTFRVLRALKTISVIP

N R R R K

C

C1 YVTEFVSLGNFSALRTFRVLRALKTISVIP
 Ec YVTEFVSLGNFSALRTFRVLRALKPISVIP
 Fc YVTEFVSLGNFSALRTFRVLRALKTISVIP
 Oa YVTEFVSLGNFSAVHTFRVLRALKTISVIP
 Bt YVTEFVSLGNFSAVHTFRVLRALKTISVIP
 Am YVKEFVSLGNFSALQTFRVLRALKTISVIP
 Pp FVTEFVNLGNFSALRTFRVLRALKTISVIP
 Pt FVTEFVNLGNFSALRTFRVLRALKTISVIP
 Pab FVTEFVNLGNFSALRTFRVLRALKTISVIP
 Hs FVTEFVNLGNFSALRTFRVLRALKTISVIP
 Mml FVTEFVNLGNFSALRTFRVLRALKTISVIP
 Cj FVTEFVNLGKFSALHTFRVLRALKTISVIP
 Sb FVTEFVNLGKFSALHTFRVLRALKTISVIP
 Gg FVTEFVNLGNFSALCTFRVLRALKTISVIP
 Nl FVTEFVSLGNFSALRTFRVLRALKTISVIP
 Oc DVTEFVKLGSFS TVRIYRVLRTLETISIVP
 *.***.**.**:: :*****:*.**:*

D

Pan FVTEFVNLGNFSALRTFRVLRVLTIL*
 Og YLTEFVNLAIFQLFALSES*
 Cp IHNRMCKLGTF*
 Cg PMAYLPLN*
 La NAYSMKFTSR*
 Mms *VTKFVYLGNF*
 Rn *VPEFVNLGNF*

Figure 6.11: Molecular conservation of sodium channel splicing in domain 1. The neonatal exon has been destroyed in multiple mammalian copies of *SCN1A*

A. The conserved cluster of sodium channel genes on human chromosome 2 as oriented by UCSC Genome Browser Feb 2009 assembly. G3 is the *GALNT3* gene which occupies a conserved position between the two pairs of sodium channels, and could be used for distinguishing *SCN2A* from *SCN1A* in genomes where the notation was incomplete. In several cases of published mammalian genomes *SCN2A* was best distinguished by the reversed orientation with respect to *SCN3A*. **B.** The invariant amino acid sequences of the neonatal exons in *SCN2A* (1.2, top) and *SCN9A* (1.7 bottom). The sequences were identical for all genomes screened. **C,D.** Amino acid sequences encoded by exon 5N in $Na_v1.1$ for species where this exon could be un-ambiguously identified, with full length sequences aligned (**B**), and truncated exons not aligned (**C**). The aligned sequences have changes highlighted according to likelihood of functional damage: conservative (green), not conserved (yellow), loss of an S4 arginine (R) or lysine (K) (purple), and the non-aligned copies with nonsense (*) at the bottom (**C**). In some cases (Oc, Og, Cp, Cg, Mm, Rn) the exon could not be identified using standard megaBLAST parameters and the location of exon 5N was ascertained using its proximity to exon 5A in *SCN1A*. The identity of *SCN1A* was confirmed in each of these cases by the location of this gene compared to *SCN3A*, *SCN2A* and *SCN9A* in the cluster. **E.** Alignments of the nucleotide sequences of the neonatal exons and flanking 3'splice sequence for all the different mammalian species where exon 5N could be found in *SCN1A*. Yellow highlights in *SCN1A* correspond to frameshifts or nonsense mutations. Purple changes in *SCN1A* indicate the site of the human polymorphism rs3812718, which appears to have emerged independently in Panda (Am). Highlighted (green) nucleotides in alignments of *SCN2A* and *SCN9A* are all synonymous changes. Species: Cj *Callithrix jacchus*; Hs *Homo sapiens*; Mml *Macaca mulatta*; Nl *Nomascus leucogenys*; Og *Otolemur garnettii*; Pp *Pan paniscus*; Pt *Pan troglodytes*; Pan *Papio anubis*; Pab *Pongo abelii*; Sb *Saimiri boliviensis*; Cp *Cavia porcellus*; Cg *Cricetulus griseus*; Mms *Mus musculus*; Rn *Rattus norvegicus*; Am *Ailuropoda melanoleuca*; Bt *Bos taurus*; Cl *Canis lupus*; Ec *Equus caballus*; Fc *Felis catus*; Oc *Oryctolagus cuniculus*; Oa *Ovis aries*; La *Loxodonta Africana*.

This variability in exon 5N of *SCN1A* does not appear to reflect a general flexibility in the sequences of neonatal isoforms of neuronal sodium channels. Neonatal exons in *SCN2A* (6N) and *SCN9A* (5N) in the same 22 mammalian species were also identified to see whether a similar degree of variation occurred. Neither *SCN2A* nor *SCN9A* contained a single amino acid substitution in any species (Figure 6.11B). Even at the nucleotide level there was a high level of conservation with infrequent silent substitutions (Figure 6.11E). This represents a highly

significant difference in rate of damage (p ($SCN1A=SCN2A$ or $SCN9A$) < 0.0001 ; Fisher's exact test, with a correction for multiple tests: $P < 0.0002$). Comparison of the rate of non-synonymous (Ka) to Synonymous (Ks) changes has been used as a proxy for detecting genes under rapid selection (Liberles & Wayne, 2002). A Ka/Ks ratio greater than 1 is indicative that a gene may be under strong selection, because this indicates mutations that change amino acids are more frequent than expected compared to silent mutations. Using a consensus 'neonatal exon' sequence containing all the observed nucleotide substitutions, a comparison was carried out with respect to presumed ancestral 'neonatal' sequence. This comparison yields a Ka/Ks = 2.4424 for *SCN1A* exon 5N, and indicates that this exon is under strong negative selective pressure in mammals (Liberles & Wayne, 2002). In contrast, neither *SCN2A* nor *SCN9A* contain a single non-synonymous mutation (Ka/Ks = 0).

Therefore, the 5N version of $Na_v1.1$ which is associated with the highest fidelity of firing in interneurons appears to be under positive selection for removal from mammalian genomes. The selective pressure removing exon 5N from $Na_v1.1$ is unknown, but highly specific to this gene, and may be associated with determining the maximal firing rates of interneurons.

6.5 Summary

To summarize, the change in rising slope after a single action potential was used here as an indicator of sodium channel availability (as suggested previously by Scott *et al.*, 2014), which is in turn indicative of the ability of the channels to recover from fast inactivation. A higher relative rising slope value for neonatal channels compared to adult ones at higher frequencies across $Na_v1.1$ and $Na_v1.2$ channels in different neuronal types suggests that there are relatively more neonatal channels available during faster stimulation, possibly as a result of increased recovery from inactivation. This is in accordance with HEK293T cell data (Chapters 3 & 4) and it is consistent with this property that is allowing $Na_v1.1$ neonatal-driven interneurons to fire more reliably at higher frequencies. Therefore, here we have managed to extrapolate a difference that was found in fast inactivation between neonatal and adult channels in HEK293T cells to a

difference in high frequency firing in neurons based on this mechanism, as it is supported by the rising slope decay data (Figure 6.12).

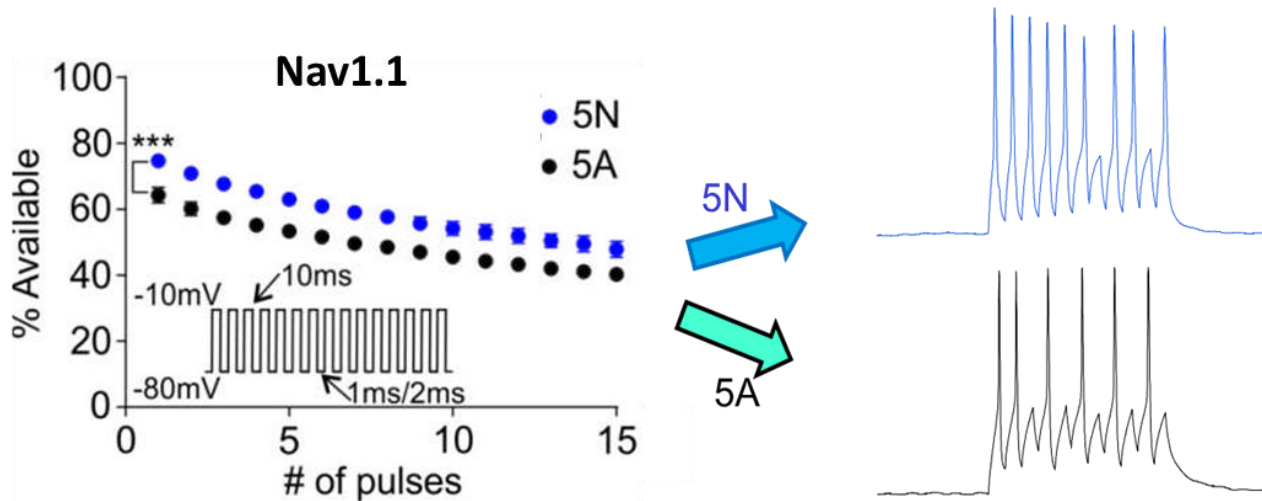


Figure 6.12: The difference in $Na_v1.1$ channel availability between isoforms in HEK293T cells is translated to a difference in firing frequency fidelity in interneurons

The data from interneurons are consistent with the data from HEK293T cells showing a difference in recovery from fast inactivation. Data suggest that neurons expressing more 5N could have shorter absolute refractory periods allowing shorter inter-spike intervals and higher firing frequency reliability in interneurons for $Na_v1.1$ isoforms.

The selective loss of neonatal $Nav1.1$ suggests that although the functional impact of this splicing is conserved across channels, the consequences of that conserved function may not be equally advantageous in different channels. While there appears to have been high pressure to conserve the neonatal forms of $Na_v1.2$ and 1.7 , neonatal 1.1 has been removed from multiple mammalian genomes. It is possible that the different expression pattern of sodium channels is linked to different impacts. The selective loss of the neonatal exon in $Na_v1.1$ may indicate that while the more subtle effects on channel availability are conserved, the ability of splicing to control firing rate may be deleterious, and the combination of rapid hyperpolarisation, thought to be predominantly set by expression of voltage-sensitive potassium channels (Bean, 2007), and fast recovering sodium channels may exceed the tolerability limit of even fast spiking interneurons.

Chapter 7: Effects of Na_v1.1 splicing on single cell response to network epileptic activity by Dynamic-Clamp

7.1 Hypothesis and Aims

Experiments up to now have shown that alternative splicing of exon 5 in sodium channels can confer higher availability for neonatal channels in HEK293T cells through increased recovery from fast inactivation during trains of fast depolarizations. Extending that to neurons, neonatal Na_v1.1 channels were able to confer higher reliability at fast firing frequency in cultured interneurons, which was consistent with higher availability of neonatal channels at higher frequencies. As has been mentioned before, an ambiguous association exists between a common polymorphism in *SCN1A* that disrupts the inclusion of the neonatal exon in Na_v1.1 channels (Tate *et al.*, 2005) and an increased likelihood of developing seizures (Abe *et al.*, 2008; Kumari *et al.*, 2013), but this has not been replicated in some studies (Manna *et al.*, 2011). Results shown here for interneurons might provide a functional (mechanistic) explanation in favor of this association, since the more reliable firing of neonatal interneurons at higher frequencies may better mitigate pyramidal cell discharges during epileptic events.

However, in order to be able to assess the link between seizure predisposition and neuronal properties conferred by Na_v1.1-5A or 5N channels, there is a need for a more direct assessment of how splicing is relevant to circuit pathology, particularly to neuronal activity during epileptiform events. To address this, we used dynamic clamp recordings as a tool for simulating epileptic synaptic activity to Na_v1.1-5A or 5N-transfected neurons in cultures. Dynamic clamp recordings have mostly been used to reintroduce a single isolated conductance in a cell to study its properties (Pavlov *et al.*, 2014; Milescu *et al.*, 2008). We decided to use the dynamic clamp approach in a different way, by introducing a recorded template of network epileptic activity in isolated neurons in order to understand the physiological/pathological implications of Na_v1.1 splicing under epileptic conditions.

This was performed by first recording the synaptic activity – in terms of changes in conductance – experienced by a neuron in an acutely provoked epileptiform event and then “feeding” that pattern of epileptic synaptic input conductances to cultured hippocampal neurons transfected with either Nav1.1 5A or 5N to examine their firing pattern in response. This approach, therefore, directly compared how neonatal and adult channels supported neuronal firing under conditions simulating epileptic synaptic activity.

Dynamic clamp recordings in this chapter were performed by Dr. Gabriele Lignani, while voltage-clamp neuronal recordings, neuronal cultures and transfections as well as data analysis were performed by the writer in collaboration with Dr. Lignani.

7.2 Setup of a neuronal and interneuronal epileptic trace template

The first step before any dynamic clamp recordings was to record epileptic traces for both excitatory neurons and interneurons. These traces would then be used as templates of epileptic activity for the dynamic clamp recordings. In order to obtain traces of epileptiform synaptic inputs, GAD67-GFP P0 mouse hippocampal neurons were plated and cultured for 21 days, to allow them to form robust synaptic connections with each other. An excitatory neuron (GFP negative) and after that an inhibitory neuron (GFP positive) were voltage-clamped at -70 mV and their spontaneous synaptic currents (AMPA current) were recorded in the presence of the convulsant 4-Aminopyridine (4-AP, 100 μ M) to mimic epileptic network activity, as used in published studies (Pozzi *et al.*, 2013) (Figure 7.1A1). The current traces recorded for both excitatory and inhibitory neurons were converted into conductance ($G=I/V$) (Figure 7.1A2) and could then be given as the command conductance to the dynamic clamp software, which dynamically injects current in patched neurons in current-clamp configuration (Figure 7.1A3). The software reads the voltage of patched neurons in real time and calculates how much current to be injected from the conductance template ($I=G*V$), allowing patched neurons to fire APs in response to the command conductance (Figure 7.1A).

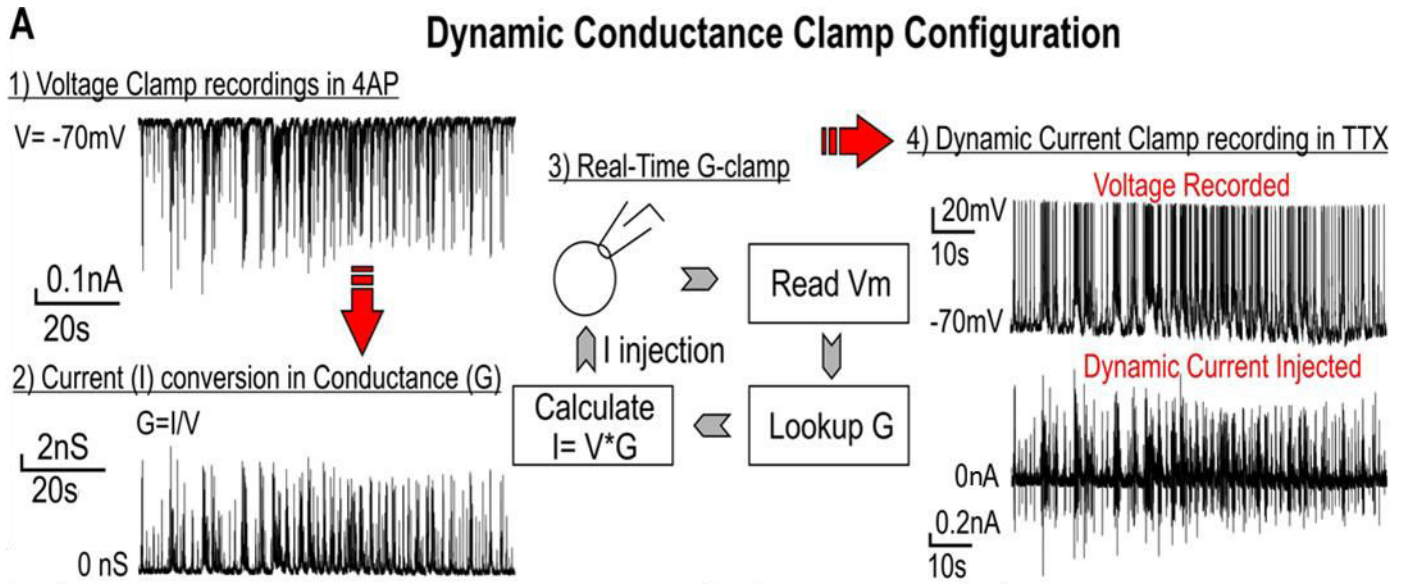


Figure 7.1: Dynamic clamp experimental procedure

A. After excitatory neuron or interneuron recordings in voltage clamp in the presence of 4AP (1), the resulting current is converted in conductance (2). Then, neurons expressing the neonatal or the adult isoform of $\text{Na}_v1.1$ were recorded in current clamp in presence of TTX and fed with the previous conductance trace generating dynamic current injections (3 & 4).

7.3 Magnitude of G_{th} – the conductance threshold

Conductance levels can vary between cells, since they depend on neuronal properties (e.g. membrane resistance) as well as – in case of transfected neurons – on the level of transfection efficiency of each individual neuron. Therefore, the conductance trace should be scaled for each neuron to a reference point, as a means of normalizing the conductance magnitude that was going to be used for each patched neuron. As a reference point, we used the conductance threshold (G_{th}) of each individual cell (i.e. the minimum conductance required to elicit an AP) (Figure 7.2A). The excitatory and inhibitory conductance traces were then scaled to different G_{th} fractions (0% – 25%) for untransfected excitatory and inhibitory neurons respectively, in order to evaluate the optimal

scale magnitude that would be used for the dynamic clamp recordings of transfected neurons (Figure 7.2 B & C). Analyzing the percent of the conductance threshold with respect to the APs elicited in current clamp and to their maximal intra-event frequency, a 15% of conductance threshold (max number of events and frequency before a plateau) was selected for all further experiments in both excitatory and inhibitory transfected neurons.

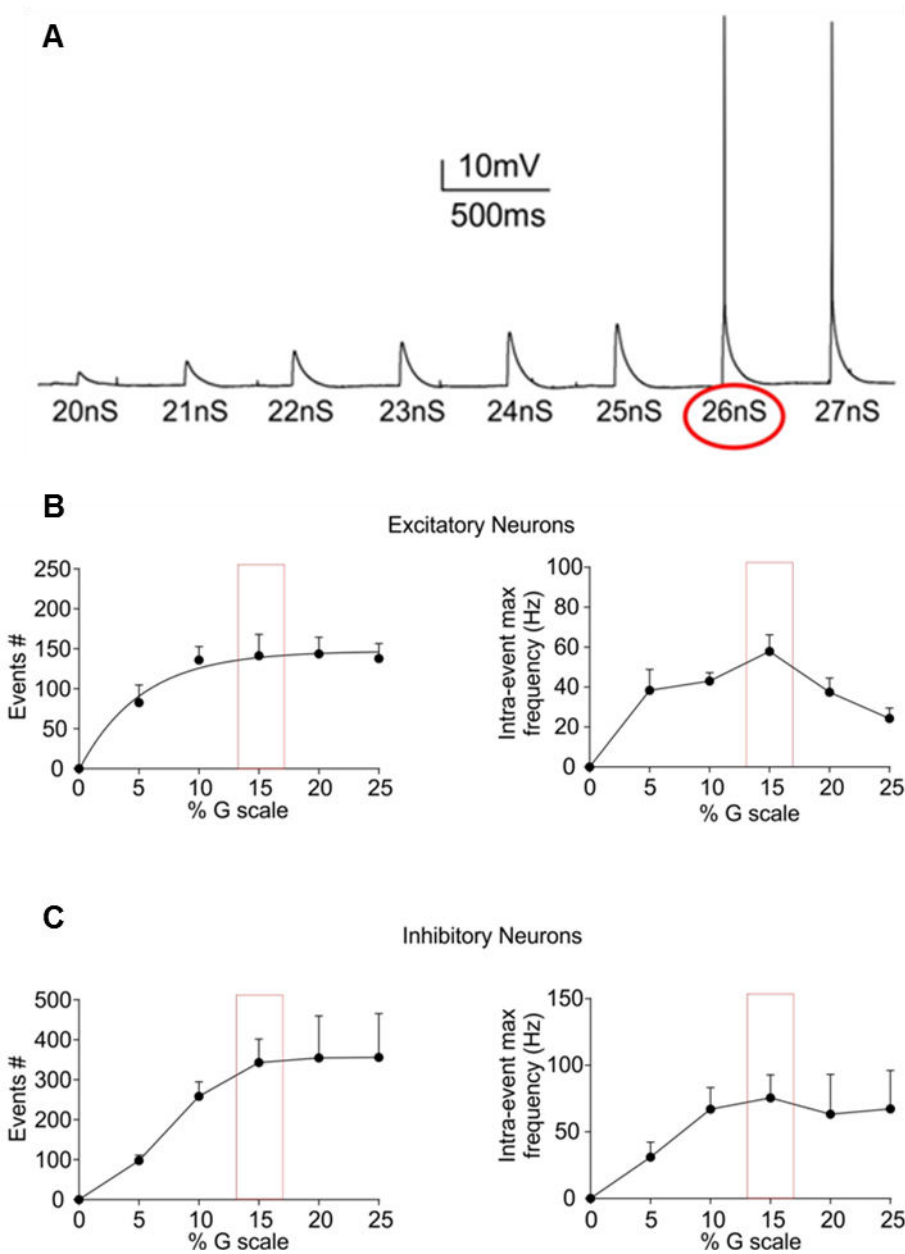


Figure 7.2: Calculation of the conductance magnitude used for both excitatory and inhibitory neurons and dynamic clamp experiments to set the magnitude of conductance threshold.

A. Representative protocol of dynamic clamp producing AMPA conductance steps ($E_{rev}=0mV$; $\tau=1ms$; $\Delta G=1nS$). The red circle is the conductance threshold in this specific experiment (repeated 10 times for each neuron recorded). **B. & C.** Number of events and intra-event maximal frequency in excitatory (B) and in inhibitory (C) neurons, against the percent of conductance threshold. The red squares represent the percent of conductance threshold used for all the dynamic clamp experiments in neurons expressing 5N or 5A splicing isoforms of $Na_v1.1$

7.4 Results

7.4.1 In interneurons $\text{Na}_v1.1\text{-5N}$ channels confer higher firing ability under epileptic conditions

$\text{Na}_v1.1$ 5A and 5N were transfected in primary neurons from GAD67-GFP mice and during the dynamic clamp recordings TTX was used to block innate sodium channel activity, similar to previous recordings (Chapter 6). GFP positive neurons (interneurons) successfully transfected with $\text{Na}_v1.1\text{-5A}$ or 5N (i.e. RFP positive cells) were patched in current clamp configuration. After the conductance threshold for each neuron was found, the conductance trace (scaled to 15% of the threshold) was used to dynamically inject current in the patched neuron in order to trigger APs in a virtual epileptic synaptic barrage. The number of APs triggered by dynamic clamp current injection and their inter spike intervals were analyzed (Figure 7.3A). Frequency analysis showed that significantly fewer cells expressing the 5A isoform reached an instantaneous firing frequency of 50 Hz than cells expressing the 5N isoform (7/14 vs 15/17; $P = 0.019$, Fisher's exact test, two-tails, Figure 7.3B), indicating that neonatal-driven interneurons were able to attain higher firing rates than adults during the same epileptiform inputs. This difference in frequency was associated with an increased numbers of events for neonatal interneurons (Figure 7.3A, C, 5N 401.2 ± 48.72 , $n = 19$; 5A 315 ± 48.38 , $n = 14$), but due to the wide distribution of event numbers between cells this difference did not reach statistical significance ($P = 0.1$, Mann Whitney U test). However, in terms of firing frequency, a cumulative frequency histogram of instantaneous firing rate showed a highly significant difference between the frequency distributions of the splice variants (Figure 7.3D; $P=0.009$, Mann-Whitney U test), with the most pronounced differences between 33 and 90.9 Hz (same frequencies used in previous current clamp experiments in Chapter 6). This was accompanied by a slower AP rising slope for cells expressing the adult splice variant (Figure 7.3E; $P<0.001$, Mann-Whitney U test). However, the presence of a small number of fast-firing cells had a disproportionate effect on the number of action potentials with very fast rising slopes.

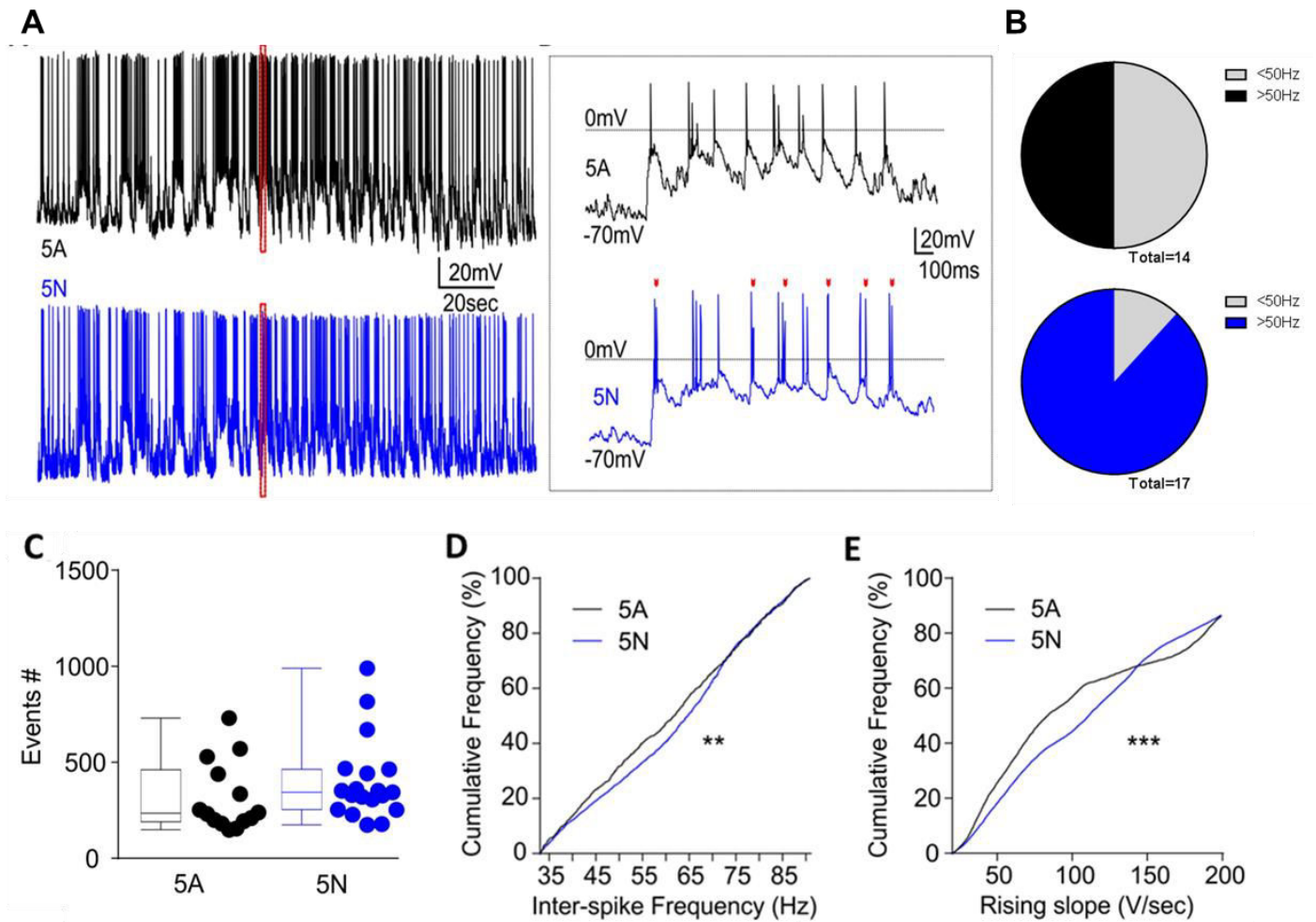


Figure 7.3: Dynamic clamp experiments demonstrate that splicing in Na_v1.1 is sufficient to alter interneuron activity during epileptiform bursts

A. Representative voltage traces of the Na_v1.1 isoforms resulting from dynamic current injection of the conductance trace (left) and zoomed representative traces of Na_v1.1 isoforms from the dotted box in A with red arrowheads indicating additional events in the cell expressing 5N compared to 5A during the series. **B.** A smaller percentage of interneurons expressing the 5A isoform reached an instantaneous firing frequency of 50 Hz (50%, black, top) than cells expressing the 5N isoform (88%, blue, bottom). **C.** Total number of APs recorded during dynamic current injection. Note the spread of points consistent with a small population of fast firing interneurons, and a cluster of interneurons firing at a slower rate for each splice variant. Number of events (5N 401.2 ± 48.72, n = 19; 5A 315 ± 48.38, n = 14; p = 0.1, Mann Whitney U test) is shown as mean ± s.e.m. **D.** Intra-spike frequency cumulative frequency analysis between 33 and 90.9 Hz (frequencies mapped to those tested in Figure 6.3) showed that the neonatal Na_v1.1 isoform have more high frequency activity during the epileptic barrage compared to the adult isoform (5A n=841; 5N n=2165; **p=0.009 Mann Whitney U test). **E.** Rising slope frequency distribution underline the differences between the splicing variants (5A n=4211; 5N n=7620; *** p<0.001 Mann Whitney U test).

Labelled interneurons in GAD-67-GFP mouse cultures cannot be distinguished in terms of different interneuronal types, therefore cells patched potentially include both fast and slow-spiking interneurons. Concurrent comparison between all three parameters analyzed before (number of events, max frequency, and maximal rising slope) showed two distinct clusters of neuronal response to the same epileptic activity for both neonatal and adult-driven interneurons (Figure 7.4A). This distribution is likely due to the presence of a small number of fast spiking interneurons in the cultures and is consistent with a cluster of cells that innately fire more rapidly than other cells (i.e. most likely parvalbumin-positive interneurons; Figure 7.4B, in white circles). Exclusion of this cell group from analysis for both splice isoforms allowed a normalized distribution of event data (Figure 7.4C) and also now revealed a highly significant difference in event number, with neonatal-driven interneurons firing more APs under epileptic activity conditions than adults (Figure 7.4D, $P = 0.007$, unpaired two-tailed Student's t-test). Removal of the putative fast spiking neurons also expanded the difference between isoforms in inter-spike frequency and rising slope frequency distribution ($P < 0.001$ Mann-Whitney test, Figure 7.4 E,F).

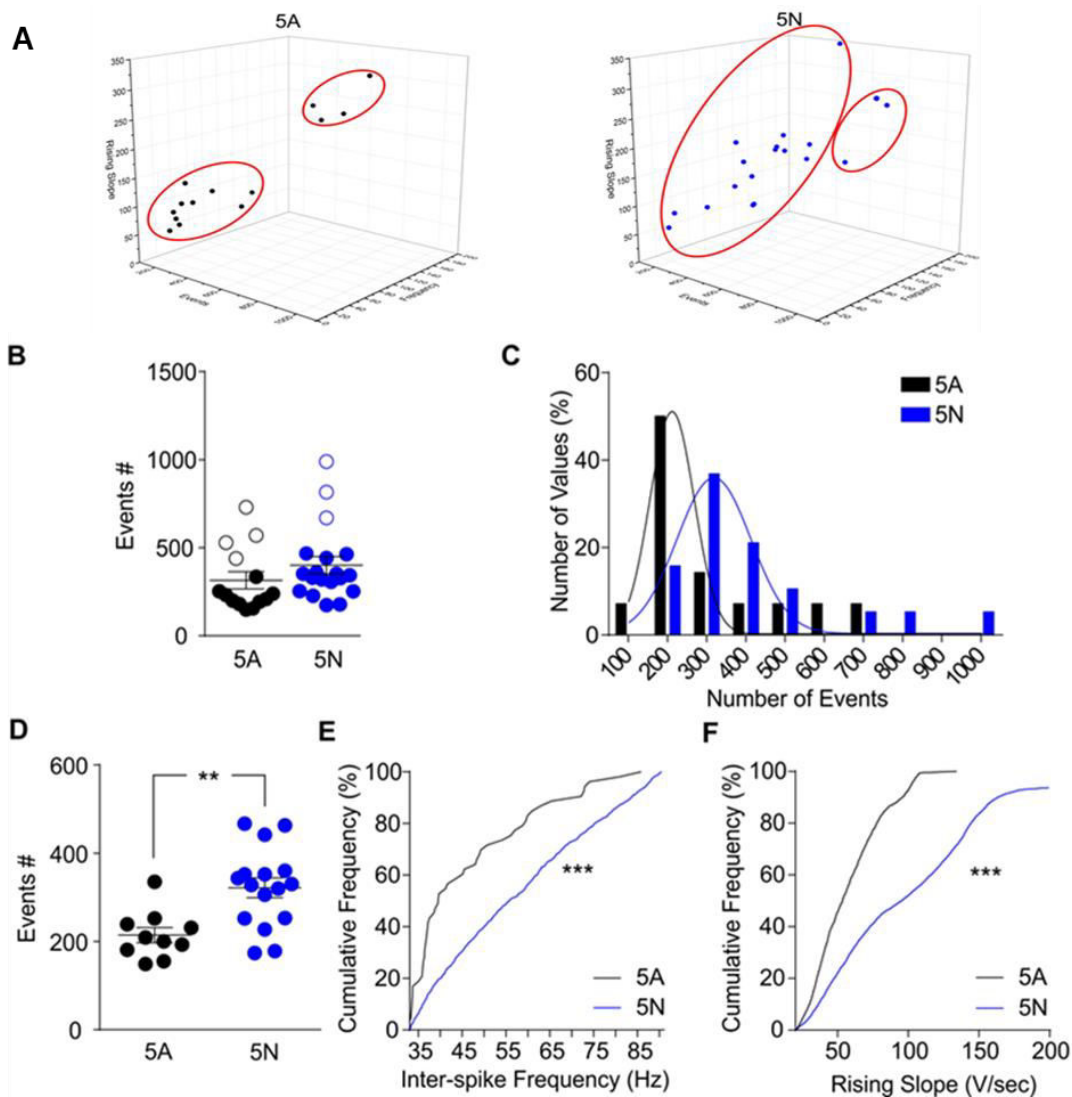


Figure 7.4: Dynamic clamp experiments in inhibitory neurons showed two clusters of neuronal response to the same epileptic activity

A. Clusters predicted by K-Means clustering for cells expressing 5A (left) and 5N (right) based on the same three parameters (number of events, max frequency, and maximal rising slope). For cells expressing 5N only frequency and events were significantly different for the two clusters, but for 5A all three parameters distinguished between the clusters. **B.** The number of events for all cells (as in Figure 7.3C), showing the cells clustering as ‘fast-spiking’ as open circles and removed from further analysis in D-E of this figure. **C.** A histogram of binned number of events shows the different distributions for 5N and 5A. **D.** Number of events with fast spiking cluster removed (5N 334.4 ± 30.16 , $n = 16$; 5A 214.4 ± 17.14 , $n = 10$; $**p = 0.007$, unpaired two-tailed Student’s T test) Lines indicate mean \pm s.e.m. **E.** Inter-spike frequency between 33 and 90.9 Hz with fast spiking neurons removed (5A $n=53$; 5N $n=829$; $***p<0.001$ Mann-Whitney test). **F.** Rising slope frequency distribution with fast spiking neurons removed (5A $n= 1943$; 5N $n=5147$; $***p<0.001$ Mann-Whitney test).

Splicing in Na_v1.1 is thus sufficient to alter how interneurons fire during epileptiform bursts, in particular allowing more cells to support bursts of higher frequency (>50 Hz) activity in response to simulated epileptic synaptic barrages. Also, the fact that Na_v1.1-5N-driven APs showed on average a higher rising slope is indicative of increased availability of this channel isoform at higher stimulations (Scott *et al.*, 2014) and is again in agreement to what was seen in current-clamp recordings for interneurons at Chapter 6.

7.4.2 Na_v1.1-5N channels also support higher availability during epileptic conditions in excitatory neurons

To test whether the effect of the neonatal isoform to confer higher firing ability under epileptic conditions was confined to interneurons only, dynamic clamp recordings were also performed in excitatory (GFP negative) neurons transfected either with Na_v1.1-5A or 5N (Figure 7.5A & B). Analysis revealed that there was no real difference in terms of how many neurons attained rapid bursts of > 50 Hz (5A: 6/7 vs 5N: 5/8; P = 0.569, Fisher's exact test, two-tails), AP events (Figure 7.5C, P>0.05, unpaired two-tailed Student's t-test) as well as in firing frequency (Figure 7.5D, P>0.05, Mann-Whitney U test) between isoforms in excitatory neurons. However, neonatal channels still elicited APs that had on average higher rising slopes (Figure 7.5E, P=0.004 Mann-Whitney U test), similar to what was seen before for the two isoforms in interneurons, and in current clamp recordings (Chapter 6). Therefore, it appears that the availability of the neonatal isoform is higher than the adult isoform during epileptic conditions, irrespective of the neuronal type in which it is expressed. Moreover, similar to what was seen in current-clamp firing reliability recordings in Chapter 6, it is only in interneurons where this difference in Na_v1.1 availability is translated into significant differences in neuronal firing rates.

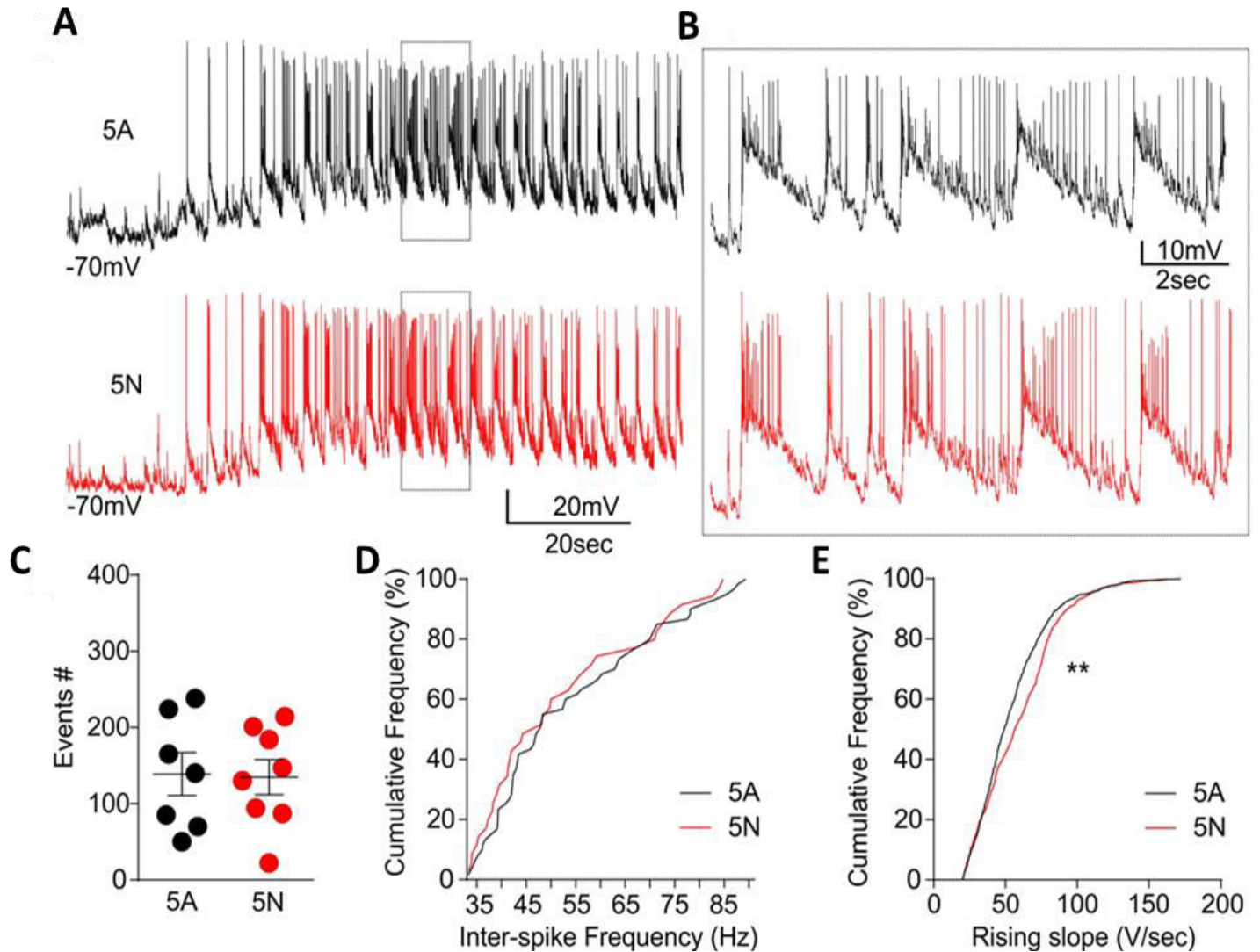


Figure 7.5: Dynamic clamp experiments in excitatory neurons demonstrate that splicing in $Na_v1.1$ is sufficient to alter only rising slope during epileptic activity

A. Representative voltage traces of the $Na_v1.1$ isoforms resulting from dynamic current injection of the epileptiform conductance trace template. **B.** Zoomed representative traces of $Na_v1.1$ isoforms from the dotted box in **A**. **C.** Total number of APs recorded during dynamic current injection showed no significant differences between $Na_v1.1$ splicing isoforms. Lines indicate mean \pm s.e.m. (5A $n=7$; 5N $n=8$). **D.** Inter-spike frequency indicates similar firing frequencies were supported by 5A and 5N between 33 and 90.9 Hz (5A $n=60$; 5N $n=35$). **E.** Rising slope frequency distribution shows a significant difference between 5A and 5N (5A $n=1011$; 5N $n=2452$; $p=0.004$ Mann-Whitney test).

7.5 Discussion and summary of the results

Dynamic clamp data indicate that inclusion of the neonatal exon is able to increase the number of high frequency bursts fired by interneurons in response to epileptiform synaptic inputs. Neonatal Na_v1.1 channels more reliably supported bursts of higher frequency (>50 Hz) and can sustain high frequency stimulation during epileptiform events better than adult channels for frequencies between 33 Hz and 90 Hz. This is in line with current-clamp data for interneurons in Chapter 6, where, at the same frequency range, neonatal-Na_v1.1 transfected interneurons showed a significantly higher firing reliability compared to neurons transfected with their adult counterparts.

In terms of APs fired during the epileptic trace, neonatal interneurons did fire a higher number with respect to adults, which reached significance when cluster analysis was used to discriminate between slow and fast-spiking interneurons. This raises the question whether the two channel isoforms have a different effect depending on which interneuronal subtype expressing them. Dissection of different types of interneurons, by using for example Cre-parvalbumin or Cre-somatostatin mouse strains, to specify the effects of each sodium channel isoform on each particular kind of interneuron would have been the next step if more time was available in order to answer this question. However, even this approach would be limited by the late onset of parvalbumin and somatostatin promoter activation (i.e. the promoter of these genes is not generally active during culture timeframes). A different effect of splicing depending on the interneuronal cell type would not be surprising, since such a cell type-specific effect has already been shown between excitatory and inhibitory neurons both in current-clamp (Chapter 6) and dynamic-clamp recordings.

The slowing of the rising phase of the action potentials conveyed by the adult isoform strongly suggests that the reduced ability to fire rapidly is due to a steady reduction in availability of channels during longer trains, as also suggested by Scott *et al.* (2014). This is likely due to their sequestration in the fast inactivated states and these data are consistent with splicing having a relatively modest effect on neuronal behavior by imposing a small reduction in channel availability when the adult exon is included. They are also in line with current-clamp data in Chapter 6, where neonatal channels showed significantly slower decay in rising slope after repetitive firing compared to adults in interneurons and this effect was also conserved in excitatory neurons,

despite the fact that this was not translated into a change in firing reliability for these cells. The same difference in maximal rising slope between neonatal and adult channels in excitatory neurons was also seen in dynamic-clamp recordings here, yet again this was not extended to differences in the epileptiform activity supported by the two isoforms in excitatory neurons. Therefore, comparison of activity in excitatory and inhibitory neurons in both current-clamp and dynamic-clamp recordings indicates that the functional difference between the two $\text{Na}_v1.1$ isoforms is most clear in interneurons. It also suggests that the biophysics of $\text{Na}_v1.1$ isoforms are particularly optimised for specifically modulating interneuronal activity. Finally, this change in interneuronal firing may be linked to the genetic association seen between variants that alter splicing of this exon and different types of epilepsy (Le Gal *et al.*, 2011; Kasperaviciute *et al.*, 2013; Kumari *et al.*, 2013, Tang *et al.*, 2014).

All together, these results reinforce the previous data on the increase AP reliability in interneurons expressing the 5N splicing isoform respect to the 5A isoform, but also draw the attention to the possible therapeutic implication of $\text{Na}_v1.1$ 5N as a means of decreasing epileptic seizures by increasing firing reliability in the inhibitory neurons.

Overview

This study has used four complementary approaches (voltage-clamp, current-clamp, dynamic-clamp and modelling) to study the biophysical and functional properties of neonatal and adult sodium channel isoforms in HEK293T cells and cultured neurons. It has shown that alternative splicing has a conserved functional effect in channel availability on three different genes within the sodium channel family (*SCN1A*, *SCN2A* and *SCN9A*). Because the study has deliberately compared channels with distinct distributions and roles, these results indicate a role for the neonatal exon that has been conserved while the genes have diverged. The data also reveal how the neonatal isoform of Na_v1.1 supports higher firing fidelity and more rapid firing during epileptiform events in interneurons and may also be subjected to selective pressure for removal among mammals. Apart from the conserved nature of the effects reported on channel availability, it cannot be ruled out that other roles for this splicing may exist, in regulating interactions with other proteins or in contributing to distinct functions in different neuronal populations, or to different roles during development of the nervous system.

As discussed in section 4.3, splicing at this site is associated with altered clinical outcomes. In animal models, and cells the function has also been explored by other groups. In the case of Na_v1.2, development of seizures is associated with a gain-of-function, and may be due to a developmental change in excitatory neurons (Gazina *et al.*, 2014; Liao *et al.*, 2010). In Na_v1.7, a similar strategy of expressing TTX-resistant variants was used to demonstrate that splicing in Na_v1.7 on its own did not change the excitability of DRG neurons, however the study was focused on the impact of a mutation on the variants and did not explore the impact of splicing on channel availability (Choi *et al.*, 2010). In *SCN1A* the lack of exon 5N in rodents has reduced the ability to model this behavior in neurons. However, since more rapid firing of interneurons at higher frequencies may better mitigate pyramidal cell discharges during potential epileptic events, expression of the neonatal exon in Na_v1.1, as in Na_v1.2 (Gazina *et al.*, 2014), may be protective against seizure activity, albeit by a distinct mechanism. The loss of exon 5N from *SCN1A* suggests that although the neonatal exon may be associated with reduced seizures, this is not supporting a drive to keep this exon, instead the evidence from published genomes indicates this exon is having an unknown negative effect on survival, leading to its loss in many mammalian genomes.

In conclusion, data here provide a roadmap for investigating how alternative splicing may produce conserved effects in different genes, and in different cell backgrounds. In particular, we show that in spite of divergence in gene function, a conserved splicing event in VGSCs can have similar functional and pharmacological consequences on different channels. Finally, results in neuronal cultures highlight the effect that splicing can have in neuronal behavior both under physiological and pathophysiological conditions and reveal a previously unknown potential mechanistic link between this splicing event in *SCN1A* and epilepsy. Future work to identify the biological importance and potential therapeutic value of manipulating alternative splicing in sodium channels will likely involve regulated genetic modifications in rodent models, an approach already being pursued by Gazina *et al.*, (2014). These tests will allow *in vivo* identification of roles played by these channel splice variants in diseased and healthy behavior.

Reference list

Abe T, Seo T, Ishitsu T, Nakagawa T, Hori M & Nakagawa K (2008). Association between *SCN1A* polymorphism and carbamazepine-resistant epilepsy. *Br J Clin Pharmacol* **66**, 204 – 307.

Agnew WS, Moore AC, Levinson SR & Raftery MA (1980). Identification of a large molecular weight peptide associated with a tetrodotoxin binding proteins from the electroplax of *Electrophorus electricus*. *Biochem. Biophys. Res. Commun.* **92**, 860 – 866.

Ahern CA, Eastwood AL, Dougherty DA & Horn R. (2008). Electrostatic contributions of aromatic residues in the local anesthetic receptor of voltage-gated sodium channels. *Circ Res.* **102**(1), 86 – 94.

Ahmad S, Dahllund L, Eriksson AB, Hellgren D, Karlsson U, Lund PE, *et al.* (2007). A stop codon mutation in *SCN9A* causes lack of pain sensation. *Hum Mol Genet* **16**, 2114 – 21.

Ahn HS, Dib-Hajj SD, Cox JJ *et al.* (2010). A new Na_v1.7 sodium channel mutation I234T in a child with severe pain. *European Journal of Pain* **14**(9), 944 – 950.

Armstrong CM & Bezanilla F (1974). Charge movement associated with the opening and closing of the activation gates of the Na channels. *J. Gen. Physiol.* **63**, 533 – 552.

Armstrong CM (1981). Sodium channels and gating currents. *Physiol. Rev.* **61**, 644 – 682.

Aurlien D, Leren TP, Tauboll E & Gjerstad L (2009). New *SCN5A* mutation in a SUDEP victim with idiopathic epilepsy. *Seizure* **18**, 158 – 60.

Aynacioglu AS, Brockmoller J, Bauer S, Sachse C, Guzelbey P, Ongen Z, *et al.* (1999). Frequency of cytochrome P450 CYP2C9 variants in a Turkish population and functional relevance for phenytoin. *Br J Clin Pharmacol* **48**, 409 – 415.

Baasch AL, Hüning I, Gilissen C, Klepper J, Veltman JA, Gillessen-Kaesbach G, *et al.* (2014). Exome sequencing identifies a de novo *SCN2A* mutation in a patient with intractable seizures, severe intellectual disability, optic atrophy, muscular hypotonia, and brain abnormalities. *Epilepsia* **55**, e25 – 29.

Barela AJ, Waddy SP, Lickfett JG, Hunter J, Anido A, Helmers SL, Goldin AL & Escayg A (2006). An epilepsy mutation in the sodium channel *SCN1A* that decreases channel excitability. *J. Neurosci.* **26**, 2714 – 2723.

Baum L, Haerian BS, Ng HK, Wong VC, Ng PW, Lui CH, Sin NC, Zhang C, Tomlinson B, Wong GW, Tan HJ, Raymond AA, Mohamed Z & Kwan P (2014). Case-control association study of polymorphisms in the voltage-gated sodium channel genes *SCN1A*, *SCN2A*, *SCN3A*, *SCN1B*, and *SCN2B* and epilepsy. *Hum Genet.* **133**, 651 – 9.

Bean BP (2007). The action potential in mammalian central neurons. *Nature reviews Neuroscience* **7**, 451 – 465.

Bechi G, Scalmani P, Schiavon E, Rusconi R, Franceschetti S & Mantegazza M. (2012). Pure haploinsufficiency for Dravet syndrome Na(V)1.1 (*SCN1A*) sodium channel truncating mutations. *Epilepsia.* **53**, 87 – 187.

Beckh S, Noda M, Lubbert H & Numa S (1989). Differential regulation of three sodium channel messenger RNAs in the rat central nervous system during development. *EMBO J* **8**, 3611 – 3616.

Bell TJ, Thaler C, Castiglioni AJ, Helton TD & Lipscombe D (2004) Cell-specific alternative splicing increases calcium channel current density in the pain pathway. *Neuron* **41**, 127 – 138

Bender RA, Brewster A, Santoro B, Ludwig A, Hofmann F, Biel M & Baram TZ (2001). Differential and age-dependent expression of hyperpolarization-activated, cyclic nucleotide-gated cation channel isoforms 1–4 suggests evolving roles in the developing rat hippocampus. *Neuroscienc.* **106**, 689 – 698.

Beneski DA & Catterall WA (1980). Covalent labeling of protein components of the sodium channel with a photoactivable derivative of scorpion toxin. *Proc. Natl. Acad. Sci. USA* **77**, 639 – 643.

Bennett PB, Valenzuela C, Chen LQ & Kallen RG (1995). On the molecular nature of the lidocaine receptor of cardiac Na channels: modification of block by alterations in the α subunit III – IV interdomain. *Circ. Res.* **77**, 584 – 592.

Berkovic SF, Heron SE, Giordano L, *et al.* (2004). Benign familial neonatal-infantile seizures: characterization of a new sodium channelopathy. *Ann Neurol* **55**, 550 – 57.

Black JA, Frezel N, Dib-Hajj SD & Waxman SG (2012). Expression of Nav1.7 in neurons extends from peripheral terminals in the skin to central preterminal branches and terminals in the dorsal horn. *Mol Pain.* **8:82**, 1 – 11.

Black JA, Liu S & Waxman SG (2009). Sodium channel activity modulates multiple functions in microglia. *Glia* **57**, 1072 – 81.

Blumenfeld H, Lampert A, Klein JP, Mission J, Chen MC, Rivera M, Dib-Hajj S, Brennan AR, Hains BC & Waxman SG (2009). Role of hippocampal sodium channel Nav1.6 in kindling epileptogenesis. *Epilepsia* **50**, 44 – 55.

Bosmans F, Martin-Eauclaire MF & Swartz KJ (2008). Deconstructing voltage sensor function and pharmacology in sodium channels. *Nature* **456**, 202 – 8.

Brackenbury WJ & Isom LL (2011). Na channel beta subunits: overachievers of the ion channel family. *Front Pharmacol* **2**, 53.

Brewster AL, Bender RA, Chen Y, Dube C, Eghbal-Ahmadi M & Baram TZ (2002). Developmental febrile seizures modulate hippocampal gene expression of hyperpolarization-activated channels in an isoform- and cell-specific manner. *J. Neurosci.* **22**, 4591 – 4599.

Brüss M, Molderings GJ, Bönisch H & Göthert M (1999). Pharmacological differences and similarities between the native mouse 5-HT₃ receptor in N1E-115 cells and a cloned short splice variant of the mouse 5-HT₃ receptor expressed in HEK 293 cells. *Naunyn Schmiedebergs Arch Pharmacol* **360**(3), 225 – 33.

Buchner DA, Trudeau M, Meisler MH (2003). SCN1M1, a Putative RNA Splicing Factor That Modifies Disease Severity in Mice. *Science* **301**, 967 – 969.

Buzatu S (2009). The temperature-induced changes in membrane potential. *Riv Biol* **102**, 199 – 207

Caldwell JH, Schaller KL, Lasher RS, Peles E & Levinson SR (2000). Sodium channel Na_v1.6 is localized at nodes of Ranvier, dendrites, and synapses. *Proc Natl Acad Sci U S A* **97**, 5616 – 5620.

Capes DL, Goldschen-Ohm MP, Arcisio-Miranda M, Bezanilla F & Chanda B (2013). Domain IV voltage-sensor movement is both sufficient and rate limiting for fast inactivation in sodium channels. *J. Gen. Physiol.* **142**, 101 – 112.

Carbone A, Fioretti FM, Fucci L, Ausio J & Piscopo M (2012). High efficiency method to obtain supercoiled DNA with a commercial plasmid purification kit. *Acta biochimica Polonica* **59**, 275 – 278.

Carter BC, Giessel AJ, Sabatini BL & Bean, BP (2012). Transient sodium current at subthreshold voltages: activation by EPSP waveforms. *Neuron* **75**, 1081 – 1093.

Carvill GL, Heavin SB, Yendle SC, McMahon JM, O’Roak BJ, Cook J *et al.* (2013). Targeted resequencing in epileptic encephalopathies identifies de novo mutations in CHD2 and SYNGAP1. *Nature Genetics* **45**(7), 10.

Catterall WA (2000). From ionic currents to molecular mechanisms: the structure and function of voltage-gated sodium channels. *Neuron* **26**, 13 – 25.

Catterall WA (2014). Sodium channels, inherited epilepsy and antiepileptic drugs. *Annu Rev Pharmacol Toxicol* **54**, 317 – 38.

Catterall WA, Goldin AL & Waxman SG (2005). Nomenclature and structure-function relationships of voltage-gated sodium channels. *Pharmacol Rev* **57**, 397 – 409.

Catterall WA, Goldin AL & Waxman SG (2005). Nomenclature and structure-function relationships of voltage-gated sodium channels. *Pharmacol Rev* **57**, 397 – 409.

Catterall WA, Kalume F, & Oakley JC (2010). Na_v1.1 channels and epilepsy. *J. Physiol. (Lond.)* **588**, 1849 – 1859.

Cestele S, Scalmani P, Rusconi R, Terragni B, Franceschetti S & Mantegazza M (2008). Self-limited hyperexcitability: functional effect of a familial hemiplegic migraine mutation of the Na_v1.1 (*SCN1A*) Na⁺ channel. *J Neurosci* **28**, 7273 – 83.

Cestele S, Schiavon E, Rusconi R, Franceschetti S & Mantegazza M. (2013). Nonfunctional Na_v1.1 familial hemiplegic migraine mutant transformed into gain of function by partial rescue of folding defects. *Proc Natl Acad Sci USA*. **110**, 17546 – 17551.

Chanda B & Bezanilla F (2002). Tracking voltage-dependent conformational changes in skeletal muscle sodium channel during activation. *J. Gen. Physiol.* **120**, 629 – 645.

Chatelier A, Dahllund L, Eriksson A, Krupp J & Chahine M. (2008) Biophysical properties of human Na_v1.7 splice variants and their regulation by protein kinase A. *J Neurophysiol* **99**, 2241 – 2250.

Chen C, Westenbroek RE, Xu X, Edwards CA, Sorenson DR, Chen Y, McEwen DP, O'Malley HA, Bharucha V, Meadows LS, Knudsen GA, Vilaythong A, Noebels JL, Saunders TL, Scheuer T, Shrager P, Catterall WA & Isom LL (2004). Mice lacking sodium channel beta1 subunits display defects in neuronal excitability, sodium channel expression, and nodal architecture. *J. Neurosci.* **24**, 4030 – 4042.

Chen K, Aradi I, Thon N, Eghbal-Ahmadi M, Baram TZ & Soltesz I (2001). Persistently modified h-channels after complex febrile seizures convert the seizure-induced enhancement of inhibition to hyperexcitability. *Nat Med.* **7**, 331 – 7.

Chen YH, Dale TJ, Romanos MA, Whitaker WR, Xie XM & Clare JJ (2000). Cloning, distribution and functional analysis of the type III sodium channel from human brain. *Eur J Neurosci* **12**, 4281 – 89.

Chioni AM, Fraser SP, Pani F, Foran P, Wilkin GP, Diss JK, *et al.* (2005). A novel polyclonal antibody specific for the Na_v1.5 voltage-gated Na(+) channel 'neonatal' splice form. *J Neurosci Methods* **147**, 88 – 98.

Choi JS, Cheng X, Foster E, Leffler A, Tyrrell L, Te Morsche RH, Eastman EM, Jansen HJ, Huehne K, Nau C, *et al.* (2010). Alternative splicing may contribute to time-dependent manifestation of inherited erythromelalgia. *Brain* **133**, 1823 – 1835.

Copley RR (2004). Evolutionary convergence of alternative splicing in ion Channels. *Trends in Genetics* **20**

Cossette P, Loukas A, Lafreniere RG, Rochefort D, Harvey-Girard E, Ragsdale DS, *et al.* (2003). Functional characterization of the D188V mutation in neuronal voltage-gated sodium channel causing generalized epilepsy with febrile seizures plus (GEFS). *Epilepsy Res* **53**, 107 – 17.

Cox JJ, Reimann F, Nicholas AK, Thornton G, Roberts E, Springell K, *et al.* (2006). An *SCN9A* channelopathy causes congenital inability to experience pain. *Nature* **444**, 894 – 8.

Cummins TR, Sheets PL & Waxman SG (2007). The roles of sodium channels in nociception: implications for mechanisms of pain. *Pain* **131**, 243 – 57.

Dar Malhotra J, Chen C, Rivolta I, Abriel H, Malhotra R, Mattei LN, Brosius FC, Kass RS & Isom LL (2001). Characterization of sodium channel alpha and beta1 subunits in rat and mouse cardiac myocytes. *Circulation* **103**, 1303 – 1310.

Darbar D, Kannankeril PJ, Donahue BS, Kucera G, Stubblefield T, Haines JL, George A Jr. & Roden DM (2008). Cardiac sodium channel (*SCN5A*) variants associated with atrial fibrillation. *Circulation* **117**, 1927 – 1935.

Davis MD & Sandoroni P (2002). Lidocaine patch for pain of erythromelalgia. *Archives of Dermatology* **138**(1), 17 – 19.

De Jonghe P (2011). Molecular genetics of Dravet syndrome. *Dev Med Child Neurol* **53**, (Suppl 2) 7 – 10.

Depienne C, Bouteiller D, Keren B, Cheuret E, Poirier K, Trouillard O, Benyahia B, Quelin C, Carpentier W, Julia S, Afenjar A, Gautier A, Rivier F, Meyer S, Berquin P, Helias M, Py I, Rivera S, Bahi-Buisson N, Gourfinkel-An I, Cazeneuve C, Ruberg M, Brice A, Nabbout R & Leguern E. (2009). Sporadic infantile epileptic encephalopathy caused by mutations in *PCDH19* resembles Dravet syndrome but mainly affects females. *PLoS Genet.* **5**, e1000381.

Depienne C, Trouillard O, Gourfinkel-An I, Saint-Martin C, Bouteiller D, *et al.* (2010). Mechanisms for variable expressivity of inherited *SCN1A* mutations causing dravet syndrome. *J Med Genet.* **47**, 404 – 410.

Deshpande LS, Lou JK, Mian A, Blair RE, Sombati S & DeLorenzo RJ (2007). In vitro status epilepticus but not spontaneous recurrent seizures cause cell death in cultured hippocampal neurons. *Epilepsy Research* **75(2-3)**, 171 – 179.

Dib-Hajj SD, Binshtok AM, Cummins TR, Jarvis MF, Samad T & Zimmermann K (2009). Voltage-gated sodium channels in pain states: role in pathophysiology and targets for treatment. *Brain Res Rev* **60**, 65 – 83.

Dib-Hajj SD, Estacion M, Jarecki BW *et al.* (2008). Paroxysmal extreme pain disorder M1627K mutation in human Na_v 1.7 renders DRG neurons hyperexcitable. *Molecular Pain* **4(37)**.

Dib-Hajj SD, Rush AM, Cummins TR *et al.* (2005). Gain-of-function mutation in Na_v1.7 in familial erythromelalgia induces bursting of sensory neurons. *Brain* **128(8)**, 1847 – 1854.

Dib-Hajj SD, Yang Y, Black JA & Waxman SG (2013). The Na_v(ν)1.7 sodium channel: from molecule to man. *Nat. Rev. Neurosci.* **14**, 49 – 62.

Doty CN. (2010). *SCN9A*: another sodium channel excited to play a role in human epilepsies. *Clin Genet.* **77**, 326 – 8.

Doyle DA, Cabral JM, Pfuetzner RA, Kuo AL, Gulbis JM, Cohen SL, Chait BT & MacKinnon R (1998). The structure of the potassium channel: molecular basis of K conduction and selectivity. *Science* **280**, 69 – 77.

Dravet C, Bureau M, Guerrini R, Giraud N & Roger J (1992). Severe myoclonic epilepsy in infants. In *Epileptic Syndromes in Infancy, Childhood and Adolescence*, 2nd edn, ed. Roger J, Dravet C, Bureau M, Dreifus FE, Perret A & Wolf P, 75 – 102. John Libbey, London.

Dravet C, Bureau M, Oguni H, Fukuyama Y & Cokar O (2005). Severe myoclonic epilepsy in infancy: Dravet syndrome. *Adv. Neurol.* **95**, 71 – 102.

Dreifuss FE (1984). Treatment of the nonconvulsive epilepsies. *Epilepsia* **24**, (Suppl 1): S45 – 54.

Drenth JPH & Waxman SG (2007). Mutations in sodium-channel gene *SCN9A* cause a spectrum of human genetic pain disorders. *J Clin Invest* **117**(12), 3603 – 3609.

Drizin I, Gregg RJ, Scanio MJ, Shi L, Gross MF, Atkinson RN, *et al.* (2008). Discovery of potent furan piperazine sodium channel blockers for treatment of neuropathic pain. *Bioorg Med Chem* **16**, 6379 – 86.

Eijkelkamp N, Linley JE, Baker MD, Minett MS, Cregg R, Werdehausen R, Rugiero F & Wood JN (2012). Neurological perspectives on voltage-gated sodium channels *Brain* **135**, 2585 – 2612

Engel J Jr (2001). A proposed diagnostic scheme for people with epileptic seizures and with epilepsy: report of the ILAE Task Force on Classification and Terminology. *Epilepsia* **42**, 796 – 803.

Estacion M, Gasser A, Dib-Hajj SD & Waxman SG (2010). A sodium channel mutation linked to epilepsy increases ramp and persistent current of Na_v1.3 and induces hyperexcitability in hippocampal neurons. *Exp Neurol* **224**, 362 – 8.

Facer P, Phil M, Punjabi PP, Abrari A, Kaba RA, Severs NJ, Chambers J, Kooner JS & Anand P (2011). Localisation of *SCN10A* gene product Na_v 1.8 and novel pain-related ion channels in human heart. *Int. Heart J.* **52**, 146 – 152.

Farmer C, Cox JJ, Fletcher EV, Woods CG, Wood JN & Schorge S (2012). Splice variants of Na(V)1.7 sodium channels have distinct beta subunit-dependent biophysical properties. *PLoS One* **7**, e41750.

Feldman DH & Lossin C (2014). The Na_v channel bench series: Plasmid preparation, *MethodsX* **1**, 6-11

Fertleman CR, Baker MD, Parker KA, Moffatt S, Elmslie FV, Abrahamsen B, *et al.* (2006). *SCN9A* mutations in paroxysmal extreme pain disorder: allelic variants underlie distinct channel defects and phenotypes. *Neuron* **52**, 767 – 74.

Fertleman CR, Ferrie CD, Aicardi J, *et al.* (2007). Paroxysmal extreme pain disorder (previously familial rectal pain syndrome). *Neurology* **69(6)**, 586 – 595.

Fletcher EV, Kullmann DM & Schorge S (2011). Alternative splicing modulates inactivation of type 1 voltage-gated sodium channels by toggling an amino acid in the first S3-S4 linker. *J Biol Chem* **286**, 36700 – 8.

Furman RE, Tanaka JC, Mueller P & Barchi RL (1986). Voltage-dependent activation in purified reconstituted sodium channels from rabbit T-tubular membranes. *Proc. Natl. Acad. Sci. USA* **83**, 488 – 492.

Fisher RS, van Emde Boas W, Blume W, *et al.* (2005). Epileptic seizures and epilepsy: definitions proposed by the International League Against Epilepsy (ILAE) and the International Bureau for Epilepsy (IBE). *Epilepsia*. **46**, 470 – 472.

Fisher R, Acevedo C, Arzimanoglou A, Bogacz A, Cross J, Elger C, *et al.* (2014). ILAE official report: a practical clinical definition of epilepsy. *Epilepsia*. **55**, 475 – 82.

Fozzard HA, Sheets MF & Hanck D (2011). The sodium channel as a target for local anesthetic drugs. *Frontiers in Pharmacology* **2**, 1 – 6.

Gastaldi M, Bartolomei F, Massacrier A, Planells R, Robaglia-Schlupp A & Cau P (1997). Increase in mRNAs encoding neonatal II and III sodium channel alpha-isoforms during kainate-induced seizures in adult rat hippocampus. *Brain Res Mol Brain Res* **44**, 179 – 190.

Gazina EV, Leaw BTW, Richards KL, Wimmer VC, Kim TH, Aumann TD, Featherby TJ, Churilov L, Hammond VE, Reid CA, et al. (2014). “Neonatal” Na_v1.2 reduces neuronal excitability and affects seizure susceptibility and behaviour. *Hum. Mol. Genet.* **24(5)**, 1457 – 68.

Gazina EV, Richards KL, Mokhtar MB, Thomas EA, Reid CA & Petrou S (2010). Differential expression of exon 5 splice variants of sodium channel α subunit mRNAs in the developing mouse brain. *Neuroscience* **166**, 195 – 200.

George AL Jr. (2005). Inherited disorders of voltage-gated sodium channels. *J. Clin. Invest.* **115**, 1990 – 1999.

Gerstein MB, Rozowsky J, Yan K-K, Wang D, Cheng C, Brown JB, Davis CA, Hillier L, Sisu C, Li JJ, et al. (2014). Comparative analysis of the transcriptome across distant species. *Nature* **512**, 445 – 448.

Goldberg YP, Macfarlane J, Macdonald ML et al. (2007). Loss-of-function mutations in the Na_v1.7 gene underlie congenital indifference to pain in multiple human populations. *Clinical Genetics* **71(4)**, 311 – 319.

Goldin AL (2001). Resurgence of sodium channel research. *Annu. Rev. Physiol.* **63**, 871 – 894.

Goldin AL (2003). Mechanisms of sodium channel inactivation. *Curr. Opin. Neurobiol.* **13**, 284 – 290.

Goldin AL, Barchi RL, Caldwell JH, Hofmann F, Howe JR, Hunter JC, Kallen RG, Mandel G, Meisler MH, Netter YB, Noda M, Tamkun MM, Waxman SG, Wood JN & Catterall WA (2000). Nomenclature of voltage-gated sodium channels. *Neuron* **28**, 365 – 368.

Gonzalez-Sulser A, Wang J, Queenan BN, Avoli M, Vicini S & Dzakpasu R (2012). Hippocampal neuron firing and local field potentials in the in vitro 4-aminopyridine epilepsy model. *Journal of Neurophysiology*, **108**(9), 2568 – 2580.

Gordon D, Merrick D, Auld V, Dunn R, Goldin AL, Davidson N & Catterall WA (1987). Tissue-specific expression of the RI and RII sodium channel subtypes. *Proc Natl Acad Sci U S A* **84**, 8682 – 8686.

Gustafson TA, Clevinger EC, O'Neill TJ, Yarowsky PJ & Krueger BK (1993). Mutually exclusive exon splicing of type III brain sodium channel alpha subunit RNA generates developmentally regulated isoforms in rat brain. *J Biol Chem* **268**, 18648 – 18653.

Guy HR & Seetharamulu P (1986). Molecular model of the action potential sodium channel. *Proc. Natl. Acad. Sci. U.S.A.* **83**, 508 – 512.

Guy HR & Seetharamulu P (1986). Molecular model of the action potential sodium channel. *Proc. Natl. Acad. Sci. USA* **508**, 508 – 512.

Haerian BS, Baum L, Kwan P, Tan HJ, Raymond AA & Mohamed Z. (2013). *SCN1A*, *SCN2A* and *SCN3A* gene polymorphisms and responsiveness to antiepileptic drugs: a multicenter cohort study and meta-analysis. *Pharmacogenomics*. **14**, 1153 – 66.

Harkin LA, McMahon JM, Iona X, Dibbens L, Pelekanos JT, Zuberi SM, Sadleir LG, Andermann E, Gill D, Farrell K, Connolly M, Stanley T, Harbord M, Andermann F, Wang J, Batish SD, Jones JG, Seltzer WK & Gardner A (2007). The Infantile Epileptic Encephalopathy Referral Consortium,. In: Sutherland G, Berkovic SF, Mulley JC & Scheffer IE (Eds.), The spectrum of *SCN1A*-related infantile epileptic encephalopathies. *Brain* **130**, 843 – 852.

Harkin LA, McMahon JM, Iona X, *et al.* (2007). The spectrum of *SCN1A*-related infantile epileptic encephalopathies. *Brain* **130**, 843 – 52.

Hartmann HA, Colom LV, Sutherland ML & Noebels JL (1999). Selective localization of cardiac SCN5A sodium channels in limbic regions of rat brain. *Nat Neurosci*, **2**, 593 – 595.

Hartshorne RP & Catterall WA (1981). Purification of the saxi- toxin receptor of the sodium channel from rat brain. *Proc. Natl. Acad. Sci. USA* **78**, 4620 – 4624.

Hartshorne RP, Keller BU, Talvenheimo JA, Catterall WA & Montal M (1985). Functional reconstitution of the purified brain sodium channel in planar lipid bilayers. *Proc. Natl. Acad. Sci. USA* **82**, 240 – 244.

Heinemann SH, Terlau H & Imoto K (1992). Molecular basis for pharmacological differences between brain and cardiac sodium channels. *Pflugers Arch.* **422**, 90 – 92.

Heinemann SH, Terlau H, Stumer W, Imoto K & Numa S (1992). Calcium channel characteristics conferred on the sodium channel by single mutations, *Nature* **356**, 441 – 443.

Heinzen EL, Yoon W, Tate SK, Sen A, Wood NW, Sisodiya SM & Goldstein DB (2007). Nova2 interacts with a cis-acting polymorphism to influence the proportions of drug-responsive splice variants of *SCN1A*. *Am J Hum Genet* **80**, 876 – 883.

Hiyama TY, Watanabe E, Ono K, Inenaga K, Tamkun MM, Yoshida S & Noda M (2002). Nax channel involved in CNS sodium-level sensing. *Nat. Neurosci* **5**, 511 – 512.

Hodgkin AL, & Huxley AF (1952). A quantitative description of membrane current and its application to conduction and excitation in nerve. *J. Physiol.* **117**, 500 – 544.

Holland KD, Kearney JA, Glauser TA, Buck G, Keddache M, Blankston JR, *et al.* (2008). Mutation of sodium channel *SCN3A* in a patient with cryptogenic pediatric partial epilepsy. *Neurosci Lett* **433**, 65 – 70.

Hsueh CH, Chen WP, Lin JL, Tsai CT, Liu YB, Juang JM, *et al.* (2009). Distinct functional defect of three novel Brugada syndrome related cardiac sodium channel mutations. *J Biomed Sci* **16**, 23.
Hung CC, Lin CJ, Chen CC, Chang CJ & Liou HH (2004). Dosage recommendation of phenytoin for patients with epilepsy with different CYP2C9/CYP2C19 polymorphisms. *Ther Drug Monit* **26**, 534 – 540.

Ilyin VI, Hodges DD, Whittemore ER, Carter RB, Cai SX, & Woodward RM (2005). V102862 (Co 102862): a potent, broad-spectrum state-dependent blocker of mammalian voltage-gated sodium channels. *British Journal of Pharmacology* **144(6)**, 801 – 812.

Isom LL (2002). The role of sodium channels in cell adhesion. *Front Biosci* **7**, 12 – 23.
Isom LL, De Jongh KS & Catterall WA (1994). Auxiliary subunits of voltage-gated ion channels. *Neuron* **12**, 1183 – 1194.

Isom LL, De Jongh KS, Patton DE, Reber BF, Offord J, Charbonneau H, Walsh K, Goldin AL & Catterall WA (1992). Primary structure and functional expression of the β 1 subunit of the rat brain sodium channel. *Science* **256**, 839 – 842.

Isom LL, Scheuer T, Brownstein AB, Ragsdale DS, Murphy BJ & Catterall WA (1995). Functional co-expression of the β 1 and type IIA α subunits of sodium channels in a mammalian cell line. *J. Biol. Chem.* **270**, 3306 – 3312.

Isom LL, Scheuer T, Brownstein AB, Ragsdale DS, Murphy BJ & Catterall WA (1995). Functional co-expression of the β 1 and type IIA α subunits of sodium channels in a mammalian cell line. *J. Biol. Chem.* **270**, 3306 – 3312.

Jarecki BW, Sheets PL, Xiao Y, Jackson JO, 2nd & Cummins TR (2009) Alternative splicing of Na(V)1.7 exon 5 increases the impact of the painful PEPD mutant channel I1461T. *Channels (Austin)* **3**, 259 – 267.

Jarvis MF, Honore P, Shieh CC, Chapman M, Joshi S, Zhang XF, *et al.* (2007). A-803467, a potent and selective Na_v1.8 sodium channel blocker, attenuates neuropathic and inflammatory pain in the rat. *Proc Natl Acad Sci USA* **104**, 8520 – 5.

Jenkins SM & Bennett V (2001). Ankyrin-G coordinates assembly of the spectrin-based membrane skeleton, voltage-gated sodium channels, and L1 CAMs at Purkinje neuron initial segments. *J Cell Biol* **155**, 739 – 746.

Jurkat-Rott K, Holzherr B, Fauler M & Lehmann-Horn F (2010). Sodium channelopathies of skeletal muscle result from gain or loss of function. *Pflugers Arch Eur J Physiol* **460**, 239 – 48.

Kaech S & Banker G (2006). Culturing hippocampal neurons. *Nature Protocols* **1**, 2406 – 2415.

Kahlig KM, Rhodes TH, Pusch M, *et al.* (2008). Divergent sodium channel defects in familial hemiplegic migraine. *Proc Natl Acad Sci USA* **105**, 9799 – 804.

Kalsotra A & Cooper TA (2011). Functional consequences of developmentally regulated alternative splicing. *Nat. Rev. Genet.* **12**, 715 – 729.

Kalume F, Yu FH, Westenbroek RE, Scheuer T & Catterall WA (2007). Reduced sodium current in Purkinje neurons from Na_v1.1 mutant mice: implications for ataxia in severe myoclonic epilepsy in infancy. *J Neurosci* **27**, 11065 – 11074.

Kapplinger JD, Tester DJ, Alders M, Benito B, Berthet M, Brugada J, *et al.* (2010). An international compendium of mutations in the *SCN5A*-encoded cardiac sodium channel in patients referred for Brugada syndrome genetic testing. *Heart Rhythm* **7**, 33 – 46.

Karoly R, Lenkey N, Juhasz AO, Vizi ES, & Mike A (2010). Fast- or slow-inactivated state preference of Na⁺ channel inhibitors: a simulation and experimental study. *PLoS Comput. Biol.* **6**, e1000818.

Kasperaviciute D, Catarino CB, Matarin M, Leu C, Novy J, Tostevin A, Leal B, Hessel EVS, Hallmann K, Hildebrand MS, *et al.* (2013). Epilepsy, hippocampal sclerosis and febrile seizures linked by common genetic variation around *SCN1A*. *Brain J. Neurol.* **136**, 3140 – 3150.

Kearney, JA & Meisler MH (2009). Single gene mutations in inherited and sporadic epilepsy. In *Encyclopedia of Basic Epilepsy Research*. Elsevier/Academic Press, London.

Kuo CC & Bean BP (1994). Naq channels must deactivate to recover from inactivation. *Neuron* **12**, 819 – 829.

Kelemen O, Convertini P, Zhang Z, Wen Y, Shen M, Falaleeva M & Stamm S (2013) Function of alternative splicing. *Gene.* **514**, 1 – 30.

Kiss T (2008). Persistent Na-channels: origin and function. A review. *Acta Biol Hung* **59**, 1 – 12.

Kobow K, El-Osta A & Blümcke I (2013). The methylation hypothesis of pharmacoresistance in epilepsy. *Epilepsia* **54**, 41 – 47.

Kopelman NM, Lancet D & Yanai I (2005). Alternative splicing and gene duplication are inversely correlated evolutionary mechanisms. *Nat. Genet.* **37**, 588 – 589.

Kuhnert SM, Phillips WJ & Davis MDP (1999). Lidocaine and mexiletine therapy for erythromelalgia. *Archives of Dermatology* **135(12)**, 1447 – 1449.

Kullmann PH, Wheeler DW, Beacom J & Horn JP (2004). Implementation of a fast 16-Bit dynamic clamp using LabVIEW-RT. *J Neurophysiol* **91**, 542 – 554.

Kumari R, Lakhan R, Kumar S, Garg RK, Misra UK, Kalita J & Mittal B (2013). *SCN1A*IVS5-91G>A polymorphism is associated with susceptibility to epilepsy but not with drug responsiveness. *Biochimie* **95**, 1350 – 1353.

Kuo CC, Chen RS, Lu L & Chen RC (1997). Carbamazepine inhibition of neuronal Na^v currents: quantitative distinction from phenytoin and possible therapeutic implications. *Mol. Pharmacol.* **51**, 1077 – 1083.

Kuo JJ, Lee RH, Zhang L & Heckman CJ (2006). Essential role of the persistent sodium current in spike initiation during slowly rising inputs in mouse spinal neurones. *J Physiol* **574**, 819 – 834.

Kwan P & Brodie MJ (2000). Early identification of refractory epilepsy. *N Engl J Med* **342**, 314 – 319.

Kwan P, Poon WS, Ng HK, Kang DE, Wong V, Ng PW, Lui CH, Sin NC, Wong KS & Baum L (2008). Multidrug resistance in epilepsy and polymorphisms in the voltage-gated sodium channel genes *SCN1A*, *SCN2A*, and *SCN3A*: correlation among phenotype, genotype, and mRNA expression. *Pharmacogenet Genomics* **18**, 989 – 998.

Kyndt F, Probst V, Potet F, Demolombe S, Chevallier JC, Baro I, *et al.* (2001). Novel *SCN5A* mutation leading either to isolated cardiac conduction defect or Brugada syndrome in a large French family. *Circulation* **104**, 3081 – 6.

Lai J, Porreca F, Hunter JC & Gold MS (2004). Voltage-gated sodium channels and hyperalgesia. *Annu Rev Pharmacol Toxicol* **44**, 371 – 97.

Lakhan R, Kumari R, Misra UK, Kalita J, Pradhan S & Mittal B (2009). Differential role of sodium channels *SCN1A* and *SCN2A* gene polymorphisms with epilepsy and multiple drug resistance in the north Indian population *Br J Clin Pharmacol* **68**, 214 – 220.

Lampert A, Dib-Hajj SD, Tyrrell L & Waxman SG (2006). Size matters: erythromelalgia mutation S241T in Nav1.7 alters channel gating. *The Journal of Biological Chemistry* **281(47)**, 36029 – 36035.

Lamsa K, Irvine EI, Giese, KP & Kullmann D (2007). NMDA receptor-dependent long-term potentiation in mouse hippocampal interneurons shows a unique dependence on Ca(2+)/calmodulin-dependent kinases. *Journal of Physiology* **584**, 885 – 894

Lee MP, Sander M & Hsieh TS, (1989). Single strand DNA cleavage reaction of duplex DNA by *Drosophila* Topoisomerase II. *J Biol Chem* **264**, 1351 – 1358.

Le Gal F, Salzman A, Crespel A, & Malafosse A (2011). Replication of association between a *SCN1A* splice variant and febrile seizures. *Epilepsia* **52**, e135 – e138.

Legroux-Crespel E, Sassolas B, Guillet G, Kupfer I, Dupre D & Misery L (2003). Treatment of familial erythromelalgia with the association of lidocaine and mexiletine. *Annales de Dermatologie et de Vénéréologie* **130(4)**, 429 – 433.

Levin SI, Khaliq ZM, Aman TK, Grieco TM, Kearney JA, Raman IM & Meisler MH (2006). Impaired motor function and learning in mice with conditional knockout of the Na channel *SCN8A* (Nav 1.6) in cerebellar Purkinje neurons and granule cells. *J. Neurophysiol.* **96**, 785 – 793.

Li T, Tian C, Scalmani P, Frassoni C, Mantegazza M, Wang Y, *et al.* (2014). Action potential initiation in neocortical inhibitory interneurons. *PLoS. Biol* **12(9)**, e1001944.

Liao Y, Deprez L, Maljevic S, Pitsch J, Claes L, Hristova D, Jordanova A, Ala-Mello S, Bellan-Koch A, Blazevic D, Schubert S, Thomas EA, Petrou S, Becker AJ, De Jonghe P & Lerche H (2010). Molecular correlates of age- dependent seizures in an inherited neonatal-infantile epilepsy. *Brain* **133**, 1403 – 1414.

Liao YJ, Safa P, Chen YR, Sobel RA, Boyden ES & Tsien RW (2008). Anti-Ca²⁺ channel antibody attenuates Ca²⁺ currents and mimics cerebellar ataxia in vivo. *Proc Natl Acad Sci USA* **105**, 2705 – 10.

Liberles DA & Wayne ML (2002). Tracking adaptive evolutionary events in genomic sequences. *Genome Biology* **3(6)**, 1018.1 – 1018.4.

Lin WH, Gunay C, Marley R, Prinz AA & Baines RA (2012). Activity-Dependent Alternative Splicing Increases Persistent Sodium Current and Promotes Seizure. *The Journal of Neuroscience* **32**, 7267 – 7277.

Lin WH, He M & Baines RA (2015). Seizure suppression through manipulating splicing of a voltage-gated sodium channel. *Brain* **138(4)**, 891 – 901.

Lin WH, Wright DE, Muraro NI & Baines RA (2009). Alternative splicing in the voltage-gated sodium channel DmNa_v regulates activation, inactivation, and persistent current. *J Neurophysiol* **102**, 1994 – 2006.

Lopez-Santiago LF, Brackenbury WJ, Chen C & Isom LL (2011). Na channel Scn1b gene regulates dorsal root ganglion nociceptor excitability in vivo. *J. Biol. Chem.* **286**, 22913 – 22923.

Loscher W, Klotz U, Zimprich F & Schmidt D (2009). The clinical impact of pharmacogenetics on the treatment of epilepsy. *Epilepsia* **50**, 1 – 23.

Lossin C, Rhodes TH, Desai RR, Vanoye CG, Wang D, Carniciu S, Devinsky O & George AL (2003). Epilepsy-associated dysfunction in the voltage-gated neuronal sodium channel *SCN1A*. *J. Neurosci.* **23**, 11289 – 11295.

Lossin C, Rhodes TH, Desai RR, Vanoye CG, Wang D, Carniciu S, Devinsky O & George AL Jr (2003). Epilepsy-associated dysfunction in the voltage-gated neuronal sodium channel *SCN1A*. *J Neurosci* **23**, 11289 – 11295.

Lossin C, Wang DW, Rhodes TH, Vanoye CG & George AL Jr. (2002). Molecular basis of an inherited epilepsy. *Neuron* **34**, 877 – 884.

Lossin C, Wang DW, Rhodes TH, Vanoye CG & George AL Jr. (2002). Molecular basis of an inherited epilepsy. *Neuron* **34**, 877 – 884.

Magistretti J, Ragsdale DS & Alonso A (1999). High conductance, sustained single channel activity responsible for the low-threshold persistent Na⁺ current in entorhinal cortex neurons. *J Neurosci* **19**, 7334 – 41.

Maier SK, Westenbroek RE, Yamanushi TT, Dobrzynski H, Boyett MR, Catterall WA & Scheuer T (2003). An unexpected requirement for brain-type sodium channels for control of heart rate in the mouse sinoatrial node. *Proc Natl Acad Sci U S A* **100**, 3507 – 3512.

Mamiya K, Ieiri I, Shimamoto J, Yukawa E, Imai J, Ninomiya H, *et al.* (1998). The effects of genetic polymorphisms of CYP2C9 and CYP2C19 on phenytoin metabolism in Japanese adult patients with epilepsy: studies in stereoselective hydroxylation and population pharmacokinetics. *Epilepsia* **39**, 1317 – 1323.

Manna I, Gambardella A, Bianchi A, Striano P, Tozzi R, Aguglia U, Beccaria F, Benna P, Campostrini R, Canevini MP, Condino F, Durisotti C, Elia M, Giallonardo AT, Iudice A, Labate A, La Neve A, Michelucci R, Muscas GC, Paravidino R, Zaccara G, Zucca C, Zara F & Perucca E (2011). A functional polymorphism in the *SCN1A* gene does not influence antiepileptic drug responsiveness in Italian patients with focal epilepsy. *Epilepsia* **52**, e40 – e44.

Mantegazza M, Curia G, Biagini G, Ragsdale DS & Avoli M (2010). Voltage-gated sodium channels as therapeutic targets in epilepsy and other neurological disorders. *Lancet Neurol* **9**, 413 – 24.

Mantegazza M, Gambardella A, Rusconi R, Schiavon E, Annesi F, Cassulini RR, Labate A, Carrideo S, Chifari R, Canevini MP, Canger R, Francheschetti S, Annesi G, Wanke E & Quattrone A (2005). Identification of an Na_v1.1 sodium channel (*SCN1A*) loss-of-function mutation associated with familial simple febrile seizures. *Proc. Natl. Acad. Sci. U.S.A.* **102**, 18177 – 18182.

Mantegazza M, Yu FH, Catterall WA & Scheuer T. (2001). Role of the C-terminal domain in inactivation of brain and cardiac sodium channels. *Proc Natl Acad Sci USA* **98**, 15348 – 53.

Marban E, Yamagishi T & Tomaselli GF (1998). Structure and function of voltage-gated sodium channels. *Journal of Physiology* **508**, 647 – 657.

Martin MS, Dutt K, Papale LA, Dube CM, Dutton SB, de Haan G, Shankar A, Tufik S, Meisler MH, Baram TZ, Goldin AL & Escayg A (2010). Altered function of the *SCN1A* voltage-gated sodium channel leads to GABAergic interneuron abnormalities. *J Biol Chem* **285**, 9823 – 2834.

Martin MS, Tang B, Papale LA, Yu FH, Catterall WA & Escayg A (2007). The voltage-gated sodium channel *SCN8A* is a genetic modifier of severe myoclonic epilepsy of infancy. *Hum Mol Genet* **16**, 2892 – 2899.

Maucksch C, Alexander Bohla A, Hoffmann F, Schleef M, Aneja MK, Elfinger M, Hartl D & Rudolph C (2009). Transgene expression of transfected supercoiled plasmid DNA concatemers in mammalian cells. *J Gene Med* **11**, 444– 453

McClatchey AI, Van den Vergh P, Pericak-Vance MA, Raskind W, Verellen C, McKenna-Yasek D, Rao K, Haines JL, Bird T, Brown RH Jr., & Gusella JF (1992). Temperature-sensitive mutations in the III-IV cytoplasmic loop region of the skeletal muscle sodium channel gene in paramyotonia congenita. *Cell* **68**, 769 – 774.

McGowan E, Hoyt SB, Li X, Lyons KA & Abbadie C (2009). A peripherally acting Na_v1.7 sodium channel blocker reverses hyperalgesia and allodynia on rat models of inflammatory and neuropathic pain. *Anesth Analg* **109**, 951 – 8.

McLean MJ & Macdonald RL (1983). Multiple actions of phenytoin on mouse spinal cord neurons in cell culture. *J. Pharmacol. Exp. Ther.* **227**, 779 – 789.

McPhee JC, Ragsdale DS, Scheuer T & Catterall WA (1996). A role for intracellular loop IVS4—S5 of the Na channel α subunit in fast inactivation. *Biophysical Journal* **70**, 318a.

Meadows LS, Chen YH, Powell AJ, Clare JJ & Ragsdale DS (2002). Functional modulation of human brain Na_v 1.3 sodium channels, expressed in mammalian cells, by auxiliary β 1, β 2 and β 3 subunits. *Neuroscience* **114**, 745 – 753.

Meisler MH & Kearney JA (2005). Sodium channel mutations in epilepsy and other neurological disorders. *J Clin Invest* **115**, 2010 – 7.

Meisler MH & Kearney JA (2005). Sodium channel mutations in epilepsy and other neurological disorders. *J Clin Investig* **115**, 2010 – 2017.

Meisler MH, O'Brien JE & Sharkey LM (2010). Sodium channel gene family: epilepsy mutations, gene interactions and modifier effects. *J Physiol* **588**, 1841 – 1848.

Meisler MH, Plummer NW, Burgess DL, Buchner DA & Sprunger LK (2004). Allelic mutations of the sodium channel *SCN8A* reveal multiple cellular and physiological functions. *Genetica* **122**, 37 – 45.

Menzler K, Hermsen A, Balkenhol K, Duddek C, Bugiel H, Bauer S, Schorge S, Reif PS, Klein KM, Haag A, Oertel WH, Hamer HM, Knake S, Trucks H, Sander T, Rosenow F, EPICURE-Consortium (2014). A common *SCN1A* splice-site polymorphism modifies the effect of carbamazepine on cortical excitability – A pharmacogenetic transcranial magnetic stimulation study. *Epilepsia*, **55**, 362–369.

Miceli F, Soldovieri M, Ambrosino P, De Maria M, Manocchio L, Medoro A & Tagliatela M (2015). Molecular pathophysiology and pharmacology of the voltage-sensing domain of neuronal ion channels. *Front. Cell. Neurosci* **9(259)**, doi:10.3389

Milescu LS, Yamanishi T, Ptak K, Mogri MZ & Smith JC (2008). Real-Time Kinetic Modeling of Voltage-Gated Ion Channels Using Dynamic Clamp. *Biophysical Journal* **95(1)**, 66 – 87.

Misra SN, Kahlig KM & George AL Jr (2008). Impaired Na_v 1.2 function and reduced cell surface expression in benign familial neonatal-infantile seizures. *Epilepsia* **49**, 1535 – 1545.

Modrek B & Lee C (2002). A genomic view of alternative splicing. *Nat Genet.* **30**, 13 – 19.

Motoike HK, Liu H, Glaaser IW, Yang A, Tateyama M & Kass RS (2004). The Na⁺ channel inactivation gate is a molecular complex: a novel role of the COOH- terminal domain. *J. Gen. Physiol.* **123**, 155 – 165.

Mu Y, Otsuka T, Horton AC, Scott DB & Ehlers MD (2003). Activity-dependent mRNA splicing controls ER export and synaptic delivery of NMDA receptors. *Neuron.* **40**, 581 – 594.

Mullen SA & Scheffer IE (2009). Translational research in epilepsy genetics. *Arch. Neurol.* **66**, 21 – 26.

Mulley JC, Scheffer IE, Petrou S, Dibbens LM, Berkovic SF & Harkin LA (2005). *SCN1A* mutations and epilepsy. *Hum. Mutat.* **25**, 535 – 542.

Mulley JC, Scheffer IE, Petrou S, Dibbens LM, Berkovic SF & Harkin LA (2005). *SCN1A* mutations and epilepsy. *Hum. Mutat.* **25**, 535 – 542.

Namadurai S, Yereddi NR, Cusdin FS, Huang CL-H, Chirgadze DY & Jackson AP (2015). A new look at sodium channel β subunits. *Open Biol.* 2015 **5**(1). PMID: 25567098.

Nassar MA, Baker MD, Levato A, Ingram R, Mallucci G, McMahon SB & Wood JN (2006). Nerve injury induces robust allodynia and ectopic discharges in Na_v1.3 null mutant mice. *Mol Pain* **2**, 33.

Nassar MA, Stirling LC, Forlani G, Baker MD, Matthews EA, Dickenson AH & Wood JN (2004). Nociceptor-specific gene deletion reveals a major role for Na_v1.7 (PN1) in acute and inflammatory pain. *Proc Natl Acad Sci U S A* **101**, 12706 – 12711.

Naylor J, Milligan CJ, Zeng F, Jones C & Beech DJ (2008). Production of a specific extracellular inhibitor of TRPM3 channels. *Br J Pharmacol* **155**, 567 – 73.

Noda M (2006). The subfornical organ, a specialized sodium channel, and the sensing of sodium levels in the brain. *Neuroscientist* **12**, 80 – 91.

Noda M, Ikeda T, Suzuki T, Takeshima H, Takahashi T, Kuno M & Numa S (1986). Expression of functional sodium channels from cloned cDNA. *Nature* **322**, 826 – 828.

Noda M, Shimizu S, Tanabe T, Takai T, Kayano T, Ikeda T, Takahashi H, Nakayama H, Kanaoka Y, Minamino N, *et al.* (1984). Primary structure of *Electrophorus electricus* sodium channel deduced from cDNA sequence. *Nature* **312**, 121 – 127.

Odani A, Hashimoto Y, Otsuki Y, Uwai Y, Hattori H, Furusho K & Inui K (1997). Genetic polymorphism of the CYP2C subfamily and its effect on the pharmacokinetics of phenytoin in Japanese patients with epilepsy. *Clin Pharmacol Ther* **62**, 287 – 292.

Ogata N, & Ohishi Y (2002). Molecular diversity of structure and function of the voltage-gated Na⁺ channels. *Jpn. J. Pharmacol.* **88**, 365 – 377.

Ogiwara I, Ito K, Sawaishi Y, Osaka H, Mazaki E, Inoue I, Montal M, Hashikawa T, Shike T, Fujiwara T, Inoue Y, Kaneda M & Yamakawa K (2009). De novo mutations of voltage-gated sodium channel α II gene *SCN2A* in intractable epilepsies. *Neurology* **73**, 1046 – 1053.

Ogiwara I, Miyamoto H, Morita N, Atapour N, Mazaki E, Inoue I, Takeuchi T, Itohara S, Yanagawa Y, Obata K, Furuichi T, Hensch TK & Yamakawa K (2007). $Na_v1.1$ localizes to axons of parvalbumin-positive inhibitory interneurons: a circuit basis for epileptic seizures in mice carrying an *SCN1A* gene mutation. *J Neurosci* **27**, 5903 – 5914.

Ohmori I, Kahlig KM, Rhodes TH, Wang DW & George AL Jr. (2006). Nonfunctional *SCN1A* is common in severe myoclonic epilepsy of infancy. *Epilepsia*, **47**, 1636 – 1642.

Oliva M, Berkovic SF, & Petrou S (2012). Sodium channels and the neurobiology of epilepsy. *Epilepsia* **53**, 1849 – 1859.

Osheroff N, Shelton ER & Brutlag DL (1983). DNA topoisomerase II from *Drosophila melanogaster*. Relaxation of supercoiled DNA. *J Biol Chem* **258**, 9536 – 9543.

Pal DK, Pong AW & Chung WK (2010). Genetic evaluation and counseling for epilepsy. *Nat Rev Neurol.* **6**, 445 – 453.

Pan Q, Shai O, Lee LJ, Frey BJ & Blencowe BJ (2008). Deep surveying of alternative splicing complexity in the human transcriptome by high-throughput sequencing. *Nat. Genet.* **40**, 1413 – 1415.

Patino GA & Isom LL (2010). Electrophysiology and beyond: multiple roles of Na^+ channel beta subunits in development and disease. *Neurosci. Lett.* **486**, 53 – 59.

Pavlov I, Savtchenko LP, Song I, Koo J, Pimashkin A, Rusakov DA & Semyanov A (2014). Tonic GABAA conductance bidirectionally controls interneuron firing pattern and synchronization in the CA3 hippocampal network. *Proceedings of the National Academy of Sciences of the United States of America* **111**(1), 504 – 509.

Payandeh J, Scheuer T, Zheng N & Catterall WA (2011). The crystal structure of a voltage-gated sodium channel. *Nature* **475**, 353 – 8.

Perucca E & Tomson T (2011). The pharmacological treatment of epilepsy in adults. *Lancet Neurol* **10**, 446 – 56.

Petrovski S, Scheffer IE, Sisodiya SM, O'Brien TJ & Berkovic SF (2009). Lack of replication of association between *SCN1A* SNP and febrile seizures. *Neurology* **73**, 1928 – 1930.

Picard F, Bertrand S, Steinlein OK & Bertrand D (1999). Mutated nicotinic receptors responsible for autosomal dominant nocturnal frontal lobe epilepsy are more sensitive to carbamazepine. *Epilepsia* **40**, 1198 – 1209.

Planells-Cases R, Caprini M, Zhang J, Rockenstein EM, Rivera RR, Murre C, Masliah E & Montal M (2000). Neuronal death and perinatal lethality in voltage-gated sodium channel α II-deficient mice. *Biophys J* **78**, 2878 – 2891.

Pozzi D, Lignani G, Ferrea E, Contestabile A, Paonessa F, D'Alessandro R, Lippiello P, Boido D, Fassio A, Meldolesi J, *et al.* (2013). REST/NRSF-mediated intrinsic homeostasis protects neuronal networks from hyperexcitability. *EMBO J.* **32**, 2994 – 3007.

Ptacek LJ, George AL Jr., Barchi RL, Griggs RC, Riggs JE, Robertson M & Leppert MF (1992). Mutations in an S4 segment of the adult skeletal muscle sodium channel cause paramyotonia congenita. *Neuron* **8**, 891 – 897.

Ptacek LJ, George AL Jr., Griggs RC, Tawil R, Kallen RG, Barchi RL, Robertson M & Leppert MF (1991). Identification of a mutation in the gene causing hyperkalemic periodic paralysis. *Cell* **67**, 1021 – 1027.

Ptak K, Zummo GG, Alheid GF, Tkatch T, Surmeier DJ & McCrimmon DR (2005). Sodium currents in medullary neurons isolated from the pre-Botzinger complex region. *J Neurosci* **25**, 5159 – 5170.

Qu Y, Curtis R, Lawson D, Gilbride K, Ge P, DiStifano PS, Silos-Santiago I, Catterall WA & Scheuer T (2001). Differential modulation of sodium channel gating and persistent sodium currents by the b1, b2 and b3 subunits. *Mol. Cell. Neurosci.* **18**, 570 – 580.

Quilichini PP, Le Van Quyen M, Ivanov A, Turner DA, Carabalona A, Gozlan H, Esclapez M, & Bernard C (2012). Hub GABA neurons mediate gamma-frequency oscillations at ictal-like event onset in the immature hippocampus. *Neuron* **74**, 57 – 64

Ragsdale DS & Avoli M (1998). Sodium channels as molecular targets for antiepileptic drugs. *Brain Res. Rev.* **26**, 16 – 28.

Ragsdale DS (2008). How do mutant Na_v1.1 sodium channels cause epilepsy? *Brain Res Rev* **58**, 149 – 159.

Ragsdale DS, McPhee JC, Scheuer T & Catterall WA (1994). Molecular determinants of state-dependent block of Na channels by local anesthetics, *Science* **265**, 1724 – 1728.

Ragsdale DS, McPhee JC, Scheuer T & Catterall WA (1996). Common molecular determinants of local anesthetic, antiarrhythmic and anticonvulsant block of voltage-gated Na channels. *Proc. Natl. Acad. Sci. U.S.A.* **93**, 9270 – 9275.

Ragsdale DS, Scheuer T & Catterall WA (1994). Frequency and voltage-dependent inhibition of type IIA Na channels, expressed in a mammalian cell line, by local anesthetic, antiarrhythmic and anticonvulsant drugs. *Mol. Pharmacol.* **40**, 756 – 765.

Rasband, MN (2010). The axon initial segment and the maintenance of neuronal polarity. *Nat. Rev. Neurosci.* **11**, 552 – 562.

Remy S, Gabriel S, Urban BW, Dietrich D, Lehmann TN, Elger CE, Heinemann U & Beck H (2003). A novel mechanism underlying drug resistance in chronic epilepsy. *Ann Neurol* **53**, 469 – 479.

Rhodes TH, Lossin C, Vanoye CG, Wang DW & George AL Jr. (2004). Non-inactivating voltage-gated sodium channels in severe myoclonic epilepsy of infancy. *Proc. Natl. Acad. Sci. U.S.A.* **101**, 11147 – 11152.

Rhodes TH, Vanoye CG, Ohmori I, Ogiwara I, Yamakawa K & George AL Jr. (2005). Sodium channel dysfunction in intractable childhood epilepsy with generalized tonic-clonic seizures. *J. Physiol.* **569**, 433 – 445.

Rogawski MA & Loscher W (2004). The neurobiology of antiepileptic drugs for the treatment of nonepileptic conditions. *Nat Med* **10**, 685 – 92.

Rojas CV, Wang J, Schwartz LS, Hoffman EP, Powell BR, & Brown RH, Jr. (1991). A Met-to-Val mutation in the skeletal muscle Na channel α -subunit in hyperkalaemic periodic paralysis. *Nature* **354**, 387 – 389.

Rudy Y & Silva JR (2006). Computational biology in the study of cardiac ion channels and cell electrophysiology. *Q. Rev. Biophys.* **39**, 57 – 116.

Rusconi R, Combi R, Cestele S, Grioni D, Franceschetti S, Dalpra L & Mantegazza M (2009). A rescuable folding defective Na_v 1.1 (*SCN1A*) sodium channel mutant causes GEFS+: common mechanism in Na_v 1.1 related epilepsies? *Hum. Mutat.* **30**, E747 – E760.

Rusconi R, Scalmani P, Cassulini RR, Giunti G, Gambardella A, Franceschetti S, Annesi G, Wanke E & Mantegazza M (2007). Modulatory proteins can rescue a trafficking defective epileptogenic Na_v 1.1 Na channel mutant. *J. Neurosci.* **27**, 11037 – 11046.

Rush AM, Dib-Hajj SD & Waxman S.G. (2005). Electrophysiological properties of two axonal sodium channels, Na_v1.2 and Na_v1.6, expressed in mouse spinal sensory neurones. *J. Physiol.* **564**, 803 – 815.

Rush AM, Dib-Hajj DS, Liu S, Cummins TR, Black JA & Waxman SG (2006). A single sodium channel mutation produces hyper- or hypoexcitability in different types of neurons. *Proc. Natl. Acad. Sci. U.S.A.* **103**, 8245 – 8250.

Ryberg E, Vub HK, Larsson N, Groblewski T, Hjorth S, Elebring T, Sjögren S & Greasley PJ (2005). Identification and characterisation of a novel splice variant of the human CB1 receptor. *FENS letters* **579(1)**, 259 – 264.

Santiago-Castillo JAD, Covarrubias M, Sánchez-Rodríguez JE, Perez-Cornejo P, & Arreola J (2010). Simulating complex ion channel kinetics with IonChannelLab. *Channels Austin Tex* **4**, 422 – 428.

Sarao R, Gupta SK, Auld VJ & Dunn RJ (1991). Developmentally regulated alternative RNA splicing of rat brain sodium channel mRNAs. *Nucleic Acids Res* **19**, 5673 – 5679.

Sato C, Ueno Y, Asai K, Takahashi K, Sato M, Engel A & Fujiyoshi Y (2001). The voltage-sensitive sodium channel is a bell-shaped molecule with several cavities. *Nature* **409**, 1047 – 1051.

Savio-Galimberti E, Gollob MH & Darbar D (2012). Voltage-gated sodium channels: biophysics, pharmacology, and related channelopathies. *Frontiers in pharmacology* **124**, 1-19.

Scalmani P, Rusconi R, Armatura E, Zara F, Avanzini G, Franceschetti S & Mantegazza M (2006). Effects in neocortical neurons of mutations of the Na_v 1.2 Na⁺ channel causing benign familial neonatal-infantile seizures. *J. Neurosci* **26**, 10100 – 10109.

Scharfman HE (2007). The Neurobiology of Epilepsy. *Current Neurology and Neuroscience Reports* **7(4)**, 348 – 354.

Scheffer IE & Berkovic SF (1997). Generalized epilepsy with febrile seizures plus. A genetic disorder with heterogeneous clinical phenotypes. *Brain* **120**, 479 – 490.

Scheffer IE, Harkin LA, Grinton BE, Dibbens LM, Turner SJ, Zielinski MA, *et al.* (2010). Temporal lobe epilepsy and GEFS + phenotypes associated with SCN1B mutations. *Brain* **130**, 100 – 9.

Scheffer IE, Zhang YH, Jansen FE & Dibbens L (2009). Dravet syndrome or genetic (generalized) epilepsy with febrile seizures plus? *Brain Dev* **31**, 394 – 400.

Schlachter K, Gruber-Sedlmayr U, Stogmann E, Lausecker M, Hotzy C, Balzar J, Schuh E, Baumgartner C, Mueller JC, Illig T, Wichmann HE, Lichtner P, Meitinger T, Strom TM, Zimprich A & Zimprich F (2009). A splice site variant in the sodium channel gene *SCN1A* confers risk of febrile seizures. *Neurology* **72**, 974 – 978.

Schneider MF & Chandler WK (1973). Voltage-dependent charge movement in skeletal muscle: a possible step in excitation–contraction coupling, *Nature* **242**, 244 – 246.

Schrempf H, Schmidt O, Kümmerlen R, Hinnah S, Müller D, Betzler M, Steinkamp T & Wagner R (1995). A prokaryotic potassium ion channel with two predicted transmembrane segments from *Streptomyces lividans*. *EMBO J.* **14**(21), 5170 – 8.

Scott RS, Henneberger C, Padmashri R, Anders S, Jensen TP, and Rusakov DA (2014). Neuronal adaptation involves rapid expansion of the action potential initiation site. *Nat. Commun.* **5**:3817. 1 – 12.

Shi X, Yasumoto S, Nakagawa E, Fukasawa T, Uchiya S & Hirose S (2009). Missense mutation of the sodium channel gene *SCN2A* causes Dravet syndrome. *Brain Dev* **31**, 758 – 762.

Singh NA, Pappas C, Dahle EJ, Claes LR, Pruess TH, De Jonghe P, Thompson J, Dixon M, Gurnett C, Peiffer A, White HS, Filloux F & Leppert MF (2009). A role of *SCN9A* in human epilepsies, as a cause of febrile seizures and as a potential modifier of Dravet syndrome. *PLoS Genet* **5**, e1000649.

Singh R, Anderman E, Whitehouse WP, Harvey AS, Keene DL, Seni MH, Crossland KM, Anderman F, Berkovic SF & Scheffer IE (2001). Severe myoclonic epilepsy of infancy: extended spectrum of GEFS+? *Epilepsia* **42**, 837 – 844.

Song T, Peng J, Ren J, Wei H, & Peng J (2015). Cloning and Characterization of Spliced Variants of the Porcine G Protein Coupled Receptor 120. *BioMed Research International* **2015**, 11 – 20.

Sontheimer H, Black JA & Waxman SG. (1996). Voltage-gated Na⁺ channels in glia: properties and possible functions. *Trends Neurosci* **19**, 325 – 31.

Sontheimer H, Black JA & Waxman SG. (1996). Voltage-gated Na⁺ channels in glia: properties and possible functions. *Trends Neurosci* **19**, 325 – 31.

Sousa F, Prazeres DMF & Queiroz JA (2009). Improvement of transfection efficiency by using supercoiled plasmid DNA purified with arginine affinity chromatography. *J Gene Med* **11**, 79– 88

Spampanato J, Escayg A, Meisler MH & Goldin AL (2001). Functional effects of two voltage-gated sodium channel mutations that cause generalized epilepsy with febrile seizures plus type 2. *J. Neurosci.* **21**, 7481 – 7490.

Spampanato J, Escayg A, Meisler MH & Goldin AL (2003). Generalized epilepsy with febrile seizures plus type 2 mutation W1204R alters voltage-dependent gating of Na_v1.1 sodium channels. *Neuroscience* **116**, 37 – 48.

Spampanato J, Kearney JA, de Haan G, McEwen DP, Escayg A, Aradi I, MacDonald BT, Levin SI, Soltesz I, Benna P, Montalenti E, Isom LL, Goldin AL & Meisler MH (2004). A novel epilepsy mutation in *SCN1A* identifies a cytoplasmic domain for beta subunit interaction. *J. Neurosci.* **24**, 10022 – 10034.

Stafstrom CE (2007). Persistent sodium current and its role in epilepsy. *Epilepsy Curr* **7**, 15 – 22.

Steinhäuser C & Seifert G (2002). Glial membrane channels and receptors in epilepsy: impact for generation and spread of seizure activity. *Eur J Pharmacol* **447**, 227 – 37.

Steijns LS, van der WJ, van Weelden MJ & de Haan K (2001). The effect of genetic polymorphism of cytochrome P450 CYP2C9 on phenytoin dose requirement. *Pharmacogenetics* **11**, 287 – 291.

Steinlein O. (2014). Genetics of Epilepsy. *Elsevier*. p.100

Struyk AF & Cannon SC (2002). Slow inactivation does not block the aqueous accessibility to the outer pore of voltage-gated Na channels. *J Gen Physiol.* **120**, 509 – 516.

Sugawara T, Tsurubuchi Y, Agarwala KL, Ito M, Fukuma G, Mazaki- Miyazaki E, *et al.* (2001). A missense mutation of the Na⁺ channel alpha II subunit gene Na_v1.2 in a patient with febrile and afebrile seizures causes channel dysfunction. *Proc Natl Acad Sci USA* **98**, 6384 – 9.

Sugiura Y, Aoki T, Sugiyama Y, Hida C, Ogata M & Yamamoto T (2000). Temperature-sensitive sodium channelopathy with heat-induced myotonia and cold-induced paralysis. *Neurology* **54**, 2179 – 2181.

Taddese A & Bean BP (2002). Subthreshold sodium current from rapidly inactivating sodium channels drives spontaneous firing of tuberomammillary neurons. *Neuron* **33**, 587 – 600.

Talvenheimo JA, Tamkun MM & Catterall WA (1982). Reconstitution of neurotoxin-stimulated sodium transport by the voltage-sensitive sodium channel purified from rat brain. *J. Biol. Chem.* **257**, 11868 – 11871.

Tamamaki N, Yanagawa Y, Tomioka Y, Miyazaki J, Obata K & Kaneko T. (2003) Green fluorescent protein expression and colocalization with calretinin, parvalbumin, and somatostatin in the GAD67-GFP knock-in mouse. *J. Comp. Neurol.* **467**, 60 – 79.

Tan BH, Pundi KN, Van Norstrand DW, Valdivia CR, Tester DJ, Medeiros-Domingo A, *et al.* (2010). Sudden infant death syndrome-associated mutations in the sodium channel beta subunits. *Heart Rhythm* **7**, 771 – 8.

Tan J, Liu Z, Nomura Y, Goldin AL & Dong K (2002). Alternative splicing of an insect sodium channel gene generates pharmacologically distinct sodium channels. *J Neurosci* **22**, 5300 – 5309.

Tang B, Dutt K, Papale L, Rusconi R, Shankar A, Hunter J, Tufik S, Yu FH, Catterall WA, Mantegazza M, Goldin AL & Escayg A (2009). A BAC transgenic mouse model reveals neuron subtype-specific effects of a Generalized Epilepsy with Febrile Seizures Plus (GEFS+) mutation. *Neurobiology of Disease* **35**, 91 – 102.

Tang B, Dutt K, Papale L, Rusconi R, Shankar A, Hunter J, Tufik S, Yu FH, Catterall WA, Mantegazza M, Goldin AL & Escayg A (2009). A BAC transgenic mouse model reveals neuron subtype-specific effects of a generalized epilepsy with febrile seizures plus (GEFS+) mutation. *Neurobiol. Dis.* **35**, 91 – 102.

Tang L, Lu X, Tao Y, Zheng J, Zhao P, Li K & Li L. (2014). *SCN1A* rs3812718 polymorphism and susceptibility to epilepsy with febrile seizures: a meta-analysis. *Gene.* **533**, 26 – 31.

Tate SK, Depondt C, Sisodiya SM, Cavalleri GL, Schorge S, Soranzo N, Thom M, Sen A, Shorvon SD, Sander JW, Wood NW & Goldstein DB (2005). Genetic predictors of the maximum doses patients receive during clinical use of the anti-epileptic drugs carbamazepine and phenytoin. *Proc Natl Acad Sci U S A* **102**, 5507 – 5512.

Tate SK, Singh R, Hung CC, Tai JJ, Depondt C, Cavalleri GL, Sisodiya SM, Goldstein DB & Liou HH (2006). A common polymorphism in the *SCN1A* gene associates with phenytoin serum levels at maintenance dose. *Pharmacogenet Genomics* **16**, 721 – 726.

Thompson CH, Kahlig KM & George AL Jr. (2011). *SCN1A* Splice Variants Exhibit Divergent Sensitivity to Commonly Used Antiepileptic Drugs *Epilepsia* **52**, 1000 – 1009.

Toman JEP (1949). The neuropharmacology of antiepileptics. *Electroencephalogr. Clin. Neurophysiol.* **1**, 33 – 44.

Trimmer JS & Rhodes KJ (2004). Localization of voltage-gated ion channels in mammalian brain. *Annu Rev Physiol* **66**, 477 – 519.

Trudeau MM, Dalton JC, Day JW, Ranum LP & Meisler MH (2006). Heterozygosity for a protein truncation mutation of sodium channel *SCN8A* in a patient with cerebellar atrophy, ataxia, and mental retardation. *J Med Genet* **43**, 527 – 30.

Ulbricht W (2005). Sodium channel inactivation: molecular determinants and modulation. *Physiol. Rev* **85**, 1271 – 1301.

Ule J, Ule A, Spencer J, Williams A, Hu JS, Cline M, Wang H, Clark T, Fraser C, Ruggiu M, *et al.* (2005). Nova regulates brain-specific splicing to shape the synapse. *Nat. Genet.* **37**, 844 – 852.

Valdivia CR, Tester DJ, Rok BA, Porter C-BJ, Munger TM, Jahangir A, *et al.* (2004). A trafficking defective, Brugada syndrome-causing *SCN5A* mutation rescued by drugs. *Cardiovasc Res* **62**, 53 – 62.

Vanoye CG, Lossin C, Rhodes TH & George AL Jr. (2002). Single channel properties of human $Na_v1.1$ and mechanisms of channel dysfunction in *SCN1A*-associated epilepsy. *J. Gen. Physiol.* **127**, 1 – 14.

Veeramah KR, O'Brien JE, Meisler MH, Cheng X, Dib-Hajj SD, Waxman SG, *et al.* (2012). De novo pathogenic *SCN8A* mutation identified by whole-genome sequencing of a family quartet affected by infantile epileptic encephalopathy and SUDEP. *Am J Hum Genet* **90**, 502 – 10.

Verkerk AO, Remme CA, Schumacher CA, Scicluna BP, Wolswinkel R, de Jonge B, Bezzina CR & Veldkamp MW (2012). Functional $Na_v1.8$ channels in intracardiac neurons: the link between *SCN10A* and cardiac electrophysiology. *Circ. Res.* [Epub ahead of print].

Wang J, Ou SW, Wang YJ, Kameyama M, Kameyama A & Zong ZH (2009). Analysis of four novel variants of $Na_v1.5/SCN5A$ cloned from the brain. *Neurosci Res* **64**, 339 – 347.

West JW, Patton DE, Scheuer T, Wang Y, Goldin AL & Catterall WA (1992). A cluster of hydrophobic amino acid residues required for fast Na channel inactivation. *Proc. Natl. Acad. Sci. USA* **89**, 10910 – 10914.

Wanisch K, Kovac S & Schorge S. (2013). Tackling obstacles for gene therapy targeting neurons: disrupting perineural nets with hyaluronidase improves transduction. *PLoS ONE* **8**,

Waxman SG (2007). Channel, neuronal and clinical function in sodium channelopathies: from genotype to phenotype. *Nat Neurosci* **10**, 405 – 409.

Westenbroek RE, Merrick DK & Catterall WA (1989). Differential subcellular localization of the RI and RII Na⁺ channel subtypes in central neurons. *Neuron* **3**, 695 – 704.

Westenbroek RE, Noebels JL & Catterall WA (1992). Elevated expression of type II Na⁺ channels in hypomyelinated axons of shiverer mouse brain. *J Neurosci* **12**, 2259 – 2267.

Wood JN & Baker M (2001). Voltage-gated sodium channels. *Current Opinion in Pharmacology* **1**, 17 – 21.

Wu MT, Huang PY, Yen CT, Chen CC & Lee MJ (2013) A novel *SCN9A* mutation responsible for primary erythromelalgia and is resistant to the treatment of sodium channel blockers. *PLoS ONE* **8(1)**, Article ID e55212.

Xu Q, Modrek B & Lee C (2002). Genome-wide detection of tissue-specific alternative splicing in the human transcriptome. *Nucleic Acids Res* **30**, 3754 – 66.

Xu R, Thomas EA, Jenkins M, Gazina EV, Chiu C, *et al.* (2007). A childhood epilepsy mutation reveals a role for developmentally regulated splicing of a sodium channel. *Mol Cell Neurosci* **35**, 292 – 301.

Yang T, Atack TC, Stroud DM, Zhang W, Hall L. & Roden DM (2012). Blocking *SCN10A* channels in heart reduces late sodium current and is antiarrhythmic. *Circ. Res.* [Epub ahead of print].

Yang YC, Hsieh JY & Kuo CC (2009). The external pore loop interacts with S6 and S3-S4 linker in domain 4 to assume an essential role in gating control and anticonvulsant action in the Na⁺ channel. *J. Gen. Physiol* **134**, 95 – 113.

Yang Y, Adowski T, Ramamurthy B, Neef A & Xu-Friedman MA (2015). High-speed dynamic-clamp interface. *J Neurophysiol* **113**(7), 2713 – 20.

Yang Y, Wang Y, Li S, Xu Z, Li H, Ma L, *et al.* (2004). Mutations in *SCN9A*, encoding a sodium channel alpha subunit, in patients with primary erythralgia. *J Med Genet* **41**, 171 – 4.

Yarov-Yarovoy V, DeCaen PG, Westenbroek RE, Pan CY, Scheuer T, Baker D, *et al.* (2012). Structural basis for gating charge movement in the voltage sensor of a sodium channel. *Proc Natl Acad Sci USA* **109**, E93 – 102.

Yu FH, Mantegazza M, Westenbroek RE, Robbins CA, Kalume F, Burton KA, Spain WJ, McKnight GS, Scheuer T & Catterall WA (2006). Reduced sodium current in GABAergic interneurons in a mouse model of severe myoclonic epilepsy in infancy. *Nat Neurosci* **9**, 1142 – 1149.

Yuan R, Zhang X, Deng Q *et al.* (2011). Two novel *SCN9A* gene heterozygous mutations may cause partial deletion of pain perception. *Pain Medicine* **12**(10), 1510 – 1514.

Zhao J, O’Leary ME & Chahine M (2011). Regulation of Na_v1.6 and Na_v1.8 peripheral nerve Na⁽⁺⁾ channels by auxiliary beta-subunits. *J Neurophysiol* **106**, 608 – 19

Zimmer T & Surber R (2008). *SCN5A* channelopathies – an update on mutations and mechanisms. *Prog Biophys Mol Biol* **98**, 120 – 36.

Zhou BT, Zhou QH, Yin JY, Li GL, Qu J, Xu XJ, Liu D, Zhou HH & Liu ZQ (2012). Effects of *SCN1A* and GABA receptor genetic polymorphisms on carbamazepine tolerability and efficacy in

Chinese patients with partial seizures: 2-year longitudinal clinical follow-up. *CNS Neurosci Ther* **18(7)**, 566 – 72

Zhou BT, Zhou QH, Yin JY, Li GL, Xu XJ, Qu J, Liu D, Zhou HH & Liu ZQ (2012). Comprehensive analysis of the association of *SCN1A* gene polymorphisms with the retention rate of carbamazepine following monotherapy for new-onset focal seizures in the Chinese Han population. *Clin Exp Pharmacol Physiol* **39(4)**, 379 – 84.

Zimmermann K, Leffler A, Babes A, Cendan CM, Carr RW, Kobayashi J, *et al.* (2007). Sensory neuron sodium channel $Na_v1.8$ is essential for pain at low temperatures. *Nature* **447**, 855 – 8.

Zimprich F, Stogmann E, Bonelli SB, Baumgartner C, Mueller JC, Meitinger T, Zimprich A & Strom TM (2008). A functional polymorphism in the *SCN1A* gene is not associated with carbamazepine dosages in Austrian patients with epilepsy. *Epilepsia* **49**, 1108 – 1109.

Appendix I: cDNA and amino acid sequence of all (TTX-sensitive and TTX-resistant) sodium channel splice variants used

The base pairs and amino acids that differ between isoforms are indicated in **red**, while the base and amino acid that is changed to confer TTX resistance is indicated in **yellow**.

SCN1A-5A cDNA sequence:

```
ATGGAGCAAACAGTGCTTGTACCACCAGGACCTGACAGCTTCAACTTCTCACCAGAGAATCTCTTGCGGCTATTGAA
AGACGCATTGCAGAAGAAAAGGCAAAGAATCCCAAACCAGACAAAAAAGATGACGACGAAAATGGCCCAAAGCCA
AATAGTGACTTGGAAGCTGGAAGAACCTTCCATTTATTTATGGAGACATTCCTCCAGAGATGGTGTCTAGAGCCCT
GGAGGACCTGGACCCCTACTATATCAATAAGAAAACCTTTTATAGTATTGAATAAAGGGAAGGCCATCTTCCGGTTCA
GTGCCACCTCTGCCCTGTACATTTAACTCCCTTCAATCCTCTTAGGAAAATAGCTATTAAGATTTTGGTACATTCATTA
TTCAGCATGCTAATTATGTGCACTATTTTGACAACTGTGTGTTTATGACAATGAGTAACCCTCCTGATTGGACAAAG
AATGTAGAATACACCTTCACAGGAATATATACTTTTGAATCACTTATAAAAATTATTGCAAGGGGATTCTGTTTAGAA
GATTTTACTTTCTTCGGGATCCATGGAACCTGGCTCGATTTCACTGTCATTACATTTGCGTACGTCACAGAGTTTGTGG
ACCTGGGCAATGTCTCGGCATTGAGAACATTCAGAGTTCTCGAGCATTGAAGACGATTTCAGTCATTCCAGGCCTG
AAAACCATTGTGGGAGCCCTGATCCAGTCTGTGAAGAAGCTCTCAGATGTAATGATCCTGACTGTGTTCTGTCTGAG
CGTATTTGCTCTAATTGGGCTGCAGCTGTTCATGGGCAACCTGAGGAATAAATGTATACAATGGCCTCCACCAATG
CTTCCTTGAGGAACATAGTATAGAAAAGAATAAACTGTGAATTATAATGGTACACTTATAAATGAAACTGTCTTTG
AGTTTGACTGGAAGTCATATATTCAAGATTCAAGATATCATTATTTCTGGAGGGTTTTTTAGATGCACTACTATGTG
GAAATAGCTCTGATGCAGGCCAATGTCCAGAGGGATATATGTGTGTGAAAGCTGGTAGAAATCCCAATTATGGCTA
CACAAGCTTTGATACCTCAGTTGGGCTTTTTTGTCTTGTTCGCCTAATGACTCAGGACTTCTGGGAAAATCTTTAT
CAACTGACATTACGTGCTGCTGGGAAAACGTACATGATATTTTTTGTGTTGGTCATTTTCcTaGGCTCATTCTACCTAA
TAAATTTGATCCTGGCTGTGGTGGCCATGGCCTACGAGGAACAGAATCAGGCCACCTTGGGAAGAAGCAGAACAGAA
AGAGGCCGAATTTCAGCAGATGATTGAACAGCTTAAAAAGCAACAGGAGGCAGCTCAGCAGGCAGCAACGGCAAC
TGCCTCAGAACATTCCAGAGAGCCCAGTGCAGCAGGCAGGCTCTCAGACAGCTCATCTGAAGCCTCTAAGTTGAGTT
CCAAGAGTGCTAAGGAAAGAAGAAATCGGAGGAAGAAAAGAAAACAGAAAGAGCAGTCTGGTGGGGAAAGAGAAA
GATGAGGATGAATTCAAAAATCTGAATCTGAGGACAGCATCAGGAGGAAAGGTTTTCGCTTCTCATTGAAGGGA
ACCGATTGACATATGAAAAGAGGTACTCCTCCCCACACCAGTCTTTGTTGAGCATCCGTGGCTCCCTATTTTACCAA
GGCGAAATAGCAGAACAAAGCCTTTTCAGCTTTAGAGGGCGAGCAAAGGATGTGGGATCTGAGAACGACTTCGCAG
ATGATGAGCACAGCACCTTTGAGGATAACGAGAGCCGTAGAGATTCTTGTGTTTGTGCCCGACGACACGGAGAGAG
ACGCAACAGCAACCTGAGTCAGACCAGTAGGTCATCCCGATGCTGGCAGTGTTCAGCGAATGGGAAGATGCAC
AGCACTGTGGATTGCAATGGTGAGGTTTCTTGGTTGGTGGACCTTCAGTTCTACATCGCCTGTTGGACAGCTTCTG
```

CCAGAGGGAACAACCACTGAAACTGAAATGAGAAAGAGAAGGTCAAGTTCTTTCCACGTTTCCATGGACTTTCTAGA
AGATCCTTCCCAAAGGCAACGAGCAATGAGTATAGCCAGCATTCTAACAATACAGTAGAAGAACTTGAAGAATCCA
GGCAGAAATGCCACCCTGTTGGTATAAATTTTCCAACATATTCTAATCTGGGACTGTTCTCCATATTGGTTAAAAGT
GAAACATGTTGTCAACCTGGTCGTGATGGACCCATTTGTTGACCTGGCCATCACCATCTGTATTGTCTTAAATACTCTT
TTCATGGCCATGGAGCACTATCCAATGACGGACCATTTCAATAATGTGCTTACAGTAGGAAACTTGGTTTTACTGGG
ATCTTTACAGCAGAAATGTTTCTGAAAATTATTGCCATGGATCCTTACTATTATTTCCAAGAAGGCTGGAATATCTTTG
ACGGTTTTATTGTGACGCTTAGCCTGGTAGAACTTGGACTCGCCAATGTGGAAGGATTATCTGTTCTCCGTTCAATTC
GATTGCTGCGAGTTTTCAAGTTGGCAAATCTTGGCCAACGTTAAATATGCTAATAAAGATCATCGGCAATCCGCTG
GGGGCTCTGGGAAATTTAACCCCTCGTCTTGGCCATCATCGTCTTCATTTTTGCCGTGGTCCGCATGCAGCTCTTGGT
AAAAGCTACAAAGATTGTGTCTGCAAGATCGCCAGTGATTGTCAACTCCCACGCTGGCACATGAATGACTTCTCCAC
TCCTCCTGATTGTGTTCCGCGTGCTGTGTGGGGAGTGGATAGAGACCATGTGGGACTGTATGGAGGTTGCTGGTCA
AGCCATGTGCCTTACTGTCTTCATGATGGTCATGGTGATTGGAAACCTAGTGGTCCTGAATCTCTTTCTGGCCTTGCTT
CTGAGCTCATTTAGTGCAGACAACCTTGCAGCCACTGATGATGATAATGAAATGAATAATCTCCAAATTGCTGTGGAT
AGGATGCACAAAGGAGTAGCTTATGTGAAAAGAAAAATATATGAATTTATTCAACAGTCTTTCATTAGGAAACAAAA
GATTTTAGATGAAATTAACCACTTGATGATCTAACAACAAGAAAGACAGTTGTATGTCCAATCATAACAGCAGAAA
TTGGGAAAGATCTTGACTATCTTAAAGATGTAATGAACTACAAGTGGTATAGGAACTGGCAGCAGTGTTGAAAA
ATACATTATTGATGAAAGTGATTACATGTCATTCATAAACAACCCAGTCTTACTGTGACTGTACCAATTGCTGTAGG
AGAATCTGACTTTGAAAATTTAAACACGGAAGACTTTAGTAGTGAATCGGATCTGGAAGAAAGCAAAGAGAAACTG
AATGAAAGCAGTAGCTCATCAGAAGGTAGCACTGTGGACATCGGCGCACCTGTAGAAGAAGCAAGCCGTTAGTGGAAC
CTGAAGAACTCTTGAACCAGAAGCTTGTTCCTGAAAGGCTGTGTACAAAGATTCAAGTGTGTCAAATCAATGTG
GAAGAAGGCAGAGGAAAACAATGGTGGAACTGAGAAGGACGTGTTCCGAATAGTTGAACATAACTGGTTTGAG
ACCTTCATTGTTTTCATGATTCTCCTTAGTAGTGGTGTCTGGCATTGAAGATATATATATTGATCAGCGAAAGACG
ATTAAGACGATGTTGGAATATGCTGACAAGTTTTCACTTACATTTTCATTCTGGAATGCTTCTAAAATGGGTGGCA
TATGGCTATCAAACATATTTACCAATGCCTGGTGTGGCTGGACTTCTTAATTGTTGATGTTTCATTGGTCAGTTAA
CAGCAAATGCCTTGGGTTACTCAGAAGTTGGAGCCATCAAATCTCAGGACACTAAGAGCTCTGAGACCTCTAAGA
GCCTTATCTCGATTTGAAGGGATGAGGGTGGTTGTGAATGCCTTTTAGGAGCAATTCCATCCATCATGAATGTGCTT
CTGGTTGTCTTATATTCTGGCTAATTTTACGCATCATGGGCGTAAATTTGTTGCTGGCAAATTCTACCACTGTATTA
ACACCACAAGTGGTGACAGTTTTGACATCGAAGACGTGAATAATCATACTGATTGCCTAAAATAATAGAAAGAAAT
GAGACTGCTCGATGGAAAAATGTGAAAGTAACTTTGATAATGTAGGATTTGGGTATCTCTTTGCTTCAAGTTGCC
ACATTCAAAGGATGGATGGATATAATGTATGCAGCAGTTGATTCCAGAAATGTGGAAGTCCAGCCTAAGTATGAAG
AAAGTCTGTACATGTATCTTACTTTGTTATTTTCATCATCTTTGGGTCCTTCTCACCTTGAACCTGTTTATTGGTGT
ATCATAGATAATTTCAACCAGCAGAAAAAGAAGTTTGGAGGTCAAGACATCTTTATGACAGAAGAACAAGAAAT
ACTATAATGCAATGAAAAAATTAGGATCGAAAAAACCGCAAAAGCCTATACTCGACCAGGAAACAAATTTCAAGG
AATGGTCTTTGACTTCGTAACCAGACAAGTTTTTACATAAGCATCATGATTCTCATCTGTCTTAAACATGGTCACAATG
ATGGTGGAAACAGATGACCAGAGTGAATATGTGACTACCATTTTGTACGCATCAATCTGGTGTTCATTGTGCTATTT
ACTGGAGAGTGTGACTGAAACTCATCTCTACGCCATTATTATTTACCATTGGATGGAATATTTTTGATTTTGTGG
TTGTCATTCTCTCATTGTAGGTATGTTTCTTGGCAGCTGATAGAAAAGTATTCGTGTCCCCTACCCTGTTCCGAGT
GATCCGTCTTGCTAGGATTGGCCGAATCCTACGTCTGATCAAAGGAGCAAAGGGATCCGCACGCTGCTCTTTGCTT
TGATGATGTCCCTCCTGCGTTGTTAACATCGGCCTCTACTCTTCTAGTCATGTTTCTACGCCATCTTTGGGATG
TCCAACTTTGCCTATGTTAAGAGGGAAGTTGGGATCGATGACATGTTCAACTTTGAGACCTTTGGCAACAGCATGAT
CTGCCTATTCAAATTACAACCTCTGCTGGCTGGGATGGATTGCTAGCACCCATTCTCAACAGTAAGCCACCCGACTG
TGACCCTAATAAAGTTAACCTGGAAGCTCAGTTAAGGGAGACTGTGGGAACCCATCTGTTGGAATTTCTTTTTGT

CAGTTACATCATCATATCCTTCCTGGTTGTGGTGAACATGTACATCGCGGTCATCCTGGAGAACTTCAGTGTTGCTAC
TGAAGAAAGTGCAGAGCCTCTGAGTGAGGATGACTTTGAGATGTTCTATGAGGTTTGGGAGAAGTTTGATCCCGAT
GCAACTCAGTTCATGGAATTTGAAAAATTATCTCAGTTTGCAGCTGCGCTTGAACCGCCTCTCAATCTGCCACAACCA
AACAAACTCCAGCTCATTGCCATGGATTTGCCCATGGTGAGTGGTGACCGGATCCACTGTCTTGATATCTTATTTGCT
TTTACAAAGCGGGTTCTAGGAGAGAGTGAGAGATGGATGCTCTACGAATACAGATGGAAGAGCGATTTCATGGCTT
CCAATCCTTCCAAGGTCTCCTATCAGCCAATCACTACTACTTTAAAACGAAAACAAGAGGAAGTATCTGCTGTCATTA
TTCAGCGTGCTTACAGACGCCACCTTTAAAGCGAACTGTAAAACAAGCTTCCTTTACGTACAATAAAAAACAAAATCA
AAGGTGGGGCTAATCTTCTTATAAAAGAAGACATGATAATTGACAGAATAAATGAAAACCTATTACAGAAAAAACT
GATCTGACCATGTCCACTTCAGCTTGTCCACCTTCTATGACCGGGTGACAAAGCCAATTGTGGAAAAACATGAGCA
AGAAGGCAAAGATGAAAAAGCCAAAGGGAAATAA

SCN1A-5A amino acid sequence:

Met EQTVLVPPGPDSFNFFTRRESLAAIERRIAEEKAKNPKPKDKKDDDENGPKPNSDLE
AGKNLPFIYGDIPPE **Met** VSEPLEDLDPYYINKKTFIVLNKKGKAIFRFSATSALYILTPF
NPLRKIAIKILVHSLFS **Met** LI **Met** CTILTNCVF **Met** T **Met** SNPPDWTKNVEYFTFTGIYTF
ESLIKIIARGFCLEDFTLRDPWNWLDFTVITFA **V** VTEFV **D** LGN **V** SALRTFRVLRALKT
ISVIPGLKTIVGALIQSVKKLSDV **Met** ILTVFCLSVFALIGLQLF **Met** GNLRNKCIQWPPT
NASLEEHSIEKNITVNYNGTLINETVFEFDWKS YIQDSRYHYFLEGFLDALLCGNSSD
AGQCPEGY **Met** CVKAGRNPNGYTSFDTFSWAFSLFRL **Met** TQD **F** WENLYQLTLRA
AGKTY **Met** IFFVLVIFLGSFYLINLILAVVA **Met** AYEEQNQATLEEA EQKEAEFQQ **Met** I
EQLKKQQAQAATATASEHSREPSAAGRLSDSSSEASKLSSKSAKERRNRRKRRK
QKEQSGGEEKDEDEFQKSESEDSIRRKGRFRFSIEGNRLTYEKRYSSPHQSLLSIRGSLF
SPRRNSRTSLFSFRGRAKDVGSENFADDEHSTFEDNESRRDSLFPVRRHGERRNSN
LSQTSRSSR **Met** LAVFPANGK **Met** HSTVDCNGEVSLVGGPSVPTSPVGQLLPEGTTTE
TE **Met** RKRRSSSFHVS **Met** DFLEDPSQRQRA **Met** SIASILTNTVEELEESRQKCPPCWY
KFSNIFLIWDCSPYWLVKVVNLVV **Met** DPFVDLAITICIVLNTLF **Met** A **Met** EHY
P **Met** TDHFNNVLTVGNLVFTGIFTAE **Met** FLKIIA **Met** DPYYYFQEGWNIFDGFIVTLSL
VELGLANVEGLSVLRSFLLRVFKLAKSWPTLN **Met** LIKIIGNSVGALGNLTLVLAIVF
IFAVVG **Met** QLFGKSYKDCVCKIASDCQLPRWH **Met** NDFHFSFLIVFRVLCGEWIE
T **Met** WDC **Met** EVAGQA **Met** CLTVF **Met** **Met** V **Met** VIGNLVVLNLFALLLSSFSADNLAA
TDDDNE **Met** NNLQIAVDR **Met** HKGVAYVVKRKIYEFIQQS FIRKQKILDEIKPLDDLNNK
KDSC **Met** SNHTAEIGKDLDYLKDVNGTTSIGIGTGSSVEKYIIDESDY **Met** SFINNPSTLV
TVPIAVGESDFENLNTEDFSSESLEESKEKLNESSSSSEGSTVDIGAPVEEQPVVEPE
ETLEPEACFTEGCVQRFKCCQINVEEGRGKQWNLRRTCFRIVEHNWFETFIV
F **Met** ILLSSGALAFEDIYDQRKTIKT **Met** LEYADKVFTYIFILE **Met** LLKWVAYGYQTYF
TNAWCWLDFLIVDVSLSLTANALGYSELGAIKSLRTRLRALRPLRALS RFEG **Met** RVV
VNALLGAIPSI **Met** NVLLVCLIFWLIFS I **Met** GVNLFAGKFYHCINTTTGDRFDIEDVNN
HTDCLKLIERNETARWKNVKNVFDNVGFGYLSLLQVATFKGW **Met** DI **Met** YAAVDSR
NVELQPKYEEESLY **Met** YLYFVIFIIFGSFFTLNLFIGVIIDNFNQQKKKFGGQDIF **Met** TE
EQKKYYNA **Met** KKLGSKKPKQPIPRPGNK FQG **Met** VFDFVTRQVFDISI **Met** ILICL
N **Met** VT **Met** **Met** VETDDQSEYVTILSRINLVFIVLFTGECVLKLISLRHYYFTIGWNIFD
FVVVILSIVG **Met** FLAELIEKYFVSPTLFRVIRLARIGRILRLIKGAKGIRTL LFA
L **Met** **Met** SLPALFNIGLLLFLV **Met** FIYAIFG **Met** SNFAYVKREVGIDD **Met** FNFETFGN
S **Met** ICLFQITTSAGWDGLLAPILNSKPPDCDPNKVNP GSSVKGDCGNPSVGIFFFVS
YIIISFLVVVN **Met** YIAVILENFSVATEESAEP LSEDDFE **Met** FYEVWEKFDPDATQ
F **Met** EFEKLSQFAAALEPPLNLPQPNKLQLIA **Met** DLP **Met** VSGDRIHCLDILFAFTKRV
LGESGE **Met** DALRIQ **Met** EERF **Met** ASNPSKVSYPITTT LKRKQEEVSAVIIQRAYRRH
LLKRTVKQASFTYNKNKIKGGANLLIKED **Met** IIDRINENSITEKTDLT **Met** STSACPPS
YDRVTKPIVEKHEQEGKDEKAKGK Stop

SCN1A-5N cDNA sequence:

ATGGAGCAAACAGTGCTTGTACCACCAGGACCTGACAGCTTCAACTTCTCACCAGAGAATCTCTTGCGGCTATTGAA
AGACGCATTGCAGAAGAAAAGGCAAAGAATCCCAAACCCAGACAAAAAAGATGACGACGAAAATGGCCCAAAGCCA
AATAGTGACTTGAAGCTGGAAAGAACCTTCCATTTATTTATGGAGACATTCCTCCAGAGATGGTGTGAGAGCCCT
GGAGGACCTGGACCCCTACTATATCAATAAGAAAACCTTTATAGTATTGAATAAAGGGAAGGCCATCTCCGGTTCA
GTGCCACCTCTGCCCTGTACATTTAACTCCCTTCAATCCTCTTAGGAAAATAGCTATTAAGATTTTGGTACATTCATTA
TTCAGCATGCTAATTATGTGCACTATTTTGACAACTGTGTGTTTATGACAATGAGTAACCCCTCTGATTGGACAAAG
AATGTAGAATACACCTTCACAGGAATATATACTTTTGAATCACTTATAAAAATTATTGCAAGGGGATTCTGTTTAGAA
GATTTTACTTTCTTCGGGATCCATGGAAGCTGGCTCGATTTCACTGTCATTACATTTGCGTTCGTCACAGAGTTTGTGA
ACCTGGGCAATTTCTCGGCATTGAGAACATTCAGAGTTCTCCGAGCATTGAAGACGATTTTCAGTCATTCAGGCCTG
AAAACCATTGTGGGAGCCCTGATCCAGTCTGTGAAGAAGCTCTCAGATGTAATGATCCTGACTGTGTTCTGTCTGAG
CGTATTTGCTCTAATTGGGCTGCAGCTGTTTCATGGGCAACCTGAGGAATAAATGTATAACAATGGCCTCCACCAATG
CTTCCTTGGAGGAACATAGTATAGAAAAGAATATAACTGTGAATTATAATGGTACACTTATAAATGAAACTGTCTTTG
AGTTTGACTGGAAGTCATATATTCAAGATTCAAGATATCATTATTTCTGGAGGGTTTTTTAGATGCACTACTATGTG
GAAATAGCTCTGATGCAGGCCAATGTCCAGAGGGATATATGTGTGTGAAAGCTGGTAGAAATCCCAATTATGGCTA
CACAAGCTTTGATACCTTCAGTTGGGCTTTTTTGTCTTGTTCGCCTAATGACTCAGGACTTCTGGGAAAATCTTTAT
CAACTGACATTACGTGCTGCTGGGAAAACGTACATGATATTTTTGTGTTGGTCATTTTCcTaGGCTCATTCTACCTAA
TAAATTTGATCCTGGCTGTGGTGGCCATGGCCTACGAGGAACAGAATCAGGCCACCTTGAAGAAGCAGAACAGAA
AGAGGCCGAATTTACAGCAGATGATTGAACAGCTTAAAAGCAACAGGAGGCAGCTCAGCAGGCAGCAACGGCAAC
TGCCTCAGAACATTCCAGAGAGCCCAGTGCAGCAGGCAGGCTCTCAGACAGCTCATCTGAAGCCTCTAAGTTGAGTT
CCAAGAGTGCTAAGGAAAGAAGAAATCGGAGGAAGAAAAGAAAACAGAAAGAGCAGTCTGGTGGGGAAAGAGAAA
GATGAGGATGAATTCAAAAATCTGAATCTGAGGACAGCATCAGGAGGAAAGGTTTTCGCTTCTCCATTGAAGGGA
ACCGATTGACATATGAAAAGAGGTA CTCTCCCCACACCAGTCTTTGTTGAGCATCCGTGGCTCCCTATTTTCACCAA
GGCGAAATAGCAGAACAAGCCTTTTCAGCTTTAGAGGGCGAGCAAAGGATGTGGGATCTGAGAACGACTTCGCAG
ATGATGAGCACAGCACCTTTGAGGATAACGAGAGCCGTAGAGATTCCTTGTGTTTGCCCCGACGACACGGAGAGAG
ACGCAACAGCAACCTGAGTCAGACCAGTAGGTCATCCCGATGCTGGCAGTGTTCAGCGAATGGGAAGATGCAC
AGCACTGTGGATTGCAATGGTGAGGTTTCTTGGTTGGTGGACCTTCAGTTCCTACATCGCCTGTTGGACAGCTTCTG
CCAGAGGGAAACAACCACTGAAACTGAAATGAGAAAGAGAAGGTCAAGTCTTTCCACGTTTCCATGGACTTTCTAGA
AGATCCTTCCCAAAGGCAACGAGCAATGAGTATAGCCAGCATTCTAACAATAACAGTAGAAGAACTTGAAGAATCCA
GGCAGAAATGCCACCCTGTTGGTATAAATTTTCCAACATATTCTTAATCTGGGACTGTTCTCCATATTGGTTAAAAGT
GAAACATGTTGTCAACCTGGTCGTGATGGACCCATTTGTTGACCTGGCCATCACCATCTGTATTGTCTTAAATACTCTT
TTCATGGCCATGGAGCACTATCCAATGACGGACCATTTCAATAATGTGCTTACAGTAGGAAACTTGGTTTTACTGGG
ATCTTTACAGCAGAAATGTTTCTGAAAATTATTGCCATGGATCCTTACTATTATTTCCAAGAAGGCTGGAATATCTTTG
ACGGTTTTATTGTGACGCTTAGCCTGGTAGAACTTGGACTCGCCAATGTGGAAGGATTATCTGTTCTCCGTTCAATTC
GATTGCTGCGAGTTTTCAAGTTGGCAAAATCTTGGCCAACGTTAAATATGCTAATAAAGATCATCGGCAATTCCGTG
GGGGCTCTGGGAAATTAACCCTCGTCTTGGCCATCATCGTCTTCATTTTTGCCGTGGTCCGCATGCAGCTCTTGGT
AAAAGCTACAAAGATTGTGTCTGCAAGATCGCCAGTGATTGTCAACTCCCACGCTGGCACATGAATGACTTCTTCCAC
TCCTTCTGATTGTGTTCCGCGTGCTGTGTGGGGAGTGGATAGAGACCATGTGGGACTGTATGGAGGTTGCTGGTCA
AGCCATGTGCCTTACTGTCTTCATGATGGTCATGGTGATTGGAAACCTAGTGGTCCTGAATCTTTTCTGGCCTTGCTT

CTGAGCTCATTAGTGCAGACAACCTTGCAGCCACTGATGATGATAATGAAATGAATAATCTCCAAATTGCTGTGGAT
AGGATGCACAAAGGAGTAGCTTATGTGAAAAGAAAAATATATGAATTTATTCAACAGTCCTTCATTAGGAAACAAAA
GATTTTAGATGAAATTAACCACTTGATGATCTAAACAACAAGAAAGACAGTTGTATGTCCAATCATACAGCAGAAA
TTGGGAAAGATCTTGACTATCTTAAAGATGTAAATGAACTACAAGTGGTATAGGAACTGGCAGCAGTGTGAAAA
ATACATTATTGATGAAAGTGATTACATGTCATTATAACAACCCAGTCTTACTGTGACTGTACCAATTGCTGTAGG
AGAATCTGACTTTGAAAATTTAAACACGGAAGACTTTAGTAGTGAATCGGATCTGGAAGAAAGCAAAGAGAACTG
AATGAAAGCAGTAGCTCATCAGAAGGTAGCACTGTGGACATCGGCGCACCTGTAGAAGAAGCCCGTAGTGGAAC
CTGAAGAACTCTGAACCAGAAGCTTGTTCCTGACTGAAGGCTGTGTACAAAGATTCAAGTGTGTCAAATCAATGTG
GAAGAAGGCAGAGGAAAAACAATGGTGGAACTGAGAAGGACGTGTTCCGAATAGTTGAACATAACTGGTTTGAG
ACCTTCATTGTTTTATGATTCTCCTTAGTAGTGGTGTCTGGCATTGGAAGATATATATATTGATCAGCGAAAGACG
ATTAAGACGATGTTGGAATATGCTGACAAGTTTTCACTTACATTTTCATTCTGGAATGCTTCTAAAATGGGTGGCA
TATGGCTATCAAACATATTTACCAATGCCTGGTGTGGCTGGACTTCTTAATTGTTGATGTTTCATTGGTCAGTTTAA
CAGCAAATGCCTTGGGTTACTCAGAACTTGGAGCCATCAAATCTCTCAGGACACTAAGAGCTCTGAGACCTCTAAGA
GCCTTATCTCGATTTGAAGGGATGAGGGTGGTTGTGAATGCCCTTTAGGAGCAATTCATCCATCATGAATGTGCTT
CTGGTTTGTCTTATATTCTGGCTAATTTTCAGCATCATGGGCGTAAATTTGTTTGTGGCAAATTTCTACCACTGTATTA
ACACCACAACCTGGTGACAGTTTTGACATCGAAGACGTGAATAATCATACTGATTGCCTAAAATAATAGAAAGAAAT
GAGACTGCTCGATGGAAAAATGTGAAAGTAACTTTGATAATGTAGGATTTGGGTATCTCTTTGCTTCAAGTTGCC
ACATTCAAAGGATGGATGGATATAATGTATGCAGCAGTTGATTCCAGAAATGTGGAACCTCAGCCTAAGTATGAAG
AAAGTCTGTACATGTATCTTTACTTTGTTATTTTCATCATCTTTGGTCCCTTCTTACCTTGAACCTGTTTATTGGTGT
ATCATAGATAATTTCAACCAGCAGAAAAAGAAGTTTGGAGGTCAAGACATCTTTATGACAGAAGAACAGAAGAAAT
ACTATAATGCAATGAAAAAATTAGGATCGAAAAAACCGCAAAGCCTATACCTCGACCAGGAAACAAATTTCAAGG
AATGGTCTTTGACTTCGTAACCAGACAAGTTTTGACATAAGCATCATGATTCTCATCTGTCTTAACATGGTCACAATG
ATGGTGGAAACAGATGACCAGAGTGAATATGTGACTACCATTTTGTACGCATCAATCTGGTGTTCATTGTGCTATTT
ACTGGAGAGTGTGTAAGTCACTCTCTACGCCATTATTATTTACCATTGGATGGAATATTTTATTGTTTGTGG
TTGTCATTCTCTCATTGTAGGTATGTTTCTTCCGAGCTGATAGAAAAGTATTTCTGTGCCCTACCCTGTTCCGAGT
GATCCGTCTTGCTAGGATTGGCCGAATCTACGTCTGATCAAAGGAGCAAAGGGGATCCGCACGCTGCTCTTTGCTT
TGATGATGTCCCTCCTGCGTTGTTAACATCGGCCTCCTACTTCTCTAGTCATGTTTCATCTACGCCATCTTTGGGATG
TCCAATTTGCCTATGTTAAGAGGGAAGTTGGGATCGATGACATGTTCAACTTTGAGACCTTTGGCAACAGCATGAT
CTGCCTATTCCAAATTACAACCTCTGCTGGCTGGGATGGATTGCTAGCACCCATTCTCAACAGTAAGCCACCCGACTG
TGACCCTAATAAAGTTAACCTGGAAGCTCAGTTAAGGGAGACTGTGGAAACCATCTGTTGGAATTTCTTTTTTGT
CAGTTACATCATCATATCCTTCTGGTTGTGGTGAACATGTACATCGCGTCTCCTGGAGAAGTTTCAAGTGTGCTAC
TGAAGAAAGTGCAGAGCCTCTGAGTGAGGATGACTTTGAGATGTTCTATGAGGTTTGGGAGAAGTTTATCCCGAT
GCAACTCAGTTCATGGAATTTGAAAAATTATCTCAGTTTGCAGCTGCGCTTGAACCGCTCTCAATCTGCCACAACCA
AACAACTCCAGCTCATTGCCATGGATTTGCCATGGTGTGAGTGGTGACCGGATCCACTGTCTTGATATCTTATTGCT
TTTACAAAGCGGGTCTAGGAGAGAGTGGAGAGATGGATGCTCTACGAATACAGATGGAAGAGCGATTCTGGCTT
CCAATCCTTCAAGGTCTCCTATCAGCCAATCACTACTTTAAAACGAAAACAAGAGGAAGTATCTGCTGTCATTA
TTCAGCGTGCTTACAGACGCCACCTTTAAAGCGAACTGTAAAACAAGCTTCTTTACGTACAATAAAAAACAAAATCA
AAGGTGGGGCTAATCTTCTATAAAAGAAGACATGATAATTGACAGAATAAATGAAAACCTTATTACAGAAAAAAT
GATCTGACCATGTCCACTTCAGCTTGTCCACCTTCTATGACCGGGTGACAAAGCCAATTGTGGAAAAACATGAGCA
AGAAGGCAAAGATGAAAAAGCCAAAGGGAATAA

SNC1A-5N amino acid sequence:

Met EQTVLVPPGPDSFNFFTRRESLAAIERRIAEEKAKNPKPKDKKDDDENGPKPNSDLE
AGKNLPFIYGDIPPE **Met** VSEPLEDLD PYYINKKTFIVLNKKGKAIFRFSATSALYILTPF
NPLRKIAIKILVHSLFS **Met** LI **Met** CTILTNCVF **Met** T **Met** SNPPDWTKNVEYFTFTGIYTF
ESLIKIIARGFCLEDFTFLRDPWNWLDFTVITFA **F** VTEFV **N** LGN **F** SALRTFRVLRALKT
ISVIPGLKTIVGALIQSVKKLSDV **Met** ILTVFCLSVFALIGLQLF **Met** GNLRNKCIQWPPT
NASLEEHSIEKNITVNYNGTLINETVFEFDWKS YIQDSRYHYFLEGFLDALLCGNSSD
AGQCPEGY **Met** CVKAGRNP NYGYTSFDTFSWAFSLFRL **Met** TQD **F** WENLYQLTLRA
AGKTY **Met** IFFVLVIFLGSFYLINLILAVVA **Met** AYEEQNQATLEEA EQKEAEFQQ **Met** I
EQLKKQQAQAATATASEHSREPSAAGRLSDSSSEASKLSSKSAKERRNRRKRRK
QKEQSGGEEKDEDEFQKSESEDSIRRKGRFRFSIEGNRLTYEKRYSSPHQSLLSIRGSLF
SPRRNSRTSLFSFRGRAKDVGSENFADDEHSTFEDNESRRDSL FVPRRHGERRNSN
LSQTSRSSR **Met** LAVFPANGK **Met** HSTVDCNGEVS LVGGPSVPTSPVGQLLPEGTTTE
TE **Met** RKRRSSSFHVS **Met** DFLEDPSQRQRA **Met** SIASILTNTVEELESRQKCPPCWY
KFSNIFLIWDCSPYWLVKVVNLVV **Met** DPFVDLAITICIVLNTLF **Met** A **Met** EHY
P **Met** TDHFNNVLT VGNLVFTGIFTAE **Met** FLKIIA **Met** DPYYYFQEGWNIFDGFIVTLSL
VELGLANVEGLSVLRSFLLRVFKLAKSWPTLN **Met** LIKIIGNSVGALGNLTLVLAIVF
IFAVVG **Met** QLFGKSYKDCVCKIASDCQLPRWH **Met** NDFHFSFLIVFRVLCGEWIE
T **Met** WDC **Met** EVAGQA **Met** CLTVF **Met** **Met** V **Met** VIGNLVVLNLF LALLLSSFSADNLAA
TDDDNE **Met** NNLQIAVDR **Met** HKGVAYVVKRKIYEFIQQS FIRKQKILDEIKPLDDLNNK
KDSC **Met** SNHTAEIGKDL DYLKDVNGTTS GIGTGSSVEKYIIDESDY **Met** SFINNP SLTV
TVPIAVGESDFENLNTEDFSSES DLEESKEKLNESSSSSEGSTVDIGAPVEEQPVVEPE
ETLEPEACFTEGCVQRFKCCQINVEEGRGKQWNLRRTCFRIVEHNWFETFIV
F **Met** ILLSSGALAFEDIYIDQRKTIKT **Met** LEYADKVFTYIFILE **Met** LLKWVAYGYQTYF
TNAWCWLD FLIVDVSLSLTANALGYSELGAIKSLRTRLRALRPLRALS RFEG **Met** RVV
VNALLGAIPSI **Met** NVLLVCLIFWLIFS I **Met** GVNLFAGKFYHCINTTTGDRFDIEDVNN
HTDCLKLIERNETARWKNVKNVFDNVGFGYLSLLQVATFKGW **Met** DI **Met** YAAVDSR
NVELQPKYEEESLY **Met** YLYFVIFIIFGSFFTLNLFIGVIIDNFNQQKKKFGGQDIF **Met** TE
EQKKYYNA **Met** KKLGSKKPKQPIPRPGNK FQG **Met** VFDFVTRQVFDISI **Met** ILICL
N **Met** VT **Met** **Met** VETDDQSEYVT TILSRINLVFIVLFTGECVLKLISLRHYYFTIGWNIFD
FVVVILSIVG **Met** FLAELIEKYFVSPTLFRVIRLARIGRILRLIKGAKGIRTL LFA
L **Met** **Met** SLPALFNIGLLLFLV **Met** FIYAIFG **Met** SNFAYVKREVGIDD **Met** FNFETFGN
S **Met** ICLFQITTSAGWDGLLAPILNSKPPDCDPNKVNP GSSVKGDCGNPSVGIFFFVS
YIIISFLVVVN **Met** YIAVILENFSVATEESA EPLSEDDFE **Met** FYEVWEKFDPDATQ
F **Met** EFEKLSQFAAALEPPLNLPQPNKLQLIA **Met** DLP **Met** VSGDRIHCLDILFAFTKRV
LGESGE **Met** DALRIQ **Met** EERF **Met** ASNPSKVS YQPITTTLKRKQEEVSAVIIQRAYRRH
LLKRTVKQASFTYNKNKIKGGANLLIKED **Met** IIDRINENSITEKTDLT **Met** STSACPPS
YDRVTKPIVEKHEQEGKDEKAKGK **Stop**

SCN2A-6A cDNA sequence:

ATGGCACAGTCAGTGCTGGTACCGCCAGGACCTGACAGCTCCGCTTCTTACCAGGGAATCCCTTGCTGCTATTGAA
CAACGCATTGCAGAAGAGAAAAGCTAAGAGACCCAAACAGGAACGCAAGGATGAGGATGATGAAAATGGCCCAAAG
CCAAACAGTGACTTGGGAAGCAGGAAAATCTCTCCATTTATTTATGGAGACATTCCCTCCAGAGATGGTGTGCTGCCC
CTGGAGGATCTGGACCCCTACTATATCAATAAGAAAACGTTTATAGTATTGAATAAAGGGAAAGCAATCTCTCGATT
CAGTGCCACCCCTGCCCTTACATTTAACTCCCTTCAACCCTATTAGAAAATTAGCTATTAAGATTTTGGTACATTCTT
TATTCAATATGCTCATTATGTGCACGATTCTTACCAACTGTGTATTTATGACCATGAGTAACCCCTCCAGACTGGACAAA
GAATGTGGAGTATACCTTTACAGGAATTTATACTTTTGAATCACTTATTAATACTTGAAGGGGCTTTTGTTTAGA
AGATTTACATTTTACGGGATCCATGGAATTGGTTGGATTTACAGTCATTACTTTTGCATATGTGACAGAGTTTGT
GGACCTGGGCAATGTCTCAGCGTTGAGAACATTGAGAGTTCTCCGAGCATTGAAAACAATTTGATCATTCCAGGCC
TGAAGACCATTGTGGGGGCCCTGATCCAGTCAGTGAAGAAGCTTTCTGATGTCATGATCTTGACTGTGTTCTGTCTAA
GCGTGTGGCGTAATAGGATTGCAAGTTGTTGTTGTTGTTGTTGTTGTTGTTGTTGTTGTTGTTGTTGTTGTTGTTGTT
TCTTCTTTGAAATAAATATCACTTCTTCTTTAACAATTCATTGGATGGGAATGGTACTACTTTCAATAGGACAGTGA
GCATATTTAACTGGGATGAATATATTGAGGATAAAAAGTCACCTTTATTTTTTAGAGGGGCAAATGATGCTCTGCTTT
GTGGCAACAGCTCAGATGCAGGCCAGTGTCTGAAGGATACATCTGTGTGAAGGCTGGTAGAAACCCCAACTATGG
CTACACGAGCTTTGACACCTTTAGTTGGGCCTTTTTGTCCTATTTTCTGTCATGACTCAAGACTTCTGGGAAAACCTT
TATCAACTGACACTACGTGCTGCTGGGAAAACGTACATGATATTTTTTGTGCTGGTCATTTTCTGGGCTCATTCTATC
TAATAAATTTGATCTTGGCTGTGGTGGCCATGGCCTATGAGGAACAGAATCAGGCCACATTGGAAGAGGCTGAACA
GAAGGAAGCTGAATTTGAGCAGATGCTCGAACAGTTGAAAAAGCAACAAGAAGAGGCTCAGGCGGCAGCTGCAGC
CGCATCTGCTGAATCAAGAGACTTCAAGTGGTGTGGTGGGATAGGAGTTTTTTCAGAGAGTTCTTCAAGTGCATCTA
AGTTGAGCTCCAAAAGTGAAAAAGAGCTGAAAAACAGAAGAAAGAAAAAGAAACAGAAAGAACAGTCTGGAGAA
GAAGAGAAAAATGACAGAGTCCGAAAATCGGAATCTGAAGACAGCATAAGAAGAAAAGGTTTCCGTTTTTCTTGG
AAGGAAGTAGGCTGACATATGAAAAGAGATTTTCTTCTCCACACCAGTCTTACTGAGCATCCGTGGCTCCCTTTTCT
CTCCAAGACGCAACAGTAGGGCGAGCCTTTTTCAGCTTTCAGAGGTCGAGCAAAGGACATTGGCTCTGAGAATGACTTT
GCTGATGATGAGCACAGCACCTTTGAGGACAATGACAGCCGAAGAGACTCTCTGTTCTGTCGCCGACAGACATGGAG
AACGGCGCCACAGCAATGTCAGCCAGGCCAGCCGTGCCTCCAGGGTGTCTCCCATCCTGCCCATGAATGGGAAGAT
GCATAGCGCTGTGGACTGCAATGGTGTGGTCTCCCTGGTCCGGGGCCCTTCTACCCTCACATCTGCTGGGCAGCTCC
TACCAGAGGGCACAACACTACTGAAACAGAAATAAGAAAAGAGACGGTCCAGTCTTATCATGTTTCCATGGATTTATTG
GAAGATCCTACATCAAGGCAAAGAGCAATGAGTATAGCCAGTATTTTGACCAACACCATGGAAGAATTTGAAGAAT
CCAGACAGAAATGCCACCATGCTGGTATAAATTTGCTAATATGTGTTTGATTTGGGACTGTTGTAAACCATGGTTAA
AGGTGAAACACCTTGTAACCTGGTTGTAATGGACCCATTTGTTGACCTGGCCATCACCATCTGCATTGTCTTAAATA
CACTCTTCATGGCTATGGAGCACTATCCCATGACGGAGCAGTTCAGCAGTGTACTGTCTGTTGGAACCTGGTCTTCA
CAGGGATCTTACAGCAGAAATGTTTCTCAAGATAATTGCCATGGATCCATATTACTTTCAAGAAGGCTGGAATA
TTTTTGATGGTTTTATTGTGAGCCTTAGTTTAATGGAACCTGGTTTGGCAAATGTGGAAGGATTGTCAGTTCTCCGAT
CATTCCGGCTGCTCCGAGTTTTCAAGTTGGCAAATCTTGGCCAACTCTAAATATGCTAATTAAGATCATTGGCAATT
CTGTGGGGGCTCTAGGAAACCTCACCTGGTATTGGCCATCATCGTCTTCATTTTGCTGTGGTCCGGATGCAGCTCT
TTGGTAAGAGCTACAAAGAATGTGTCTGCAAGATTTCCAATGATTGTGAACTCCACGCTGGCACATGCATGACTTTT
TCCACTCTTCTGATCGTGTCCGCGTGTGTGGAGAGTGGATAGAGACCATGTGGGACTGTATGGAGGTCGCT
GGCCAAACCATGTGCCTTACTGTCTTCATGATGGTGTGATTGGAAATCTAGTGGTCTGAACCTCTTCTTGGCC

TTGCTTTTGAGTTCCTTCAGTTCTGACAATCTTGCTGCCACTGATGATGATAACGAAATGAATAATCTCCAGATTGCTG
TGGGAAGGATGCAGAAAGGAATCGATTTTGTAAAAGAAAAATACGTGAATTTATTCAGAAAGCCTTTGTTAGGAA
GCAGAAAGCTTTAGATGAAATTAACCGCTTGAAGATCTAAATAATAAAAAAGACAGCTGTATTTCCAACCATACCA
CCATAGAAATAGGCCAAAGACCTCAATTATCTCAAAGACGGAATGGAACACTAGTGGCATAGGCAGCAGTGTAGA
AAAATATGTCGTGGATGAAAGTGATTACATGTCATTTATAAAACAACCCTAGCCTCACTGTGACAGTACCAATTGCTGT
TGGAGAATCTGACTTTGAAAATTTAAATACTGAAGAATTCAGCAGCGAGTCAGATATGGAGGAAAGCAAAGAGAAG
CTAAATGCAACTAGTTCATCTGAAGGCAGCACGGTTGATATTGGAGCTCCCGCCGAGGGAGAACAGCCTGAGGTTG
AACCTGAGGAATCCCTTGAACCTGAAGCCTGTTTTACAGAAGACTGTGTACGGAAGTTCAAGTGTGTGTCAGATAAGC
ATAGAAGAAGGCAAAGGGAAACTCTGGTGGAAATTTGAGGAAAACATGCTATAAGATAGTGGAGCACAATTGGTTC
GAAACCTTCATTGTCTTCATGATTCTGCTGAGCAGTGGGGCTCTGGCCTTTGAAGATATATACATTGAGCAGCGAAA
AACCATTAAGACCATGTTAGAATATGCTGACAAGGTTTTCACTTACATATTCATTCTGGAATGCTGCTAAAGTGGGT
TGCATATGGTTTTCAAGTGTATTTTACCAATGCCTGGTGGCTAGACTTCTGATTGTTGATGTCTCACTGGTTAGC
TTAACTGCAAATGCCTTGGGTTACTCAGAACTTGGTGCCATCAAATCCCTCAGAACACTAAGAGCTCTGAGGCCACTG
AGAGCTTTGTCCCGTTTGAAGGAATGAGGGTTGTTGTAATGCTCTTTTAGGAGCCATTCCATCTATCATGAATGTA
CTTCTGGTTTGTCTGATCTTTTGGCTAATATTCAGTATCATGGGAGTGAATCTCTTTGCTGGCAAGTTTTACCATTGTA
TTAATTACACCACTGGAGAGATGTTTGATGTAAGCGTGGTCAACAACACTACAGTGAGTGCAAAGCTCTCATTGAGAGC
AATCAAACCTGCCAGGTGGAAAAATGTGAAAGTAACTTTGATAACGTAGGACTTGGATATCTGTCTCTACTTCAAGT
AGCCACGTTTAAAGGGATGGATGGATATTATGTATGCAGCTGTTGATTCACGAAATGTAGAATTACAACCCAAGTATG
AAGACAACCTGTACATGTATCTTTATTTTGTATCTTTATTATTTTTGTTTCACTTTTACCTTGAATCTTTTCATTGGTG
TCATCATAGATAACTTCAACCAACAGAAAAAGAAAGTTTGGAGGTCAAGACATTTTTATGACAGAAGAACAGAAGAA
ATACTACAATGCAATGAAAAAAGTGGTTCAAAGAAACCACAAAAACCCATACCTCGACCTGCTAACAAATTCCAAG
GAATGGTCTTTGATTTTGAACCAACAAGTCTTTGATATCAGCATCATGATCCTCATCTGCCTAACATGGTCACCAT
GATGGTGGAAACCGATGACCAGAGTCAAGAAATGACAAACATTCTGTAAGTGGATTAATCTGGTGTATTATTGTTCTGT
TCACTGGAGAATGTGTGCTGAAACTGATCTCTCTCGTTACTACTATTTCACTATTGGATGGAATATTTTTGATTTTGT
GGTGGTCACTTCTCCATTGTAGGAATGTTTCTGGCTGAACTGATAGAAAAGTATTTTGTGTCCCCTACCCTGTTCCG
AGTGATCCGTCTTGCCAGGATTGGCCGAATCCTACGTCTGATCAAAGGAGCAAAGGGGATCCGCACGCTGCTCTTTG
CTTTGATGATGTCCCTCCTGCGTTGTTAACATCGGCCTCCTCTTTTCTGGTCACTTTCATCTACGCCATCTTTGGG
ATGTCCAATTTTGCCTATGTTAAGAGGGAAAGTTGGGATCGATGACATGTTCAACTTTGAGACCTTTGGCAACAGCAT
GATCTGCCTGTTCCAAATTACAACCTCTGCTGGCTGGGATGGATTGCTAGCACCTATTCTTAATAGTGGACCTCCAGA
CTGTGACCCTGACAAAGATCACCTGGAAGCTCAGTTAAAGGAGACTGTGGGAACCCATCTGTTGGGATTTTCTTTTT
TGTCAGTTACATCATCATATCCTTCTGGTTGTGGTGAACATGTACATCGCGGTCATCCTGGAGAATTCAGTGTTC
TACTGAAGAAAGTGCAGAGCCTCTGAGTGAGGATGACTTTGAGATGTTCTATGAGGTTTGGGAGAAGTTTGATCCC
GATGCGACCCAGTTTATAGAGTTTGCCAAACTTTCTGATTTTGCAGATGCCCTGGATCCTCCTCTTCTCATAGCAAAC
CCAACAAAGTCCAGCTCATTGCCATGGATCTGCCATGGTGAGTGGTGACCGGATCCACTGTCTTGACATCTTATTTG
CTTTTACAAGCGTGTTTTGGGTGAGAGTGGAGAGATGGATGCCCTTGAATACAGATGGAAGAGCGATTTCATGGC
ATCAAACCCCTCAAAGTCTCTTATGAGCCATTACGACCACGTTGAAACGCAAACAAGAGGAGGTGTCTGCTATTAT
TATCCAGAGGGCTTACAGACGCTACCTCTTGAAGCAAAAAGTTAAAAAGGTATCAAGTATATACAAGAAAGACAAA
GGCAAAGAATGTGATGGAACACCCATCAAAGAAGATACTCTCATTGATAAACTGAATGAGAATTCAACTCCAGAGA
AAACCGATATGACGCCTTCCACCACGTCTCCACCCTCGTATGATAGTGTGACCAAACCGAAAAAGAAAAATTTGAA
AAAGACAAATCAGAAAAGGAAGACAAAGGGAAAGATATCAGGGAAAGTAAAAAGTAA

SCN2A-6A amino acid sequence:

MetAQSVLVPPGPDSFRFFFTRESLAAIEQRIAEKAKRPKQERKDEDDENGPKPNSDL
EAGKSLPFIYGDIPPE **Met**VSVPLEDLDPYYINKKTFIVLNKGKAISRFSATPALYILTPF
NPIRKLAIKILVHSLFN **Met**LI **Met**CTILTNCV **Met**T **Met**SNPPDWTKNVEYTFGTIYTF
ESLIKILARGFCLEDFTLRDPWNWLDFTVITFAYVTEFV **D**LGNVSALRTRVLRALK
TISVIPGLKTIVGALIQSVKKLSDV **Met**ILTVFCLSVFALIGLQLF **Met**GNLRNKCLQWP
PDNSSFEINITSFFNNSLDGNGTTFNRTVSIFNWDEYIEDKSHFYFLEGQNDALLCGN
SSDAGQCPEGYICVKAGRNPNYGYTSFDTFSWAFLSLFRL **Met**TQD **F**WENLYQLTLR
AAGKTY **Met**IFFVLVIFLGSFYLINLILAVVA **Met**AYEEQNQATLEEAQEKEAEFQ
Q **Met**LEQLKKQEEEAQAAAAAASAESRDFSGAGGIGVFSESSSVASKLSSKSEKELKN
RRKKKKQKEQSGEEKNDRVRKSESEDSIRRKGFRRFSLEGSRLTYEKRFSSPHQSLLSI
RGSLSFPRRNSRASLFSFRGRAKDIGSENDFADDEHSTFEDNDSRRDSLFPVPHRGE
RRHSNVSQASRASRVLPILP **Met**NGK **Met**HSAVDCNGVVSLVGGPSTLTSAGQLLPEG
TTTETEIRKRRSSSYHVS **Met**DLLEDPTSRQRA **Met**SIASILTNT **Met**EELEESRQKCPP
CWYKFAN **Met**CLIWDCCKPWLKVKHLVNLVV **Met**DPFVDLAITICIVLNTL
F **Met**A **Met**EHYP **Met**TEQFSSVLSVGNLVFTGIFTAE **Met**FLKIIA **Met**DPYFFFQEGWN
IFDGFIVSLSL **Met**ELGLANVEGLSVLRSFRLLRVFKLAKSWPTLN **Met**LIKIIGNSVGA
LGNLTLVLAIIVFIFAVVG **Met**QLFGKSYKECVCKISNDCELPRWH **Met**HDFHHSFLIVF
RVLCGEWIET **Met**WDC **Met**EVAGQT **Met**CLTVF **Met** **Met**VMetVIGNLVVLNLFALLLS
SFSSDNLAATDDDNE **Met**NNLQIAVGR **Met**QKGFDFVKKIREFIQKAFVRKQKALDE
IKPLEDLNKKDSCISNHTTIEIGKDLNYLKDGNNGTTSIGSSVEKYVVDSESY **Met**SF
INNPSTVTVPIAVGESDFENLNTEEFSSSED **Met**EESKEKLNATSSSEGSTVDIGAPA
EGEQPEVEPEESLEPEACFTEDCVRKFKCCQISIEEGKGLWWNLRKTCYKIVEHNW
FETFIVF **Met**ILLSSGALAFEDIYIEQRKTIKT **Met**LEYADKVFTYIFILE **Met**LLKWVAYG
FQVYFTNAWCWLDLIVDVSLSLTANALGYSELGAIKSLRTLRLRPLRALSFE
G **Met**RVVVNALLGAIPSI **Met**NVLLVCLIFWLIFS **Met**GVNLFAGKFYHCINYTTG
E **Met**FDVSVVNNYSECKALIESNQARWKNVKVNFNDNVGLGYLSLLQVATFKG
W **Met**DI **Met**YAAVDSRNVELQPKYEDNLY **Met**YLYFVIFIIFGSFFTLNLFIVGVIIDNFN
QQKKKFGGQDIF **Met**TEEQKKYYNA **Met**KKLGSKKPQKPIPRPANKFQG **Met**VDFVFT
KQVFDISI **Met**ILICLN **Met**VT **Met** **Met**VETDDQSQE **Met**TNILYWINLVFIVLFTGECVL
KLISLRYYYFTIGWNIFDFVVLVLSIVG **Met**FLAELIEKYFVSPTLFRVIRLARIGRILRLI
KGAKGIRTLFAL **Met** **Met**SLPALFNIGLLLFLV **Met**FIYAIFG **Met**SNFAYVKREVGID
D **Met**FNFETFGNS **Met**ICLFQITTSAGWDGLLAPILNSGPPDCDPDKDHPGSSVKGDC
GNPSVGIFFFVSYIIISFLVVVN **Met**YIAVILENFSVATEESAEPLEDDFE **Met**FYEVW
EKFDPPDATQFIEFAKLSDFADALDPPLLIAPKPNKVQLIA **Met**DLP **Met**VSGDRIHCLDIL
FAFTKRVLGESGE **Met**DALRIQ **Met**EERF **Met**ASNPSKVSYPEPITTTLKRKQEEVSAIIIQ
RAYRRYLLKQKVKVSSIYKKDKGKECDGTPIKEDTLIDKLNENSTPEKTD **Met**TPSTT
SPPSYDSVTKPEKEKFEKDKSEKEDKGKDIRESKK **Stop**

SCN2A-5N cDNA sequence:

ATGGCACAGTCAGTGCTGGTACCGCCAGGACCTGACAGCTCCGCTTCTTACCAGGGAATCCCTTGCTGCTATTGAA
CAACGCATTGCAGAAGAGAAAAGCTAAGAGACCCAAACAGGAACGCAAGGATGAGGATGATGAAAATGGCCCAAAG
CCAAACAGTGACTTGGGAAGCAGGAAAATCTCTCCATTTATTTATGGAGACATTCCCTCCAGAGATGGTGTGCTGCCC
CTGGAGGATCTGGACCCCTACTATATCAATAAGAAAACGTTTATAGTATTGAATAAAGGGAAAGCAATCTCTCGATT
CAGTGCCACCCCTGCCCTTACATTTAACTCCCTTCAACCCTATTAGAAAATTAGCTATTAAGATTTTGGTACATTCTT
TATTCAATATGCTCATTATGTGCACGATTCTTACCAACTGTGTATTTATGACCATGAGTAACCCCTCCAGACTGGACAAA
GAATGTGGAGTATACCTTTACAGGAATTTATACTTTTGAATCACTTATTAATACTTGAAGGGGCTTTTGTTTAGA
AGATTTACATTTTACGGGATCCATGGAATTGGTTGGATTTACAGTCATTACTTTTGCATATGTGACAGAGTTTGT
GAACTGGGCAATGTCTCAGCGTTGAGAACATTCAGAGTTCTCCGAGCATTGAAAACAATTTAGTCATTCCAGGCC
TGAAGACCATTGTGGGGGCCCTGATCCAGTCAGTGAAGAAGCTTTCTGATGTCATGATCTTGACTGTGTTCTGTCTAA
GCGTGTGGCGTAATAGGATTGCAGTTGTTTCATGGGCAACCTACGAAATAAATGTTTGAATGGCCTCCAGATAAT
TCTTCCTTTGAAATAAATATCACTTCCTTCTTAAACAATTCATTGGATGGGAATGGTACTACTTTCAATAGGACAGTGA
GCATATTTAACTGGGATGAATATATTGAGGATAAAAAGTCACTTTTATTTTTAGAGGGGCAAATGATGCTCTGCTTT
GTGGCAACAGCTCAGATGCAGGCCAGTGTCTGAAGGATACATCTGTGTGAAGGCTGGTAGAAACCCCAACTATGG
CTACACGAGCTTTGACACCTTTAGTTGGGCCTTTTTGTCCTATTTTCTCATGACTCAAGACTTCTGGGAAAACCTT
TATCAACTGACACTACGTGCTGCTGGGAAAACGTACATGATATTTTTTGTGCTGGTCATTTTCTGGGCTCATTCTATC
TAATAAATTTGATCTTGGCTGTGGTGGCCATGGCCTATGAGGAACAGAATCAGGCCACATTGGAAGAGGCTGAACA
GAAGGAAGCTGAATTTAGCAGATGCTCGAACAGTTGAAAAAGCAACAAGAAGAGGCTCAGGCGGCAGCTGCAGC
CGCATCTGCTGAATCAAGAGACTTCAGTGGTGTGGTGGGATAGGAGTTTTTTCAGAGAGTTCTTCAGTAGCATCTA
AGTTGAGCTCCAAAAGTGAAAAAGAGCTGAAAAACAGAAGAAAGAAAAAGAAACAGAAAGAACAGTCTGGAGAA
GAAGAGAAAAATGACAGAGTCCGAAAATCGGAATCTGAAGACAGCATAAGAAGAAAAGGTTTCCGTTTTCTTTGG
AAGGAAGTAGGCTGACATATGAAAAGAGATTTTCTTCTCCACACCAGTCTTACTGAGCATCCGTGGCTCCCTTTCT
CTCCAAGACGCAACAGTAGGGCGAGCCTTTTTCAGCTTCAGAGGTCGAGCAAAGGACATTGGCTCTGAGAATGACTTT
GCTGATGATGAGCACAGCACCTTTGAGGACAATGACAGCCGAAGAGACTCTCTGTTCTGTCGCCGACAGACATGGAG
AACGGCGCCACAGCAATGTCAGCCAGGCCAGCCGTGCCTCCAGGGTGTCTCCCATCCTGCCCATGAATGGGAAGAT
GCATAGCGCTGTGGACTGCAATGGTGTGGTCTCCCTGGTCCGGGGCCCTTCTACCCTCACATCTGCTGGGCAGCTCC
TACCAGAGGGCACAACTACTGAAACAGAAATAAGAAAAGAGACGGTCCAGTTCCTATCATGTTTCCATGGATTTATTG
GAAGATCCTACATCAAGGCAAAGAGCAATGAGTATAGCCAGTATTTTGACCAACACCATGGAAGAATTTGAAGAAT
CCAGACAGAAATGCCACCATGCTGGTATAAATTTGCTAATATGTGTTTGATTTGGGACTGTTGTAAACCATGGTTAA
AGGTGAAACACCTTGTAACCTGGTTGTAATGGACCCATTTGTTGACCTGGCCATCACCATCTGCATTGTCTTAAATA
CACTCTTCATGGCTATGGAGCACTATCCCATGACGGAGCAGTTCAGCAGTGTACTGTCTGTTGGAACCTGGTCTTCA
CAGGGATCTTACAGCAGAAATGTTTCTCAAGATAATTGCCATGGATCCATATTACTTTCAAGAAGGCTGGAATA
TTTTTGATGGTTTTATTGTGAGCCTTAGTTTAATGGAACCTGGTTTGGCAAATGTGGAAGGATTGTCAGTTCTCCGAT
CATTCCGGCTGCTCCGAGTTTTCAAGTTGGCAAATCTTGGCCAACTCTAAATATGCTAATTAAGATCATTGGCAATT
CTGTGGGGGCTCTAGGAAACCTCACCTGGTATTGGCCATCATCGTCTTCATTTTGCTGTGGTCCGCATGCAGCTCT
TTGGTAAGAGCTACAAAGAATGTGTCTGCAAGATTTCCAATGATTGTGAACTCCACGCTGGCACATGCATGACTTTT
TCCACTCCTTCTGATCGTGTCCGCGTGTGTGGAGAGTGGATAGAGACCATGTGGGACTGTATGGAGGTCGCT
GGCCAAACCATGTGCCTTACTGTCTTCATGATGGTTCATGGTATTGGAAATCTAGTGGTCTGAACCTCTTCTGGCC

TTGCTTTTGAGTTCCTTCAGTTCTGACAATCTTGCTGCCACTGATGATGATAACGAAATGAATAATCTCCAGATTGCTG
TGGGAAGGATGCAGAAAGGAATCGATTTTGTAAAAGAAAAATACGTGAATTTATTCAGAAAGCCTTTGTTAGGAA
GCAGAAAGCTTTAGATGAAATTAACCGCTTGAAGATCTAAATAATAAAAAAGACAGCTGTATTTCCAACCATACCA
CCATAGAAATAGGCCAAAGACCTCAATTATCTCAAAGACGGAATGGAACACTACTAGTGGCATAGGCAGCAGTGTAGA
AAAATATGTCGTGGATGAAAGTGATTACATGTCATTTATAAAACAACCCTAGCCTCACTGTGACAGTACCAATTGCTGT
TGGAGAATCTGACTTTGAAAATTTAAATACTGAAGAATTCAGCAGCGAGTCAGATATGGAGGAAAGCAAAGAGAAG
CTAAATGCAACTAGTTCATCTGAAGGCAGCACGGTTGATATTGGAGCTCCCGCCGAGGGAGAACAGCCTGAGGTTG
AACCTGAGGAATCCCTTGAACCTGAAGCCTGTTTTACAGAAGACTGTGTACGGAAGTTCAAGTGTGTGTCAGATAAGC
ATAGAAGAAGGCAAAGGGAAACTCTGGTGGAATTTGAGGAAAACATGCTATAAGATAGTGGAGCACAATTGGTTC
GAAACCTTCATTGTCTTCATGATTCTGCTGAGCAGTGGGGCTCTGGCCTTTGAAGATATATACATTGAGCAGCGAAA
AACCATTAAGACCATGTTAGAATATGCTGACAAGGTTTTCACTTACATATTCATTCTGGAATGCTGCTAAAGTGGGT
TGCATATGGTTTTCAAGTGTATTTTACCAATGCCTGGTGCTGGCTAGACTTCTGATTGTTGATGTCTCACTGGTTAGC
TTAACTGCAAATGCCTTGGGTTACTCAGAACTTGGTGCCATCAAATCCCTCAGAACACTAAGAGCTCTGAGGCCACTG
AGAGCTTTGTCCCGTTTTGAAGGAATGAGGGTTGTTGTAATGCTCTTTTAGGAGCCATTCCATCTATCATGAATGTA
CTTCTGGTTTTGTCTGATCTTTTGGCTAATATTCAGTATCATGGGAGTGAATCTCTTTGCTGGCAAGTTTTACCATTGTA
TTAATTACACCACTGGAGAGATGTTTGATGTAAGCGTGGTCAACAACACTACAGTGAGTGCAAAGCTCTCATTGAGAGC
AATCAAACCTGCCAGGTGGAAAAATGTGAAAGTAACTTTGATAACGTAGGACTTGGATATCTGTCTCTACTTCAAGT
AGCCACGTTTAAGGGATGGATGGATATTATGTATGCAGCTGTTGATTACGAAATGTAGAATTACAACCCAAGTATG
AAGACAACCTGTACATGTATCTTTATTTTGTATCTTTATTATTTTTGTTTCACTTTTACCTTGAATCTTTTCATTGGTG
TCATCATAGATAACTTCAACCAACAGAAAAAGAAAGTTTGGAGGTCAAGACATTTTTATGACAGAAGAACAGAAGAA
ATACTACAATGCAATGAAAAAAGTGGTTCAAAGAAACCACAAAAACCCATACCTCGACCTGCTAACAAATTCGAAG
GAATGGTCTTTGATTTTGAACCAACAAGTCTTTGATATCAGCATCATGATCCTCATCTGCCTAACATGGTCACCAT
GATGGTGGAAACCGATGACCAGAGTCAAGAAATGACAAACATTCTGTAAGTAACTGATGATAAGTAACTGATGATAAG
TCACTGGAGAATGTGTGCTGAAACTGATCTCTCTTCGTTACTACTATTTCACTATTGGATGGAATATTTTTGATTTTGT
GGTGGTCACTTCTCCATTGTAGGAATGTTTCTGGCTGAACTGATAGAAAAGTATTTTGTGTCCCCTACCCTGTTCCG
AGTGATCCGTCTTGCCAGGATTGGCCGAATCCTACGTCTGATCAAAGGAGCAAAGGGGATCCGCACGCTGCTCTTTG
CTTTGATGATGTCCCTCCTGCGTTGTTAACATCGGCCTCCTTCTTTTCTGGTCATGTTTCTACGCCATCTTTGGG
ATGTCCAATTTTGCCTATGTTAAGAGGGAAAGTTGGGATCGATGACATGTTCAACTTTGAGACCTTTGGCAACAGCAT
GATCTGCCTGTTCCAAATTACAACCTCTGCTGGCTGGGATGGATTGCTAGCACCTATTCTTAATAGTGGACCTCCAGA
CTGTGACCCTGACAAAGATCACCTGGAAGCTCAGTTAAAGGAGACTGTGGGAACCCATCTGTTGGGATTTTCTTTTT
TGTCAGTTACATCATCATATCCTTCTGGTTGTGGTGAACATGTACATCGCGGTCATCCTGGAGAATTCAGTGTTGC
TACTGAAGAAAGTGCAGAGCCTCTGAGTGAGGATGACTTTGAGATGTTCTATGAGGTTTGGGAGAAGTTTGATCCC
GATGCGACCCAGTTTATAGAGTTTGCCAAACTTTCTGATTTTGCAGATGCCCTGGATCCTCCTCTTCTCATAGCAAAC
CCAACAAAGTCCAGCTCATTGCCATGGATCTGCCATGGTGAGTGGTGACCGGATCCACTGTCTTGACATCTTATTTG
CTTTTACAAGCGTGTGTTTGGGTGAGAGTGGAGAGATGGATGCCCTTGAATACAGATGGAAGAGCGATTTCATGGC
ATCAAACCCCTCAAAGTCTCTTATGAGCCATTACGACCACGTTGAAACGCAAACAAGAGGAGGTGTCTGCTATTAT
TATCCAGAGGGCTTACAGACGCTACCTCTTGAAGCAAAAAGTTAAAAAGGTATCAAGTATATACAAGAAAGACAAA
GGCAAAGAATGTGATGGAACCCCATCAAAGAAGATACTCTCATTGATAAACTGAATGAGAATTCAACTCCAGAGA
AAACCGATATGACGCCTTCCACCACGTCTCCACCCTCGTATGATAGTGTGACCAAACCGAAAAAGAAAAATTTGAA
AAAGACAAATCAGAAAAGGAAGACAAAGGGAAAGATATCAGGGAAAGTAAAAAGTAA

SCN2A-5N amino acid sequence:

MetAQSVLVPPGPDSFRFFFTRESLAAIEQRIAEKAKRPKQERKDEDDENGPKPNSDL
EAGKSLPFIYGDIPPE **Met**VSVPLEDLDPYYINKKTFIVLNKGKAISRFSATPALYILTPF
NPIRKLAIKILVHSLFN **Met**LI **Met**CTILTNCV **Met**T **Met**SNPPDWTKNVEYTFGTIYTF
ESLIKILARGFCLEDFTLRDPWNWLDFTVITFAYVTEFV **N**LGNVSALRTRVLRALK
TISVIPGLKTIVGALIQSVKKLSDV **Met**ILTVFCLSVFALIGLQLF **Met**GNLRNKCLQWP
PDNSSFEINITSFFNNSLDGNGTTFNRTVSIFNWDEYIEDKSHFYFLEGQNDALLCGN
SSDAGQCPEGYICVKAGRNPNYGYTSFDTFSWAFLSLFRL **Met**TQD **F**WENLYQLTLR
AAGKTY **Met**IFFVLVIFLGSFYLINLILAVVA **Met**AYEEQNQATLEEAQEKEAEFQ
Q **Met**LEQLKKQEEEAQAAAAAASAESRDFSGAGGIGVFSESSSVASKLSSKSEKELKN
RRKKKKQKEQSGEEKNDRVRKSESEDSIRRKGFRRFSLEGSRLTYEKRFSSPHQSLLSI
RGSLSFPRRNSRASLFSFRGRAKDIGSENDFADDEHSTFEDNDSRRDSLFPVPHRGE
RRHSNVSQASRASRVLPILP **Met**NGK **Met**HSAVDCNGVVSLVGGPSTLTSAGQLLPEG
TTTETEIRKRRSSSYHVS **Met**DLLEDPTSQRRA **Met**SIASILTNT **Met**EELEESRQKCPP
CWYKFAN **Met**CLIWDCCKPWLKVKHLVNLVV **Met**DPFVDLAITICIVLNTL
F **Met**A **Met**EHYP **Met**TEQFSSVLSVGNLVFTGIFTAE **Met**FLKIIA **Met**DPYFFFQEGWN
IFDGFIVSLSL **Met**ELGLANVEGLSVLRSFRLLRVFKLAKSWPTLN **Met**LIKIIGNSVGA
LGNLTLVLAIIVFIFAVVG **Met**QLFGKSYKECVCKISNDCELPRWH **Met**HDFHHSFLIVF
RVLCGEWIET **Met**WDC **Met**EVAGQT **Met**CLTVF **Met** **Met**V **Met**VIGNLVVLNLFALLLS
SFSSDNLAATDDDNE **Met**NNLQIAVGR **Met**QKGI DFVKKIREFIQKAFVRKQKALDE
IKPLEDLNKKDSCISNHTTIEIGKDLNYLKDGNNGTTSIGIGSSVEKYVVDSDY **Met**SF
INNPSTVTVPIAVGESDFENLNTEEFSSSD **Met**EESKEKLNATSSSEGSTVDIGAPA
EGEQPEVEPEESLEPEACFTEDCVRKFKCCQISIEEGKGLWWNLRKTCYKIVEHNW
FETFIVF **Met**ILLSSGALAFEDIYIEQRKTIKT **Met**LEYADKVFTYIFILE **Met**LLKWVAYG
FQVYFTNAWCWLDFLIVDVSLSLTANALGYSELGAIKSLRTLRLRPLRALS RFE
G **Met**RVVVNALLGAIPSI **Met**NVLLVCLIFWLIFS **Met**GVNLFAGKFYHCINYTTG
E **Met**FDVSVVNNYSECKALIESNQARWKNVKVNFNDNVGLGYLSLLQVATFKG
W **Met**DI **Met**YAAVDSRNVELQPKYEDNLY **Met**YLYFVIFIIFGSFFTLNLFIVGVIIDNFN
QQKKKFGGQDIF **Met**TEEQKKYYNA **Met**KKLGSKKPQKPIPRPANKFQG **Met**VDFVFT
KQVFDISI **Met**ILICLN **Met**VT **Met** **Met**VETDDQSQE **Met**TNILYWINLVFIVLFTGECVL
KLISLRYYYFTIGWNIFDFVVLVLSIVG **Met**FLAELIEKYFVSPTLFRVIRLARIGRILRLI
KGAKGIRTLFAL **Met** **Met**SLPALFNIGLLLFLV **Met**FIYAIFG **Met**SNFAYVKREVGID
D **Met**FNFETFGNS **Met**ICLFQITTSAGWDGLLAPILNSGPPDCDPDKDHPGSSVKGDC
GNPSVGIFFFVSYIIISFLVVVN **Met**YIAVILENFSVATEESAEPLEDDFE **Met**FYEVW
EKFDPPDATQFIEFAKLSDFADALDPPLLIAPKPNKVQLIA **Met**DLP **Met**VSGDRIHCLDIL
FAFTKRVLGESGE **Met**DALRIQ **Met**EERF **Met**ASNPSKVSYPITTTLKRKQEEVSAIIIQ
RAYRRYLLKQKVKKVSSIYKKDKGKECDGTPIKEDTLIDKLNENSTPEKTD **Met**TPSTT
SPPSYDSVTKPEKEKFEKDKSEKEDKGKDIRESKK **Stop**

SNC9A-5A cDNA sequence:

ATGGCAATGTTGCCTCCCCAGGACCTCAGAGCTTTGTCCATTTACAAAACAGTCTCTTGCCTCATTGAACAACGC
ATTGCTGAAAGAAAATCAAAGGAACCCAAAGAAGAAAAGAAAGATGATGATGAAGAAGCCCCAAAGCCAAGCAGT
GACTTGGAAGCTGGCAAACAACCTGCCCTTCATCTATGGGGACATTCCTCCCGCATGGTGTGAGAGCCCTGGAGGA
CTTGACCCTACTATGCAGACAAAAGACTTTTCATAGTATTGAACAAAGGGAAAACAATCTTCCGTTTCAATGCCAC
ACCTGCTTTATATATGCTTTCTCCTTTCAGTCCTCTAAGAAGAATATCTATTAAGATTTTAGTACACTCCTTATTCAGCA
TGCTCATCATGTGCACTATTCTGACAACTGCATATTTATGACCATGAATAACCCGCCGGACTGGACCAAAAATGTGC
AGTACACTTTTACTGGAATATATACTTTTGAATCACTTGTAAAAATCCTTGCAAGAGGCTTCTGTGTAGGAGAATTCA
CTTTTCTTCGTGACCCGTGGAACCTGGCTGGATTTTGTGTCATTGTTTTTGCATGACAGAAATTTGTAGACCTAG
GCAATGTTTCAGCTCTTCGAACTTTCAGAGTATTGAGAGCTTTGAAAATCTTCTGTAATCCCAGGCCTGAAGACAA
TTGTAGGGGCTTTGATCCAGTCAGTGAAGAAGCTTTCTGATGTCATGATCCTGACTGTGTTCTGTCTGAGTGTGTTG
CACTAATTGGACTACAGCTGTTTCATGGGAAACCTGAAGCATAAATGTTTTCGAAATCACTTGAAAATAATGAAACAT
TAGAAAGCATAATGAATACCTAGAGAGTGAAGAAGACTTTAGAAAATATTTTTATTACTTGAAGGATCCAAAGAT
GCTCTCCTTTGTGGTTTCAGCACAGATTCAGGTCAGTGTCCAGAGGGGTACACCTGTGTGAAAATTGGCAGAAACCC
TGATTATGGCTACACGAGCTTTGACACTTTTCAGCTGGCCTTCTTAGCCTTGTGTTAGGCTAATGACCCAAGATTACTG
GGAAAACCTTTACCAACAGACGCTGCGTGCTGCTGGCAAACCTACATGATCTTCTTTGTCGTAGTGATTTTCCTGGG
CTCCTTTTATCTAATAAACTTGATCCTGGCTGTGGTTGCCATGGCATATGAAGAACAGAACCAGGCAAACATTGAAG
AAGCTAAACAGAAAGAATTAGAATTTCAACAGATGTTAGACCGTCTTAAAAAAGAGCAAGAAGAAGCTGAGGCAAT
TGCAGCGCAGCGGCTGAATATACAAGTATTAGGAGAAGCAGAATTATGGGCCTCTCAGAGAGTTCTTCTGAAACA
TCCAAACTGAGCTCTAAAAGTGCTAAAGAAAAGAAGAAACAGAAGAAAGAAAAAGAATCAAAGAAGCTCTCCAGT
GGAGAGGAAAAGGGAGATGCTGAGAAATTGTCGAAATCAGAATCAGAGGACAGCATCAGAAGAAAAGTTTCCAC
CTTGGTGTGCAAGGGCATAGGCGAGCACATGAAAAGAGGTTGTCTACCCCAATCAGTCACTACTCAGCATTCTGGG
CTCCTTGTGTTTCTGCAAGGCGAAGCAGCAGAACAAGTCTTTTTAGTTTCAAAGGCAGAGGAAGAGATATAGGATCTG
AGACTGAATTTGCCGATGATGAGCACAGCATTTTTGGAGACAATGAGAGCAGAAGGGGCTCACTGTTTGTGCCCA
CAGACCCAGGAGCGACGCAGCAGTAACATCAGCCAAGCCAGTAGGTCCCACCAATGCTGCCGGTGAACGGGAA
AATGCACAGTGTGTGGACTGCAACGGTGTGGTCTCCCTGGTTGATGGACGCTCAGCCCTCATGCTCCCAATGGAC
AGCTTCTGCCAGAGGGCACGACCAATCAAATACACAAGAAAAGGCGTTGTAGTTCCTATCTCCTTTCAGAGGATATG
CTGAATGATCCCAACCTCAGACAGAGCAATGAGTAGAGCAAGCATATTAACAAACTGTGGAAGAAGCTTGAAG
AGTCCAGACAAAATGTCCACCTTGGTGGTACAGATTTGCACACAAATCTTGATCTGGAATTGCTCTCCATATTGGA
TAAAATTCAAAAAGTGTATCTATTTTATTGTAATGGATCCTTTTGTAGATCTTGCAATTACCATTTGCATAGTTTTAAC
ACATTATTTATGGCTATGGAACACCACCAATGACTGAGGAATTCAAAAATGTAATGCTATAGGAAATTTGGTCTTT
ACTGGAATCTTTCAGCTGAAATGGTATTAATAACTGATTGCCATGGATCCATATGAGTATTTCCAAGTAGGCTGGAA
TATTTTTGACAGCCTTATTGTGACTTTAAGTTTGTGGAGCTCTTCTAGCAGATGTGGAAGGATTGTCAGTTCTGCG
ATCATTGACTGCTCCGAGTCTCAAGTTGGCAAATCCTGGCCAACATTGAACATGCTGATTAAGATCATTGGTAA
CTCAGTAGGGGCTCTAGGTAACCTCACCTTAGTGTGGCCATCATCGTCTTCATTTTGCTGTGGTCCGCATGCAGCT
CTTTGGTAAGAGCTACAAAGAATGTGTCTGCAAGATCAATGATGACTGTACGCTCCACGGTGGCACATGAACGACT
TCTTCCACTCCTTCTGATTGTGTTCCGCGTGTGTGTGGAGAGTGGATAGAGACCATGTGGGACTGTATGGAGGTC
GCTGGTCAAGCTATGTGCCTTATTGTTTACATGATGGTCATGGTCATTGGAAAACCTGGTGGTCTAAACCTATTTCTG
GCCTTATTATTGAGCTCATTAGTTCAGACAATCTTACAGCAATTGAAGAAGACCCTGATGCAAACAACCTCCAGATT

GCAGTGA CTAGAATTA AAAAGGGAATAAATTATGTGAAACAAACCTTACGTGAATTTATTCTAAAAGCATTTCCTCAA
AAAGCCAAAGATTTCCAGGGAGATAAGACAAGCAGAAGATCTGAATACTAAGAAGGAAAACCTATATTTCTAACCAT
ACACTTGCTGAAATGAGCAAAGGTCACAATTTCTCAAGGAAAAAGATAAAATCAGTGGTTTTGGAAGCAGCGTGG
ACAAACACTTGATGGAAGACAGTGATGGTCAATCATTATTACAATCCCAGCCTCACAGTGACAGTGCCAATTGCA
CCTGGGGAATCCGATTTGGAAAATATGAATGCTGAGGAACTTAGCAGTGATTCGGATAGTGAATACAGCAAAGTGA
GATTAACCGGTCAAGCTCCTCAGAGTGCAGCACAGTTGATAACCCCTTGCCTGGAGAAGGAGAAGAAGCAGAGGC
TGAACCTATGAATCCGATGAGCCAGAGGCCTGTTTCACAGATGGTTGTGTACGGAGGTTCTCATGCTGCCAAGTTA
ACATAGAGTCAGGGAAAGGAAAAATCTGGTGAACATCAGGAAAACCTGCTACAAGATTGTTGAACACAGTTGGTT
TGAAAGCTTCATTGTCCTCATGATCCTGCTCAGCAGTGGTGCCCTGGCTTTTGAAGATATTTATATTGAAAGGAAAA
GACCATTAAGATTATCCTGGAGTATGCAGACAAGATCTTCACTTACATCTTCACTTCTGGAATGCTTCTAAAATGGAT
AGCATATGGTTATAAAACATATTTACCAATGCCTGGTGTGGCTGGATTTCCTAATTGTTGATGTTTCTTGGTTACT
TTAGTGGCAAACACTCTTGGCTACTCAGATCTTGGCCCATTAATCCCTTCGGACACTGAGAGCTTTAAGACCTCTA
AGAGCCTTATCTAGATTTGAAGGAATGAGGGTCGTTGTGAATGCACTCATAGGAGCAATTCCTTCCATCATGAATGT
GCTACTTGTGTCTTATATTCTGGCTGATATTCAGCATCATGGGAGTAAATTTGTTTGGTGGCAAGTTCTATGAGTG
TATTAACACCACAGATGGGTACGGTTTCTGCAAGTCAAGTTCAAATCGTTCCGAATGTTTTGCCCTTATGAATGT
TAGTCAAATGTGCGATGGAAAAACCTGAAAGTGAACCTTGTATAATGTCGGACTTGGTTACCTATCTCTGCTTCAAGT
TGCAACTTTAAGGGATGGACGATTATTATGTATGCAGCAGTGGATTCTGTTAATGTAGACAAGCAGCCCAAATATG
AATATAGCCTCTACATGTATATTTATTTTGTGCTCTTATCATCTTGGGTCACTTCTTCACTTTGAACCTGTTCAATTGGT
GTCATCATAGATAATTTCAACCAACAGAAAAAGAGCTTGGAGGTCAAGACATCTTTATGACAGAAGAACAGAAGA
AATACTATAATGCAATGAAAAAGCTGGGGTCCAAGAAGCCACAAAAGCCAATTCCTCGACCAGGGAACAAAATCCA
AGGATGTATATTTGACCTAGTGACAAATCAAGCCTTTGATATTAGTATCATGGTTCTTATCTGTCTCAACATGGTAACC
ATGATGGTAGAAAAGGAGGGTCAAAGTCAACATATGACTGAAGTTTTATATTGGATAAATGTGGTTTTTATAATCCT
TTTCACTGGAGAATGTGTGCTAAAACCTGATCTCCCTCAGACACTACTACTTCACTGTAGGATGGAATATTTTTGATTTT
GTGGTTGTGATTATCTCCATTGTAGGTATGTTTCTAGCTGATTTGATTGAAACGATTTTTGTGTCCCTACCTGTTCC
GAGTGATCCGTCTTGCCAGGATTGGCCGAATCCTACGTCTAGTCAAAGGAGCAAAGGGGATCCGCACGCTGCTCTTT
GCTTTGATGATGTCCCTTCTGCGTTGTTTAAACATCGGCCTCCTGCTCTTCTGGTCATGTTTCTACGCCATCTTTGG
AATGTCCAACCTTGCCTATGTTAAAAAGGAAGATGGAATTAATGACATGTTCAATTTTGGAGACCTTTGGCAACAGTAT
GATTTGCCTGTTCCAAATTACAACCTCTGCTGGCTGGGATGGATTGCTAGCACCTATTCTTAACAGTAAGCCACCCGA
CTGTGACCCAAAAAAGTTTATCCTGGAAGTTTCAAGTTGAAGGAGACTGTGGTAACCCATCTGTTGGAATATTCTACTT
TGTTAGTTATATCATCATATCCTTCTGGTTGTGGTGAACATGTACATTGCAGTCATACTGGAGAATTTTAGTGTGGC
ACTGAAGAAAGTACTGAACCTCTGAGTGAGGATGACTTTGAGATGTTCTATGAGGTTTGGGAGAAGTTTGTATCCCG
ATGCGACCCAGTTTATAGAGTTCTTAAACTCTGATTTTGCAGCTGCCCTGGATCCTCCTTCTCATAGCAAACCC
CAACAAAGTCCAGCTCATTGCCATGGATCTGCCATGGTTAGTGGTGACCGGATCCATTGTCTTGACATCTTATTTGC
TTTTACAAAGCGTGTGTTTGGGTGAGAGTGGGGAGATGGATTCTTTCGTTACAGATGGAAGAAAGGTTTCTATGTCTG
CAAATCCTTCAAAGTGTCTATGAACCCATCACAACCACACTAAAACGGAAACAAGAGGATGTGTCTGCTACTGTC
ATTCAGCGTGCTTATAGACGTTACCGCTTAAAGGCAAAATGTCAAAAATATATCAAGTATATACATAAAAGATGGAGA
CAGAGATGATGATTTACTCAATAAAAAAGATATGGCTTTTGTATAATGTTAATGAGAACTCAAGTCCAGAAAAACAG
ATGCCACTTCATCCACCCTCTCCACCTTCATATGATAGTGAACAAAGCCAGACAAGAGAAATATGAACAAGACA
GAACAGAAAAGGAAGACAAAGGGAAAGACAGCAAGGAAAGCAAAAATAG

SCN9A-5A amino acid sequence:

Met A Met L P P P G P Q S F V H F T K Q S L A L I E Q R I A E R K S K E P K E E K K D D D E E A P K P S S D L E A
G K Q L P F I Y G D I P P G **Met** V S E P L E D L D P Y Y A D K K T F I V L N K G K T I F R F N A T P A L Y **Met** L S P
F S P L R R I S I K I L V H S L F S **Met** L I **Met** C T I L T N C I F **Met** T **Met** N N P P D W T K N V E Y T F T G I Y T F
E S L V K I L A R G F C V G E F T F L R D P W N W L D F V V I V F A Y **V** T E F V **D** L G N V S A L R T F R V L R A L
K T I S V I P G L K T I V G A L I Q S V K K L S D V **Met** I L T V F C L S V F A L I G L Q L F **Met** G N L K H K C F R N S
L E N N E T L E S I **Met** N T L E S E E D F R K Y F Y L E G S K D A L L C G F S T D S G Q C P E G Y T C V K I G R N
P D Y G Y T S F D T F S W A F L A L F R L **Met** T Q D **Y** W E N L Y Q Q T L R A A G K T Y **Met** I F F V V V I F L G S
F Y L I N L I L A V V A **Met** A Y E E Q N Q A N I E E A K Q K E L E F Q Q **Met** L D R L K K E Q E E A E A I A A A A A
E Y T S I R R S R I **Met** G L S E S S S E T S K L S S K S A K E R R N R R K K N Q K K L S S G E E K G D A E K L S K S
E S E D S I R R K S F H L G V E G H R R A H E K R L S T P N Q S P L S I R G S L F S A R R S S R T S L F S F K G R G R
D I G S E T E F A D D E H S I F G D N E S R R G S L F V P H R P Q E R R S S N I S Q A S R S P P **Met** L P V N G
K **Met** H S A V D C N G V V S L V D G R S A L **Met** L P N G Q L L P E G T T N Q I H K K R R C S S Y L L S E
D **Met** L N D P N L R Q R A **Met** S R A S I L T N T V E E L E E S R Q K C P P W W Y R F A H K F L I W N C S P Y W
I K F K K C I Y F I V **Met** D P F V D L A I T I C I V L N T L F **Met** A **Met** E H H P **Met** T E E F K N V L A I G N L V F T
G I F A A E **Met** V L K L I A **Met** D P Y E Y F Q V G W N I F D S L I V T L S L V E L F L A D V E G L S V L R S F R L L
R V F K L A K S W P T L N **Met** L I K I I G N S V G A L G N L T L V L A I I V F I F A V V G **Met** Q L F G K S Y K E C V
C K I N D D C T L P R W H **Met** N D F F H S F L I V F R V L C G E W I E T **Met** W D C **Met** E V A G Q A **Met** C L I
V Y **Met** **Met** V **Met** V I G N L V L N L F L A L L L S S F S S D N L T A I E E D P D A N N L Q I A V T R I K K G I N
Y V K Q T L R E F I L K A F S K K P K I S R E I R Q A E D L N T K K E N Y I S N H T L A E **Met** S K G H N F L K E K D
K I S G F G S S V D K H L **Met** E D S D G Q S F I H N P S L T V T V P I A P G E S D L E N **Met** N A E E L S S D S D S
E Y S K V R L N R S S S E C S T V D N P L P G E G E E A E A E P **Met** N S D E P E A C F T D G C V R R F S C C Q V
N I E S G K G K I W W N I R K T C Y K I V E H S W F E S F I V L **Met** I L L S S G A L A F E D I Y I E R K K T I K I I L E
Y A D K I F T Y I F I L E **Met** L L K W I A Y G Y K T Y F T N A W C W L D F L I V D V S L V T L V A N T L G Y S D L G
P I K S L R T L R A L R P L R A L S R F E G **Met** R V V V N A L I G A I P S I **Met** N V L L V C L I F W L I F S I **Met** G
V N L F A G K F Y E C I N T T D G S R F P A S Q V P N R S E C F A L **Met** N V S Q N V R W K N L K V N F D N V G
L G Y L S L L Q V A T F K G W T I I **Met** Y A A V D S V N V D K Q P K Y E Y S L Y **Met** Y I Y F V V F I I F G S F F T L
N L F I G V I I D N F N Q Q K K L G G Q D I F **Met** T E E Q K K Y Y N A **Met** K K L G S K K P Q K P I P R P G N K I
Q G C I F D L V T N Q A F D I S I **Met** V L I C L N **Met** V T **Met** **Met** V E K E G Q S Q H **Met** T E V L Y W I N V V F
I I L F T G E C V L K L I S L R H Y Y F T V G W N I F D F V V V I I S I V **GMet** F L A D L I E T Y F V S P T L F R V I R L
A R I G R I L R L V K G A K G I R T L L F A L **Met** **Met** S L P A L F N I G L L L F L V **Met** F I Y A I F G **Met** S N F A Y
V K K E D G I N D **Met** F N F E T F G N S **Met** I C L F Q I T T S A G W D G L L A P I L N S K P P D C D P K K V H P
G S S V E G D C G N P S V G I F Y F V S Y I I I S F L V V V N **Met** Y I A V I L E N F S V A T E E S T E P L S E D D F
E **Met** F Y E V W E K F D P D A T Q F I E F S K L S D F A A A L D P P L L I A K P N K V Q L I A **Met** D L P **Met** V S
G D R I H C L D I L F A F T K R V L G E S G E **Met** D S L R S Q **Met** E E R F **Met** S A N P S K V S Y E P I T T T L K R
K Q E D V S A T V I Q R A Y R R Y R L R Q N V K N I S S I Y I K D G R D D D L L N K K D **Met** A F D N V N E N S
S P E K T D A T S S T T S P P S Y D S V T K P D K E K Y E Q D R T E K E D K G K D S K E S K K **Stop**

SNC9A-5N cDNA sequence:

ATGGCAATGTTGCCTCCCCAGGACCTCAGAGCTTTGTCCATTTACAAAACAGTCTCTTGCCCTCATTGAACAACGC
ATTGCTGAAAGAAAATCAAAGGAACCCAAAGAAGAAAAGAAAGATGATGATGAAGAAGCCCCAAAGCCAAGCAGT
GACTTGGAAGCTGGCAAACAACTGCCCTTCATCTATGGGGACATTCCTCCCGCATGGTGTGAGAGCCCCTGGAGGA
CTTGACCCTACTATGCAGACAAAAGACTTTTCATAGTATTGAACAAAGGGAAAACAATCTTCCGTTTCAATGCCAC
ACCTGCTTTATATATGCTTTCTCCTTTCAGTCCTCTAAGAAGAATATCTATTAAGATTTTAGTACACTCCTTATTCAGCA
TGCTCATCATGTGCACTATTCTGACAACTGCATATTTATGACCATGAATAACCCGCCGGACTGGACCAAAAATGTG
AGTACACTTTTACTGGAATATATACTTTTGAATCACTTGTAAAAATCCTTGCAAGAGGCTTCTGTGTAGGAGAATTCA
CTTTTCTTTCGTGACCCGTGGAAGTGGCTGGATTTTGTGTCATTGTTTTTTCGTATTACAGAAATTTGTAACCTAGG
CAATGTTTCAGCTCTTCGAACTTTCAGAGTATTGAGAGCTTTGAAAATCTTGTAAATCCCAGGCCTGAAGACAAT
TGTAGGGGCTTTGATCCAGTCAGTGAAGAAGCTTTCTGATGTCATGATCCTGACTGTGTTCTGTCTGAGTGTGTTTGC
ACTAATTGGACTACAGCTGTTTCATGGGAAACCTGAAGCATAAATGTTTTCGAAATTCACCTGAAAATAATGAAACATT
AGAAAGCATAATGAATACCCTAGAGAGTGAAGAAGACTTTAGAAAATATTTTTATTACTTGAAGGATCCAAAGATG
CTCTCCTTTGTGGTTTTAGCACAGATTCAGGTGAGTGTCCAGAGGGGTACACCTGTGTGAAAATTGGCAGAAACCT
GATTATGGCTACACGAGCTTTGACACTTTCAGCTGGGCTTCTTAGCCTGTTTAGGCTAATGACCCAAGATTACTGG
GAAAACCTTTACCAACAGACGCTGCGTGCTGCTGGCAAACCTACATGATCTTCTTGTGCTAGTGATTTTCTGGGC
TCCTTTTATCTAATAAACTTGATCCTGGCTGTGGTTGCCATGGCATATGAAGAACAGAACCCAGGCAAACATTGAAGA
AGCTAAACAGAAAGAATTAGAATTTCAACAGATGTTAGACCGTCTTAAAAAAGAGCAAGAAGAAGCTGAGGCAATT
GCAGCGGCAGCGGCTGAATATACAAGTATTAGGAGAAGCAGAATTATGGGCTCTCAGAGAGTTCTTCTGAAACAT
CCAACTGAGCTCTAAAAGTGCTAAAGAAAGAAGAAACAGAAAGAAAGAAAAGAATCAAAGAAGCTCTCCAGTG
GAGAGGAAAAGGGAGATGCTGAGAAATTGTGCAATCAGAATCAGAGGACAGCATCAGAAGAAAAAGTTTCCACC
TTGGTGTGCAAGGGCATAGGCGAGCAGCATGAAAAGAGTTGTCTACCCCAATCAGTCACTCAGCATTCTGTTGGC
TCCTTGTCTTCTGCAAGGCGAAGCAGCAGAACAAGTCTTTTGTAGTTTCAAAGGCAGAGGAAGAGATATAGGATCTGA
GACTGAATTTGCCGATGATGAGCACAGCATTTTGGAGACAATGAGAGCAGAAGGGGCTCACTGTTTGTGCCCCAC
AGACCCAGGAGCGACGACGAGTAACATCAGCCAAGCCAGTAGGTCCCCACCAATGCTGCCGGTGAACGGGAAA
ATGCACAGTGTGTGGACTGCAACGGTGTGGTCTCCCTGGTTGATGGACGCTCAGCCCTCATGCTCCCAATGGACA
GCTTCTGCCAGAGGGCAGACCAATCAAATACACAAGAAAAGGCGTTGTAGTTCCTATCTCCTTTCAGAGGATATGC
TGAATGATCCCAACCTCAGACAGAGCAATGAGTAGAGCAAGCATATTAACAAACACTGTGGAAGAATTGAAGA
GTCCAGACAAAATGTCCACCTTGGTGGTACAGATTTGCACACAAATCTTGATCTGGAATTGCTCTCCATATTGGAT
AAAATTCAAAAAGTGTATCTATTTTATTGTAATGGATCCTTTTGTAGATCTTGCAATTACCATTTGCATAGTTTTAAC
ACATTATTTATGGCTATGGAACACCACCAATGACTGAGGAATTCAAAAATGTAATTGCTATAGGAAATTTGGTCTTT
ACTGGAATCTTTCAGCTGAAATGGTATTAATAACTGATTGCCATGGATCCATATGAGTATTTCCAAGTAGGCTGGAA
TATTTTTGACAGCCTTATTGTGACTTTAAGTTTGTGGAGCTCTTCTAGCAGATGTGGAAGGATTGTCAGTTCTGCG
ATCATTGACTGCTCCGAGTCTTCAAGTTGGCAAATCCTGGCCAACATTGAACATGCTGATTAAGATCATTGGTAA
CTCAGTAGGGGCTCTAGGTAACCTCACCTTAGTGTGGCCATCATCGTCTTCAATTTTGTGTTGGTCCGCATGCAGCT
CTTTGGTAAGAGCTACAAAGAATGTGTCTGCAAGATCAATGATGACTGTACGCTCCACGGTGGCACATGAACGACT
TCTTCCACTCCTTCTGATTGTGTTCCGCGTGCTGTGTGGAGAGTGGATAGAGACCATGTGGGACTGTATGGAGGTC
GCTGGTCAAGCTATGTGCCTTATTGTTTACATGATGGTCATGGTCATTGGAAAACCTGGTGGTCTAAACCTATTTCTG
GCCTTATTATTGAGCTCATTAGTTCAGACAATCTTACAGCAATTGAAGAAGACCCTGATGCAAACAACCTCCAGATT

GCAGTGA CTAGAATTA AAAAGGGAATAAATTATGTGAAACAAACCTTACGTGAATTTATTCTAAAAGCATTTCCTCAA
AAAGCCAAAGATTTCCAGGGAGATAAGACAAGCAGAAGATCTGAATACTAAGAAGGAAAACCTATATTTCTAACCAT
ACACTTGCTGAAATGAGCAAAGGTCACAATTTCTCAAGGAAAAAGATAAAATCAGTGGTTTTGGAAGCAGCGTGG
ACAAACACTTGATGGAAGACAGTGATGGTCAATCATTATTACAATCCCAGCCTCACAGTGACAGTGCCAATTGCA
CCTGGGGAATCCGATTTGGAAAATATGAATGCTGAGGAACTTAGCAGTGATTCGGATAGTGAATACAGCAAAGTGA
GATTAACCCGGTCAAGCTCCTCAGAGTGCAGCACAGTTGATAACCCCTTGCCTGGAGAAGGAGAAGAAGCAGAGGC
TGAACCTATGAATTCCGATGAGCCAGAGGCCTGTTTCACAGATGGTTGTGTACGGAGGTTCTCATGCTGCCAAGTTA
ACATAGAGTCAGGGAAAGGAAAAATCTGGTGAACATCAGGAAAACCTGCTACAAGATTGTTGAACACAGTTGGTT
TGAAAGCTTCATTGTCCTCATGATCCTGCTCAGCAGTGGTGCCTGGCTTTTGAAGATATTTATATTGAAAGGAAAA
GACCATTAAGATTATCCTGGAGTATGCAGACAAGATCTTCACTTACATCTTCATTCTGGAAATGCTTCTAAAATGGAT
AGCATATGGTTATAAAACATATTTACCAATGCCTGGTGTGGCTGGATTTCCTAATTGTTGATGTTTCTTGGTTACT
TTAGTGGCAAACACTCTTGGCTACTCAGATCTTGGCCCATTAATCCCTTCGGACACTGAGAGCTTTAAGACCTCTA
AGAGCCTTATCTAGATTTGAAGGAATGAGGGTCGTTGTGAATGCACTCATAGGAGCAATTCCTTCCATCATGAATGT
GCTACTTGTGTCTTATATTCTGGCTGATATTCAGCATCATGGGAGTAAATTTGTTTGCTGGCAAGTTCTATGAGTG
TATTAACACCACAGATGGGTACGGTTTCTGCAAGTCAAGTTCAAATCGTTCCGAATGTTTTGCCCTTATGAATGT
TAGTCAAATGTGCGATGGAAAAACCTGAAAGTGAACCTTGTATAATGTCGGACTTGGTTACCTATCTCTGCTTCAAGT
TGCAACTTTAAGGGATGGACGATTATTATGTATGCAGCAGTGGATTCTGTTAATGTAGACAAGCAGCCCAAATATG
AATATAGCCTCTACATGTATATTTATTTGTCGTCTTATCATCTTGGGTCACTTCACTTTGAACCTGTTCAATTGGT
GTCATCATAGATAATTTCAACCAACAGAAAAAGGCTTGGAGGTCAAGACATCTTATGACAGAAGAACAGAAGA
AATACTATAATGCAATGAAAAAGCTGGGGTCCAAGAAGCCACAAAAGCCAATTCCTCGACCAGGGAACAAAATCCA
AGGATGTATATTTGACCTAGTGACAAATCAAGCCTTTGATATTAGTATCATGGTTCTTATCTGTCTCAACATGGTAACC
ATGATGGTAGAAAAGGAGGGTCAAAGTCAACATATGACTGAAGTTTTATATTGGATAAATGTGGTTTTTATAATCCT
TTTCACTGGAGAATGTGTGCTAAAACCTGATCTCCCTCAGACACTACTACTTCACTGTAGGATGGAATATTTTTGATTTT
GTGGTTGTGATTATCTCCATTGTAGGTATGTTTCTAGCTGATTTGATTGAAACGATTTTTGTGTCCCTACCTGTTCC
GAGTGATCCGTCTTGCCAGGATTGGCCGAATCCTACGTCTAGTCAAAGGAGCAAAGGGGATCCGCACGCTGCTCTTT
GCTTTGATGATGTCCCTCCTGCGTTGTTTAAACATCGGCCTCCTGCTCTTCTGGTCATGTTTCTACGCCATCTTTGG
AATGTCCAACCTTGCCTATGTTAAAAAGGAAGATGGAATTAATGACATGTTCAATTTTGGAGACCTTTGGCAACAGTAT
GATTTGCCTGTTCAAATTACAACCTCTGCTGGCTGGGATGGATTGCTAGCACCTATTCTTAACAGTAAGCCACCCGA
CTGTGACCCAAAAAAGTTCATCCTGGAAGTTCAGTTGAAGGAGACTGTGGTAACCCATCTGTTGGAATATTCTACTT
TGTTAGTTATATCATCATATCCTTCTGGTTGTGGTGAACATGTACATTGCAGTCATACTGGAGAATTTTAGTGTGCC
ACTGAAGAAAGTACTGAACCTCTGAGTGAGGATGACTTTGAGATGTTCTATGAGGTTTGGGAGAAGTTTGTATCCCG
ATGCGACCCAGTTTATAGAGTTCTCTAAACTCTCTGATTTTGCAGCTGCCCTGGATCCTCCTCTCATAGCAAACCC
CAACAAAGTCCAGCTCATTGCCATGGATCTGCCATGGTTAGTGGTGACCGGATCCATTGTCTTGACATCTTATTTGC
TTTTACAAAGCGTGTGTTTGGGTGAGAGTGGGGAGATGGATTCTTTCGTTACAGATGGAAGAAAGGTTTCTATGCTG
CAAATCCTTCAAAGTGTCTATGAACCCATCACAACCACACTAAAACGGAAACAAGAGGATGTGTCTGCTACTGTC
ATTCAGCGTGCTTATAGACGTTACCGCTTAAAGGCAAAATGTCAAAAATATATCAAGTATATACATAAAAGATGGAGA
CAGAGATGATGATTTACTCAATAAAAAAGATATGGCTTTTGTATAATGTTAATGAGAACTCAAGTCCAGAAAAACAG
ATGCCACTTCATCCACCCTCTCCACCTTCATATGATAGTGAACAAAGCCAGACAAAGAGAAATATGAACAAGACA
GAACAGAAAAGGAAGACAAAGGGAAAGACAGCAAGGAAAGCAAAAATAG

SCN9A-5N amino acid sequence:

Met A Met L P P P G P Q S F V H F T K Q S L A L I E Q R I A E R K S K E P K E E K K D D D E E A P K P S S D L E A
G K Q L P F I Y G D I P P G **Met** V S E P L E D L D P Y Y A D K K T F I V L N K G K T I F R F N A T P A L Y **Met** L S P
F S P L R R I S I K I L V H S L F S **Met** L I **Met** C T I L T N C I F **Met** T **Met** N N P P D W T K N V E Y T F T G I Y T F
E S L V K I L A R G F C V G E F T F L R D P W N W L D F V V I V F A Y **L** T E F V **N** L G N V S A L R T F R V L R A L K
T I S V I P G L K T I V G A L I Q S V K K L S D V **Met** I L T V F C L S V F A L I G L Q L F **Met** G N L K H K C F R N S L
E N N E T L E S I **Met** N T L E S E E D F R K Y F Y L E G S K D A L L C G F S T D S G Q C P E G Y T C V K I G R N P
D Y G Y T S F D T F S W A F L A L F R L **Met** T Q D **Y** W E N L Y Q Q T L R A A G K T Y **Met** I F F V V V I F L G S F
Y L I N L I L A V V A **Met** A Y E E Q N Q A N I E E A K Q K E L E F Q Q **Met** L D R L K K E Q E E A E A I A A A A A E
Y T S I R R S R I **Met** G L S E S S S E T S K L S S K S A K E R R N R R K K N Q K K L S S G E E K G D A E K L S K S E
S E D S I R R K S F H L G V E G H R R A H E K R L S T P N Q S P L S I R G S L F S A R R S S R T S L F S F K G R G R
D I G S E T E F A D D E H S I F G D N E S R R G S L F V P H R P Q E R R S S N I S Q A S R S P P **Met** L P V N G
K **Met** H S A V D C N G V V S L V D G R S A L **Met** L P N G Q L L P E G T T N Q I H K K R R C S S Y L L S E
D **Met** L N D P N L R Q R A **Met** S R A S I L T N T V E E L E E S R Q K C P P W W Y R F A H K F L I W N C S P Y W
I K F K K C I Y F I V **Met** D P F V D L A I T I C I V L N T L F **Met** A **Met** E H H P **Met** T E E F K N V L A I G N L V F T
G I F A A E **Met** V L K L I A **Met** D P Y E Y F Q V G W N I F D S L I V T L S L V E L F L A D V E G L S V L R S F R L L
R V F K L A K S W P T L N **Met** L I K I I G N S V G A L G N L T L V L A I I V F I F A V V G **Met** Q L F G K S Y K E C V
C K I N D D C T L P R W H **Met** N D F F H S F L I V F R V L C G E W I E T **Met** W D C **Met** E V A G Q A **Met** C L I
V Y **Met** **Met** V **Met** V I G N L V V L N L F L A L L L S S F S S D N L T A I E E D P D A N N L Q I A V T R I K K G I N
Y V K Q T L R E F I L K A F S K K P K I S R E I R Q A E D L N T K K E N Y I S N H T L A E **Met** S K G H N F L K E K D
K I S G F G S S V D K H L **Met** E D S D G Q S F I H N P S L T V T V P I A P G E S D L E N **Met** N A E E L S S D S D S
E Y S K V R L N R S S S E C S T V D N P L P G E G E E A E A E P **Met** N S D E P E A C F T D G C V R R F S C C Q V
N I E S G K G K I W W N I R K T C Y K I V E H S W F E S F I V L **Met** I L L S S G A L A F E D I Y I E R K K T I K I I L E
Y A D K I F T Y I F I L E **Met** L L K W I A Y G Y K T Y F T N A W C W L D F L I V D V S L V T L V A N T L G Y S D L G
P I K S L R T L R A L R P L R A L S R F E G **Met** R V V V N A L I G A I P S I **Met** N V L L V C L I F W L I F S I **Met** G
V N L F A G K F Y E C I N T T D G S R F P A S Q V P N R S E C F A L **Met** N V S Q N V R W K N L K V N F D N V G
L G Y L S L L Q V A T F K G W T I I **Met** Y A A V D S V N V D K Q P K Y E Y S L Y **Met** Y I Y F V V F I I F G S F F T L
N L F I G V I I D N F N Q Q K K K L G G Q D I F **Met** T E E Q K K Y Y N A **Met** K K L G S K K P Q K P I P R P G N K I
Q G C I F D L V T N Q A F D I S I **Met** V L I C L N **Met** V T **Met** **Met** V E K E G Q S Q H **Met** T E V L Y W I N V V F
I I L F T G E C V L K L I S L R H Y Y F T V G W N I F D F V V V I I S I V **GMet** F L A D L I E T Y F V S P T L F R V I R L
A R I G R I L R L V K G A K G I R T L L F A L **Met** **Met** S L P A L F N I G L L L F L V **Met** F I Y A I F G **Met** S N F A Y
V K K E D G I N D **Met** F N F E T F G N S **Met** I C L F Q I T T S A G W D G L L A P I L N S K P P D C D P K K V H P
G S S V E G D C G N P S V G I F Y F V S Y I I I S F L V V V N **Met** Y I A V I L E N F S V A T E E S T E P L S E D D F
E **Met** F Y E V W E K F D P D A T Q F I E F S K L S D F A A A L D P P L L I A K P N K V Q L I A **Met** D L P **Met** V S
G D R I H C L D I L F A F T K R V L G E S G E **Met** D S L R S Q **Met** E E R F **Met** S A N P S K V S Y E P I T T T L K R
K Q E D V S A T V I Q R A Y R R Y R L R Q N V K N I S S I Y I K D G R D D D L L N K K D **Met** A F D N V N E N S
S P E K T D A T S S T T S P P S Y D S V T K P D K E K Y E Q D R T E K E D K G K D S K E S K K **Stop**

SCN1A-5A **TTX-Resistant** cDNA sequence:

ATGGAGCAAACAGTGCTTGTACCACCAGGACCTGACAGCTTCAACTTCTCACCAGAGAATCTCTTGCGGCTATTGAA
AGACGCATTGCAGAAGAAAAGGCAAAGAATCCCAAACCAGACAAAAAAGATGACGACGAAAATGGCCCAAAGCCA
AATAGTGACTTGAAGCTGGAAAGAACCTTCCATTTATTTATGGAGACATTCCTCCAGAGATGGTGTGAGAGCCCT
GGAGGACCTGGACCCCTACTATATCAATAAGAAAACCTTTATAGTATTGAATAAAGGGAAGGCCATCTCCGGTTCA
GTGCCACCTCTGCCCTGTACATTTAACTCCCTTCAATCCTCTTAGGAAAATAGCTATTAAGATTTTGGTACATTCATTA
TTCAGCATGCTAATTATGTGCACTATTTTGACAACTGTGTGTTTATGACAATGAGTAACCCCTCTGATTGGACAAAG
AATGTAGAATACACCTTCACAGGAATATATACTTTTGAATCACTTATAAAAATTATTGCAAGGGGATTCTGTTTAGAA
GATTTTACTTTCTTCGGGATCCATGGAAGTGGCTCGATTTCACTGTCATTACATTTGCGTACGTCACAGAGTTTGTGG
ACCTGGGCAATGCTCTCGGCATTGAGAACATTCAGAGTTCTCCGAGCATTGAAGACGATTTAGTCATTCCAGGCCTG
AAAACCATTGTGGGAGCCCTGATCCAGTCTGTGAAGAAGCTCTCAGATGTAATGATCCTGACTGTGTTCTGTCTGAG
CGTATTGCTCTAATTGGGCTGCAGCTGTTTCATGGGCAACCTGAGGAATAAATGTATAACAATGGCCTCCACCAATG
CTTCCTTGGAGGAACATAGTATAGAAAAGAATATAACTGTGAATTATAATGGTACACTTATAAATGAAACTGTCTTTG
AGTTTGACTGGAAGTCATATATTCAAGATTCAAGATATCATTATTTCTGGAGGGTTTTTTAGATGCACTACTATGTG
GAAATAGCTCTGATGCAGGCCAATGTCCAGAGGGATATATGTGTGTGAAAGCTGGTAGAAATCCCAATTATGGCTA
CACAAGCTTTGATACCTTCAGTTGGGCTTTTTTGTCTTGTTCGCCTAATGACTCAGGACTCTGGGAAAATCTTTAT
CAACTGACATTACGTGCTGCTGGGAAAACGTACATGATATTTTTGTGTTGGTCATTTTCcTaGGCTCATTCTACCTAA
TAAATTTGATCCTGGCTGTGGTGGCCATGGCCTACGAGGAACAGAATCAGGCCACCTTGAAGAAGCAGAACAGAA
AGAGGCCGAATTTAGCAGATGATTGAACAGCTTAAAAGCAACAGGAGGCAGCTCAGCAGGCAGCAACGGCAAC
TGCCTCAGAACATTCCAGAGAGCCCAGTGCAGCAGGCAGGCTCTCAGACAGCTCATCTGAAGCCTCTAAGTTGAGTT
CCAAGAGTGCTAAGGAAAGAAGAAATCGGAGGAAGAAAAGAAAACAGAAAGAGCAGTCTGGTGGGGAAAGAGAAA
GATGAGGATGAATTTCAAAAATCTGAATCTGAGGACAGCATCAGGAGGAAAGGTTTTTCGCTTCTCCATTGAAGGGA
ACCGATTGACATATGAAAAGAGGTAATCCTCCCCACACCAGTCTTTGTTGAGCATCCGTGGCTCCCTATTTTACCAA
GGCGAAATAGCAGAACAAGCCTTTTTCAGCTTTAGAGGGCGAGCAAAGGATGTGGGATCTGAGAACGACTTCGCAG
ATGATGAGCACAGCACCTTTGAGGATAACGAGAGCCGTAGAGATTCCTTGTGTTTGCCCCGACGACACGGAGAGAG
ACGCAACAGCAACCTGAGTCAGACCAGTAGGTCATCCCGGATGCTGGCAGTGTTCAGCGAATGGGAAGATGCAC
AGCACTGTGGATTGCAATGGTGGAGTTTCTTGGTGGTGGACCTTCAGTTCTACATCGCCTGTTGGACAGCTTCTG
CCAGAGGGAAACAACCACTGAAACTGAAATGAGAAAGAGAAGGTCAAGTTCTTTCCACGTTTCCATGGACTTTCTAGA
AGATCCTTCCCAAAGGCAACGAGCAATGAGTATAGCCAGCATTCTAACAATAACAGTAGAAGAACTTGAAGAATCCA
GGCAGAAATGCCACCCTGTTGGTATAAATTTTCCAACATATTCTTAATCTGGGACTGTTCTCCATATTGGTTAAAAGT
GAAACATGTTGTCAACCTGGTCGTGATGGACCCATTTGTTGACCTGGCCATCACCATCTGTATTGTCTTAAATACTCTT
TTCATGGCCATGGAGCACTATCCAATGACGGACCATTTCAATAATGTGCTTACAGTAGGAAACTTGGTTTTTCACTGGG
ATCTTTACAGCAGAAATGTTTCTGAAAATTATTGCCATGGATCCTTACTATTATTTCCAAGAAGGCTGGAATATCTTTG
ACGGTTTTATTGTGACGCTTAGCCTGGTAGAACTTGGACTCGCCAATGTGGAAGGATTATCTGTTCTCCGTTCAATTC
GATTGCTGCGAGTTTTCAAGTTGGCAAAATCTTGGCCAACGTTAAATATGCTAATAAAGATCATCGGCAATTCCGTG
GGGGCTCTGGGAAATTAACCCTCGTCTTGGCCATCATCGTCTTCATTTTTGCCGTGGTCCGCATGCAGCTCTTTGGT
AAAAGCTACAAAGATTGTGTCTGCAAGATCGCCAGTGATTGTCAACTCCCACGCTGGCACATGAATGACTTCTTCCAC
TCCTTCTGATTGTGTTCCGCGTGCTGTGTGGGGAGTGGATAGAGACCATGTGGGACTGTATGGAGGTTGCTGGTCA
AGCCATGTGCCTTACTGTCTTCATGATGGTCATGGTGATTGGAAACCTAGTGGTCCTGAATCTTTTCTGGCCTTGCTT

CTGAGCTCATTAGTGCAGACAACCTTGCAGCCACTGATGATGATAATGAAATGAATAATCTCCAAATTGCTGTGGAT
AGGATGCACAAAGGAGTAGCTTATGTGAAAAGAAAAATATATGAATTTATTCAACAGTCCTTCATTAGGAAACAAAA
GATTTTAGATGAAATTAACCACTTGATGATCTAAACAACAAGAAAGACAGTTGTATGTCCAATCATACAGCAGAAA
TTGGGAAAGATCTTGACTATCTTAAAGATGTAAATGAACTACAAGTGGTATAGGAACTGGCAGCAGTGTGAAAA
ATACATTATTGATGAAAGTGATTACATGTCATTCATAACAACCCAGTCTTACTGTGACTGTACCAATTGCTGTAGG
AGAATCTGACTTTGAAAATTTAAACACGGAAGACTTTAGTAGTGAATCGGATCTGGAAGAAAGCAAAGAGAACTG
AATGAAAGCAGTAGCTCATCAGAAGGTAGCACTGTGGACATCGGCGCACCTGTAGAAGAAGCCCGTAGTGGAAC
CTGAAGAACTCTGAACCAGAAGCTTGTTCCTGACTGAAGGCTGTGTACAAAGATTCAAGTGTGTCAAATCAATGTG
GAAGAAGGCAGAGGAAAAACAATGGTGGAACTGAGAAGGACGTGTTCCGAATAGTTGAACATAACTGGTTTGAG
ACCTTCATTGTTTTATGATTCTCCTTAGTAGTGGTGTCTGGCATTGGAAGATATATATATTGATCAGCGAAAGACG
ATTAAGACGATGTTGGAATATGCTGACAAGTTTTCACTTACATTTTTATTCTGGAATGCTTCTAAAATGGGTGGCA
TATGGCTATCAAACATATTTACCAATGCCTGGTGTGGCTGGACTTCTTAATTGTTGATGTTTCATTGGTCAGTTTAA
CAGCAAATGCCTTGGGTTACTCAGAACTTGGAGCCATCAAATCTCTCAGGACACTAAGAGCTCTGAGACCTCTAAGA
GCCTTATCTCGATTTGAAGGGATGAGGGTGGTTGTGAATGCCCTTTAGGAGCAATCCATCCATCATGAATGTGCTT
CTGGTTTGTCTTATATTCTGGCTAATTTTCAGCATCATGGGCGTAAATTTGTTTGTGGCAAATTTCTACCACTGTATTA
ACACCACAACCTGGTGACAGTTTTGACATCGAAGACGTGAATAATCATACTGATTGCCTAAAATAATAGAAAGAAAT
GAGACTGCTCGATGGAAAAATGTGAAAGTAACTTTGATAATGTAGGATTTGGGTATCTCTTTGCTTCAAGTTGCC
ACATTCAAAGGATGGATGGATATAATGTATGCAGCAGTTGATTCCAGAAATGTGGAACCTCAGCCTAAGTATGAAG
AAAGTCTGTACATGTATCTTTACTTTGTTATTTTCATCATCTTTGGTCCCTTCTTACCTTGAACCTGTTTATTGGTGT
ATCATAGATAATTTCAACCAGCAGAAAAAGAAGTTTGGAGGTCAAGACATCTTTATGACAGAAGAACAGAAGAAAT
ACTATAATGCAATGAAAAAATTAGGATCGAAAAAACCAGAAAAGCCTATACCTCGACCAGGAAACAAATTTCAAGG
AATGGTCTTTGACTTCGTAACCAGACAAGTTTTGACATAAGCATCATGATTCTCATCTGTCTTAACATGGTCACAATG
ATGGTGGAAACAGATGACCAGAGTGAATATGTGACTACCATTTTGTACGCATCAATCTGGTGTTCATTGTGCTATTT
ACTGGAGAGTGTGACTGAAACTCATCTCTACGCCATTATTATTTACCATTGGATGGAATATTTTATTGTTTGGG
TTGTCATTCTCTCATTGTAGGTATGTTTCTTGGCAGCTGATAGAAAAGTATTCGTGTCCCTACCCTGTTCCGAGT
GATCCGTCTTGCTAGGATTGGCCGAATCTACGTCTGATCAAAGGAGCAAAGGGGATCCGCACGCTGCTCTTTGCTT
TGATGATGTCCCTCCTGCGTTGTTAACATCGGCCTCCTACTTCTCTAGTCATGTTTCATCTACGCCATCTTTGGGATG
TCCAATTTGCCTATGTTAAGAGGGAAGTTGGGATCGATGACATGTTCAACTTTGAGACCTTTGGCAACAGCATGAT
CTGCCTATTCAAATTACAACCTCTGCTGGCTGGGATGGATTGCTAGCACCCATTCTCAACAGTAAGCCACCCGACTG
TGACCCTAATAAAGTTAACCTGGAAGCTCAGTTAAGGGAGACTGTGGAAACCATCTGTTGGAATTTCTTTTTTGT
CAGTTACATCATATCCTTCTGGTTGTGGTGAACATGTACATCGCGTCTCCTGGAGAAGTTTCAAGTGTGCTAC
TGAAGAAAGTGCAGAGCCTCTGAGTGAGGATGACTTTGAGATGTTCTATGAGGTTTGGGAGAAGTTTATCCCGAT
GCAACTCAGTTCATGGAATTTGAAAAATTATCTCAGTTTGCAGCTGCGCTTGAACCGCTCTCAATCTGCCACAACCA
AACAACTCCAGCTCATTGCCATGGATTTGCCATGGTGTGAGTGGTGACCGGATCCACTGTCTTGATATCTTATTGCT
TTTACAAAGCGGGTCTAGGAGAGAGTGGAGAGATGGATGCTCTACGAATACAGATGGAAGAGCGATTCTGGCTT
CCAATCCTTCAAGGTCTCCTATCAGCCAATCACTACTTTAAAACGAAAACAAGAGGAAGTATCTGCTGTCATTA
TTCAGCGTGCTTACAGACGCCACCTTTTAAAGCGAACTGTAAAACAAGCTTCTTTACGTACAATAAAAAACAAAATCA
AAGGTGGGGCTAATCTTCTTATAAAAAGAAGACATGATAATTGACAGAATAAATGAAAACCTTATTACAGAAAAAAT
GATCTGACCATGTCCACTTCAGCTTGTCCACCTTCTATGACCGGGTGACAAAGCCAATTGTGGAAAAACATGAGCA
AGAAGGCAAAGATGAAAAAGCCAAAGGGAATAA

SCN1A-5A **TTX-Resistant** amino acid sequence:

Met EQTVLVPPGPDSFNFFTRRESLAAIERRIAEEKAKNPKPKDKKDDDENGPKPNSDLE
AGKNLPFIYGDIPPE **Met** VSEPLEDLDPYYINKKTFIVLNKKGKAIFRFSATSALYILTPF
NPLRKIAIKILVHSLFS **Met** LI **Met** CTILTNCVF **Met** T **Met** SNPPDWTKNVEYFTFTGIYTF
ESLIKIIARGFCLEDFTLRDPWNWLDFTVITFA **V** VTEFV **D** LGN **V** SALRTFRVLRALKT
ISVIPGLKTIVGALIQSVKKLSDV **Met** ILTVFCLSVFALIGLQLF **Met** GNLRNKCIQWPPT
NASLEEHSIEKNITVNYNGTLINETVFEFDWKSYYIQDSRYHYFLEGFLDALLCGNSSD
AGQCPEGY **Met** CVKAGRNPNGYTSFDTFSWAFSLFRL **Met** TQD **S** WENLYQLTLRA
AGKTY **Met** IFFVLVIFLGSFYLINLILAVVA **Met** AYEEQNQATLEEAQKEAEFQQ **Met** I
EQLKKQQAQAATATASEHSREPSAAGRLSDSSSEASKLSSKSAKERRNRRKKR
QKEQSGGEEKDEDEFQKSESEDSIRRKGRFRFSIEGNRLTYEKRYSSPHQSLLSIRGSLF
SPRRNSRTSLFSFRGRAKDVGSENFADDEHSTFEDNESRRDSLFPVRRHGERRNSN
LSQTSRSSR **Met** LAVFPANGK **Met** HSTVDCNGEVS LVGGPSVPTSPVGQLLPEGTTTE
TE **Met** RKRRSSSFHVS **Met** DFLEDPSQRQRA **Met** SIASILTNTVEELEESRQKCPPCWY
KFSNIFLIWDCSPYWLVKVVNLVV **Met** DPFVDLAITICIVLNTLF **Met** A **Met** EHY
P **Met** TDHFNNVLTVGNLVFTGIFTAE **Met** FLKIIA **Met** DPYYYFQEGWNIFDGFIVTLSL
VELGLANVEGLSVLRSFLLRVFKLAKSWPTLN **Met** LIKIIGNSVGALGNLTLVLAIVF
IFAVVG **Met** QLFGKSYKDCVCKIASDCQLPRWH **Met** NDFHFSFLIVFRVLCGEWIE
T **Met** WDC **Met** EVAGQA **Met** CLTVF **Met** **Met** V **Met** VIGNLVVLNLFALLLSSFSADNLAA
TDDDNE **Met** NNLQIAVDR **Met** HKGVAYVVKRKIYEFIQQS FIRKQKILDEIKPLDDLNNK
KDSC **Met** SNHTAEIGKDL DYLKDVNGTTS GIGTGSSVEKYIIDESDY **Met** SFINNPSTLV
TVPIAVGESDFENLNTEDFSSES DLEESKEKLNESSSSSEGSTVDIGAPVEEQPVVEPE
ETLEPEACFTEGCVQRFKCCQINVEEGRGKQWWNLRRTCFRIVEHNWFETFIV
F **Met** ILLSSGALAFEDIYIDQRKTIKT **Met** LEYADKVFTYIFILE **Met** LLKWVAYGYQTYF
TNAWCWLD FLIVDVS LVS LTANALGYSELGAIKSLRTRLRALRPLRALS RFEG **Met** RVV
VNALLGAIPSI **Met** NVLLVCLIFWLIFS I **Met** GVNLFAGKFYHCINTTTGDRFDIEDVNN
HTDCLKLIERNETARWKNVKNVFDNVGFGYLSLLQVATFKGW **Met** DI **Met** YAAVDSR
NVELQPKYEEESLY **Met** YLYFVIFIIFGSFFTLNLFIGVIIDNFNQQKKKFGGQDIF **Met** TE
EQKKYYNA **Met** KKLGSKKPKPIPRPGNKFGQ **Met** VFDFVTRQVFDISI **Met** ILICL
N **Met** VT **Met** **Met** VETDDQSEYVTILSRINLVFIVLFTGECVLKLSLRHYYFTIGWNIFD
FVVVILSIVG **Met** FLAELIEKYFVSPTLFRVIRLARIGRILRLIKGAKGIRTL LFA
L **Met** **Met** SLPALFNIGLLLFLV **Met** FIYAIFG **Met** SNFAYVKREVGIDD **Met** FNFETFGN
S **Met** ICLFQITTSAGWDGLLAPILNSKPPDCDPNKVNP GSSVKGDCGNPSVGIFFFVS
YIIISFLVVVN **Met** YIAVILENFSVATEESAEP LSEDDFE **Met** FYEVWEKFDPDATQ
F **Met** EFEKLSQFAAALEPPLNLPQPNKLQLIA **Met** DLP **Met** VSGDRIHCLDILFAFTKRV
LGESGE **Met** DALRIQ **Met** EERF **Met** ASNPSKVSYPITTT LKRKQEEVSAVIIQRAYRRH
LLKRTVKQASFTYNKNKIKGGANLLIKED **Met** IIDRINENSITEKTDLT **Met** STSACPPS
YDRVTKPIVEKHEQEGKDEKAKGK Stop

SCN1A-5N **TTX-Resistant** cDNA sequence:

ATGGAGCAAACAGTGCTTGTACCACCAGGACCTGACAGCTTCAACTTCTCACAGAGAATCTCTTGC GGCTATTGAA
AGACGCATTGCAGAAGAAAAGGCAAAGAATCCCAAACCAGACAAAAAAGATGACGACGAAAATGGCCCAAAGCCA
AATAGTGACTTGAAGCTGGAAAGAACCTTCCATTTATTTATGGAGACATTCCTCCAGAGATGGTGTGAGAGCCCT
GGAGGACCTGGACCCCTACTATATCAATAAGAAAACCTTTATAGTATTGAATAAAGGGAAGGCCATCTCCGGTTCA
GTGCCACCTCTGCCCTGTACATTTAACTCCCTTCAATCCTCTTAGGAAAATAGCTATTAAGATTTTGGTACATTCATTA
TTCAGCATGCTAATTATGTGCACTATTTTGACAACTGTGTGTTTATGACAATGAGTAACCCCTCTGATTGGACAAAG
AATGTAGAATACACCTTCACAGGAATATATACTTTTGAATCACTTATAAAAATTATTGCAAGGGGATTCTGTTTAGAA
GATTTTACTTTCTTCGGGATCCATGGAAGCTGGCTCGATTTCACTGTCATTACATTTGCGTTCGTCACAGAGTTTGTGA
ACCTGGGCAATTTCTCGGCATTGAGAACATTCAGAGTTCTCCGAGCATTGAAGACGATTTTCAGTCATTCAGGCCTG
AAAACCATTGTGGGAGCCCTGATCCAGTCTGTGAAGAAGCTCTCAGATGTAATGATCCTGACTGTGTTCTGTCTGAG
CGTATTGCTCTAATTGGGCTGCAGCTGTTTCATGGGCAACCTGAGGAATAAATGTATAACAATGGCCTCCACCAATG
CTTCCTTGGAGGAACATAGTATAGAAAAGAATATAACTGTGAATTATAATGGTACACTTATAAATGAAACTGTCTTTG
AGTTTGACTGGAAGTCATATATTCAAGATTCAAGATATCATTATTTCTGGAGGGTTTTTTAGATGCACTACTATGTG
GAAATAGCTCTGATGCAGGCCAATGTCCAGAGGGATATATGTGTGTGAAAGCTGGTAGAAATCCCAATTATGGCTA
CACAAGCTTTGATACCTTCAGTTGGGCTTTTTTGTCTTGTTCGCCTAATGACTCAGGACTCTGGGAAAATCTTTAT
CAACTGACATTACGTGCTGCTGGGAAAACGTACATGATATTTTTGTGTTGGTCATTTTCcTaGGCTCATTCTACCTAA
TAAATTTGATCCTGGCTGTGGTGGCCATGGCCTACGAGGAACAGAATCAGGCCACCTTGAAGAAGCAGAACAGAA
AGAGGCCGAATTTACGAGATGATTGAACAGCTTAAAAGCAACAGGAGGCAGCTCAGCAGGCAGCAACGGCAAC
TGCCTCAGAACATTCCAGAGAGCCCAGTGCAGCAGGCAGGCTCTCAGACAGCTCATCTGAAGCCTCTAAGTTGAGTT
CCAAGAGTGCTAAGGAAAGAAGAAATCGGAGGAAGAAAAGAAAACAGAAAGAGCAGTCTGGTGGGGAAAGAGAAA
GATGAGGATGAATTTCAAAAATCTGAATCTGAGGACAGCATCAGGAGGAAAGGTTTTCGCTTCTCCATTGAAGGGA
ACCGATTGACATATGAAAAGAGGTA CTCTCCCCACACCAGTCTTTGTTGAGCATCCGTGGCTCCCTATTTTACCAA
GGCGAAATAGCAGAACAAGCCTTTTCAGCTTTAGAGGGCGAGCAAAGGATGTGGGATCTGAGAACGACTTCGCAG
ATGATGAGCACAGCACCTTTGAGGATAACGAGAGCCGTAGAGATTCTTTGTTTGCCCCGACGACACGGAGAGAG
ACGCAACAGCAACCTGAGTCAGACCAGTAGGTCATCCCGGATGCTGGCAGTGTTCAGCGAATGGGAAGATGCAC
AGCACTGTGGATTGCAATGGTGAGGTTTCTTGGTTGGTGGACCTTCAGTTCTACATCGCCTGTTGGACAGCTTCTG
CCAGAGGGAAACAACCACTGAAACTGAAATGAGAAAGAGAAGGTCAAGTTCTTTCCACGTTTCCATGGACTTTCTAGA
AGATCCTTCCCAAAGGCAACGAGCAATGAGTATAGCCAGCATTCTAACAATAACAGTAGAAGAACTTGAAGAATCCA
GGCAGAAATGCCACCCTGTTGGTATAAATTTTCCAACATATTCTTAATCTGGGACTGTTCTCCATATTGGTTAAAAGT
GAAACATGTTGTCAACCTGGTCGTGATGGACCCATTTGTTGACCTGGCCATCACCATCTGTATTGTCTTAAATACTCTT
TTCATGGCCATGGAGCACTATCCAATGACGGACCATTTCAATAATGTGCTTACAGTAGGAAACTTGGTTTTACTGGG
ATCTTTACAGCAGAAATGTTTCTGAAAATTATTGCCATGGATCCTTACTATTATTTCCAAGAAGGCTGGAATATCTTTG
ACGTTTTTATTGTGACGCTTAGCCTGGTAGAACTTGGACTCGCCAATGTGGAAGGATTATCTGTTCTCCGTTCAATTC
GATTGCTGCGAGTTTTCAAGTTGGCAAAATCTTGGCCAACGTTAAATATGCTAATAAAGATCATCGGCAATTCCGTG
GGGGCTCTGGGAAATTAACCCTCGTCTTGGCCATCATCGTCTTCATTTTTGCCGTGGTCCGCATGCAGCTCTTTGGT
AAAAGCTACAAAGATTGTGTCTGCAAGATCGCCAGTGATTGTCAACTCCCACGCTGGCACATGAATGACTTCTTCCAC
TCCTTCTGATTGTGTTCCGCGTGCTGTGTGGGGAGTGGATAGAGACCATGTGGGACTGTATGGAGGTTGCTGGTCA
AGCCATGTGCCTTACTGTCTTCATGATGGTCATGGTGATTGGAAACCTAGTGGTCCTGAATCTTTTCTGGCCTTGCTT

CTGAGCTCATTTAGTGCAGACAACCTTGCAGCCACTGATGATGATAATGAAATGAATAATCTCCAAATTGCTGTGGAT
AGGATGCACAAAGGAGTAGCTTATGTGAAAAGAAAAATATATGAATTTATTCAACAGTCCTTCATTAGGAAACAAAA
GATTTTAGATGAAATTAACCACTTGATGATCTAAACAACAAGAAAGACAGTTGTATGTCCAATCATACAGCAGAAA
TTGGGAAAGATCTTGACTATCTTAAAGATGTAAATGAACTACAAGTGGTATAGGAACTGGCAGCAGTGTGAAAA
ATACATTATTGATGAAAGTGATTACATGTCATTCATAACAACCCAGTCTTACTGTGACTGTACCAATTGCTGTAGG
AGAATCTGACTTTGAAAATTTAAACACGGAAGACTTTAGTAGTGAATCGGATCTGGAAGAAAGCAAAGAGAACTG
AATGAAAGCAGTAGCTCATCAGAAGGTAGCACTGTGGACATCGGCGCACCTGTAGAAGAAGCCCGTAGTGGAAC
CTGAAGAACTCTGAACCAGAAGCTTGTTCCTGACTGAAGGCTGTGTACAAAGATTCAAGTGTGTCAAATCAATGTG
GAAGAAGGCAGAGGAAAAACAATGGTGGAACTGAGAAGGACGTGTTCCGAATAGTTGAACATAACTGGTTTGAG
ACCTTCATTGTTTTATGATTCTCCTTAGTAGTGGTGTCTGGCATTGGAAGATATATATATTGATCAGCGAAAGACG
ATTAAGACGATGTTGGAATATGCTGACAAGTTTTCACTTACATTTTTATTCTGGAAATGCTTCTAAAATGGGTGGCA
TATGGCTATCAAACATATTTACCAATGCCTGGTGTGGCTGGACTTCTTAATTGTTGATGTTTCATTGGTCAGTTTAA
CAGCAAATGCCTTGGGTTACTCAGAACTTGGAGCCATCAAATCTCTCAGGACACTAAGAGCTCTGAGACCTCTAAGA
GCCTTATCTCGATTTGAAGGGATGAGGGTGGTTGTGAATGCCCTTTAGGAGCAATCCATCCATCATGAATGTGCTT
CTGGTTTGTCTTATATTCTGGCTAATTTTCAGCATCATGGGCGTAAATTTGTTTGTGGCAAATTTCTACCACTGTATTA
ACACCACAACCTGGTGACAGTTTTGACATCGAAGACGTGAATAATCATACTGATTGCCTAAAATAATAGAAAGAAAT
GAGACTGCTCGATGGAAAAATGTGAAAGTAACTTTGATAATGTAGGATTTGGGTATCTCTTTGCTTCAAGTTGCC
ACATTCAAAGGATGGATGGATATAATGTATGCAGCAGTTGATTCCAGAAATGTGGAACCTCAGCCTAAGTATGAAG
AAAGTCTGTACATGTATCTTTACTTTGTTATTTTCATCATCTTTGGTCCCTTCTTACCTTGAACCTGTTTATTGGTGT
ATCATAGATAATTTCAACCAGCAGAAAAAGAAAGTTTGGAGGTCAAGACATCTTTATGACAGAAGAACAGAAGAAAT
ACTATAATGCAATGAAAAAATTAGGATCGAAAAAACCGCAAAGCCTATACCTCGACCAGGAAACAAATTTCAAGG
AATGGTCTTTGACTTCGTAACCAGACAAGTTTTGACATAAGCATCATGATTCTCATCTGTCTTAACATGGTCACAATG
ATGGTGGAAACAGATGACCAGAGTGAATATGTGACTACCATTTTGTACGCATCAATCTGGTGTTCATTGTGCTATTT
ACTGGAGAGTGTGTAAGTCACTCTCTACGCCATTATTTTACCATTGGATGGAATATTTTATTGTTTGGTGG
TTGTCATTCTCTCATTGTAGGTATGTTTCTTCCGAGCTGATAGAAAAGTATTCGTGTCCCTACCCTGTTCCGAGT
GATCCGTCTTGCTAGGATTGGCCGAATCTACGTCTGATCAAAGGAGCAAAGGGGATCCGCACGCTGCTCTTTGCTT
TGATGATGTCCCTCCTGCGTTGTTAACATCGGCCTCCTACTCTTCTAGTCATGTTTCTACGCCATCTTTGGGATG
TCCAATTTGCCTATGTTAAGAGGGAAGTTGGGATCGATGACATGTTCAACTTTGAGACCTTTGGCAACAGCATGAT
CTGCCTATTCAAATTACAACCTCTGCTGGCTGGGATGGATTGCTAGCACCCATTCTCAACAGTAAGCCACCCGACTG
TGACCCTAATAAAGTTAACCTGGAAGCTCAGTTAAGGGAGACTGTGGAAACCCATCTGTTGGAATTTCTTTTTGT
CAGTTACATCATCATCCTTCTGGTGTGGTGAACATGTACATCGCGTCTCCTGGAGAAGTTTCAAGTGTGCTAC
TGAAGAAAGTGCAGAGCCTCTGAGTGAGGATGACTTTGAGATGTTCTATGAGGTTTGGGAGAAGTTTATCCCGAT
GCAACTCAGTTCATGGAATTTGAAAAATTATCTCAGTTTGCAGCTGCGCTTGAACCGCTCTCAATCTGCCACAACCA
AACAACTCCAGCTCATTGCCATGGATTTGCCATGGTGAAGTGGTGAACCGGATCCACTGTCTTGATATCTTATTGCT
TTTACAAAGCGGGTCTAGGAGAGAGTGGAGAGATGGATGCTCTACGAATACAGATGGAAGAGCGATTCTGGCTT
CCAATCTTCAAGGTCTCCTATCAGCCAATCACTACTTTTAAACGAAAACAAGAGGAAGTATCTGCTGTCATTA
TTCAGCGTGCTTACAGACGCCACCTTTTAAAGCGAACTGTAAAACAAGCTTCTTTACGTACAATAAAAAACAAATCA
AAGGTGGGGCTAATCTTCTTATAAAAGAAGACATGATAATTGACAGAATAAATGAAAACCTTATTACAGAAAAAAT
GATCTGACCATGTCCACTTCAGCTTGTCCACCTCTATGACCGGGTGACAAAGCCAATTGTGGAAAAACATGAGCA
AGAAGGCAAAGATGAAAAAGCCAAAGGGAATAA

SNC1A-5N **TTX-Resistant** amino acid sequence:

Met EQTVLVPPGPDSFNFFTRRESLAAIERRIAEEKAKNPKPKDKKDDDENGPKPNSDLE
AGKNLPFIYGDIPPE **Met** VSEPLEDLDPPYINKKTFIVLNKKGKAIFRFSATSALYILTPF
NPLRKIAIKILVHSLFS **Met** LI **Met** CTILTNCVF **Met** T **Met** SNPPDWTKNVEYFTFTGIYTF
ESLIKIIARGFCLEDFTFLRDPWNWLDFTVITFA **F** VTEFV **N** LGN **F** SALRTFRVLRALKT
ISVIPGLKTIVGALIQSVKKLSDV **Met** ILTVFCLSVFALIGLQLF **Met** GNLRNKCIQWPPT
NASLEEHSIEKNITVNYNGTLINETVFEFDWKSYSIQDSRYHYFLEGFLDALLCGNSSD
AGQCPEGY **Met** CVKAGRNPNGYTSFDTFSWAFSLFRL **Met** TQD **S** WENLYQLTLRA
AGKTY **Met** IFFVLVIFLGSFYLINLILAVVA **Met** AYEEQNQATLEEAQKEAEFQQ **Met** I
EQLKKQQAQAATATASEHSREPSAAGRLSDSSSEASKLSSKSAKERRNRRKKRK
QKEQSGGEEKDEDEFQKSESEDSIRRKGRFRFSIEGNRLTYEKRYSSPHQSLLSIRGSLF
SPRRNSRTSLFSFRGRAKDVGSENFADDEHSTFEDNESRRDSLFPVRRHGERRNSN
LSQTSRSSR **Met** LAVFPANGK **Met** HSTVDCNGEVSLVGGPSVPTSPVGQLLPEGTTTE
TE **Met** RKRRSSSFHVS **Met** DFLEDPSQRQRA **Met** SIASILTNTVEELEESRQKCPPCWY
KFSNIFLIWDCSPYWLVKVVNLVV **Met** DPFVDLAITICIVLNTLF **Met** A **Met** EHY
P **Met** TDHFNNVLTVGNLVFTGIFTAE **Met** FLKIIA **Met** DPYYYFQEGWNIFDGFIVTSL
VELGLANVEGLSVLRSFLLRVFKLAKSWPTLN **Met** LIKIIGNSVGALGNLTLVLAIVF
IFAVVG **Met** QLFGKSYKDCVCKIASDCQLPRWH **Met** NDFHFSFLIVFRVLCGEWIE
T **Met** WDC **Met** EVAGQA **Met** CLTVF **Met** **Met** V **Met** VIGNLVVLNLFALLLSSFSADNLAA
TDDDNE **Met** NNLQIAVDR **Met** HKGVAYVVKRKIYEFIQQSFIRKQKILDEIKPLDDLNNK
KDSC **Met** SNHTAEIGKDLDYLKDVNGTTSIGIGTGSSVEKYIIDESDY **Met** SFINNPSTLV
TVPIAVGESDFENLNTEDFSSESLEESKEKLNESSSSSSEGSTVDIGAPVEEQPVVEPE
ETLEPEACFTEGCVQRFKCCQINVEEGRGKQWWNLRRTCFRIVEHNWFETFIV
F **Met** ILLSSGALAFEDIYIDQRKTIKT **Met** LEYADKVFTYIFILE **Met** LLKWVAYGYQTYF
TNAWCWLDFLIVDVSLSLTANALGYSELGAIKSLRTRLRALRPLRALS RFEG **Met** RVV
VNALLGAIPSI **Met** NVLLVCLIFWLIFS **Met** GVNLFAGKFYHCINTTTGDRFDIEDVNN
HTDCLKLIERNETARWKNVKNVFDNVGFGYLSLLQVATFKGW **Met** DI **Met** YAAVDSR
NVELQPKYEEESLY **Met** YLYFVIFIIFGSFFTLNLFIGVIIDNFNQQKKKFGGQDIF **Met** TE
EQKKYYNA **Met** KKLGSKKPKPIPRPGNKFGG **Met** VFDFVTRQVFDISI **Met** ILICL
N **Met** VT **Met** **Met** VETDDQSEYVTILSRINLVFIVLFTGECVLKLSLRHYYFTIGWNIFD
FVVVILSIVG **Met** FLAELIEKYFVSPTLFRVIRLARIGRILRLIKGAKGIRTL LFA
L **Met** **Met** SLPALFNIGLLLFLV **Met** FIYAIFG **Met** SNFAYVKREVGIDD **Met** FNFETFGN
S **Met** ICLFQITTSAGWDGLLAPILNSKPPDCDPNKVNPSSVKGDCGNPSVGIFFFVS
YIIISFLVVVN **Met** YIAVILENFSVATEESAEPLEDDFE **Met** FYEVWEKFDPDATQ
F **Met** EFEKLSQFAAALEPPLNLPQPNKLQLIA **Met** DLP **Met** VSGDRIHCLDILFAFTKRV
LGESGE **Met** DALRIQ **Met** EERF **Met** ASNPSKVSYPITTTLKRKQEEVSAVIIQRAYRRH
LLKRTVKQASFTYNKNKIKGGANLLIKED **Met** IIDRINENSITEKTDLT **Met** STSACPPS
YDRVTKPIVEKHEQEGKDEKAKGK **Stop**

SCN2A-6A **TTX-Resistant** cDNA sequence:

ATGGCACAGTCAGTGCTGGTACCGCCAGGACCTGACAGCTCCGCTTCTTACCAGGGAATCCCTTGCTGCTATTGAA
CAACGCATTGCAGAAGAGAAAAGCTAAGAGACCCAAACAGGAACGCAAGGATGAGGATGATGAAAATGGCCCAAAG
CCAAACAGTGACTTGGGAAGCAGGAAAATCTCTCCATTTATTTATGGAGACATTCCCTCCAGAGATGGTGTGCTGCCC
CTGGAGGATCTGGACCCCTACTATATCAATAAGAAAACGTTTATAGTATTGAATAAAGGGAAAGCAATCTCTCGATT
CAGTGCCACCCCTGCCCTTACATTTAACTCCCTTCAACCCTATTAGAAAATTAGCTATTAAGATTTTGGTACATTCTT
TATTCAATATGCTCATTATGTGCACGATTCTTACCAACTGTGTATTTATGACCATGAGTAACCCCTCCAGACTGGACAAA
GAATGTGGAGTATACCTTTACAGGAATTTATACTTTTGAATCACTTATTAATAACTTGAAGGGGCTTTTGTGTTAGA
AGATTTACATTTTTACGGGATCCATGGAATTGGTTGGATTTACAGTCATTACTTTTGCATATGTGACAGAGTTTGT
G**G**ACTGGGCAATGTCTCAGCGTTGAGAACATTAGAGTTCTCCGAGCATTGAAAACAATTTAGTCATTCCAGGCC
TGAAGACCATTGTGGGGGCCCTGATCCAGTCAGTGAAGAAGCTTTCTGATGTCATGATCTTGACTGTGTTCTGTCTAA
GCGTGTGTTGCGCTAATAGGATTGCAGTTGTTTATGAGGCAACCTACGAAATAAATGTTTGAATGGCCTCCAGATAAT
TCTTCCTTTGAAATAAATATCACTTCCTTCTTAAACAATTCATTGGATGGGAATGGTACTACTTTCAATAGGACAGTGA
GCATATTTAACTGGGATGAATATATTGAGGATAAAAAGTCACTTTTATTTTTAGAGGGGCAAATGATGCTCTGCTTT
GTGGCAACAGCTCAGATGCAGGCCAGTGTCTGAAGGATACATCTGTGTGAAGGCTGGTAGAAACCCCAACTATGG
CTACACGAGCTTTGACACCTTTAGTTGGGCCTTTTTGTCTTATTTTGTCTCATGACTCAAGACT**C**CTGGGAAAACCTT
TATCAACTGACACTACGTGCTGCTGGGAAAACGTACATGATATTTTTTGTGCTGGTCATTTTCTGGGCTCATTCTATC
TAATAAATTTGATCTTGGCTGTGGTGGCCATGGCCTATGAGGAACAGAATCAGGCCACATTGGAAGAGGCTGAACA
GAAGGAAGCTGAATTTAGCAGATGCTCGAACAGTTGAAAAAGCAACAAGAAGAGGCTCAGGCGGCAGCTGCAGC
CGCATCTGCTGAATCAAGAGACTTCACTGGTGTGGTGGGATAGGAGTTTTTTCAGAGAGTTCTTCACTAGCATCTA
AGTTGAGCTCCAAAAGTGAAAAAGAGCTGAAAAACAGAAGAAAGAAAAAGAAACAGAAAGAACAGTCTGGAGAA
GAAGAGAAAAATGACAGAGTCCGAAAATCGGAATCTGAAGACAGCATAAGAAGAAAAGTTTTCCGTTTTCTTGG
AAGGAAGTAGGCTGACATATGAAAAGAGATTTTCTTCTCCACACCAGTCTTACTGAGCATCCGTGGCTCCCTTTCT
CTCCAAGACGCAACAGTAGGGCGAGCCTTTTCACTTCAAGAGTCTGAGCAAAGGACATTGGCTCTGAGAATGACTTT
GCTGATGATGAGCACAGCACCTTTGAGGACAATGACAGCCGAAGAGACTCTCTGTTCTGCGCACAGACATGGAG
AACGGCGCCACAGCAATGTCAGCCAGGCCAGCCGTGCCTCCAGGGTGTCTCCCATCCTGCCCATGAATGGGAAGAT
GCATAGCGCTGTGGACTGCAATGGTGTGGTCTCCCTGGTCCGGGGCCCTTCTACCCCTCACATCTGCTGGGCAGCTCC
TACCAGAGGGCACAACTACTGAAACAGAAATAAGAAAAGAGACGGTCCAGTTCTTATCATGTTTCCATGGATTTATTG
GAAGATCCTACATCAAGGCAAAGAGCAATGAGTATAGCCAGTATTTTGACCAACACCATGGAAGAATTTGAAGAAT
CCAGACAGAAATGCCACCATGCTGGTATAAATTTGCTAATATGTGTTTGATTTGGGACTGTTGTAAACCATGGTTAA
AGGTGAAACACCTTGTAACCTGGTTGTAATGGACCCATTTGTTGACCTGGCCATCACCATCTGCATTGTCTTAAATA
CACTCTTATGGCTATGGAGCACTATCCCATGACGGAGCAGTTCAGCAGTGTACTGTCTGTTGGAACCTGGTCTTCA
CAGGGATCTTACAGCAGAAATGTTTCTCAAGATAATTGCCATGGATCCATATTACTTTCAAGAAGGCTGGAATA
TTTTTGATGGTTTTATTGTGAGCCTTAGTTTAATGGAACCTGGTTTGGCAAATGTGGAAGGATTGTCAGTTCTCCGAT
CATTCCGGCTGCTCCGAGTTTTCAAGTTGGCAAATCTTGGCCAACTCTAAATATGCTAATTAAGATCATTGGCAATT
CTGTGGGGGCTCTAGGAAACCTCACCTGGTATTGGCCATCATCGTCTTCATTTTGCTGTGGTCCGCATGCAGCTCT
TTGGTAAGAGCTACAAAGAATGTGTCTGCAAGATTTCCAATGATTGTGAACTCCACGCTGGCACATGCATGACTTTT
TCCACTCCTTCTGATCGTGTCCGCGTGTGTGGAGAGTGGATAGAGACCATGTGGGACTGTATGGAGGTCGCT
GGCCAAACCATGTGCCTTACTGTCTTATGATGGTGTGATTGGAAATCTAGTGGTCTGAACCTCTTCTGGCC

TTGCTTTTGAGTTCCTTCAGTTCTGACAATCTTGCTGCCACTGATGATGATAACGAAATGAATAATCTCCAGATTGCTG
TGGGAAGGATGCAGAAAGGAATCGATTTTGTTAAAAGAAAAATACGTGAATTTATTCAGAAAGCCTTTGTTAGGAA
GCAGAAAGCTTTAGATGAAATTAACCGCTTGAAGATCTAAATAATAAAAAAGACAGCTGTATTTCCAACCATACCA
CCATAGAAATAGGCCAAAGACCTCAATTATCTCAAAGACGGAATGGAACACTAGTGGCATAGGCAGCAGTGTAGA
AAAATATGTCGTGGATGAAAGTGATTACATGTCATTTATAAAACAACCCTAGCCTCACTGTGACAGTACCAATTGCTGT
TGGAGAATCTGACTTTGAAAATTTAAATACTGAAGAATTCAGCAGCGAGTCAGATATGGAGGAAAGCAAAGAGAAG
CTAAATGCAACTAGTTCATCTGAAGGCAGCACGGTTGATATTGGAGCTCCCGCCGAGGGAGAACAGCCTGAGGTTG
AACCTGAGGAATCCCTTGAACCTGAAGCCTGTTTTACAGAAGACTGTGTACGGAAGTTCAAGTGTGTGTCAGATAAGC
ATAGAAGAAGGCAAAGGGAAACTCTGGTGGAAATTTGAGGAAAACATGCTATAAGATAGTGGAGCACAATTGGTTC
GAAACCTTCATTGTCTTCATGATTCTGCTGAGCAGTGGGGCTCTGGCCTTTGAAGATATATACATTGAGCAGCGAAA
AACCATTAAGACCATGTTAGAATATGCTGACAAGGTTTTCACTTACATATTCATTCTGGAATGCTGCTAAAGTGGGT
TGCATATGGTTTTCAAGTGTATTTTACCAATGCCTGGTGGCTAGACTTCTGATTGTTGATGTCTCACTGGTTAGC
TTAACTGCAAATGCCTTGGGTTACTCAGAACTTGGTGCCATCAAATCCCTCAGAACACTAAGAGCTCTGAGGCCACTG
AGAGCTTTGTCCCGTTTTGAAGGAATGAGGGTTGTTGTAATGCTCTTTTAGGAGCCATTCCATCTATCATGAATGTA
CTTCTGGTTTTGTCTGATCTTTTGCTAATATTCAGTATCATGGGAGTGAATCTCTTTGCTGGCAAGTTTTACCATTGTA
TTAATTACACCACTGGAGAGATGTTTGATGTAAGCGTGGTCAACAACACTACAGTGAGTGCAAAGCTCTCATTGAGAGC
AATCAAACCTGCCAGGTGGAAAAATGTGAAAGTAACTTTGATAACGTAGGACTTGGATATCTGTCTCTACTTCAAGT
AGCCACGTTTAAGGGATGGATGGATATTATGTATGCAGCTGTTGATTCACGAAATGTAGAATTACAACCCAAGTATG
AAGACAACCTGTACATGTATCTTTATTTTGTATCTTTATTATTTTTGTTTCACTTTTACCTTGAATCTTTTCATTGGTG
TCATCATAGATAACTTCAACCAACAGAAAAAGAAAGTTTGGAGGTCAAGACATTTTTATGACAGAAGAACAGAAGAA
ATACTACAATGCAATGAAAAAAGTGGTTCAAAGAAACCACAAAAACCCATACCTCGACCTGCTAACAAATTCGAAG
GAATGGTCTTTGATTTTGAACCAACAAGTCTTTGATATCAGCATCATGATCCTCATCTGCCTAACATGGTCACCAT
GATGGTGGAAACCGATGACCAGAGTCAAGAAATGACAAACATTCTGACTGGATTAATCTGGTGTATTATTGTTCTGT
TCACTGGAGAATGTGTGCTGAAACTGATCTCTCTTCGTTACTACTATTTCACTATTGGATGGAATATTTTTGATTTTGT
GGTGGTCACTTCTCCATTGTAGGAATGTTTCTGGCTGAACTGATAGAAAAGTATTTTGTGTCCCCTACCCTGTTCCG
AGTGATCCGTCTTGCCAGGATTGGCCGAATCCTACGTCTGATCAAAGGAGCAAAGGGGATCCGCACGCTGCTCTTTG
CTTTGATGATGTCCCTCCTGCGTTGTTAACATCGGCCTCCTCTTTTCTGGTCATGTTTCTACGCCATCTTTGGG
ATGTCCAATTTTGCCTATGTTAAGAGGGAAAGTTGGGATCGATGACATGTTCAACTTTGAGACCTTTGGCAACAGCAT
GATCTGCCTGTTCCAAATTACAACCTCTGCTGGCTGGGATGGATTGCTAGCACCTATTCTTAATAGTGGACCTCCAGA
CTGTGACCCTGACAAAGATCACCTGGAAGCTCAGTTAAAGGAGACTGTGGGAACCCATCTGTTGGGATTTTCTTTTT
TGTCAGTTACATCATCATATCCTTCTGGTTGTGGTGAACATGTACATCGCGGTCATCCTGGAGAATTCAGTGTTC
TACTGAAGAAAGTGCAGAGCCTCTGAGTGAGGATGACTTTGAGATGTTCTATGAGGTTTGGGAGAAGTTTGATCCC
GATGCGACCCAGTTTATAGAGTTTGCCAAACTTTCTGATTTTGCAGATGCCCTGGATCCTCCTCTTCTCATAGCAAAC
CCAACAAAGTCCAGCTCATTGCCATGGATCTGCCATGGTGAGTGGTGACCGGATCCACTGTCTTGACATCTTATTTG
CTTTTACAAGCGTGTTTTGGGTGAGAGTGGAGAGATGGATGCCCTTGAATACAGATGGAAGAGCGATTTCATGGC
ATCAAACCCCTCAAAGTCTCTTATGAGCCATTACGACCACGTTGAAACGCAAACAAGAGGAGGTGTCTGCTATTAT
TATCCAGAGGGCTTACAGACGCTACCTCTTGAAGCAAAAAGTTAAAAAGGTATCAAGTATATACAAGAAAGACAAA
GGCAAAGAATGTGATGGAACACCCATCAAAGAAGATACTCTCATTGATAAACTGAATGAGAATTCAACTCCAGAGA
AAACCGATATGACGCCTTCCACCACGTCTCCACCCTCGTATGATAGTGTGACCAAACCGAAAAAGAAAAATTTGAA
AAAGACAAATCAGAAAAGGAAGACAAAGGGAAAGATATCAGGGAAAGTAAAAAGTAA

SCN2A-6A **TTX-Resistant** amino acid sequence:

MetAQSVLVPPGPDSFRFFFTRESLAAIEQRIAEKAKRPKQERKDEDDENGPKPNSDL
EAGKSLPFIYGDIPPE **Met**VSVPLEDLDPPYYINKKTFIVLNKGKAISRFSATPALYILTPF
NPIRKLAIKILVHSLFN **Met**LI **Met**CTILTNCV **Met**T **Met**SNPPDWTKNVEYTFGTIYTF
ESLIKILARGFCLEDFTFLRDPWNWLDFTVITFAYVTEFV **D**LGNVSALRTFRVLRALK
TISVIPGLKTIVGALIQSVKKLSDV **Met**ILTVFCLSVFALIGLQLF **Met**GNLRNKCLQWP
PDNSSFEINITSFFNNSLDGNGTTFNRTVSIFNWDEYIEDKSHFYFLEGQNDALLCGN
SSDAGQCPEGYICVKAGRNPNYGYTSFDTFSWAFLSLFRL **Met**TQD **S**WENLYQLTLR
AAGKTY **Met**IFFVLVIFLGSFYLINLILAVVA **Met**AYEEQNQATLEEAQEKEAEFQ
Q **Met**LEQLKKQEEEAQAAAAAASAESRDFSGAGGIGVFSESSSVASKLSSKSEKELKN
RRKKKKQKEQSGEEKNDRVRKSESEDSIRRKGFRRFSLEGSRLTYEKRFSSPHQSLLSI
RGSLSFPRRNSRASLFSFRGRAKDIGSENDFADDEHSTFEDNDSRRDSLFPVPHRGE
RRHSNVSQASRASRVLPILP **Met**NGK **Met**HSAVDCNGVVSLVGGPSTLTSAGQLLPEG
TTTETEIRKRRSSSYHVS **Met**DLLEDPTSQRRA **Met**SIASILTNT **Met**EELEESRQKCPP
CWYKFAN **Met**CLIWDCCKPWLKVKHLVNLVV **Met**DPFVDLAITICIVLNTL
F **Met**A **Met**EHYP **Met**TEQFSSVLSVGNLVFTGIFTAE **Met**FLKIIA **Met**DPYFFFQEGWN
IFDGFIVSLSL **Met**ELGLANVEGLSVLRSFRLLRVFKLAKSWPTLN **Met**LIKIIGNSVGA
LGNLTLVLAIIVFIFAVVG **Met**QLFGKSYKECVCKISNDCELPRWH **Met**HDFHHSFLIVF
RVLCGEWIET **Met**WDC **Met**EVAGQT **Met**CLTVF **Met** **Met**VMetVIGNLVVLNLFALLLS
SFSSDNLAATDDDNE **Met**NNLQIAVGR **Met**QKGFDFVKKIREFIQKAFVRKQKALDE
IKPLEDLNKKDSCISNHTTIEIGKDLNYLKDGNNGTTSIGIGSSVEKYVVDSESY **Met**SF
INNPSTVTVPIAVGESDFENLNTEEFSSSED **Met**EESKEKLNATSSSEGSTVDIGAPA
EGEQPEVEPEESLEPEACFTEDCVRKFKCCQISIEEGKGLWWNLRKTCYKIVEHNW
FETFIVF **Met**ILLSSGALAFEDIYIEQRKTIKT **Met**LEYADKVFTYIFILE **Met**LLKWVAYG
FQVYFTNAWCWLDLIVDVSLSLTANALGYSELGAIKSLRTLRLRPLRALSFE
G **Met**RVVVNALLGAIPSI **Met**NVLLVCLIFWLIFS **Met**GVNLFAGKFYHCINYTTG
E **Met**FDVSVVNNYSECKALIESNQARWKNVKNVFDNVGLGYLSLLQVATFKG
W **Met**DI **Met**YAAVDSRNVELQPKYEDNLY **Met**YLYFVIFIIFGSFFTLNLFIVGVIIDNFN
QQKKKFGGQDIF **Met**TEEQKKYYNA **Met**KKLGSKKPQKPIPRPANKFQG **Met**VDFVFT
KQVFDISI **Met**ILICLN **Met**VT **Met** **Met**VETDDQSQE **Met**TNILYWINLVFIVLFTGECVL
KLISLRYYYFTIGWNIFDFVVLVLSIVG **Met**FLAELIEKYFVSPTLFRVIRLARIGRILRLI
KGAKGIRTLFAL **Met** **Met**SLPALFNIGLLLFLV **Met**FIYAIFG **Met**SNFAYVKREVGID
D **Met**FNFETFGNS **Met**ICLFQITTSAGWDGLLAPILNSGPPDCDPDKDHPGSSVKGDC
GNPSVGIFFFVSYIIISFLVVVN **Met**YIAVILENFSVATEESAEPLEDDFE **Met**FYEVW
EKFDPPDATQFIEFAKLSDFADALDPPLLIAPKPNKVQLIA **Met**DLP **Met**VSGDRIHCLDIL
FAFTKRVLGESGE **Met**DALRIQ **Met**EERF **Met**ASNPSKVSYPEPITTTLKRKQEEVSAIIIQ
RAYRRYLLKQKVKVSSIYKKDKGKECDGTPIKEDTLIDKLNENSTPEKTD **Met**TPSTT
SPPSYDSVTKPEKEKFEKDKSEKEDKGKDIRESKK **Stop**

SCN2A-5N TTX-Resistant cDNA sequence:

ATGGCACAGTCAGTGCTGGTACCGCCAGGACCTGACAGCTCCGCTTCTTACCAGGAATCCCTTGCTGCTATTGAA
CAACGCATTGCAGAAGAGAAAAGCTAAGAGACCCAAACAGGAACGCAAGGATGAGGATGATGAAAATGGCCCAAAG
CCAAACAGTGACTTGGGAAGCAGGAAAATCTCTCCATTTATTTATGGAGACATTCCCTCCAGAGATGGTGTGCTGCCC
CTGGAGGATCTGGACCCCTACTATATCAATAAGAAAACGTTTATAGTATTGAATAAAGGGAAAGCAATCTCTCGATT
CAGTGCCACCCCTGCCCTTACATTTAACTCCCTTCAACCCTATTAGAAAATTAGCTATTAAGATTTTGGTACATTCTT
TATTCAATATGCTCATTATGTGCACGATTCTTACCAACTGTGTATTTATGACCATGAGTAACCCCTCCAGACTGGACAAA
GAATGTGGAGTATACCTTTACAGGAATTTATACTTTTGAATCACTTATTTAAAATACTTGAAGGGGCTTTTGTTTAGA
AGATTTACATTTTTACGGGATCCATGGAATTGGTTGGATTTACAGTCATTACTTTTGCATATGTGACAGAGTTTGT
GAACTGGGCAATGTCTCAGCGTTGAGAACATTCAGAGTTCTCCGAGCATTGAAAACAATTTAGTCATTCCAGGCC
TGAAGACCATTGTGGGGGCCCTGATCCAGTCAGTGAAGAAGCTTTCTGATGTCATGATCTTGACTGTGTTCTGTCTAA
GCGTGTGGCGTAATAGGATTGCAAGTTGTTGTTGTTGTTGTTGTTGTTGTTGTTGTTGTTGTTGTTGTTGTTGTTGTT
TCTTCCTTTGAAATAAATATCACTTCCTTCTTTAAACAATTCATTGGATGGGAATGGTACTACTTTCAATAGGACAGTGA
GCATATTTAACTGGGATGAATATATTGAGGATAAAAAGTCACTTTTATTTTTAGAGGGGGCAAATGATGCTCTGCTTT
GTGGCAACAGCTCAGATGCAGGCCAGTGTCTGAAGGATACATCTGTGTGAAGGCTGGTAGAAACCCCAACTATGG
CTACACGAGCTTTGACACCTTTAGTTGGGCCTTTTTGTCCTATTTTGTCTCATGACTCAAGACTCTGGGAAAACCTT
TATCAACTGACACTACGTGCTGCTGGGAAAACGTACATGATATTTTTTGTGCTGGTCATTTTCTGGGCTCATTCTATC
TAATAAATTTGATCTTGGCTGTGGTGGCCATGGCCTATGAGGAACAGAATCAGGCCACATTGGAAGAGGCTGAACA
GAAGGAAGCTGAATTTAGCAGATGCTCGAACAGTTGAAAAAGCAACAAGAAGAGGCTCAGGCGGCAGCTGCAGC
CGCATCTGCTGAATCAAGAGACTTCAGTGGTGTGGTGGGATAGGAGTTTTTTTCCAGAGAGTTCTTCCAGTAGCATCTA
AGTTGAGCTCCAAAAGTGAAAAAGAGCTGAAAAACAGAAGAAAGAAAAAGAAACAGAAAGAACAGTCTGGAGAA
GAAGAGAAAAATGACAGAGTCCGAAAATCGGAATCTGAAGACAGCATAAGAAGAAAAGGTTTCCGTTTTTCTTGG
AAGGAAGTAGGCTGACATATGAAAAGAGATTTTCTTCTCCACACCAGTCTTACTGAGCATCCGTGGCTCCCTTTTCT
CTCCAAGACGCAACAGTAGGGCGAGCCTTTTCCAGTTTCCAGAGGTCGAGCAAAGGACATTGGCTCTGAGAATGACTTT
GCTGATGATGAGCACAGCACCTTTGAGGACAATGACAGCCGAAGAGACTCTCTGTTCTGTCGCCGACAGACATGGAG
AACGGCGCCACAGCAATGTCAGCCAGGCCAGCCGTGCCTCCAGGGTGCTCCCCATCCTGCCCATGAATGGGAAGAT
GCATAGCGCTGTGGACTGCAATGGTGTGGTCTCCCTGGTGGGGGCCCTTCTACCCTCACATCTGCTGGGCAGCTCC
TACCAGAGGGCACAACTACTGAAACAGAAATAAGAAAAGAGACGGTCCAGTTCTTATCATGTTTCCATGGATTTATTG
GAAGATCCTACATCAAGGCAAAGAGCAATGAGTATAGCCAGTATTTTGACCAACACCATGGAAGAATTTGAAGAAT
CCAGACAGAAATGCCACCATGCTGGTATAAATTTGCTAATATGTGTTTGATTTGGGACTGTTGTAACCATGGTTAA
AGGTGAAACACCTTGTAACCTGGTTGTAATGGACCCATTTGTTGACCTGGCCATCACCATCTGCATTGTCTTAAATA
CACTCTTCATGGCTATGGAGCACTATCCCATGACGGAGCAGTTCAGCAGTGTACTGTCTGTTGGAACCTGGTCTTCA
CAGGGATCTTACAGCAGAAATGTTTCTCAAGATAATTGCCATGGATCCATATTACTTTTCAAGAAGGCTGGAATA
TTTTTGATGGTTTTATTGTGAGCCTTAGTTTAAATGGAACCTGGTTTGGCAAATGTGGAAGGATTGTCAGTTCTCCGAT
CATTCCGGCTGCTCCGAGTTTTCAAGTTGGCAAATCTTGGCCAACTCTAAATATGCTAATTAAGATCATTGGCAATT
CTGTGGGGGCTCTAGGAAACCTCACCTGGTATTGGCCATCATCGTCTTCATTTTGCTGTGGTGGCATGCAGCTCT
TTGGTAAGAGCTACAAAGAATGTGTCTGCAAGATTTCCAATGATTGTGAACTCCCACGCTGGCACATGCATGACTTTT
TCCACTCCTTCTGATCGTGTCCGCGTGTGTGGAGAGTGATAGAGACCATGTGGGACTGTATGGAGGTCGCT
GGCCAAACCATGTGCCTTACTGTCTTCATGATGGTTCATGGTATTGGAAATCTAGTGGTCTGAACCTCTTCTGGCC

TTGCTTTTGAGTTCCTTCAGTTCTGACAATCTTGCTGCCACTGATGATGATAACGAAATGAATAATCTCCAGATTGCTG
TGGGAAGGATGCAGAAAGGAATCGATTTTGTAAAAGAAAAATACGTGAATTTATTCAGAAAGCCTTTGTTAGGAA
GCAGAAAGCTTTAGATGAAATTAACCGCTTGAAGATCTAAATAATAAAAAAGACAGCTGTATTTCCAACCATACCA
CCATAGAAATAGGCCAAAGACCTCAATTATCTCAAAGACGGAATGGAACACTAGTGGCATAGGCAGCAGTGTAGA
AAAATATGTCGTGGATGAAAGTGATTACATGTCATTTATAAAACAACCCTAGCCTCACTGTGACAGTACCAATTGCTGT
TGGAGAATCTGACTTTGAAAATTTAAATACTGAAGAATTCAGCAGCGAGTCAGATATGGAGGAAAGCAAAGAGAAG
CTAAATGCAACTAGTTCATCTGAAGGCAGCACGGTTGATATTGGAGCTCCCGCCGAGGGAGAACAGCCTGAGGTTG
AACCTGAGGAATCCCTTGAACCTGAAGCCTGTTTTACAGAAGACTGTGTACGGAAGTTCAAGTGTGTGTCAGATAAGC
ATAGAAGAAGCAAAGGGAAACTCTGGTGAATTTGAGGAAAACATGCTATAAGATAGTGGAGCACAATTGGTTC
GAAACCTTCATTGTCTTCATGATTCTGCTGAGCAGTGGGGCTCTGGCCTTTGAAGATATATACATTGAGCAGCGAAA
AACCATTAAGACCATGTTAGAATATGCTGACAAGGTTTTCACTTACATATTCATTCTGGAATGCTGCTAAAGTGGGT
TGCATATGGTTTTCAAGTGTATTTTACCAATGCCTGGTGGCTAGACTTCTGATTGTTGATGTCTCACTGGTTAGC
TTAACTGCAAATGCCTTGGGTTACTCAGAACTTGGTGCCATCAAATCCCTCAGAACACTAAGAGCTCTGAGGCCACTG
AGAGCTTTGTCCCGTTTTGAAGGAATGAGGGTTGTTGTAATGCTCTTTTAGGAGCCATTCCATCTATCATGAATGTA
CTTCTGGTTTTGTCTGATCTTTTGGCTAATATTCAGTATCATGGGAGTGAATCTCTTTGCTGGCAAGTTTTACCATTGTA
TTAATTACACCACTGGAGAGATGTTTGATGTAAGCGTGGTCAACAACACTACAGTGAGTGCAAAGCTCTCATTGAGAGC
AATCAAACCTGCCAGGTGGAAAAATGTGAAAGTAACTTTGATAACGTAGGACTTGGATATCTGTCTCTACTTCAAGT
AGCCACGTTTAAGGGATGGATGGATATTATGTATGCAGCTGTTGATTACGAAATGTAGAATTACAACCCAAGTATG
AAGACAACCTGTACATGTATCTTTATTTTGTATCTTTATTATTTTTGTTTCACTTTTACCTTGAATCTTTTCATTGGTG
TCATCATAGATAACTTCAACCAACAGAAAAAGAAAGTTTGGAGGTCAAGACATTTTTATGACAGAAGAACAGAAGAA
ATACTACAATGCAATGAAAAAAGTGGTTCAAAGAAACCACAAAAACCCATACCTCGACCTGCTAACAAATTCGAAG
GAATGGTCTTTGATTTTGAACCAACAAGTCTTTGATATCAGCATCATGATCCTCATCTGCCTAACATGGTCACCAT
GATGGTGGAAACCGATGACCAGAGTCAAGAAATGACAAACATTCTGTAAGTGGATTAATCTGGTGTATTATTGTTCTGT
TCACTGGAGAATGTGTGCTGAAACTGATCTCTCTCGTTACTACTATTTCACTATTGGATGGAATATTTTTGATTTTGT
GGTGGTCACTTCTCCATTGTAGGAATGTTTCTGGCTGAACTGATAGAAAAGTATTTTGTGTCCCCTACCCTGTTCCG
AGTGATCCGTCTTGCCAGGATTGGCCGAATCCTACGTCTGATCAAAGGAGCAAAGGGGATCCGCACGCTGCTCTTTG
CTTTGATGATGTCCCTCCTGCGTTGTTAACATCGGCCTCCTCTTTTCTGGTCACTTTCATCTACGCCATCTTTGGG
ATGTCCAATTTTGCCTATGTTAAGAGGGAAAGTTGGGATCGATGACATGTTCAACTTTGAGACCTTTGGCAACAGCAT
GATCTGCCTGTTCCAAATTACAACCTCTGCTGGCTGGGATGGATTGCTAGCACCTATTCTTAATAGTGGACCTCCAGA
CTGTGACCCTGACAAAGATCACCTGGAAGCTCAGTTAAAGGAGACTGTGGGAACCCATCTGTTGGGATTTTCTTTTT
TGTCAGTTACATCATCATATCCTTCTGGTTGTGGTGAACATGTACATCGCGGTCATCCTGGAGAATTCAGTGTTC
TACTGAAGAAAGTGCAGAGCCTCTGAGTGAGGATGACTTTGAGATGTTCTATGAGGTTTGGGAGAAGTTTGATCCC
GATGCGACCCAGTTTATAGAGTTTGCCAAACTTTCTGATTTTGCAGATGCCCTGGATCCTCCTCTTCTCATAGCAAAC
CCAACAAAGTCCAGCTCATTGCCATGGATCTGCCATGGTGAGTGGTGACCGGATCCACTGTCTTGACATCTTATTTG
CTTTTACAAGCGTGTTTTGGGTGAGAGTGGAGAGATGGATGCCCTTGAATACAGATGGAAGAGCGATTTCATGGC
ATCAAACCCCTCAAAGTCTCTTATGAGCCATTACGACCACGTTGAAACGCAAACAAGAGGAGGTGTCTGCTATTAT
TATCCAGAGGGCTTACAGACGCTACCTCTTGAAGCAAAAAGTTAAAAAGGTATCAAGTATATACAAGAAAGACAAA
GGCAAAGAATGTGATGGAACCCCATCAAAGAAGATACTCTCATTGATAAACTGAATGAGAATTCAACTCCAGAGA
AAACCGATATGACGCCTTCCACCACGTCTCCACCCTCGTATGATAGTGTGACCAAACCGAAAAAGAAAAATTTGAA
AAAGACAAATCAGAAAAGGAAGACAAAGGGAAAGATATCAGGGAAAGTAAAAAGTAA

SCN2A-5N **TTX-Resistant** amino acid sequence:

MetAQSVLVPPGPDSFRFFFTRESLAAIEQRIAEKAKRPKQERKDEDDENGPKPNSDL
EAGKSLPFIYGDIPPE **Met**VSVPLEDLDPPYYINKKTFIVLNKGKAISRFSATPALYILTPF
NPIRKLAIKILVHSLFN **Met**LI **Met**CTILTNCV **Met**T **Met**SNPPDWTKNVEYTFGTIYTF
ESLIKILARGFCLEDFTLRDPWNWLDFTVITFAYVTEFV **N**LGNVSALRTRVLRALK
TISVIPGLKTIVGALIQSVKKLSDV **Met**ILTVFCLSVFALIGLQLF **Met**GNLRNKCLQWP
PDNSSFEINITSFFNNSLDGNGTTFNRTVSIFNWDEYIEDKSHFYFLEGQNDALLCGN
SSDAGQCPEGYICVKAGRNPNYGYTSFDTFSWAFLSLFRL **Met**TQD **S**WENLYQLTLR
AAGKTY **Met**IFFVLVIFLGSFYLINLILAVVA **Met**AYEEQNQATLEEAQEKEAEFQ
Q **Met**LEQLKKQEEEAQAAAAAASAESRDFSGAGGIGVFSESSSVASKLSSKSEKELKN
RRKKKKQKEQSGEEKNDRVRKSESEDSIRRKGRFRSLEGSRLTYEKRFSSPHQSLLSI
RGSLSFPRRNSRASLFSFRGRAKDIGSENDFADDEHSTFEDNDSRRDSLFPVPHRGE
RRHSNVSQASRASRVLPILP **Met**NGK **Met**HSAVDCNGVVSLVGGPSTLTSAGQLLPEG
TTTETEIRKRRSSSYHVS **Met**DLLEDPTSQRRA **Met**SIASILTNT **Met**EELEESRQKCPP
CWYKFAN **Met**CLIWDCCKPWLKVKHLVNLVV **Met**DPFVDLAITICIVLNTL
F **Met**A **Met**EHYP **Met**TEQFSSVLSVGNLVFTGIFTAE **Met**FLKIIA **Met**DPYFFFQEGWN
IFDGFIVSLSL **Met**ELGLANVEGLSVLRSFRLLRVFKLAKSWPTLN **Met**LIKIIGNSVGA
LGNLTLVLAIIVFIFAVVG **Met**QLFGKSYKECVCKISNDCELPRWH **Met**HDFHHSFLIVF
RVLCGEWIET **Met**WDC **Met**EVAGQT **Met**CLTVF **Met** **Met**VMetVIGNLVVLNLFALLLS
SFSSDNLAATDDDNE **Met**NNLQIAVGR **Met**QKGI DFVKKIREFIQKAFVRKQKALDE
IKPLEDLNKKDSCISNHTTIEIGKDLNYLKDGNGTTSIGSSVEKYVVDSESY **Met**SF
INNPSTVTVPIAVGESDFENLNTEEFSSSED **Met**EESKEKLNATSSSEGSTVDIGAPA
EGEQPEVEPEESLEPEACFTEDCVRKFKCCQISIEEGKGLWWNLRKTCYKIVEHNW
FETFIVF **Met**ILLSSGALAFEDIYIEQRKTIKT **Met**LEYADKVFTYIFILE **Met**LLKWVAYG
FQVYFTNAWCWLDFLIVDVSLSLTANALGYSELGAIKSLRTLRLRPLRALS RFE
G **Met**RVVVNALLGAIPSI **Met**NVLLVCLIFWLIFS **Met**GVNLFAGKFYHCINYTTG
E **Met**FDVSVVNNYSECKALIESNQARWKNVKVNFNDNVGLGYLSLLQVATFKG
W **Met**DI **Met**YAAVDSRNVELQPKYEDNLY **Met**YLYFVIFIIFGSFFTLNLFIVGVIIDNFN
QQKKKFGGQDIF **Met**TEEQKKYYNA **Met**KKLGSKKPQKPIPRPANKFQG **Met**VDFDVT
KQVFDISI **Met**ILICLN **Met**VT **Met** **Met**VETDDQSQE **Met**TNILYWINLVFIVLFTGECVL
KLISLRYYYFTIGWNIFDFVVLVLSIVG **Met**FLAELIEKYFVSPTLFRVIRLARIGRILRLI
KGAKGIRTLFAL **Met** **Met**SLPALFNIGLLLFLV **Met**FIYAIFG **Met**SNFAYVKREVGID
D **Met**FNFETFGNS **Met**ICLFQITTSAGWDGLLAPILNSGPPDCDPDKDHPGSSVKGDC
GNPSVGIFFFVSYIIISFLVVVN **Met**YIAVILENFSVATEESAEPLEDDFE **Met**FYEVW
EKFDPPDATQFIEFAKLSDFADALDPPLLIAPKPNKVQLIA **Met**DLP **Met**VSGDRIHCLDIL
FAFTKRVLGESGE **Met**DALRIQ **Met**EERF **Met**ASNPSKVSYPITTTLKRKQEEVSAIIIQ
RAYRRYLLKQKVKKVSSIYKKDKGKECDGTPIKEDTLIDKLNENSTPEKTD **Met**TPSTT
SPPSYDSVTKPEKEKFEKDKSEKEDKGKDIRESKK **Stop**

SNC9A-5A **TTX-Resistant** cDNA sequence:

ATGGCAATGTTGCCTCCCCAGGACCTCAGAGCTTTGTCCATTTACAAAACAGTCTCTTGCCCTCATTGAACAACGC
ATTGCTGAAAGAAAATCAAAGGAACCCAAAGAAGAAAAGAAAGATGATGATGAAGAAGCCCCAAAGCCAAGCAGT
GACTTGGAAGCTGGCAAACAACTGCCCTTCATCTATGGGGACATTCCTCCCGCATGGTGTGAGAGCCCTGGAGGA
CTTGACCCTACTATGCAGACAAAAGACTTTTCATAGTATTGAACAAAGGGAAAACAATCTCCGTTTCAATGCCAC
ACCTGCTTTATATATGCTTTCTCCTTTCAGTCCTCTAAGAAGAATATCTATTAAGATTTTAGTACACTCCTTATTCAGCA
TGCTCATCATGTGCACTATTCTGACAACTGCATATTTATGACCATGAATAACCCGCCGGACTGGACCAAAAATGTGC
AGTACACTTTTACTGGAATATATACTTTTGAATCACTTGTAAAAATCCTTGCAAGAGGCTTCTGTGTAGGAGAATTCA
CTTTTCTTCGTGACCCGTGGAAGTGGCTGGATTTTGTGTCATTGTTTTTGCATGACAGAAATTTGTAGACCTAG
GCAATGTTTCAGCTCTTCGAACTTTCAGAGTATTGAGAGCTTTGAAAATCTTCTGTAATCCCAGGCCTGAAGACAA
TTGTAGGGGCTTTGATCCAGTCAGTGAAGAAGCTTTCTGATGTCATGATCCTGACTGTGTTCTGTCTGAGTGTGTTG
CACTAATTGGACTACAGCTGTTTCATGGGAAACCTGAAGCATAAATGTTTTCGAAATTCACTTGAAAATAATGAAACAT
TAGAAAGCATAATGAATACCTAGAGAGTGAAGAAGACTTTAGAAAATATTTTTATTACTTGAAGGATCCAAAGAT
GCTCTCCTTTGTGGTTTCAGCACAGATTCAGGTCAGTGTCCAGAGGGGTACACCTGTGTGAAAATTGGCAGAAACCC
TGATTATGGCTACACGAGCTTTGACACTTTCAGCTGGCCTTCTTAGCCTTGTGTTAGGCTAATGACCCAAGATTCTG
GGAAAACCTTTACCAACAGACGCTGCGTGCTGCTGGCAAACCTACATGATCTTCTTTGTCGTAGTGATTTTCCTGGG
CTCCTTTTATCTAATAAACTTGATCCTGGCTGTGGTTGCCATGGCATATGAAGAACAGAACCAGGCAAACATTGAAG
AAGCTAAACAGAAAGAATTAGAATTTCAACAGATGTTAGACCGTCTTAAAAAAGAGCAAGAAGAAGCTGAGGCAAT
TGCAGCGCAGCGGCTGAATATACAAGTATTAGGAGAAGCAGAATTATGGGCCTCTCAGAGAGTTCTTCTGAAACA
TCCAAACTGAGCTCTAAAAGTGCTAAAGAAAAGAAGAAACAGAAGAAAGAAAAGAATCAAAGAAGCTCTCCAGT
GGAGAGGAAAAGGGAGATGCTGAGAAATTGTCGAAATCAGAATCAGAGGACAGCATCAGAAGAAAAGTTTCCAC
CTTGGTGTGCAAGGGCATAGGCGAGCACATGAAAAGAGGTTGTCTACCCCAATCAGTCACTACTCAGCATTCTGGG
CTCCTTGTGTTTCTGCAAGGCGAAGCAGCAGAACAAGTCTTTTTAGTTTCAAAGGCAGAGGAAGAGATATAGGATCTG
AGACTGAATTTGCCGATGATGAGCACAGCATTTTTGGAGACAATGAGAGCAGAAGGGGCTCACTGTTTGTGCCCA
CAGACCCAGGAGCGACGCAGCAGTAACATCAGCCAAGCCAGTAGGTCCCACCAATGCTGCCGGTGAACGGGAA
AATGCACAGTGCTGTGGACTGCAACGGTGTGGTCTCCCTGGTTGATGGACGCTCAGCCCTCATGCTCCCAATGGAC
AGCTTCTGCCAGAGGGCACGACCAATCAAATACACAAGAAAAGGCGTTGTAGTTCCTATCTCCTTTCAGAGGATATG
CTGAATGATCCCAACCTCAGACAGAGAGCAATGAGTAGAGCAAGCATATTAACAAACTGTGGAAGAAGTGAAG
AGTCCAGACAAAATGTCCACCTTGGTGGTACAGATTTGCACACAAATCTTGATCTGGAATTGCTCTCCATATTGGA
TAAAATTCAAAAAGTGTATCTATTTTATTGTAATGGATCCTTTTGTAGATCTTGCAATTACCATTTGCATAGTTTTAAC
ACATTATTTATGGCTATGGAACACCACCAATGACTGAGGAATTCAAAATGTACTTGCTATAGGAAATTTGGTCTTT
ACTGGAATCTTTCAGCTGAAATGGTATTAATAACTGATTGCCATGGATCCATATGAGTATTTCCAAGTAGGCTGGAA
TATTTTTGACAGCCTTATTGTGACTTTAAGTTTGTGGAGCTCTTCTAGCAGATGTGGAAGGATTGTCAGTTCTGCG
ATCATTGAGACTGCTCCGAGTCTCAAGTTGGCAAATCCTGGCCAACATTGAACATGCTGATTAAGATCATTGGTAA
CTCAGTAGGGGCTCTAGGTAACCTCACCTTAGTGTGGCCATCATCGTCTTCATTTTGCTGTGGTCCGCATGCAGCT
CTTTGGTAAGAGCTACAAAGAATGTGTCTGCAAGATCAATGATGACTGTACGCTCCACGGTGGCACATGAACGACT
TCTTCCACTCCTTCTGATTGTGTTCCGCGTGTGTGGAGAGTGGATAGAGACCATGTGGGACTGTATGGAGGTC
GCTGGTCAAGCTATGTGCCTTATTGTTTACATGATGGTCATGGTCATTGGAAAACCTGGTGGTCTAAACCTATTTCTG
GCCTTATTATTGAGCTCATTAGTTCAGACAATCTTACAGCAATTGAAGAAGACCCTGATGCAAACAACCTCCAGATT

GCAGTGA CTAGAATTA AAAAGGGAATAAATTATGTGAAACAAACCTTACGTGAATTTATTCTAAAAGCATTTCCTCAA
AAAGCCAAAGATTTCCAGGGAGATAAGACAAGCAGAAGATCTGAATACTAAGAAGGAAAACCTATATTTCTAACCAT
ACACTTGCTGAAATGAGCAAAGGTCACAATTTCTCAAGGAAAAAGATAAAATCAGTGGTTTTGGAAGCAGCGTGG
ACAAACACTTGATGGAAGACAGTGATGGTCAATCATTATTACAATCCCAGCCTCACAGTGACAGTGCCAATTGCA
CCTGGGGAATCCGATTTGGAAAATATGAATGCTGAGGAACTTAGCAGTGATTCGGATAGTGAATACAGCAAAGTGA
GATTAACCGGTCAAGCTCCTCAGAGTGCAGCACAGTTGATAACCCCTTGCCTGGAGAAGGAGAAGAAGCAGAGGC
TGAACCTATGAATCCGATGAGCCAGAGGCCTGTTTCACAGATGGTTGTGTACGGAGGTTCTCATGCTGCCAAGTTA
ACATAGAGTCAGGGAAAGGAAAAATCTGGTGAACATCAGGAAAACCTGCTACAAGATTGTTGAACACAGTTGGTT
TGAAAGCTTCATTGTCCTCATGATCCTGCTCAGCAGTGGTGCCTGGCTTTTGAAGATATTTATATTGAAAGGAAAA
GACCATTAAGATTATCCTGGAGTATGCAGACAAGATCTTCACTTACATCTTCACTTCTGGAATGCTTCTAAAATGGAT
AGCATATGGTTATAAAACATATTTACCAATGCCTGGTGTGGCTGGATTTCCTAATTGTTGATGTTTCTTGGTTACT
TTAGTGGCAAACACTCTTGGCTACTCAGATCTTGGCCCATTAATCCCTTCGGACACTGAGAGCTTTAAGACCTCTA
AGAGCCTTATCTAGATTTGAAGGAATGAGGGTCGTTGTGAATGCACTCATAGGAGCAATTCCTTCCATCATGAATGT
GCTACTTGTGTCTTATATTCTGGCTGATATTCAGCATCATGGGAGTAAATTTGTTTGGTGGCAAGTTCTATGAGTG
TATTAACACCACAGATGGGTACGGTTTCTGCAAGTCAAGTTCAAATCGTTCCGAATGTTTTGCCCTTATGAATGT
TAGTCAAATGTGCGATGGAAAAACCTGAAAGTGAACCTTGTATAATGTCGGACTTGGTTACCTATCTCTGCTTCAAGT
TGCAACTTTAAGGGATGGACGATTATTATGTATGCAGCAGTGGATTCTGTTAATGTAGACAAGCAGCCCAAATATG
AATATAGCCTCTACATGTATATTTATTTTGTGCTCTTATCATCTTGGGTCACTTCTCACTTTGAACCTGTTCAATTGGT
GTCATCATAGATAATTTCAACCAACAGAAAAAGGCTTGGAGGTCAAGACATCTTATGACAGAAGAACAGAAGA
AATACTATAATGCAATGAAAAAGCTGGGGTCCAAGAAGCCACAAAAGCCAATTCCTCGACCAGGGAACAAAATCCA
AGGATGTATATTTGACCTAGTGACAAATCAAGCCTTTGATATTAGTATCATGGTTCTTATCTGTCTCAACATGGTAACC
ATGATGGTAGAAAAGGAGGGTCAAAGTCAACATATGACTGAAGTTTTATATTGGATAAATGTGGTTTTTATAATCCT
TTTCACTGGAGAATGTGTGCTAAAACCTGATCTCCCTCAGACACTACTACTTCACTGTAGGATGGAATATTTTTGATTTT
GTGGTTGTGATTATCTCCATTGTAGGTATGTTTCTAGCTGATTTGATTGAAACGATTTTTGTGTCCCTACCTGTTCC
GAGTGATCCGTCTTGCCAGGATTGGCCGAATCCTACGTCTAGTCAAAGGAGCAAAGGGGATCCGCACGCTGCTCTTT
GCTTTGATGATGTCCCTCTGCGTTGTTTAAACATCGGCCTCCTGCTCTTCTGGTCATGTTTCTACGCCATCTTTGG
AATGTCCAACCTTGCCTATGTTAAAAAGGAAGATGGAATTAATGACATGTTCAATTTTGGAGACCTTTGGCAACAGTAT
GATTTGCCTGTTCAAATTACAACCTCTGCTGGCTGGGATGGATTGCTAGCACCTATTCTTAACAGTAAGCCACCCGA
CTGTGACCCAAAAAAGTTTATCCTGGAAGTTTCAAGTTGAAGGAGACTGTGGTAACCCATCTGTTGGAATATTCTACTT
TGTTAGTTATATCATCATATCCTTCTGGTTGTGGTGAACATGTACATTGCAGTCATACTGGAGAATTTTAGTGTGGC
ACTGAAGAAAGTACTGAACCTCTGAGTGAGGATGACTTTGAGATGTTCTATGAGGTTTGGGAGAAGTTTGTATCCCG
ATGCGACCCAGTTTATAGAGTTCTCTAAACTCTGATTTTGCAGCTGCCCTGGATCCTCCTCTTCTCATAGCAAAC
CAACAAAGTCCAGCTCATTGCCATGGATCTGCCATGGTTAGTGGTGACCGGATCCATTGTCTTGACATCTTATTTGC
TTTTACAAAGCGTGTGTTTGGGTGAGAGTGGGGAGATGGATTCTTTCGTTACAGATGGAAGAAAGGTTTCTATGCTG
CAAATCCTTCAAAGTGTCTATGAACCCATACAACCACACTAAAACGGAAACAAGAGGATGTGTCTGCTACTGTC
ATTCAGCGTGCTTATAGACGTTACCGCTTAAAGGCAAAATGTCAAAAATATATCAAGTATATACATAAAAGATGGAGA
CAGAGATGATGATTTACTCAATAAAAAAGATATGGCTTTTGTATAATGTTAATGAGAACTCAAGTCCAGAAAAACAG
ATGCCACTTCATCCACCCTCTCCACCTTCATATGATAGTGAACAAAGCCAGACAAAGAGAAATATGAACAAGACA
GAACAGAAAAGGAAGACAAAGGGAAGACAGCAAGGAAAGCAAAAAATAG

SCN9A-5A TTX-Resistant amino acid sequence:

Met A Met L P P P G P Q S F V H F T K Q S L A L I E Q R I A E R K S K E P K E E K K D D D E E A P K P S S D L E A
G K Q L P F I Y G D I P P G **Met** V S E P L E D L D P Y Y A D K K T F I V L N K G K T I F R F N A T P A L Y **Met** L S P
F S P L R R I S I K I L V H S L F S **Met** L I **Met** C T I L T N C I F **Met** T **Met** N N P P D W T K N V E Y T F T G I Y T F
E S L V K I L A R G F C V G E F T F L R D P W N W L D F V V I V F A Y **V** T E F V **D** L G N V S A L R T F R V L R A L
K T I S V I P G L K T I V G A L I Q S V K K L S D V **Met** I L T V F C L S V F A L I G L Q L F **Met** G N L K H K C F R N S
L E N N E T L E S I **Met** N T L E S E E D F R K Y F Y L E G S K D A L L C G F S T D S G Q C P E G Y T C V K I G R N
P D Y G Y T S F D T F S W A F L A L F R L **Met** T Q D **S** W E N L Y Q Q T L R A A G K T Y **Met** I F F V V V I F L G S
F Y L I N L I L A V V A **Met** A Y E E Q N Q A N I E E A K Q K E L E F Q Q **Met** L D R L K K E Q E E A E A I A A A A A
E Y T S I R R S R I **Met** G L S E S S S E T S K L S S K S A K E R R N R R K K N Q K K L S S G E E K G D A E K L S K S
E S E D S I R R K S F H L G V E G H R R A H E K R L S T P N Q S P L S I R G S L F S A R R S S R T S L F S F K G R G R
D I G S E T E F A D D E H S I F G D N E S R R G S L F V P H R P Q E R R S S N I S Q A S R S P P **Met** L P V N G
K **Met** H S A V D C N G V V S L V D G R S A L **Met** L P N G Q L L P E G T T N Q I H K K R R C S S Y L L S E
D **Met** L N D P N L R Q R A **Met** S R A S I L T N T V E E L E E S R Q K C P P W W Y R F A H K F L I W N C S P Y W
I K F K K C I Y F I V **Met** D P F V D L A I T I C I V L N T L F **Met** A **Met** E H H P **Met** T E E F K N V L A I G N L V F T
G I F A A E **Met** V L K L I A **Met** D P Y E Y F Q V G W N I F D S L I V T L S L V E L F L A D V E G L S V L R S F R L L
R V F K L A K S W P T L N **Met** L I K I I G N S V G A L G N L T L V L A I I V F I F A V V G **Met** Q L F G K S Y K E C V
C K I N D D C T L P R W H **Met** N D F F H S F L I V F R V L C G E W I E T **Met** W D C **Met** E V A G Q A **Met** C L I
V Y **Met** **Met** V **Met** V I G N L V V L N L F L A L L L S S F S S D N L T A I E E D P D A N N L Q I A V T R I K K G I N
Y V K Q T L R E F I L K A F S K K P K I S R E I R Q A E D L N T K K E N Y I S N H T L A E **Met** S K G H N F L K E K D
K I S G F G S S V D K H L **Met** E D S D G Q S F I H N P S L T V T V P I A P G E S D L E N **Met** N A E E L S S D S D S
E Y S K V R L N R S S S E C S T V D N P L P G E G E E A E A E P **Met** N S D E P E A C F T D G C V R R F S C C Q V
N I E S G K G K I W W N I R K T C Y K I V E H S W F E S F I V L **Met** I L L S S G A L A F E D I Y I E R K K T I K I I L E
Y A D K I F T Y I F I L E **Met** L L K W I A Y G Y K T Y F T N A W C W L D F L I V D V S L V T L V A N T L G Y S D L G
P I K S L R T L R A L R P L R A L S R F E G **Met** R V V V N A L I G A I P S I **Met** N V L L V C L I F W L I F S I **Met** G
V N L F A G K F Y E C I N T T D G S R F P A S Q V P N R S E C F A L **Met** N V S Q N V R W K N L K V N F D N V G
L G Y L S L L Q V A T F K G W T I I **Met** Y A A V D S V N V D K Q P K Y E Y S L Y **Met** Y I Y F V V F I I F G S F F T L
N L F I G V I I D N F N Q Q K K K L G G Q D I F **Met** T E E Q K K Y Y N A **Met** K K L G S K K P Q K P I P R P G N K I
Q G C I F D L V T N Q A F D I S I **Met** V L I C L N **Met** V T **Met** **Met** V E K E G Q S Q H **Met** T E V L Y W I N V V F
I I L F T G E C V L K L I S L R H Y Y F T V G W N I F D F V V V I I S I V **GMet** F L A D L I E T Y F V S P T L F R V I R L
A R I G R I L R L V K G A K G I R T L L F A L **Met** **Met** S L P A L F N I G L L L F L V **Met** F I Y A I F G **Met** S N F A Y
V K K E D G I N D **Met** F N F E T F G N S **Met** I C L F Q I T T S A G W D G L L A P I L N S K P P D C D P K K V H P
G S S V E G D C G N P S V G I F Y F V S Y I I I S F L V V V N **Met** Y I A V I L E N F S V A T E E S T E P L S E D D F
E **Met** F Y E V W E K F D P D A T Q F I E F S K L S D F A A A L D P P L L I A K P N K V Q L I A **Met** D L P **Met** V S
G D R I H C L D I L F A F T K R V L G E S G E **Met** D S L R S Q **Met** E E R F **Met** S A N P S K V S Y E P I T T T L K R
K Q E D V S A T V I Q R A Y R R Y R L R Q N V K N I S S I Y I K D G R D D D L L N K K D **Met** A F D N V N E N S
S P E K T D A T S S T T S P P S Y D S V T K P D K E K Y E Q D R T E K E D K G K D S K E S K K **Stop**

SNC9A-5N **TTX-Resistant** cDNA sequence:

ATGGCAATGTTGCCTCCCCAGGACCTCAGAGCTTTGTCCATTTACAAAACAGTCTCTTGCCCTCATTGAACAACGC
ATTGCTGAAAGAAAATCAAAGGAACCCAAAGAAGAAAAGAAAGATGATGATGAAGAAGCCCCAAAGCCAAGCAGT
GACTTGGAAGCTGGCAAACAACCTGCCCTTCATCTATGGGGACATTCCTCCCGCATGGTGTGAGAGCCCTGGAGGA
CTTGACCCTACTATGCAGACAAAAGACTTTTCATAGTATTGAACAAAAGGAAAACAATCTTCCGTTTCAATGCCAC
ACCTGCTTTATATATGCTTTCTCCTTTCAGTCCTCTAAGAAGAATATCTATTAAGATTTTAGTACACTCCTTATTCAGCA
TGCTCATCATGTGCACTATTCTGACAACTGCATATTTATGACCATGAATAACCCGCCGGACTGGACCAAAAATGTGC
AGTACACTTTTACTGGAATATATACTTTTGAATCACTTGTAAAAATCCTTGCAAGAGGCTTCTGTGTAGGAGAATTCA
CTTTTCTTCGTGACCCGTGGAACCTGGCTGGATTTTGTGTCATTGTTTTTTCGTATTACAGAAATTTGTAACTAGG
CAATGTTTCAGCTCTTCGAACTTTCAGAGTATTGAGAGCTTTGAAAATCTTGTAAATCCCAGGCCTGAAGACAAT
TGTAGGGGCTTTGATCCAGTCAGTGAAGAAGCTTTCTGATGTCATGATCCTGACTGTGTTCTGTCTGAGTGTGTTTGC
ACTAATTGGACTACAGCTGTTTCATGGGAAACCTGAAGCATAAATGTTTTCGAAATTCACCTGAAAATAATGAAACATT
AGAAAGCATAATGAATACCCTAGAGAGTGAAGAAGACTTTAGAAAATATTTTTATTACTTGAAGGATCCAAAGATG
CTCTCCTTTGTGGTTTTAGCACAGATTCAGGTGAGTGTCCAGAGGGGTACACCTGTGTGAAAATTGGCAGAAACCT
GATTATGGCTACACGAGCTTTGACACTTTCAGCTGGGCTTCTTAGCCTGTTTAGGCTAATGACCCAAGATTCTGG
GAAAACCTTTACCAACAGACGCTGCGTGCTGCTGGCAAACCTACATGATCTTCTTTGTCGTAGTGATTTTCTGGGC
TCCTTTTATCTAATAAACTTGATCCTGGCTGTGGTTGCCATGGCATATGAAGAACAGAACCCAGGCAAACATTGAAGA
AGCTAAACAGAAAGAATTAGAATTTCAACAGATGTTAGACCGTCTTAAAAAAGAGCAAGAAGAAGCTGAGGCAATT
GCAGCGGCAGCGGCTGAATATACAAGTATTAGGAGAAGCAGAATTATGGGCCTCTCAGAGAGTTCTTCTGAAACAT
CCAACTGAGCTCTAAAAGTGCTAAAGAAAGAAGAAACAGAAAGAAAGAAAAGAATCAAAGAAGCTCTCCAGTG
GAGAGGAAAAGGGAGATGCTGAGAAATTGTGCAATCAGAATCAGAGGACAGCATCAGAAGAAAAAGTTTCCACC
TTGGTGTGCAAGGGCATAGGCGAGCAGCATGAAAAGAGTTGTCTACCCCAATCAGTCACCACTCAGCATTCTGTGGC
TCCTTGTCTTCTGCAAGGCGAAGCAGCAGAACAAGTCTTTTTAGTTTCAAAGGCAGAGGAAGAGATATAGGATCTGA
GACTGAATTTGCCGATGATGAGCACAGCATTTTGGAGACAATGAGAGCAGAAGGGGCTCACTGTTTGTGCCCCAC
AGACCCAGGAGCGACGACGAGTAACATCAGCCAAGCCAGTAGGTCCCCACCAATGCTGCCGGTGAACGGGAAA
ATGCACAGTGCTGTGGACTGCAACGGTGTGGTCTCCCTGGTTGATGGACGCTCAGCCCTCATGCTCCCAATGGACA
GCTTCTGCCAGAGGGCAGACCAATCAAATACACAAGAAAAGGCGTTGTAGTTCCTATCTCCTTTCAGAGGATATGC
TGAATGATCCCAACCTCAGACAGAGCAATGAGTAGAGCAAGCATATTAACAAACACTGTGGAAGAATTGAAGA
GTCCAGACAAAATGTCCACCTTGGTGGTACAGATTTGCACACAAATCTTGATCTGGAATTGCTCTCCATATTGGAT
AAAATTCAAAAAGTGTATCTATTTTATTGTAATGGATCCTTTTGTAGATCTTGCAATTACCATTTGCATAGTTTTAAC
ACATTATTTATGGCTATGGAACACCACCAATGACTGAGGAATTCAAAAATGTAATTGCTATAGGAAATTTGGTCTTT
ACTGGAATCTTTCAGCTGAAATGGTATTAATAACTGATTGCCATGGATCCATATGAGTATTTCCAAGTAGGCTGGAA
TATTTTTGACAGCCTTATTGTGACTTTAAGTTTGTGGAGCTCTTCTAGCAGATGTGGAAGGATTGTCAGTTCTGCG
ATCATTGAGACTGCTCCGAGTCTCAAGTTGGCAAATCCTGGCCAACATTGAACATGCTGATTAAGATCATTGGTAA
CTCAGTAGGGGCTCTAGGTAACCTCACCTTAGTGTGGCCATCATCGTCTTCATTTTTGCTGTGGTCCGCATGCAGCT
CTTTGGTAAGAGCTACAAAGAATGTGTCTGCAAGATCAATGATGACTGTACGCTCCACGGTGGCACATGAACGACT
TCTTCCACTCCTTCTGATTGTGTTCCGCGTGCTGTGTGGAGAGTGGATAGAGACCATGTGGGACTGTATGGAGGTC
GCTGGTCAAGCTATGTGCCTTATTGTTTACATGATGGTCATGGTCATTGGAAAACCTGGTGGTCCATAACCTATTTCTG
GCCTTATTATTGAGCTCATTAGTTCAGACAATCTTACAGCAATTGAAGAAGACCCTGATGCAAACAACCTCCAGATT

GCAGTGA CTAGAATTA AAAAGGGAATAAATTATGTGAAACAAACCTTACGTGAATTTATTCTAAAAGCATTTCCTCAA
AAAGCCAAAGATTTCCAGGGAGATAAGACAAGCAGAAGATCTGAATACTAAGAAGGAAAACCTATATTTCTAACCAT
ACACTTGCTGAAATGAGCAAAGGTCACAATTTCTCAAGGAAAAAGATAAAATCAGTGGTTTTGGAAGCAGCGTGG
ACAAACACTTGATGGAAGACAGTGATGGTCAATCATTATTACAATCCCAGCCTCACAGTGACAGTGCCAATTGCA
CCTGGGGAATCCGATTTGGAAAATATGAATGCTGAGGAACTTAGCAGTGATTCGGATAGTGAATACAGCAAAGTGA
GATTAACCGGTCAAGCTCCTCAGAGTGCAGCACAGTTGATAACCCCTTGCCTGGAGAAGGAGAAGAAGCAGAGGC
TGAACCTATGAATCCGATGAGCCAGAGGCCTGTTTCACAGATGGTTGTGTACGGAGGTTCTCATGCTGCCAAGTTA
ACATAGAGTCAGGGAAAGGAAAAATCTGGTGAACATCAGGAAAACCTGCTACAAGATTGTTGAACACAGTTGGTT
TGAAAGCTTCATTGTCCTCATGATCCTGCTCAGCAGTGGTGCCCTGGCTTTTGAAGATATTTATATTGAAAGGAAAA
GACCATTAAGATTATCCTGGAGTATGCAGACAAGATCTTCACTTACATCTTCACTTCTGGAATGCTTCTAAAATGGAT
AGCATATGGTTATAAAACATATTTACCAATGCCTGGTGTGGCTGGATTTCCTAATTGTTGATGTTTCTTGGTTACT
TTAGTGGCAAACACTCTTGGCTACTCAGATCTTGGCCCATTAATCCCTTCGGACACTGAGAGCTTTAAGACCTCTA
AGAGCCTTATCTAGATTTGAAGGAATGAGGGTCGTTGTGAATGCACTCATAGGAGCAATTCCTTCCATCATGAATGT
GCTACTTGTGTCTTATATTCTGGCTGATATTCAGCATCATGGGAGTAAATTTGTTTGCTGGCAAGTTCTATGAGTG
TATTAACACCACAGATGGGTACGGTTTCTGCAAGTCAAGTTCAAATCGTTCCGAATGTTTTGCCCTTATGAATGT
TAGTCAAATGTGCGATGGAAAAACCTGAAAGTGAACCTTGTATAATGTCGGACTTGGTTACCTATCTCTGCTTCAAGT
TGCAACTTTAAGGGATGGACGATTATTATGTATGCAGCAGTGGATTCTGTTAATGTAGACAAGCAGCCCAAATATG
AATATAGCCTCTACATGTATATTTATTTGTCGTCTTATCATCTTGGGTCACTTCACTTTGAACCTGTTCAATTGGT
GTCATCATAGATAATTTCAACCAACAGAAAAAGAGCTTGGAGGTCAAGACATCTTATGACAGAAGAACAGAAGA
AATACTATAATGCAATGAAAAAGCTGGGGTCCAAGAAGCCACAAAAGCCAATTCCTCGACCAGGGAACAAAATCCA
AGGATGTATATTTGACCTAGTGACAAATCAAGCCTTTGATATTAGTATCATGGTTCTTATCTGTCTCAACATGGTAACC
ATGATGGTAGAAAAGGAGGGTCAAAGTCAACATATGACTGAAGTTTTATATTGGATAAATGTGGTTTTTATAATCCT
TTCACTGGAGAATGTGTGCTAAAACCTGATCTCCCTCAGACACTACTACTTCACTGTAGGATGGAATATTTTTGATTTT
GTGGTTGTGATTATCTCCATTGTAGGTATGTTTCTAGCTGATTTGATTGAAACGATTTTTGTGTCCCTACCTGTTCC
GAGTGATCCGTCTTGCCAGGATTGGCCGAATCCTACGTCTAGTCAAAGGAGCAAAGGGGATCCGCACGCTGCTCTTT
GCTTTGATGATGTCCCTCCTGCGTTGTTTAAACATCGGCCTCCTGCTTCTCTGGTCATGTTTCTACGCCATCTTTGG
AATGTCCAACCTTGCCTATGTTAAAAAGGAAGATGGAATTAATGACATGTTCAATTTTGAGACCTTTGGCAACAGTAT
GATTTGCCTGTTCAAATTACAACCTCTGCTGGCTGGGATGGATTGCTAGCACCTATTCTTAACAGTAAGCCACCCGA
CTGTGACCCAAAAAAGTTTATCCTGGAAGTTTCAAGTTGAAGGAGACTGTGGTAACCCATCTGTTGGAATATTCTACTT
TGTTAGTTATATCATCATATCCTTCTGGTTGTGGTGAACATGTACATTGCAGTCATACTGGAGAATTTTAGTGTGGC
ACTGAAGAAAGTACTGAACCTCTGAGTGAGGATGACTTTGAGATGTTCTATGAGGTTTGGGAGAAGTTTGATCCCG
ATGCGACCCAGTTTATAGAGTTCTTAAACTCTGATTTTGCAGCTGCCCTGGATCCTCCTTCTCATAGCAAACCC
CAACAAAGTCCAGCTCATTGCCATGGATCTGCCATGGTTAGTGGTGACCGGATCCATTGTCTTGACATCTTATTTGC
TTTTACAAAGCGTGTGTTGGGTGAGAGTGGGGAGATGGATTCTTTCGTTACAGATGGAAGAAAGGTTTCTGTCTG
CAAATCCTTCAAAGTGTCTATGAACCCATCACAACCACACTAAAACGGAAACAAGAGGATGTGTCTGCTACTGTC
ATTCAGCGTGCTTATAGACGTTACCGCTTAAAGGCAAAATGTCAAAAATATATCAAGTATATACATAAAAGATGGAGA
CAGAGATGATGATTTACTCAATAAAAAAGATATGGCTTTTGTATAATGTTAATGAGAACTCAAGTCCAGAAAAACAG
ATGCCACTTCATCCACCCTCTCCACCTTCATATGATAGTGAACAAAGCCAGACAAAGAGAAATATGAACAAGACA
GAACAGAAAAGGAAGACAAAGGGAAAGACAGCAAGGAAAGCAAAAATAG

SCN9A-5N **TTX-Resistant** amino acid sequence:

Met A Met L P P P G P Q S F V H F T K Q S L A L I E Q R I A E R K S K E P K E E K K D D D E E A P K P S S D L E A
G K Q L P F I Y G D I P P G **Met** V S E P L E D L D P Y Y A D K K T F I V L N K G K T I F R F N A T P A L Y **Met** L S P
F S P L R R I S I K I L V H S L F S **Met** L I **Met** C T I L T N C I F **Met** T **Met** N N P P D W T K N V E Y T F T G I Y T F
E S L V K I L A R G F C V G E F T F L R D P W N W L D F V V I V F A Y **L** T E F V **N** L G N V S A L R T F R V L R A L K
T I S V I P G L K T I V G A L I Q S V K K L S D V **Met** I L T V F C L S V F A L I G L Q L F **Met** G N L K H K C F R N S L
E N N E T L E S I **Met** N T L E S E E D F R K Y F Y L E G S K D A L L C G F S T D S G Q C P E G Y T C V K I G R N P
D Y G Y T S F D T F S W A F L A L F R L **Met** T Q D **S** W E N L Y Q Q T L R A A G K T Y **Met** I F F V V V I F L G S F
Y L I N L I L A V V A **Met** A Y E E Q N Q A N I E E A K Q K E L E F Q Q **Met** L D R L K K E Q E E A E A I A A A A A E
Y T S I R R S R I **Met** G L S E S S S E T S K L S S K S A K E R R N R R K K N Q K K L S S G E E K G D A E K L S K S E
S E D S I R R K S F H L G V E G H R R A H E K R L S T P N Q S P L S I R G S L F S A R R S S R T S L F S F K G R G R
D I G S E T E F A D D E H S I F G D N E S R R G S L F V P H R P Q E R R S S N I S Q A S R S P P **Met** L P V N G
K **Met** H S A V D C N G V V S L V D G R S A L **Met** L P N G Q L L P E G T T N Q I H K K R R C S S Y L L S E
D **Met** L N D P N L R Q R A **Met** S R A S I L T N T V E E L E E S R Q K C P P W W Y R F A H K F L I W N C S P Y W
I K F K K C I Y F I V **Met** D P F V D L A I T I C I V L N T L F **Met** A **Met** E H H P **Met** T E E F K N V L A I G N L V F T
G I F A A E **Met** V L K L I A **Met** D P Y E Y F Q V G W N I F D S L I V T L S L V E L F L A D V E G L S V L R S F R L L
R V F K L A K S W P T L N **Met** L I K I I G N S V G A L G N L T L V L A I I V F I F A V V G **Met** Q L F G K S Y K E C V
C K I N D D C T L P R W H **Met** N D F F H S F L I V F R V L C G E W I E T **Met** W D C **Met** E V A G Q A **Met** C L I
V Y **Met** **Met** V **Met** V I G N L V V L N L F L A L L L S S F S S D N L T A I E E D P D A N N L Q I A V T R I K K G I N
Y V K Q T L R E F I L K A F S K K P K I S R E I R Q A E D L N T K K E N Y I S N H T L A E **Met** S K G H N F L K E K D
K I S G F G S S V D K H L **Met** E D S D G Q S F I H N P S L T V T V P I A P G E S D L E N **Met** N A E E L S S D S D S
E Y S K V R L N R S S S E C S T V D N P L P G E G E E A E A E P **Met** N S D E P E A C F T D G C V R R F S C C Q V
N I E S G K G K I W W N I R K T C Y K I V E H S W F E S F I V L **Met** I L L S S G A L A F E D I Y I E R K K T I K I I L E
Y A D K I F T Y I F I L E **Met** L L K W I A Y G Y K T Y F T N A W C W L D F L I V D V S L V T L V A N T L G Y S D L G
P I K S L R T L R A L R P L R A L S R F E G **Met** R V V V N A L I G A I P S I **Met** N V L L V C L I F W L I F S I **Met** G
V N L F A G K F Y E C I N T T D G S R F P A S Q V P N R S E C F A L **Met** N V S Q N V R W K N L K V N F D N V G
L G Y L S L L Q V A T F K G W T I I **Met** Y A A V D S V N V D K Q P K Y E Y S L Y **Met** Y I Y F V V F I I F G S F F T L
N L F I G V I I D N F N Q Q K K L G G Q D I F **Met** T E E Q K K Y Y N A **Met** K K L G S K K P Q K P I P R P G N K I
Q G C I F D L V T N Q A F D I S I **Met** V L I C L N **Met** V T **Met** **Met** V E K E G Q S Q H **Met** T E V L Y W I N V V F
I I L F T G E C V L K L I S L R H Y Y F T V G W N I F D F V V V I I S I V **GMet** F L A D L I E T Y F V S P T L F R V I R L
A R I G R I L R L V K G A K G I R T L L F A L **Met** **Met** S L P A L F N I G L L L F L V **Met** F I Y A I F G **Met** S N F A Y
V K K E D G I N D **Met** F N F E T F G N S **Met** I C L F Q I T T S A G W D G L L A P I L N S K P P D C D P K K V H P
G S S V E G D C G N P S V G I F Y F V S Y I I I S F L V V V N **Met** Y I A V I L E N F S V A T E E S T E P L S E D D F
E **Met** F Y E V W E K F D P D A T Q F I E F S K L S D F A A A L D P P L L I A K P N K V Q L I A **Met** D L P **Met** V S
G D R I H C L D I L F A F T K R V L G E S G E **Met** D S L R S Q **Met** E E R F **Met** S A N P S K V S Y E P I T T T L K R
K Q E D V S A T V I Q R A Y R R Y R L R Q N V K N I S S I Y I K D G D R D D D L L N K K D **Met** A F D N V N E N S
S P E K T D A T S S T T S P P S Y D S V T K P D K E K Y E Q D R T E K E D K G K D S K E S K K **Stop**